University of Glasgow

Exploring the Spliceosome using Hinokiflavone Based Probes

Helmi Kreinin

PhD thesis

University of Glasgow

School of Chemistry

September 2017

Abstract

The spliceosome is the cellular machinery involved in producing mature messenger RNA from pre-mRNA before it is translated into protein by the cells. Improved understanding of this vital cellular process would allow us to design better drugs to combat diseases that depend on splicing mismanagement. Small molecules that affect splicing would be useful in furthering our understanding of this complex cellular mechanism.

Hinokiflavone, a biflavonoid natural product, was found to affect splicing in cells. In this work we describe the total synthesis of hinokiflavone, after exploring alternative synthetic routes.

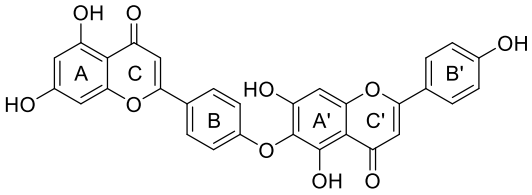

Hinokiflavone

Several different series of hinokiflavone analogues were also designed and three of these structural analogues displayed the same bioactivity as hinokiflavone. Various biological assays in which hinokiflavone and the analogues were active were then examined. It was found that these molecules modulate splicing by inhibiting SENP activity. The SENP enzyme removes SUMO, a post-translational modification involved in the cellular control over splicing, hence its inhibition has a marked effect on cellular metabolism.

Author's Declaration

This thesis represents the original work of Helmi Kreinin unless explicitly stated otherwise in the text. No part of this thesis has previously been submitted for a degree at the University of Glasgow or any other university. The research was carried out predominantly at the University of Glasgow (UK) in the Loudon laboratory under the supervision of Professor Richard C. Hartley during the period between October 2013 and March 2017, biological testing was carried out at the University of Dundee (UK) under the supervision of Professor Angus I. Lamond.

Acknowledgements

I would like to thank first and foremost Professor Richard C. Hartley for being the best supervisor any PhD student could hope for. Thank you for your infinite patience and ever helpful comments.

Thank you to all the biologists in Dundee for their brilliant work, especially Angus and Andrea.

I would like to also thank the past and present members of the Hartley group. especially Stuart, Claire, Lewis, Laura, Justyna, Masha and everyone else who has been part of our struggle in brick-dust land. I couldn't have made it through without your help and emotional support.

I would also like to thank the Sutherland group for being such nice lab/office buddies. Kerry, Nikki, Johnny, Ewen, Réka and the rest of the friendly, brilliant people in this group. I would like to also thank the France, Clark and Prunet group members who have made this organic section a friendly place to work in.

Nothing could be possible without our brilliant support staff, especially Stuart, Ted and Karen. Thank you for making the trains run.

I can never thank my family enough, they have made me who I am and continually support and encourage me. Emme, Halliki, aitah!

Lewis, I am only here because of your help. Mina ei ole puuksutaja, sina oled puuksu karu.

Abbreviations

Ac	Acetate
ADP	adenosine diphosphate
amu	atomic mass unit
Ar	aromatic
aq.	aqueous
ATP	adenosine triphosphate
ATR	attenuated total reflectance
br	broad
BnBr	benzyl bromide
BuOH	butanol
BTPP	*tert*-butylimino-tri(pyrrolidino)phosphorane
cat.	catalytic
COSY	correlation spectroscopy
d	doublet
DCM	dichloromethane
DEPT	Distortionless enhancement by polarization transfer
dd	doublet of doublets
ddd	doublet of doublet of doublets

DMAP 4-Dimethylaminopyridine

DMF *N*,*N*'-dimethylformamide

DMSO dimethylsulfoxide

DNA deoxyribonucleic acid

DIPEA N,N-diisopropylethylamine

dt doublet of triplets

EI electron ionisation

eq. equivalents

ESI electrospray ionisation

Et ethyl

Et_2O diethyl ether

EtOAc ethyl acetate

EtOH ethanol

EDC 1-Ethyl-3-(3-dimethylaminopropyl)-carbodiimide

g gram(s)

h hour(s)

HBTU N,N,N′,N′-Tetramethyl-O-(1H-benzotriazol-1-yl)-uronium hexafluorophosphate

HMBC heteronuclear multiple bond correlation

HPLC high performance liquid chromatography

HRMS	high-resolution mass spectrometry
HSQC	heteronuclear single quantum coherence
IR	infrared
J NMR	coupling constant
^{i}Pr	isopropyl
L	litre or ligand
LDA	lithium diisopropylamine
LHS	left hand side
LRMS	low resolution mass spectroscopy
lit.	literature
M	molar
m	multiplet
Me	methyl
MeOD	d_4-deuterated methanol
MeOH	methanol
mg	milligram(s)
mL	millilitre(s)
mM	millimolar
mol	mole(s)

mp	melting point
NEDD	neural precursor cell expressed developmentally downregulated
NMR	nuclear magnetic resonance
NOESY	nuclear overhouser effect
Pd/C	palladium on carbon
Ph	phenyl
PG	protecting group
ppm	parts per million
q	quartet
RHS	right hand side
RNA	ribonucleic acid
rt	room temperature
s	singlet
sept.	septet
S_N1	monomolecular nucleophilic substitution
S_N2	bimolecular nucleophilic substitution
S_NAr	nucleophilic aromatic substitution
t	triplet
tt	triplet of triplets

THF	tetrahydrofuran
THP	tetrahydropyran
TLC	thin layer chromatography
µL	microlitre
µM	micromolar
°C	degrees Celsius

Table of Contents

1 Introduction

1.1 Pre-mRNA splicing

A core dogma of biology is that "DNA is transcribed to RNA is translated to protein".[1] This phrase outlines the flow of information from the genetic code, written in DNA, to the proteome and phenotype that we can see in the organism. Unfortunately, this dogma is a gross oversimplification of the actual flow of information. There are several processes complicating the picture, such as epigenetics, post translational modification and splicing, the latter of which will be discussed in more detail below.[2]

The genes coding for proteins in eukaryotes are not continuous. This means that the coding exons, so called because they exit the nucleus to be translated, are interrupted by several non-coding introns. The pre-messenger RNA transcribed from the DNA is spliced, the introns are cut out, before the mature RNA exits the nucleus to be translated into a polypeptide by the ribosome (*figure 1*). The splicing itself is done by molecular machinery called the spliceosome.[1]

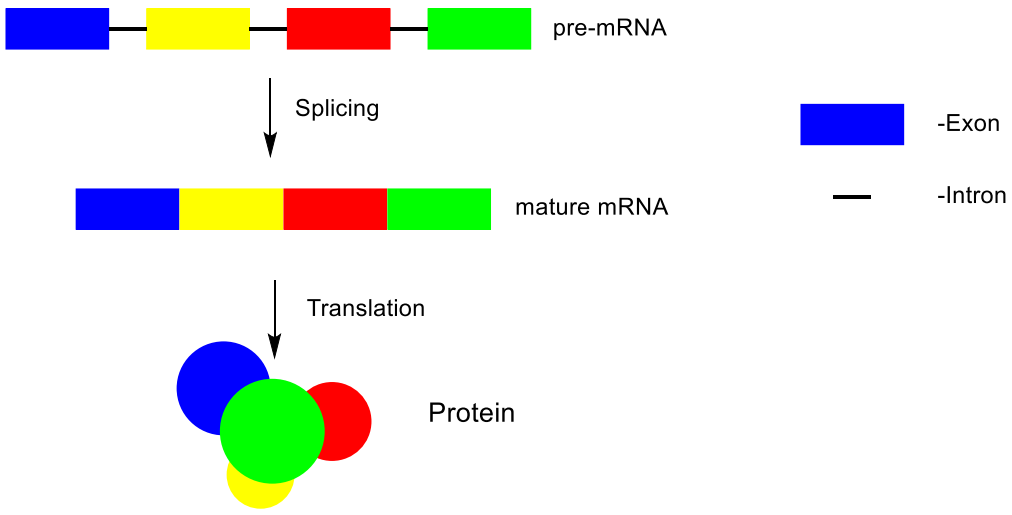

Figure 1 Splicing
Pre-mRNA (composed of exons (coloured rectangles) and introns (black lines) is spliced to form mRNA (coloured rectangles) that is translated into protein (coloured circles).

The spliceosome is a dynamic ribonucleoprotein machinery, which assembles and disassembles every time a mature RNA is produced. Mass spectrometric analysis on the splicing assembly found 300 polypeptides associated with it, so it is easy to see why it has been called a "megamolecular behemoth".[3] Since the

components assemble and disassemble continually as the spliceosome works, it is a complicated machine to study.

The actual steps being catalysed are simple: to cut out the introns and join the exons together. Two transesterification steps take place on the phosphate group of the RNA backbone (*figure 2*). The first transesterification step forms the lariat intermediate and the second step joins the two exons together. The intron is released in the form of a lariat and the mRNA exits the nucleus to be translated.[1]

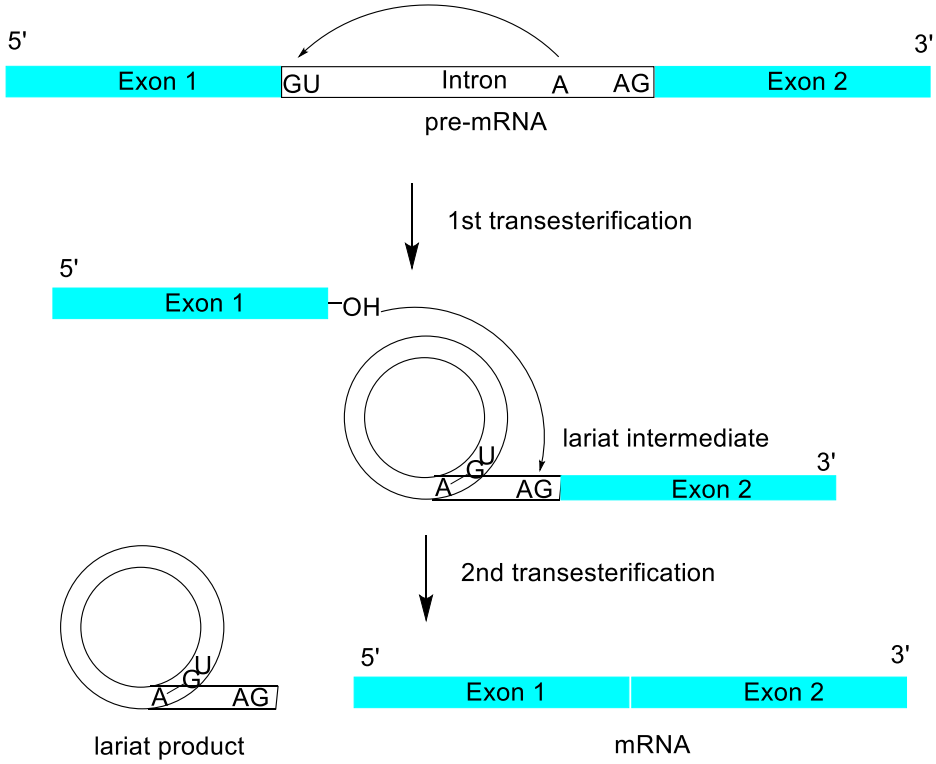

Figure 2 Splicing mechanism
The exons (blue rectangles) are joined together after two catalytic steps. The intron (white rectangle) is cyclised to form a cyclic (white lariat) side product.

1.1.1 Structure of the spliceosome

The reason the eukaryote spliceosome contains a range of proteins and cofactors to do two easy transesterification reactions is control. The cell requires both spatial and temporal control over splicing; different splice sites are activated and deactivated in different cells and at different times during development. Splicing at the correct splice site is necessary to provide the correct protein after translation. The non-catalytic parts of the spliceosome are believed to be

involved in the control of splicing, making sure that correct splice sites are spliced at appropriate times in the right cells.[4]

Splicing at the correct site can be problematic. Exons are relatively short, only 150 nucleotides on average, compared to introns that are believed to have an average chain length of 3000 nucleotides. It has been estimated that 90% of the average pre-mRNA is made up of introns and hence removed in the splicing process. The splicing machinery is very good at selectively removing the introns. It does so by marking the splice sites with several different markers to ensure correct splicing and then double checking the mature mRNA several times over.[4]

First of all, there are specific sequences in the introns marking the splice sites. There are conserved sequences that mark both the start and the end of introns, GU and AG sequences respectively. There is also a conserved sequence at the branch point of the intron, where the lariat is joined up, that always contains an adenine. The end and beginning of the pre-mRNA are protected by a 5'cap, a modified guanine amino acid, and a polyadenyline tail to prevent the pre-mRNA from being degraded. These stay on during splicing, thus enhancing translation by also ensuring the stability of the mature mRNA.[1]

There is also a serine/arginine rich protein family, called SR proteins, these molecules bind to the pre-mRNA controlling the splice site along with marker proteins deposited by the RNA polymerase during transcription. Splicing is also controlled by post-translational modifications, such as phosphorylation, methylation or ubiquitination, of proteins taking part in splicing.[4] Lastly there are intronic and exonic splicing enhancers and silencers providing more subtle control over splicing for the cell.

The spliceosome is a dynamic assembly and hence assembles and disassembles every time a mature RNA is produced (*figure 3*). The snRNPs (small nuclear ribonucleo proteins), U1, U2, U4, U5 and U6, associate with the pre-mRNA in a specific order also. First, the early (E) complex is formed; this step is not ATP-dependent. The spliceosome is committed to splicing after the formation of the E complex. U2 then associates with the E complex in an ATP-dependent step forming the A complex. Further association with U4, U5 and U6 produces the B complex that then undergoes structural changes to form the mature

spliceosome, complex C. During the rearrangement U1 and U4 are expelled from the structure. The two transesterification reactions then occur, which are believed to be catalysed by an active site formed by U2 and U6. After the transesterification reactions the complex disassembles and the mRNA is released.[5]

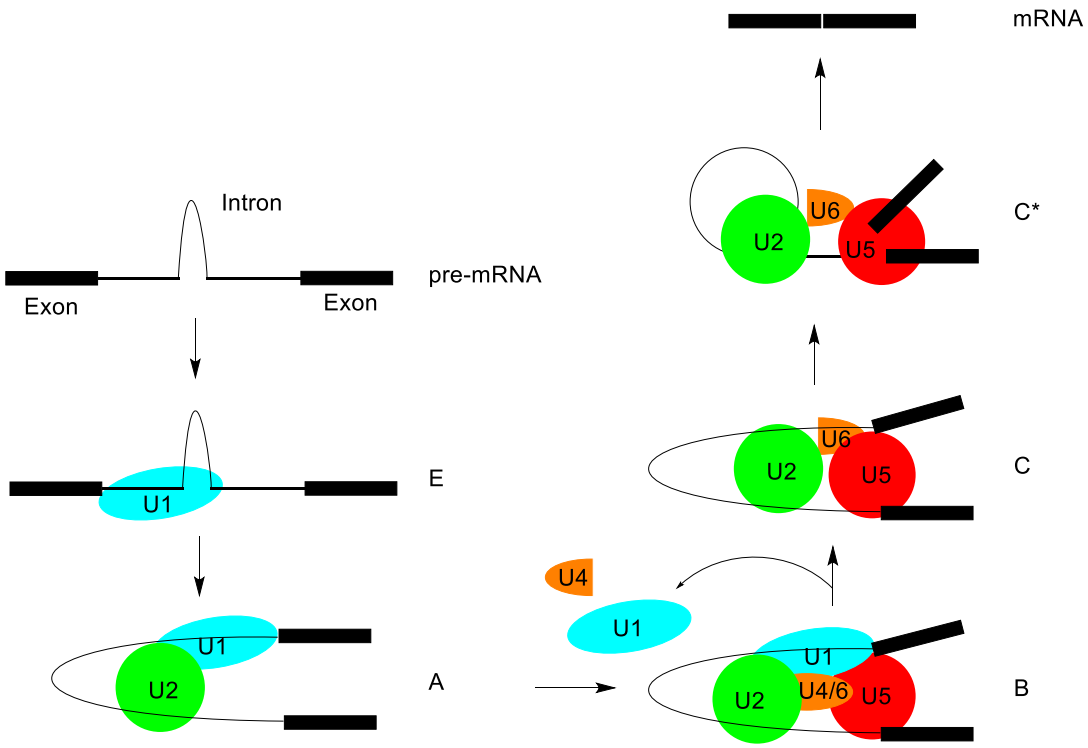

Figure 3 Core Spliceosome
The snRNPs (U1, U2, U4-6 represented by coloured shapes) assemble on the pre-mRNA (exons represented by black rectangles, intron by black line) in a specific order. Each assembly is known as a splicing complex (labelled on the right hand side of the complex).

1.1.2 Alternative splicing

One of the surprising discoveries made after the human genome project was completed was the realisation of how small our genome actually is. The human proteome is 10-100 times bigger than the number of genes actually coding for it.[2] Splicing offers eukaryotes a remarkable advantage; it allows for a much more complex proteasome than the genome would suggest (*figure 4*). This is because genes can be spliced in different ways. In humans up to 95% of all the multi-exon genes undergo alternative splicing.[1] This can be done by various different mechanisms that all result in the ability of the cell to create many variants of proteins depending on spatial and temporal requirements.[2, 3, 6]

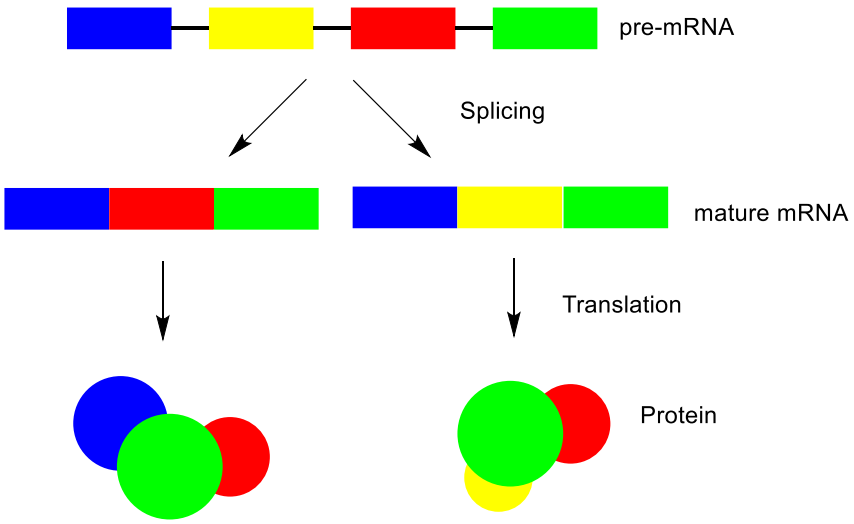

Figure 4 Alternative splicing
Pre-mRNA (composed of exons (coloured rectangles) and introns (black lines) can be spliced to form different mRNA (coloured rectangles) that is then translated into different proteins (coloured circles) by, for example leaving out the yellow exon in one mRNA and the red exon in the other mRNA.

This means that one gene contains the potential for making multiple variants of the same protein depending on how it is spliced. A very good example of this is the gene for the potassium channel KCNMA1 in the human body that has 13 exons and hence more than a 1000 potential protein variants that could be produced by alternative splicing. Of course, not all of these variants are actually produced only 6-7 splice sites are utilised to produce the different variants of the channel.[7]

Several different alternative splicing strategies exist. Exon skipping is believed to be the most common and intron retention the rarest alternative splicing event. Alternative splice sites are believed to be more common than mutually exclusive exons which make up only about 13% of these events (*figure 5*). It is also rather common to skip two exons in a row, but less common to see three exons skipped. These observations have been explained by proposing an inverted relationship to the complexity of the event, so more complex splicing events occur less frequently.[8]

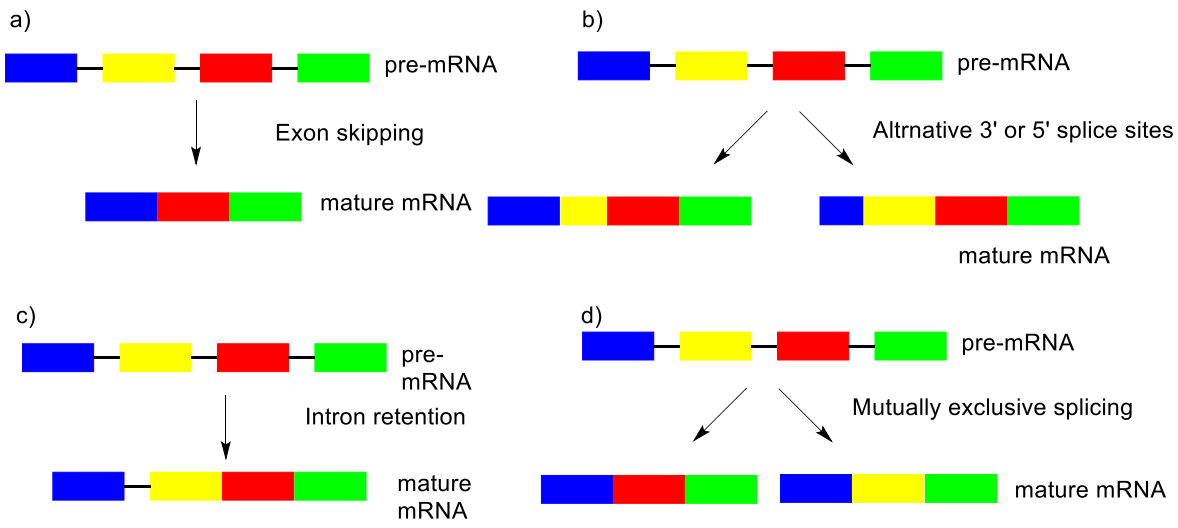

Figure 5 Alternative splicing types
Figure *a)* represents exon skipping, *b)* represents alternative 3' or 5' splice sites that produce exons of different lengths (yellow exon), *c)* represents intron retention where intron (black line is present in the mature mRNA and *d)* represents mutual exclusive exons where either the yellow exon is included or the red exon but not both in the mature mRNA.

The alternatively spliced protein variants can have slightly different functions, as in the different potassium channels in the body. They can also have completely opposing functions. For example several genes, such as BCL-X and MCL1, code for both pro- and anti-apoptotic variants. The outcome, and the fate of the cell, depends on splicing.[6]

Alternative splicing is regulated at many different levels, such as splicing enhancers and silencers located within the pre-mRNA itself. It can also be regulated by histone modification on the DNA level. Transcription rate of splicing factors has an effect on splicing control, as do post-translational modifications of splicing factors such as phosphorylation, methylation and ubiquitination.[9] More evidence has accumulated in recent years to confirm the epigenetic control over the availability of various splicing factors. This in turn has an effect on alternative splicing. This suggests that the splicing is very much controlled by the cell itself as well as environmental factors and cellular signalling.[3]

1.1.3 Importance of accuracy

Faults in the splicing mechanism are important to human disease. It is estimated that as much as 50% of all point mutations causing genetic diseases affect splicing sites and are not in the mRNA that goes on to be translated into the protein.[10] A mutation can affect the splicing in several ways. One possibility is

that the mutation moves the splice site further to the 3' or 5' end potentially including extra useless amino acids or cutting out nucleotides that should have coded for amino acids in the protein. These added nucleotides can also lead to shifted reading frames that can cause further problems. An example of this includes familial dysautonomia, in this disease a point mutation of a T to G moves the normal splice site and leads to exon skipping. The exon skipping results in a shifted reading frame for translation, containing a premature stop codon resulting in a truncated, useless protein.[10]

Splicing is also important in cancer development. Very different splice variants are often found in cancer cells.[10] This can be due to a mutation that directly affects an oncogene or a tumour repressor gene, like in the case of receptor tyrosine kinase gain-of-function mutations that have been found in multiple gastrointestinal stromal tumours. The mutation affects splicing creating an alternatively spliced receptor that has a constitutively active conformation, which contributes to tumour development.[10]

However, in many cancers there are no underlying mutations and the splicing is controlled by splicing modulators in the cell. For example, in some lineages of thyroid, small intestine, kidney and lung cancer, the SR proteins regulating splicing are over-expressed leading to modified cellular activity. It is, as of yet, unclear whether the change in splicing regulators is the cause of the cancer or whether it is the already cancerous cells that change the splicing modulators to benefit the cancer, although some splicing factors have been shown to be oncogenes. Overexpressed they lead to the development of cancer.[10]

It should also be mentioned that viruses use the human splicing machinery when replicating in human cells as they do not have their own cellular machinery and replicate using the host cells resources. In fact, studies in viruses have sometimes illuminated our understanding of gene regulation. Hence, it was the study of adenoviruses that first led to the discovery of the exon-intron architecture of our genes.[11, 12] Viruses have evolved control mechanisms over alternative splicing as well, the influenza virus for example uses the same pre-mRNA sequence to make both a matrix protein, important structurally, and an ion channel by utilising alternative splicing. Further studies into the relationship between viruses and the eukaryotic spliceosome might yield more insights into

the spliceosome's mechanism of action. It might even lead to new drug targets that could be utilised for making small molecule antivirals. This might overcome the problem that there is a shortage of general antiviral drugs that are effective against more than one virus strain.[13]

There has been research into correcting genetic mutation that affect splicing and cause disease. The two approaches most widely studied are the use of small molecules and antisense oligonucleotides.[10] Since many of the splicing events are modulated by post-translational modifications of proteins such as phosphorylation or methylation, small molecules that affect these modifications can have a large effect on splicing also. For example GSK3 is a kinase that phosphorylates SR proteins that regulate splicing. Inhibiting GSK3 can affect splicing. Unfortunately, kinases such as GSK3 phosphorylate multiple SR proteins and so the inhibition of them will most likely have several unwanted and unpredictable side effects.[14]

Using antisense oligonucleotides can be a much more specific way to target alternative splicing, because direct base-pairing of nucleotide sequences can be used to direct the bonding. These short antisense sequences, or AONs, can be prepared to exactly match the RNA desired, hence minimising side-effects.[10] Since there is a lot of RNA in the splicesomal assembly the AONs can be used in different approaches, for example, AONs binding directly to splice sites can correct the reading frame affected by mutation.[10] Clinical trials have been completed for intravenous administration of an AON doing precisely this to treat Duchenne's muscular dystrophy. Even though the dystrophyn protein produced with this treatment is not complete, as the exon skipping induced by the mutation is not corrected, it is partially functioning because of the corrected reading frame and hence eases the symptoms experienced by the sufferers.[15, 16]

1.1.4 Studying the spliceosome

Better understanding of the spliceosome and its associated proteins could facilitate better treatments of diseases resulting from mutations affecting splicing as well as the various cancers associated with changes of splicing. Historically, research on the spliceosome mainly used mass spectroscopic methods to identify components of the spliceosome.[4] It was very difficult to

imagine how the different complexes worked together as a lot of structural changes are believed to take place during splicing itself.

Recent improvements in the cryo electron microscopy techniques has allowed the scientific community to take a closer look at the protein and RNA structures involved in the splicing apparatus. In fact, over the last several years there has been a "quantum leap" in our mechanistic understanding of the spliceosome.[17] There now exist atomic detail images of the activated B complex, C and C* complexes. This gives us an unprecedented understanding of the core spliceosome and the various ways the splicing factors interact with each other.[5] However, it does not tell us how splicing is regulated in cells.

Small molecules that interact specifically and selectively with the spliceosome, splice-modulators, have also facilitated the mechanistic study of the spliceosome. The most well studied group of splicing-modulators is believed to interact with the SF3b multiprotein component on the U2 snRNP.[18] This group includes polyketides that can be categorised into three distinct families based on natural products, examples of these three groups can be seem in *figure 6*: pladienolide D **1** is an example of the 12-membered macrolides, herboxidine **2** is shown here as an example of the family of pyran containing SF3b inhibitors and spliceostatin A **3** is an aptly named representative of the di-pyran polyketide splicing inhibitors.

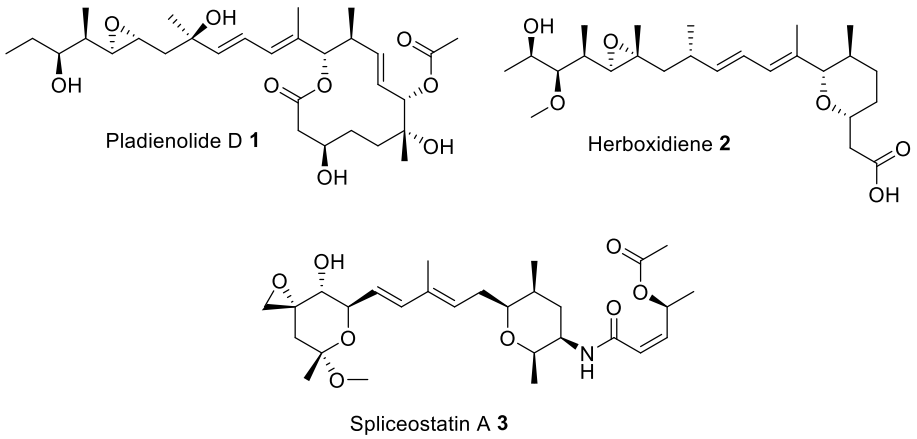

Figure 6 Splicing inhibitors

There have been several clinical studies on polyketides targeting SF3b, most of them based on the 12-membered macrolide structure and targeting cancers.

E7107 **4** (*figure 7*) showed great potential against solid tumours, however failed phase 1 clinical trials due to toxicity. 6-Deoxypladienolide D **5** has shown promise against acute myeloid leukaemia and is in phase 1 clinical trials.[18] Most likely these will not be the only SF3b targeting drug candidates for long, as synthetic versions of this class of natural products are being explored all the time.

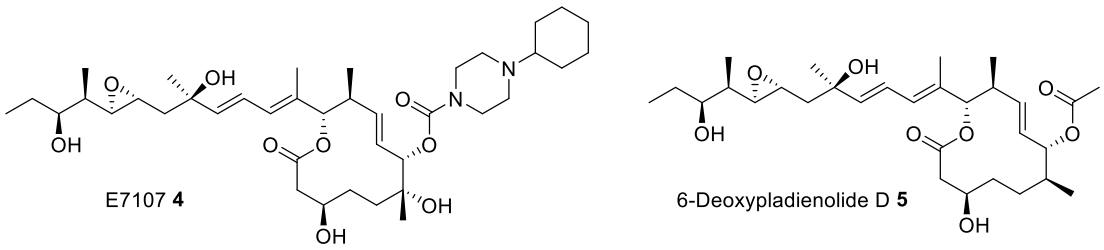

Figure 7 Splicing inhibitor drug candidates

Other small molecule splicing modulators include leucettine **6**, a naturally occurring kinase inhibitor (*figure 8*). The effect of leucettine **6** on the spliceosome is due to the regulatory effect of its target kinase on the spliceosome resulting in alternative splicing patterns.[19] Another example is isoginkgetin **7**, a biflavone known to stall the spliceosome and hence stop splicing from taking place.[20]

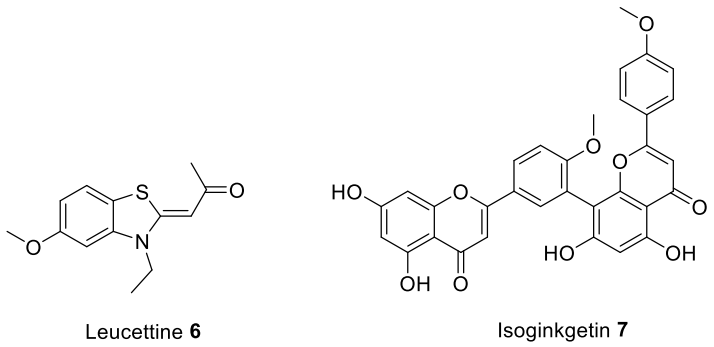

Figure 8 Splicing inhibitors

Other small molecule probes that can modulate alternative splicing or arrest the spliceosome assembly at a specific complex would be useful for the study of this complex and interesting molecular machine.

1.2 Hinokiflavone

Hinokiflavone **9** was first isolated in 1958 from *Coniferae* along with other biflavonoids ginkegetin and sciadopitysin.[21] The structure of hinokiflavone **9** (*figure 9*) was later proposed by Fukui and Kawano[22] and the proposed compound **8** synthesised by Nakazawa in 1967.[23, 24] The structure first proposed turned out to be wrong when the synthesised material **8** was compared to the natural product **9** by IR, melting point and micro analysis (*figure 9*). The structure was therefore revised and the new, now correct compound **9** synthesised by Nakazawa.[23, 24] This synthesis (see section 2.2.3), however does not report a final yield for the hinokiflavone **9** formed so we can assume that this synthesis did not yield a quantifiable amount of product. In 1987 the first NMR study of hinokiflavone **9** was published, which confirmed the structure proposed by Nakazawa by analysing isolated hinokiflavone **9**.[25]

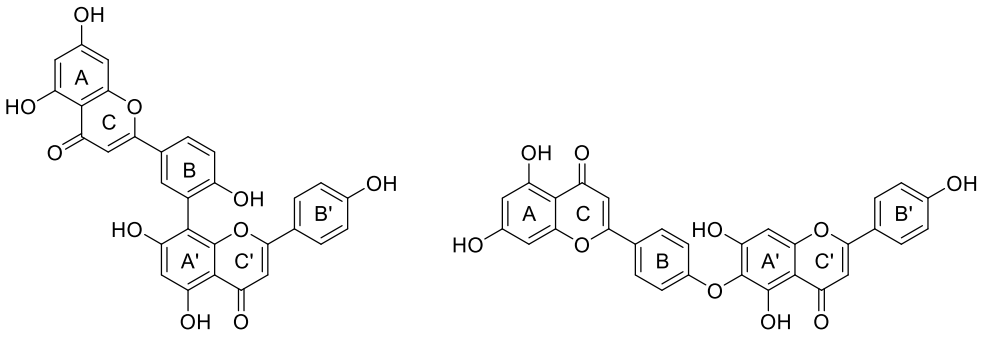

Original, incorrect structure **8** Structure of Hinokiflavone **9**

Figure 9 Hinokiflavone

Since the original synthesis efforts, no more synthetic approaches towards hinokiflavone **9** have been published, however numerous isolation protocols and patents for the isolation of hinokiflavone **9** have appeared in the literature. Hinokiflavone **9** can be isolated from a multitude of plants, most of them found in Japan or far east Asia, such as the oriental Thuja, the Japanese Wax tree and the Japanese Cyprous. [26-28]

The interest in isolating hinokiflavone **9** is justified by the amount of research into various biological activities of hinokiflavone **9**. It is now used in routine screening with other flavones against viral strains and cancer cell lines.[17] There have been several recent patents released for using hinokiflavone **9** in

formulations designed to treat diabetes [29] and gastrointestinal motility issues [30] among others. In depth computer aided studies have been undertaken to demonstrate its activity as a matrix metalloproteinase-9 inhibitor, active in inflammation and cancer [31] and it has been investigated as a BACE-1 inhibitor to tackle Alzheimer's disease.[32]

1.2.1 Hinokiflavone as a spliceosome inhibitor

After isoginkgetin was identified as a splicing inhibitor by high throughput screening in 2008[20] Professor Angus Lamond and colleagues investigated if other biflavones also showed splice-modulating activity. Hinokiflavone **9**, amentoflavone **10** and sciadoptysin (*figure 10*) were found to stall the spliceosome assembly *in vitro*.

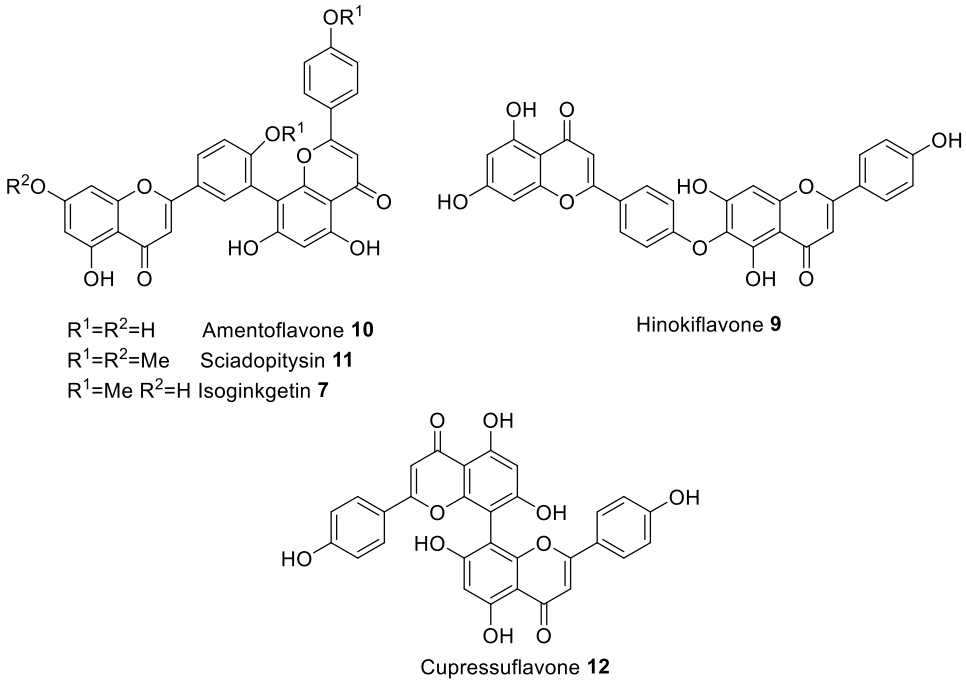

Figure 10 Biflavones tested by Lamond *et al*.

The biflavones (500 μM) were screened for effects on splicing by subjecting pre-mRNA to either DMSO or biflavones in the presence of HeLa nuclear extract. Model pre-mRNAs used were Ad1 and HPV18 E6/7. The nuclear extract was then analysed using on-gel separation techniques. Hinokiflavone **9** and amentoflavone **10** had a more marked effect than isoginkgetin **7**, a known splicing inhibitor, in that only the non-spliced RNA can be seen in the gel and none of the spliced, shorter isoform. In the cases of isoginkgetin **7** and sciadoptysin **11** small amounts

of spliced RNA could be seen. No splicing inhibition was observed with cupressuflavone **12** (*figure 11*).

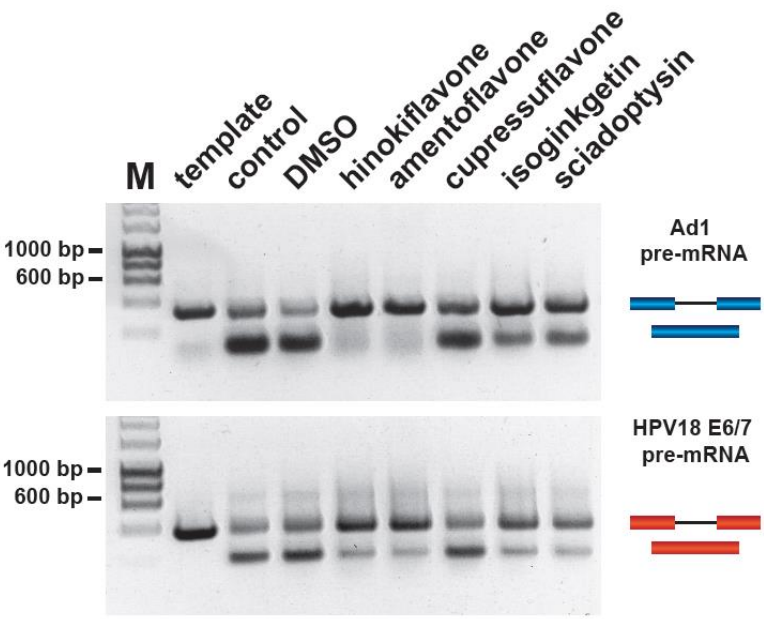

Figure 11 – *In vitro* splicing assay
Pre-mRNA, 30% HeLa nuclear extract and compound/DMSO incubated for 30 min at 90 ºC. RNA amplified by RT-CPR then separated on 1% agarose gel with SYBR safe DNA gel stain. Intron retention in Ad1 and HPV18E6/7 as a result of treatment with 500 µM of compound/DMSO.

In cellulo studies were then carried out for these same biflavones **7**, **9-12**. Only hinokiflavone **9** and isoginkgetin **7** affected splicing in cells. Hence efforts were concentrated on testing hinokiflavone **9**.

More in depth studies on the effect of hinokiflavone **9** on the splicing of endogenous pre-mRNA were then carried out. Hinokiflavone **9** does not stall slicing completely, but changes alternative splicing. Hinokiflavone **9** was tested in three human cell lines (*figure 12*). Cells were then harvested and analysed for alternative splicing on various example pre-mRNAs. Two examples illustrating alternative splicing by exon skipping shown here are MCL1 and FAS. Hsp40 and RIOK3 demonstrate intron inclusion after the addition of hinokiflavone **9**. Here, the cell type to produce the most marked change in splicing was the NB4 cells. It is interesting to note that hinokiflavone **9** induced different alternative splicing events depending on the cell type and the pre-mRNA being spliced.

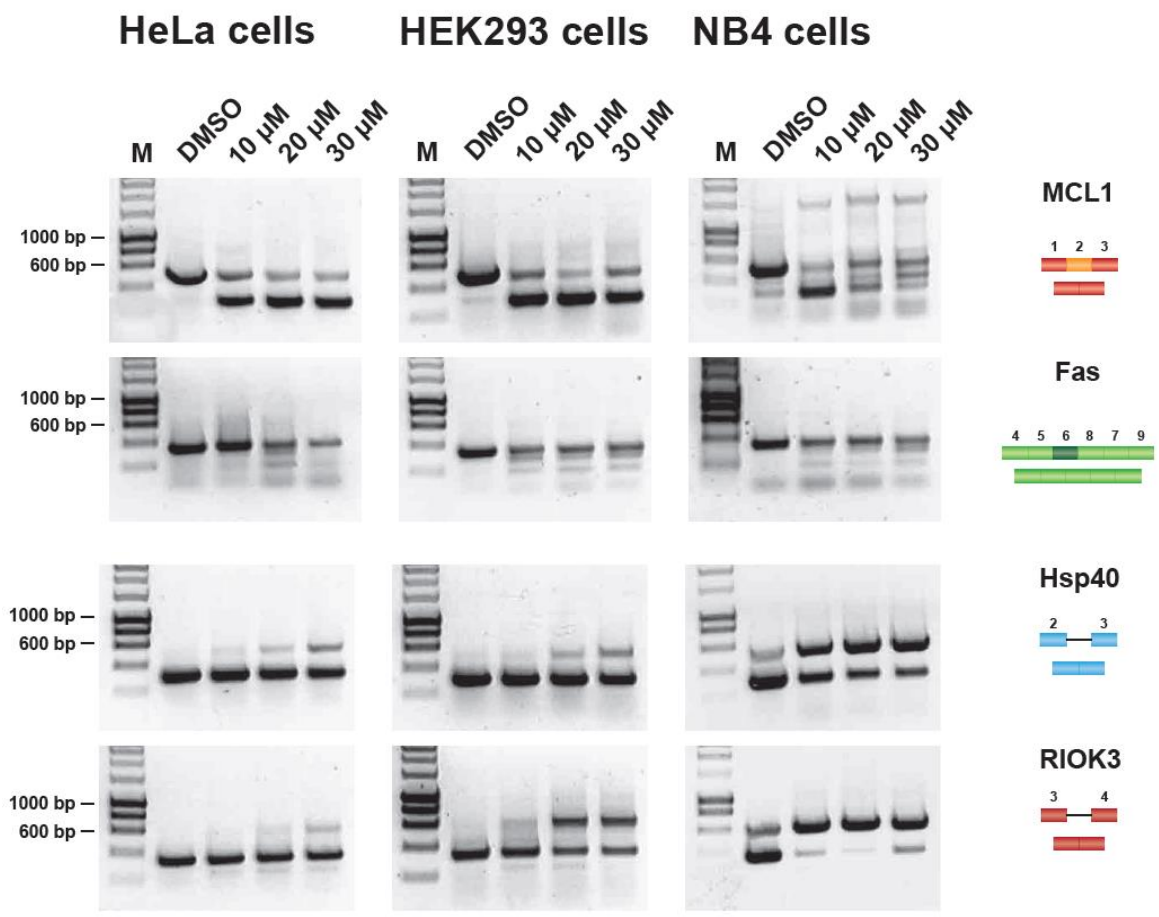

Figure 12 – Changes in alternative splicing in cells
HeLa, HEK293 and NB4 cells treated with compound/DMSO incubated 24 h. total RNA was extracted, reverse transcribed then amplified by semi quantitative RT-PCR using primers specific to sequences examined. Separated on 1% agarose gel with SYBR safe DNA gel stain.

The Lamond group then focused on understanding exactly how hinokiflavone **9** was affecting the splicing process and where in the splicing cycle it was having its effect. For this the formed splicing complexes were monitored for their relative abundance on a native gel (*figure 13*).

When experiments were done to actually look at the spliceosomal complexes, the reason for hinokiflavone **9** modulating splicing became clear. Only H/E complex and A complex were formed in the presence of hinokiflavone **9** (*figure 13*). Neither of the later complexes B or C are visible in the gel. Splicing is stalled at complex A and cannot proceed.

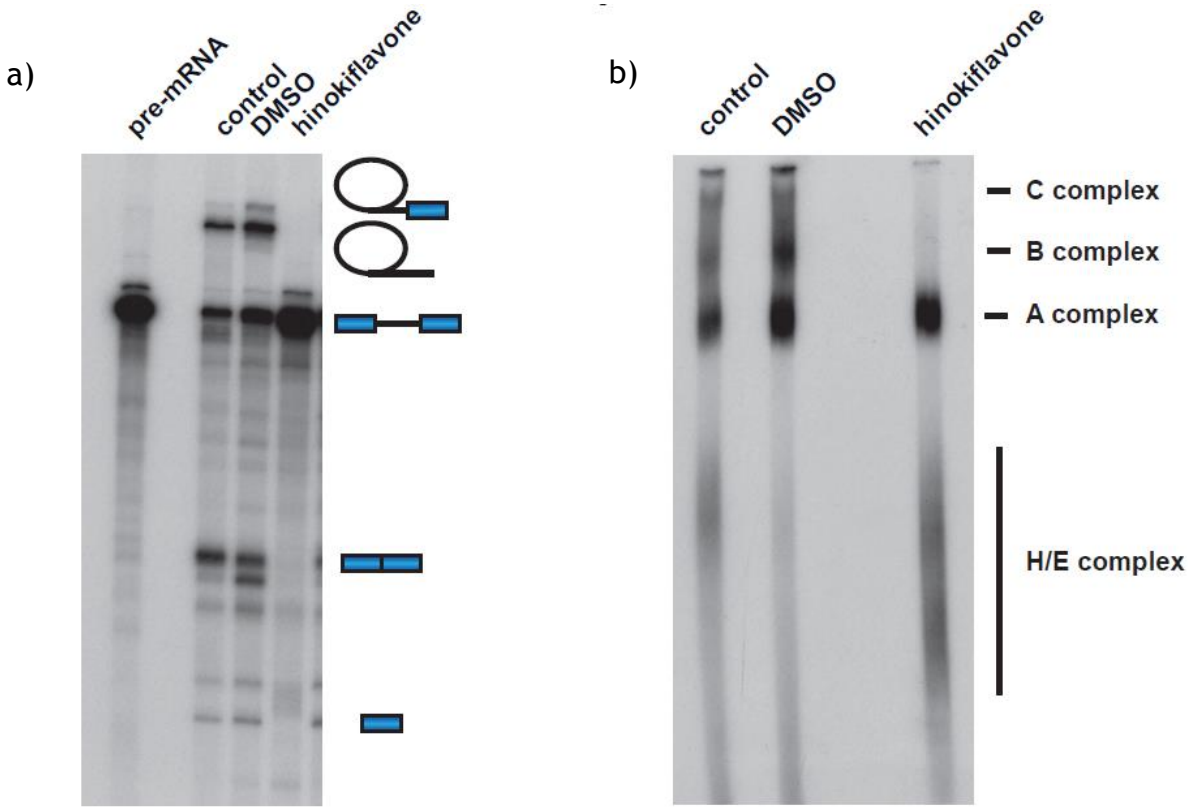

Figure 13-Hinokiflavone stalls the splicceosome at the A complex formation
^{32}P labelled Ad1 pre-mRNA, 30% HeLa nuclear extract and hinokiflavone/DMSO incubated for 30 min at 90 ºC. Analysed on native agarose gel, visualized using phosphor imaging. Figure 13a) shows various splicing products (pre-mRNA, mRNA, lariat intermediate and lariat product). Figure 13b) shows separated splicing complexes.

To further study the effect of hinokiflavone **9** on cells, HeLa cells were incubated with 20 μM hinokiflavone **9** for 24 hours (*figure 14*). After that various spliceosomal proteins (splicing factors) were stained with specific antibodies so they could be visualised by fluorescence microscopy. SC35, U1A, DDX46, U2AF65, SART1 and SR-proteins are present in the E and A complexes or promote the formation of these complexes, they are also all relocalised in megaspeckles when the cells are treated with hinokiflavone **9**.

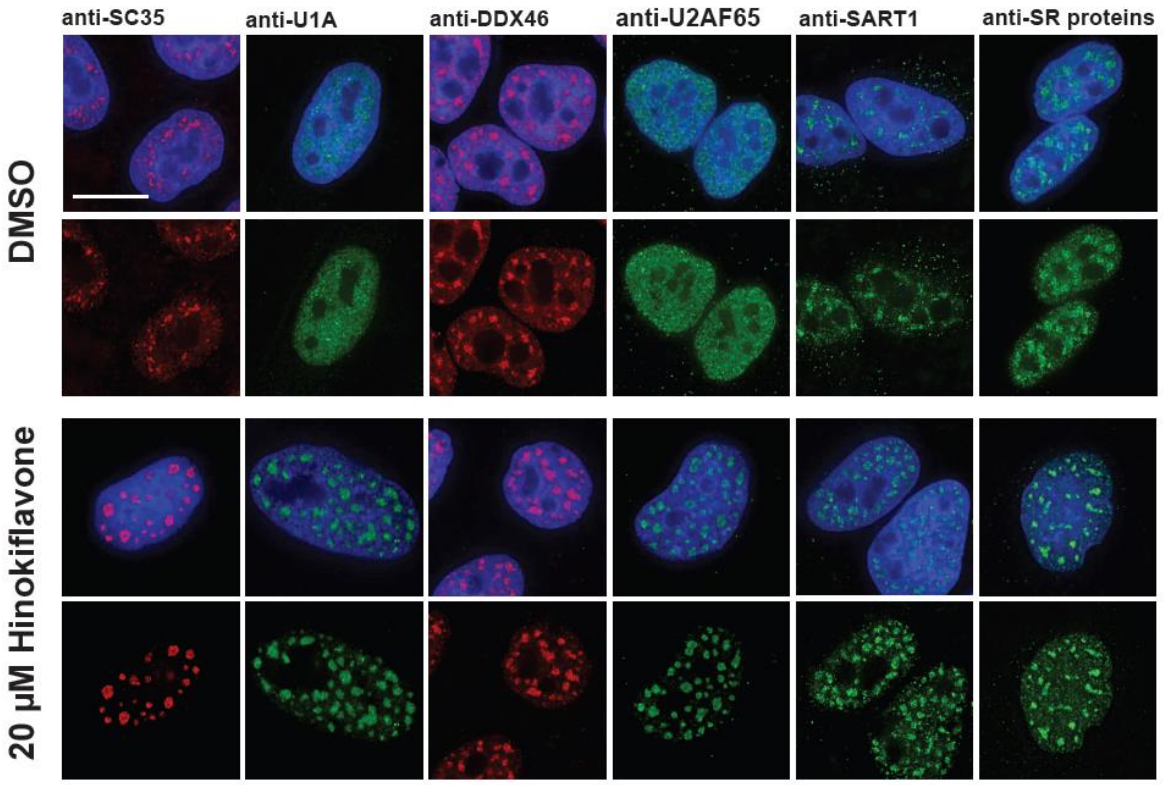

Figure 14 - Immunofluorescence assay
HeLa cells incubated with 20µM hinokiflavone/DMSO for 24 h. The cells were then fixed with 4% paraformaldehyde, permeabilised with 0.5% Triton X100 and incubated with the primary antibodies, 1 hour at RT, then incubated with the secondary dye-conjugated antibodies. Visualised with fluorescence microscope (cells stained with DAPI (blue) to show DNA and nucleus).

SC35 is the best studied of the SR-proteins (serine-arginine proteins). SC35 binds to the pre-mRNA as it is being transcribed and acts as a splice site indicator and splicing stimulator by encouraging the binding of U1 to the pre-mRNA. The other SR-proteins have similar roles, acting as splicing promotors. Staining for SC35 protein and the other SR proteins in the DMSO control are located in splicing speckles but in the hinokiflavone **9** treated cells these proteins are localised in the circular megaspeckles.

U1 A is one of the proteins associated with the U1 snRNA to form the U1 snRNP. The U1 snRNP is the first snRNP to associate with the pre-mRNA during splicing, forming the E complex, and then stays associated to the pre-mRNA through the A and B complexes. It is therefore not surprising to see that U1 A protein also accumulate in the megaspeckles after the addition of hinokiflavone **9**.

DDX46 protein is a component of the U2 snRNP while U2AF65 helps the U2 associate with the pre-mRNA. U2 associates with the pre-mRNA to form the A

complex. U2 snRNP stays attached to the pre-mRNA until the end of the splicing process. Both proteins can be found in the megaspeckles formed due to hinokiflavone **9**.

The same experiment was carried out in HeLa cells incubated with 20 μM of hinokiflavone **9** for 24 hours, this time staining for late stage spliceosomal complex associated proteins (*figure 15*). None of the splicing factors associated with spliceosomal complexes B, C and C* relocate to the megaspeckles. Instead, these late stage associated splicing factors were as dispersed in the nucleus as they had been in the DMSO control.

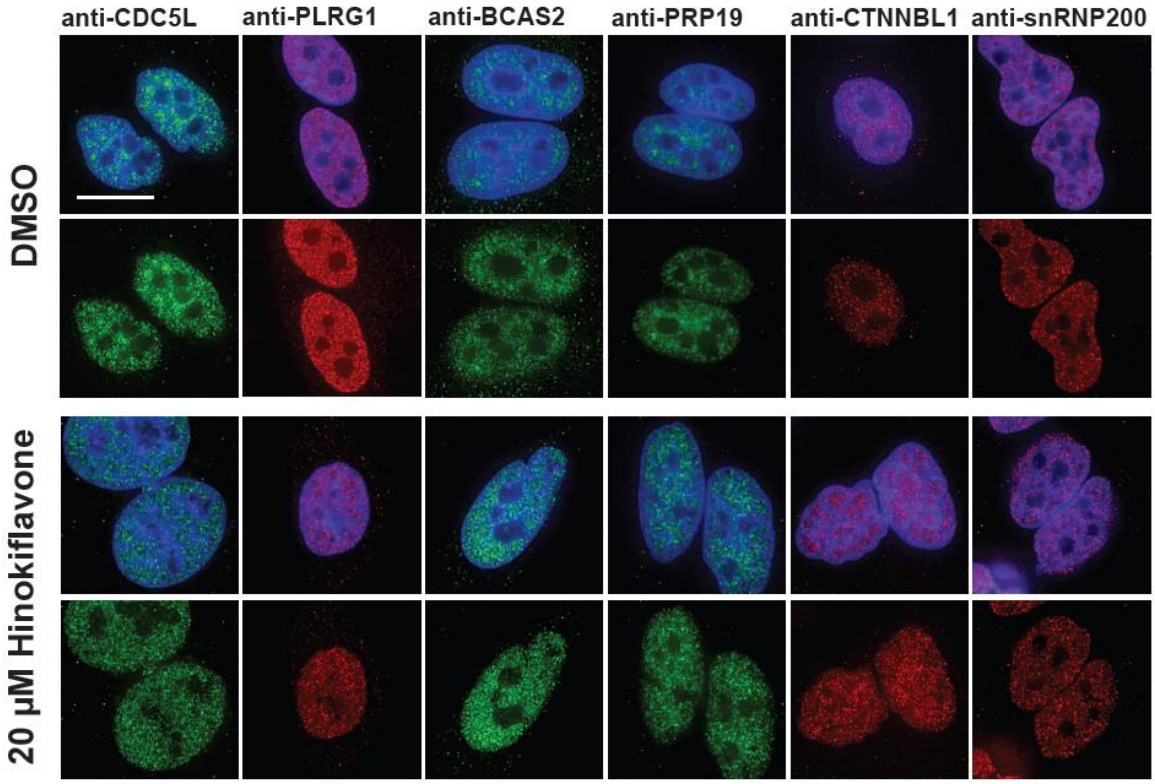

Figure 15 - Immunofluorescence assay
HeLa cells incubated with 20μM hinokiflavone/DMSO for 24 h. The cells then fixed with 4% paraformaldehyde, permeabilised with 0.5% Triton X100 and incubated with the primary antibodies, 1 hour at RT, then secondary dye-conjugated antibodies. Visualised with fluorescence microscope (cells stained with DAPI (blue) to show DNA and nucleus).

PRP19 protein is part of the PRP19 protein complex. It associates with the spliceosome after the release of U1, in the C complex and is present throughout the two transesterification steps. It does not accumulate in the megaspeckles as it is associated with the late spliceosomal activity.

snRNP200 is a subunit of the U5 snRNP and hence associates with the pre-mRNA to form the B complex. As can be seen from *figure 15* it also does not accumulate in the megaspeckles observed in the hinokiflavone **26** treated cells.

To study the effect of hinokiflavone on pre-mRNA splicing, it was important to be able to make synthetic hinokiflavone **9**. A synthetic route to hinokiflavone **9** would also be necessary if further studies were to use larger amounts of the natural product than was commercially available. This was likely to happen if animal studies were to be undertaken. As hinokiflavone **9** was exhibiting such interesting biological activity this was not at all unlikely.

2 Flavonoids

Since hinokiflavone **9** is a biflavone, a closer look into the structure, reactivity and strategies to synthesise flavones will be examined (*figure 16*). Flavones are a subgroup of compounds belonging in the flavonoid family of natural products.[33] All flavanoids are biosynthesised from chalcones **13** in plants and take their ring labels from chalcones **13**.[34] Flavones **14** have the general structure shown in *figure 16,* which is comprised of a chromone **16** ring system with aromatic ring attached at the 2 position. Flavonols **15** are a very important subset of flavones **14** with a hydroxyl substituent at the C-3 position. Even though flavones include flavonols, usually when talking of flavones we tend to talk of compounds that are unsubstituted on the C-3 position and use the name flavonols for the C-3 substituted flavones. There are several other families of flavonoids such as flavans **17** that do not have any oxygens attached at the C-3 and C-4 positions, flavanones **18** that are flavans **17** with the carbonyl in the C-4 position and dihydroflavones **19** that are flavanones **18** with a C-3 hydroxyl substituent. Isoflavones **20** differ in the position of the B ring on the chromone substructure. The flavonoids are the most abundant class of secondary metabolites mainly found in land plants with over 3000 compounds known.[35] These differ from each other by the presence of additional functionalisation, mainly by the presence of additional hydroxyl groups on carbons C-5, C-6, C-7, C-8, C-2', C-3' etc. Methoxy substitution and or sugar moieties are also common.[34]

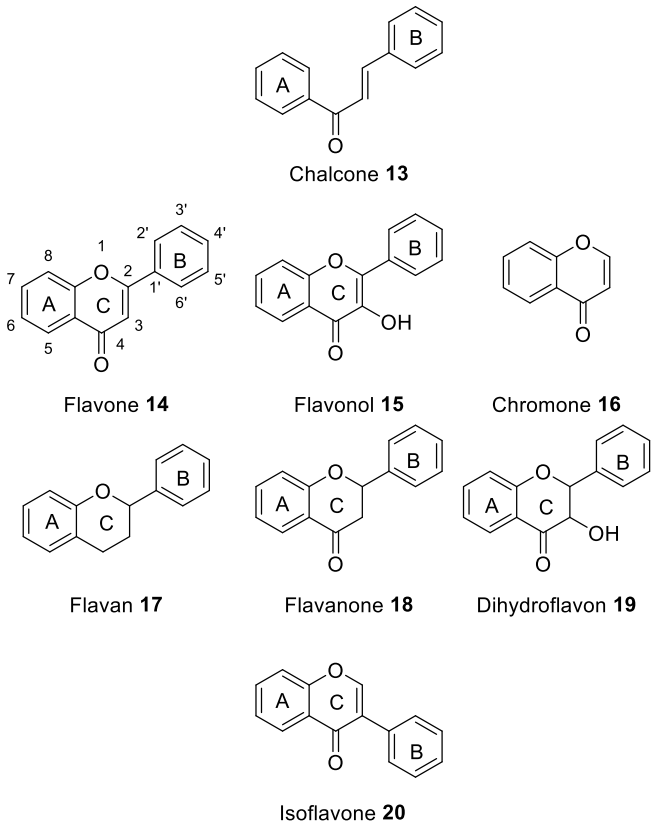

Figure 16 Chalcones, flavonoids, isoflavonoids and chromones

Flavones **14** are one of the major classes of flavonoids. Flavones **14** are ubiquitous in our diets as they can be found in most fruit and vegetables. The daily flavanoid intake for a European adult is estimated to be about 20 mg/day.[35] Flavones **14** have also been found to be a highly biologically active natural product family. Many of them have anticancer, anti-inflammatory and antioxidant properties.[36] Different flavonoids, such as quercetin, are available as food supplements and some have been tested in clinical studies.[35, 37-39]

The structural features of flavones **14** have a profound effect on their physical properties. Flavones **14** have an extensive aromatic system that makes these molecules prefer π-stacking (*figure 17)*.[36] They also tend to have several hydroxyl groups on the A and B rings that together with the ketone of the C ring facilitates extensive hydrogen bonding. As a consequence of both the π-stacking and H-bonding encouraging intermolecular bonding, flavones tend to be poorly soluble in almost all solvents.

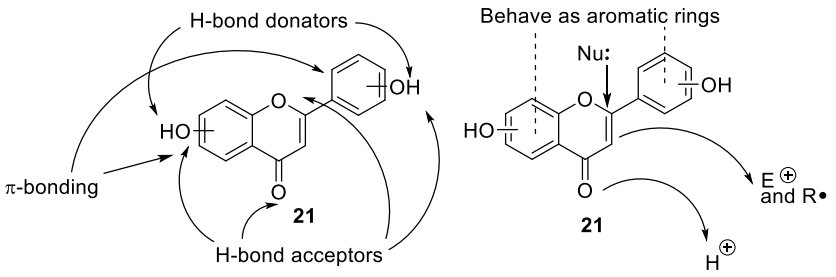

Figure 17 Flavone reactivity

Reactivity of flavones **21** depends on their substitution pattern as well as their general structure. The A and B rings typically behave like aromatic rings, undergoing substitution reactions. If they have hydroxyl functionalisation, the A and B rings behave as phenols (*figure 17)*.[40] The ketone of the flavone behaves differently from other ketones due to the extensive conjugation, for example it does not react with hydroxylamine to form oximes. The C ring can open under basic conditions to form the 1,3-diketone, undergoing retro-Baker-Venkataraman reaction (see *scheme 11*).[40] It is also possible to selectively alkylate the C3 position by using radical chemistry.[41] Flavones **21** are known to react with radicals in nature, but so far few synthetic reports of radical flavonoid chemistry have been recorded.[41]

The phenolic hydroxyl groups on the A and B rings also have different reactivities (*figure 18*). The most notable difference is the hydroxyl group on C5, it is hydrogen bonded to the carbonyl group and hence much harder to deprotonate and alkylate than the other phenols.[42, 43] It should be mentioned that any particular flavone will not have hydroxyl substituents on all the available positions, but only a small collection of them, 5-hydroxy- and 7-hydroxy-flavones being some of the common modifications to the core. The rates of de-acetylation in peracetylated flavones follow this order: 7 > 4' > 3 > 5 > 3'. This indicates that the 7-position is the most stable phenoxide, followed by 4' etc.[42] The reactivity differences are varied by substituents other than hydroxyl groups. These differences in reactivity are slight, however, and hard to take advantage of, hence the use of protecting groups is common if any position is to be selectively alkylated.[43]

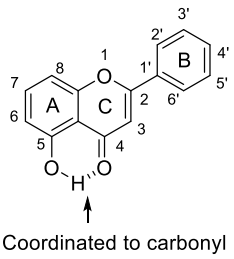

Figure 18 Flavone reactivity

2.1 Synthesis of Flavones

There exist a multitude of different approaches for the synthesis of flavones **14**. Since these are an abundant class of natural products with continually emerging new bioactivities, flavones **14** are constantly investigated as leads for new drugs and as such new synthetic routes emerge every year.[44-47] The most widely and often used synthetic approaches are those that were first described in the early twentieth century, but several catalytic and novel approaches have been described recently as well.[36]

The synthetic approaches towards flavones **22** can be broken into three broad categories, illustrated by the retrosynthesis in *scheme 1*. The cyclic ether can be formed by the oxidative cyclisation of a chalcone **23** (disconnection a). Alternatively, the same bond can be formed by the intramolecular addition of the phenolic hydroxyl to an alkyne in which case the synthesis would proceed though alkyne **24**. In each case, it is the C ring that is formed last. Flavones can also be made by the rearrangement of aromatic esters **25** (disconnection b) and this is one of the most common synthetic routes to flavones with a number of named reactions having this common disconnection. The B ring **27** can also be attached to a chromone **26** by the formation of an sp^2–sp^2 carbon–carbon bond (see disconnection c). All of these approaches are discussed in more detail below.

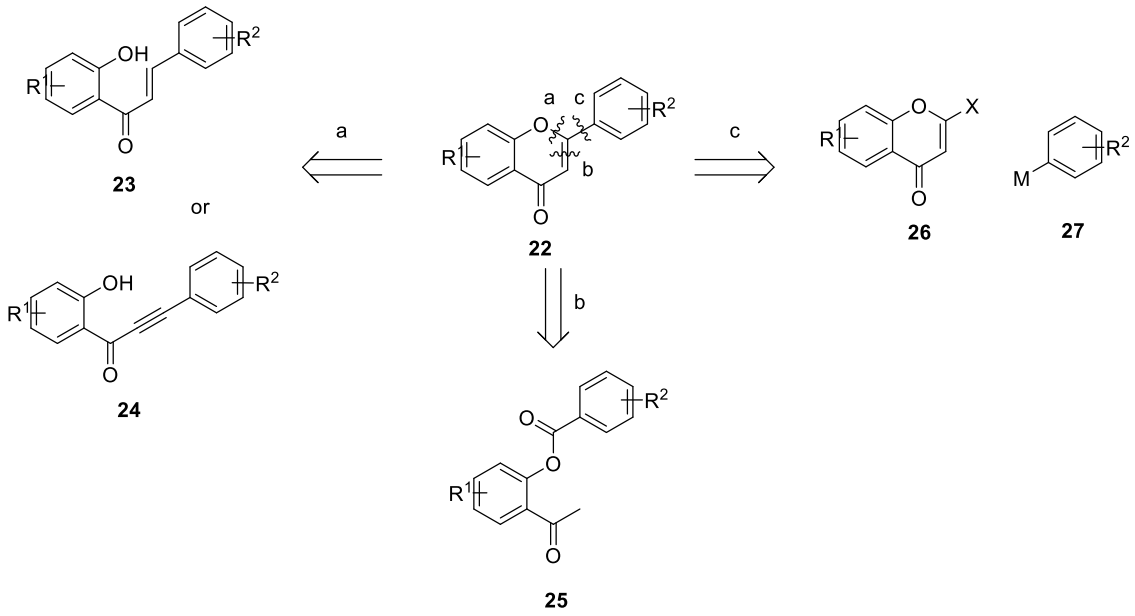

Scheme 1 Flavone retrosynthesis

2.1.1 Synthesis *via* chalcones

A common way to make flavones **22** is to make the corresponding chalcone **23**, (disconnection a in *scheme 1*) mimicking the biosynthetic pathway (retrosynthesis shown in *scheme 2*).[36] Chalcones **23**, in turn, can be made by the Claisen-Smith condensation of a 2-hydroxyacetophenone **28** and a benzaldehyde derivative **29**. This method of making flavones is well established, and there are several other methods based on modified Claisen rearrangement.[36]

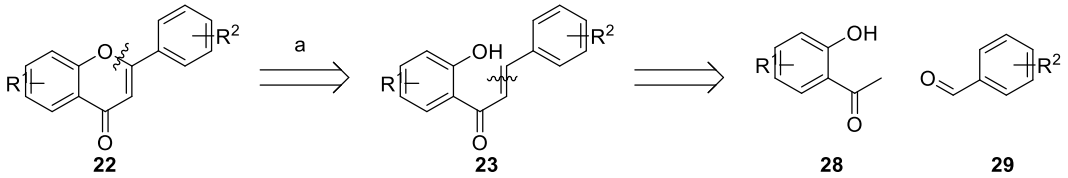

Scheme 2

The ring closing-dehydrogenation steps are usually catalysed by either Br_2 or I_2 in the presence of an oxidant such as DMSO although SeO_2 or other halogen containing reagents have also been used.[36] The proposed mechanism is shown in *scheme 3*. The reaction mechanism is believed to proceed though iodination of the double bond to give iodinium ion **30** that then promotes the intramolecular attack by the phenolic hydroxyl to close the six-membered ring to flavanone **31**. Elimination of HI then reforms the double bond between C2 and C3 thus forming

the flavone **22**. Usually only catalytic amounts of iodine are used under high temperatures in DMSO. DMSO is reduced to dimethylsulfide to regenerate iodine.

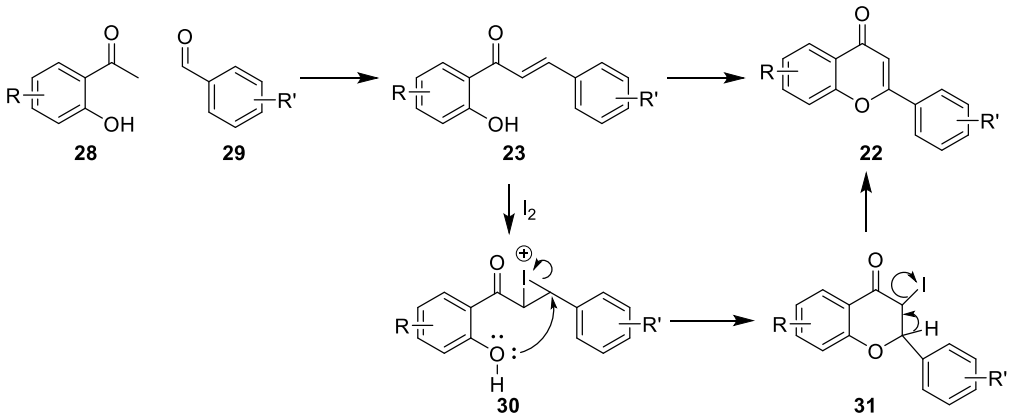

Scheme 3

Using the chalcone **23** to make the flavone **22** can be especially useful if the reactions are done to synthesise libraries for biological screening because chalcones **23** have interesting biological activities themselves and are therefore often included in screening libraries containing flavonoids. By designing the synthesis of flavones **22** through chalcones **23** two interesting classes of compounds can be obtained from the same route. A nice example of this technique was employed by Tan *et al.* when looking for a potential new antibacterial against *Flavobacterium columnare,* the cause of columnaris disease in channel catfish.[48] They included a number of flavonoids in their screen including several trimethoxyflavones **33** and their parent trimethoxychalcones **32** (*scheme 4*).[48] Unfortunately none of the compounds from their screen turned out to be better against *Flavobacterium columnare* than their original lead wogonin **34** (*figure 19*).

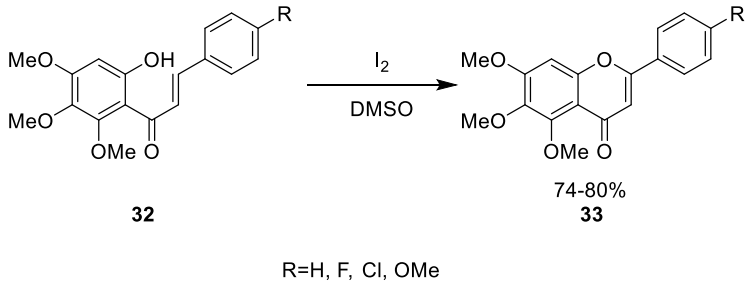

Scheme 4

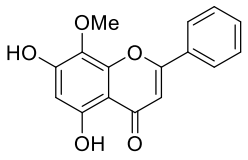

Wogonin **34**

Figure 19

2.1.2 Synthesis *via* alkyne

Considering this strategic disconnection a further, cyclisation to form the C ring can also proceed from alkyne **23** (retrosynthesis shown in *scheme 5*). There are two main synthetic routes to obtain alkynes **24** that can cyclise to form flavones, route 1 involves the palladium-catalysed coupling of an acyl halide **35** and a terminal alkyne **36**. Route 2 relies on palladium-catalysed carboxylation of an *ortho*-halophenol **37** and a terminal alkyne **36**. The second route requires simpler substrates, but does involve the use of pressurised carbon monoxide that can be a safety hazard.

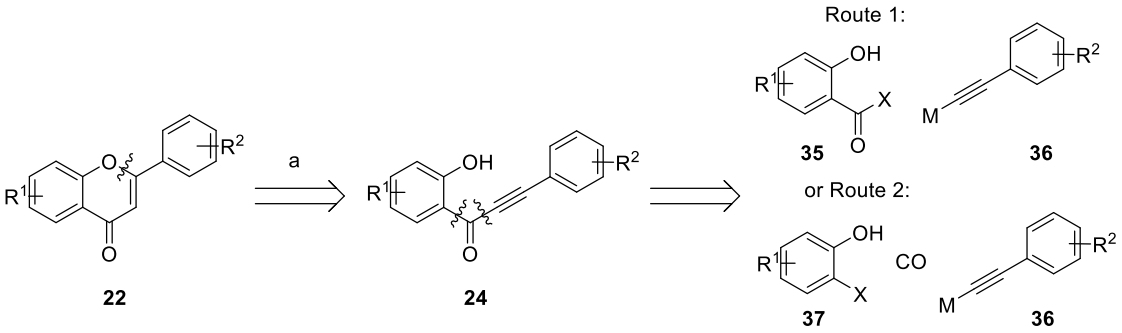

Scheme 5

The first example of synthesising a flavone **14** using an alkyne analogue **40** of a chalcone was reported by Luxen *et al*. in 1985 (*scheme 6*). They synthesised one example using this method, making their starting alkyne from benzoyl chloride **38** and a phenyl acetylene **39** in the presence of copper iodide.[49]

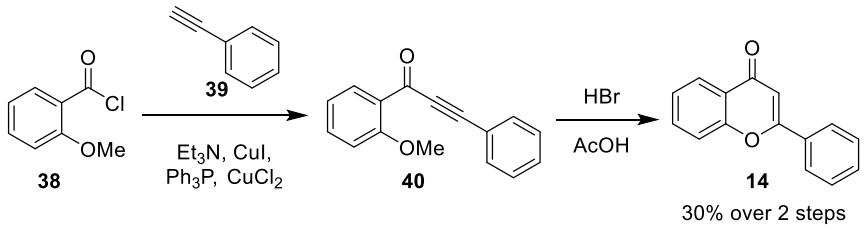

Scheme 6

Recently this approach has received attention again and improvements have been made over the original synthesis proposed by Luxen *et al.*, both in the synthesis of the alkyne **24** and in the cyclisation reaction as well as milder reaction conditions.[50, 51] The most recent report by Yang *et al.* reported overall yields of 93-99% for their library of 24 flavones **22**, including both aromatic and aliphatic R^2 groups and a range of electron donating and withdrawing groups for both R^1 and R^2 (*scheme 7*).[51] They used trimethoxytriazine activated benzoic acids **41** to form the alkyne intermediate **43** that they then cyclised using piperazine to yield the flavones **22**.

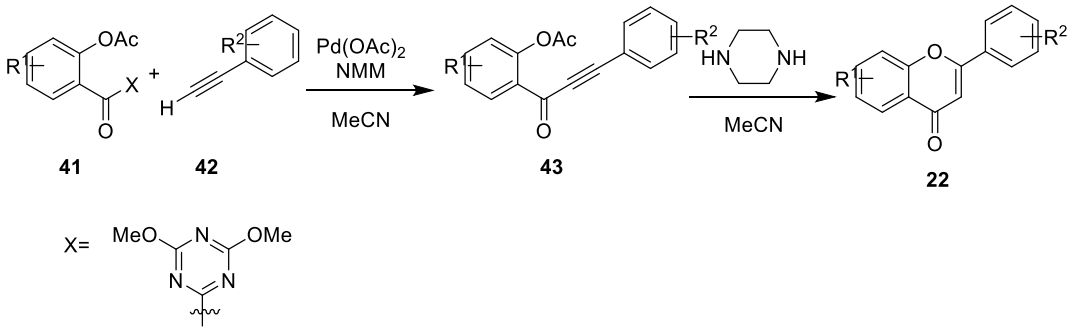

Scheme 7

Route 2 involves the insertion of a carbonyl group to construct the ketone of the C ring, usually by palladium catalysed carbonylation reaction. There are a few different protocols for carrying out this one pot addition-cyclisation reaction (s*cheme 8*). Liu *et al.* synthesised a small array of flavones **46** using a very low catalyst loading in 70-90% yield.[52] Xue *et al.* did the same reaction on aryl fluorides in 2011 with a slightly higher catalyst loading also for a small library or flavones with yields between 84-98%.[53] Neither paper had many (or any at all in Xue's case) different substituents on the A ring, though both had at least one example with a methoxy and a fluoro group on the B ring.

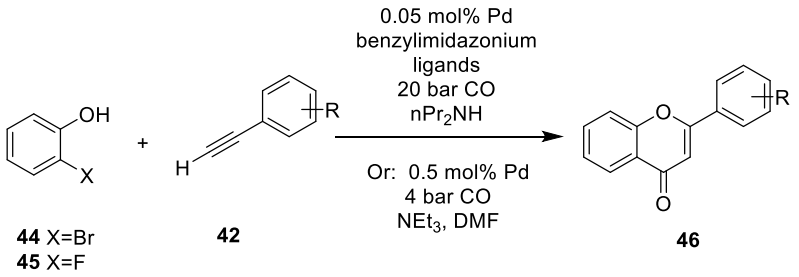

Scheme 8

2.1.3 Synthesis *via* 2-hydroxyacetophenone

The oldest and most commonly used synthetic route to flavones **22** proceeds *via* disconnection b (*scheme 9*). There are numerous very similar named reactions, such as Baker-Venkataraman, Allan-Robinson and Kostanecki acylation, which form the arylester **25** under different reaction conditions. Although first described in the beginning and middle of the twentieth century these reactions continue to be used for the synthesis of flavones.

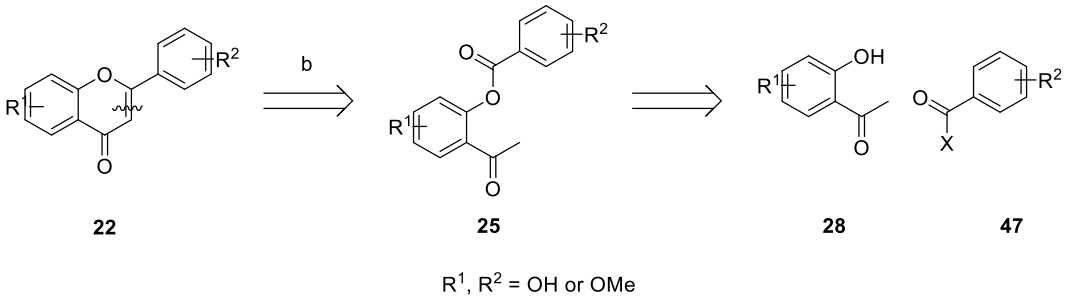

Scheme 9

These reactions proceed through a rearrangement *via* the ß-diketone intermediate **49** (*scheme 10*).[36, 54] ß-diketone **49** can be formed by the Baker-Venkataraman (B-V) rearrangement from a *ortho*-esterified acetophenone **25** that can be easily synthesised by esterification of an *o*-hydroxylacetophenenone **28** with either a benzoic acid **48** or an acid chloride (*scheme 2*).

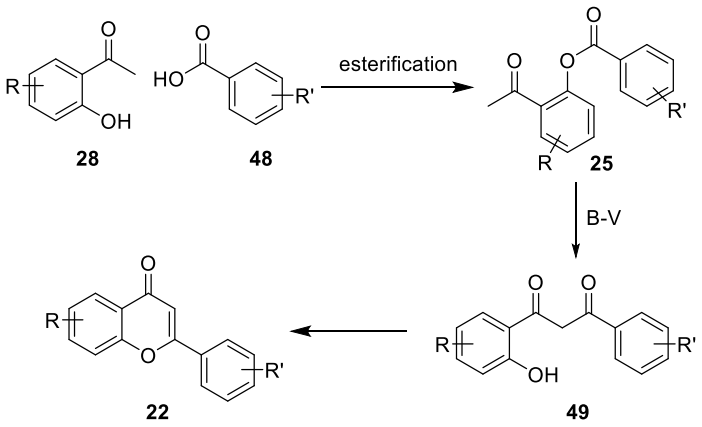

Scheme 10

The Baker-Venkataraman rearrangement to form the diketone **49** proceeds through the enolate **50** (*scheme 11*). This then ring closes in an intramolecular Claisen reaction to form intermediate **51** that opens to form the deprotonated diketone **52**. The diketone **49** need not be isolated; the cyclisation can be catalysed by the same base which catalysed the diketone **49** formation. A mild base is usually used for this reaction, such as potassium carbonate. If the diketone **49** is isolated the cyclisation to form the flavone **22** is usually carried out under strongly acidic conditions instead.[55]

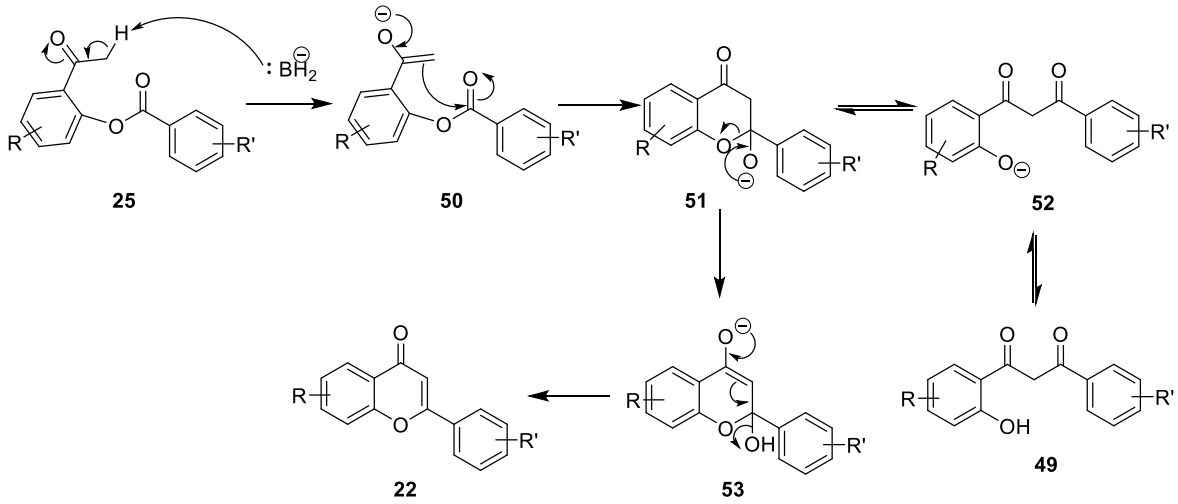

Scheme 11

Baker-Venkataraman synthesis of flavones **22** was first described in 1933 and has continued to be used to this day.[55] Recently, when looking for a novel lead for COX2 inhibitors, Badiger and co-workers opted to screen a small library of flavone derivatives **59** (R=heterocycles) synthesised by a Baker-Venkataraman

reaction (*scheme 12*). They started their synthesis from methyl protected acetophenone **54** and benzyoyl chloride **55** to form the ester **56** that was then rearranged to the diketone **57** using potassium hydroxide. The diketone **57** was then cyclised using sulfuric acid in acetic acid to form the dimethoxyflavone **58**. Deprotection and further functionalisation yielded the flavone library **59**. Some naturally occurring flavonoids had been described as COX2 inhibitors, and by synthesising a library, using this reliable way of making flavones, they hoped to find a more selective inhibitor for COX2 without COX1 activity.[56] COX2 is involved in the inflammatory response and hence is an important target for new anti-inflammatory drugs but COX1 is involved in normal cell metabolism and hence its inhibition would lead to side effects.

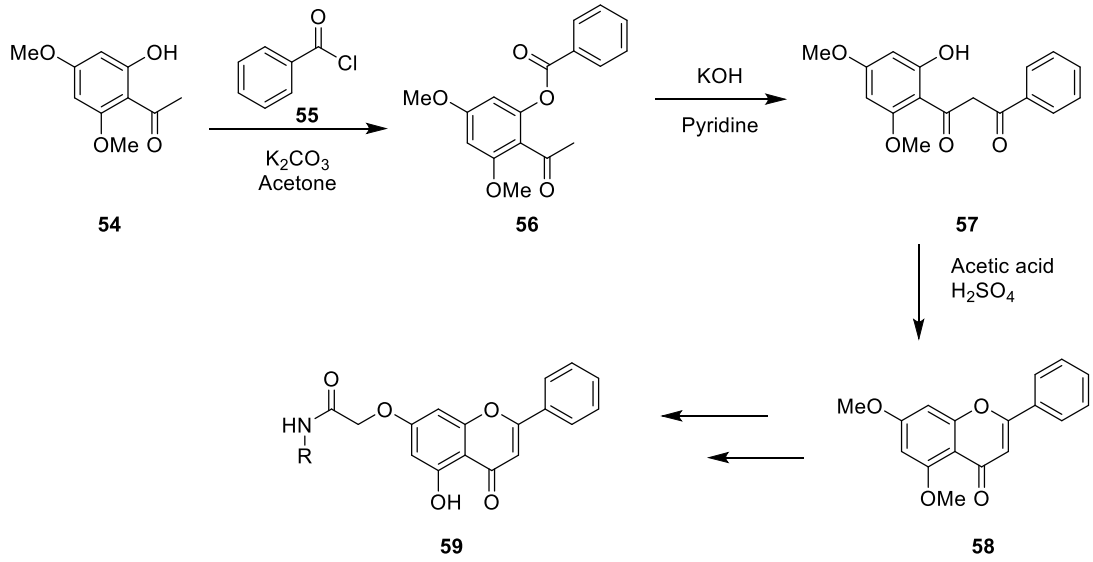

Scheme 12

A very similar synthetic route, the Allan–Robinson method (*scheme 13*), of making flavones proceeds through the same diketone intermediate **49**, this time made from an acetophenone and an acid anhydride. As the acid anhydride and the starting acetophenone can both be substituted this method allows for the formation of both flavones **22** and flavanols **15**, as well as chromones **16** if an aliphatic acid chloride is used instead. A recent example for the use of Allan-Robinson condensation can be found in another library of flavonoids synthesised to investigate the structure activity relationship between flavonoid functionalisation and inhibition of cell proliferation of the HT29 (a human colonic cancer) cell line. The following flavonols **62** were synthesised as part of the screen.[57]

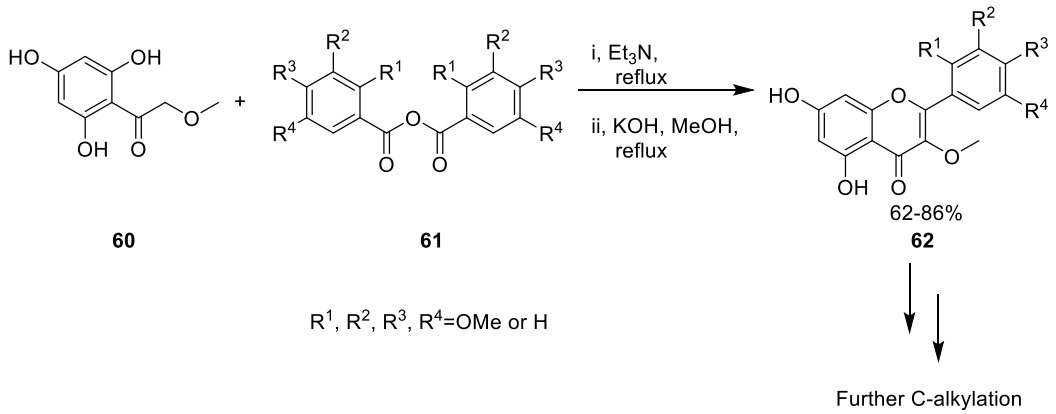

Scheme 13

Yet a different method for forming flavones *via* the b disconnection is the Kostanecki acylation, mainly used to synthesise chromones **16** and coumarins **70** but can also be used to make flavones **14** (*scheme 14*). Aromatic R groups lead to the formation of flavones **14** and aliphatic R groups can be used to make chromones **16**. Coumarins **70** can be synthesised instead by encouraging enolate **68** formation (here R=Me).[58, 59]

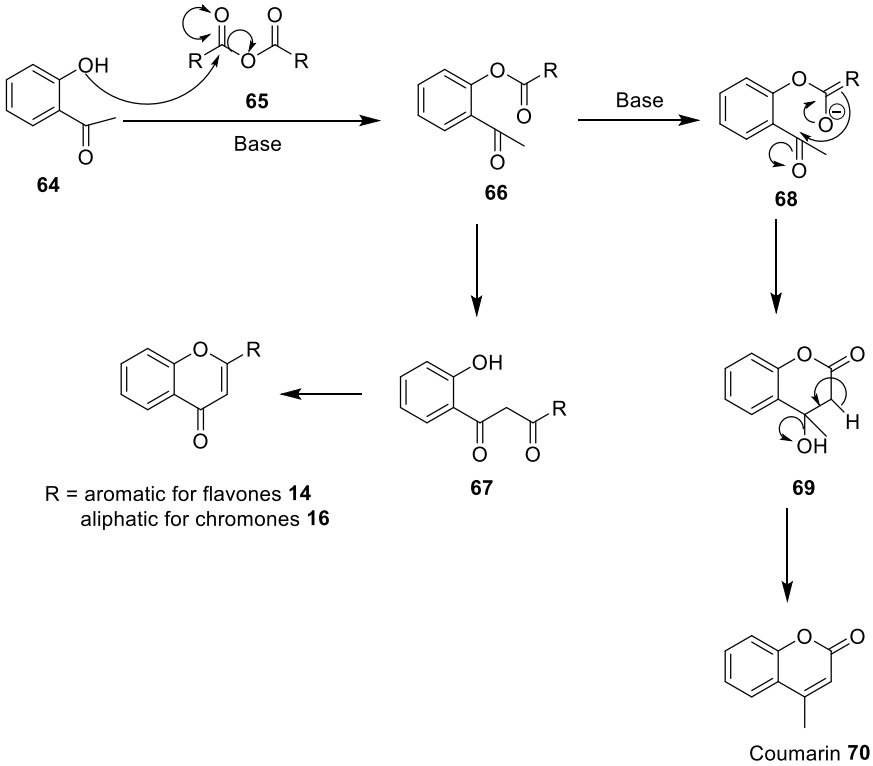

Scheme 14

2.1.4 Synthesis *via* attachment of B-ring to chromone

Flavones can also be synthesised using disconnection c, most often by metal-catalysed cross-coupling using 2-chlorochromones and arylboronic acids for example (*scheme 15*).[60] The other option is to cross couple chromone-2-carboxylic acid with an aryl halide in the presence of a palladium and silver carbonate mixture.[61] Direct coupling of a chromone and an arylboronic acid has also been reported in the presence of palladium catalyst.[62]

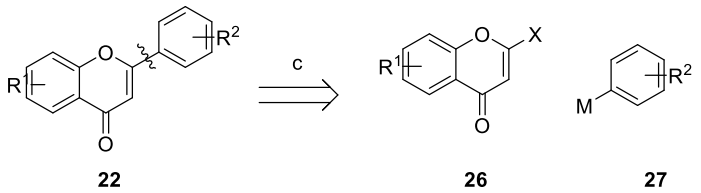

Scheme 15

Simple Suzuki cross coupling was employed by Kraus *et al*. to synthesise a small collection of flavones **73** using chlorochromones **71** and aryboronic acids **72** (*scheme 16*).[63] A total of five substituted flavones **73** were synthesised in good yield.

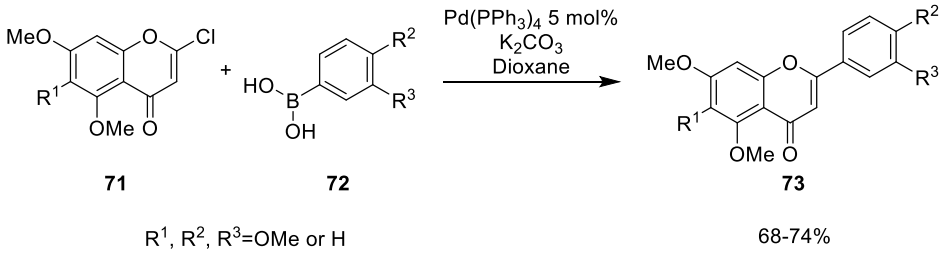

Scheme 16

An example of using palladium-catalysed Heck type reaction[64] to make a flavone can be seen in the synthesis of frutinone A **77** (*scheme 17*). A simple chromone **16** was heated in the presence of arylboronic acid **74**, palladium acetate, a Lewis acid and oxidants under air to form the flavone **75**. A further palladium catalysed insertion of carbon monoxide was then carried out after the methyl deprotection of the flavone phenol to yield frutinone **77**.[65] This demonstrates the strength of palladium catalysed reactions to form complex aromatic natural products efficiently.

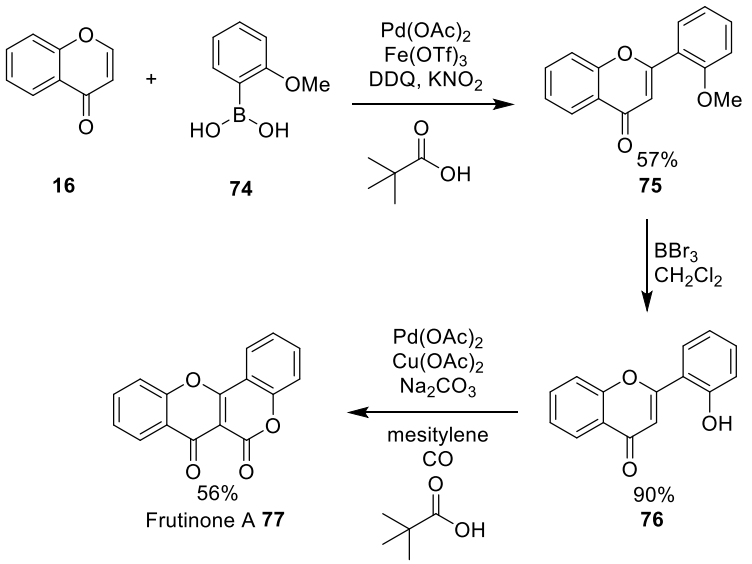

Scheme 17

More recently a transition metal free decarbonylative coupling has been described by Golshani *et al*. where the B ring is attached as an aryl boronic acid **79** to a chromone-2-carboxylic acid **78**.[66] [67] Moderate to good yields were achieved on a small library of methyl, chloro and hydroxyl substituted flavones **22** (*scheme 18*).

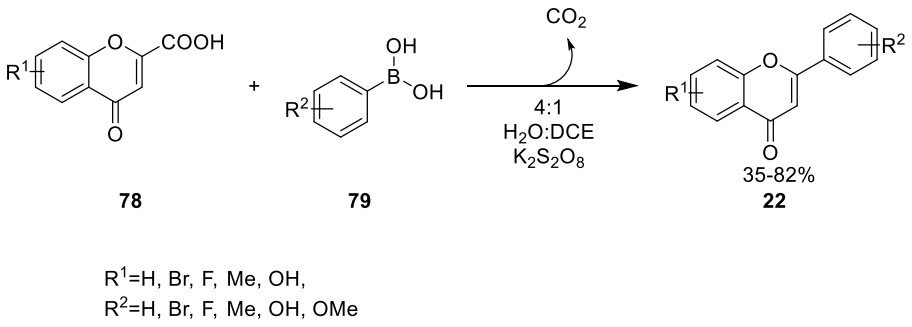

Scheme 18

These cross coupling reactions towards the synthesis of flavones have all been reported relatively recently, implying a continued interest in the synthesis of bioactive natural products. The continued need to come up with better synthetic routes illustrates the difficulty in dealing with this family of natural products. Depending on the substitution pattern, the reactivity of the flavonoid will change, making some compounds harder to synthesise than others with different substitution patterns. The newer cross coupling reactions seem to have a problem with reactivity under some conditions, whereas the older robust

methods suffer from harsh conditions and high temperatures that can also lead to low yields.[50] The synthesis of flavonoids is still not trivial, even though efforts towards better methods to make them have been going on for almost a hundred years.

2.2 Biflavones

Biflavonoids are dimers of flavonoids. They are usually divided into two groups, those with C-C linkages for example amentoflavone **10**, and those with C-O-C linkages between the monomer units such as ochnaflavone **80** (*figure 20*).

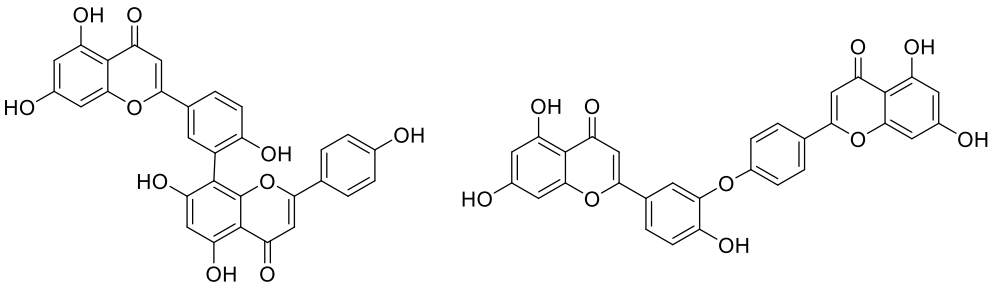

Amentoflavone **10** Ochnaflavone **80**

Figure 20 Examples of biflavones

There are relatively few plants that produce biflavonoids, but they have been found to have many different types of biological activity, most notably anti-inflammatory activity.[34, 68] There have also been relatively few reports of total synthesis of biflavones,[69] with even fewer from the last decades, however with resent interest in the bioactivity of biflavones there might be more published in the coming years.

The synthesis efforts towards biflavones can also be categorised into two groups, those that leave the biflavone coupling step to the end of the synthesis, and those that start the synthesis from there. Synthesising two monomers and then coupling them is the more convergent approach and theoretically leads to a shorter, higher yielding synthesis. This seems to be the more popular synthetic approach in recent literature.[68, 70]

Yet as some flavones can be highly substituted, these couplings can fail due to steric hindrance. Starting the synthesis from the middle and building up the

flavone skeleton once the central bridging bond has been made seems to be the strategy used for the total synthesis of natural biflavones that have multiple hydroxyl groups. Both of these approaches are described in more detail below.

2.2.1 Synthesis of C-linked biflavones

Cupressuflavone **12** was one of the first biflavones to be synthesised. It was synthesised by Murti *et al.* in 1966.[71] To synthesise the biflavone, iodo monomers **81** with the phenolic hydroxyls protected as methyl ethers, were coupled together using a copper catalyst in an Ullman style reaction (*scheme 19*).[72] Considering the steric hindrance around the new C-C bond, the poor yield of biflavone **82** was considered acceptable. The hexamethoxy cupressuflavone **82** was then deprotected using boron tribromide. No yield for cupressuflavone **12** was reported for this reaction at all and from the descriptions in the paper it can be assumed that the deprotection did not proceed smoothly. Several partially demethylated side products were isolated. Some amount of the desired cupressuflavone **12** was isolated however, as the authors successfully compared to the natural isolated cupressuflavone **12** samples.[71]

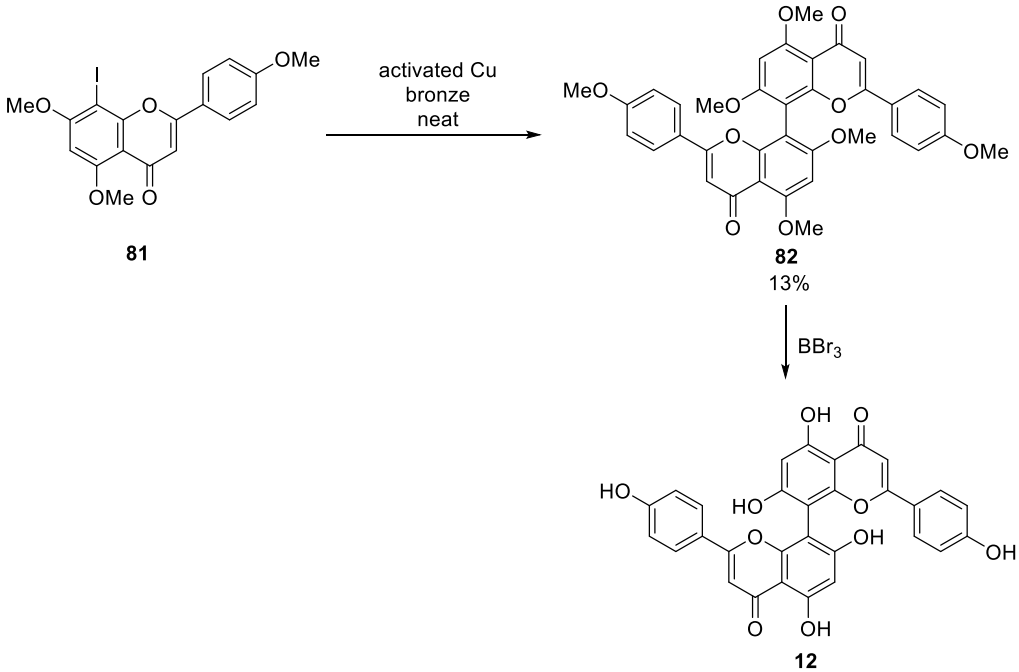

81 **82** 13% **12**

Scheme 19

The second synthetic approach to cupressuflavone **12** from 1976 employs a different strategy.[73] While still using Ullman coupling Ahmad *et al.* opted to

synthesise the central C–C bond first and then build up the flavone (*scheme 20*). Hence the synthesis begun from trimethoxy-8-iodoflavone **83**, and the dimer **84** was formed by Ullman coupling, Friedel Crafts acylation completed their bis(acetophenone) derivative **86**. They then deprotected only the methoxy group that would lead to a phenoxide coordinated tothe carbonyl group.. They then used the desired deprotection product and benzaldehyde **87** to form the chalcone **88**. After cyclisation using selenium dioxide the protected biflavone **82** was deprotected and dimethylcupressuflavone **89** was isolated. There were several problems with this synthetic approach, namely both the boron tribromide deprotection steps gave mixtures of products and did not go to completion.[73] It did illustrate that this alternative approach to synthesising biflavones was viable.

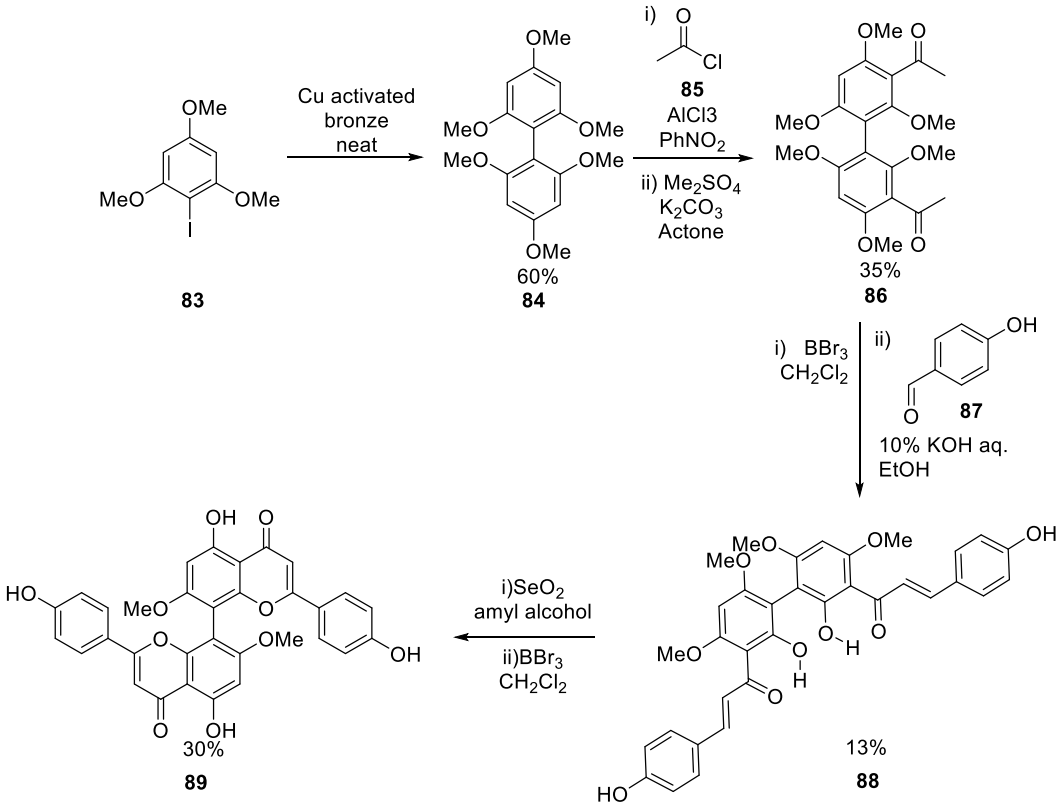

Scheme 20

There have been a few of examples of C-C biflavones synthesised by Suzuki coupling in the more recent literature.[70, 74-76] For example the unsubstituted analogues of cupressuflavone **91** (C8-C8), succedaneaflavone **90** (C6-C6) and agathisflavone **92** (C6-C8) as well as three other biflavones with C7-C6 **94**, C7-C7 **93** and C8-C7 **95** linkages (*figure 22*) were synthesised by Kohari *et al*..[70] Even

though these analogues **90**-**95** do not have any hydroxyl groups, and are hence much simpler, the yields for the Suzuki coupling, though optimised, were poor in cases (especially for compounds **91**, **92** and **95**). This was reportedly due to the steric hindrance of these particular conformations. It can be assumed that increased bulk from functional groups on these flavones would lead to perhaps even lower yields. In fact, none of the reported biflavones synthesised recently has been fully substituted, with biflavone skeletons synthesised instead of naturally occurring polyphenolic biflavones.[70, 74, 75]

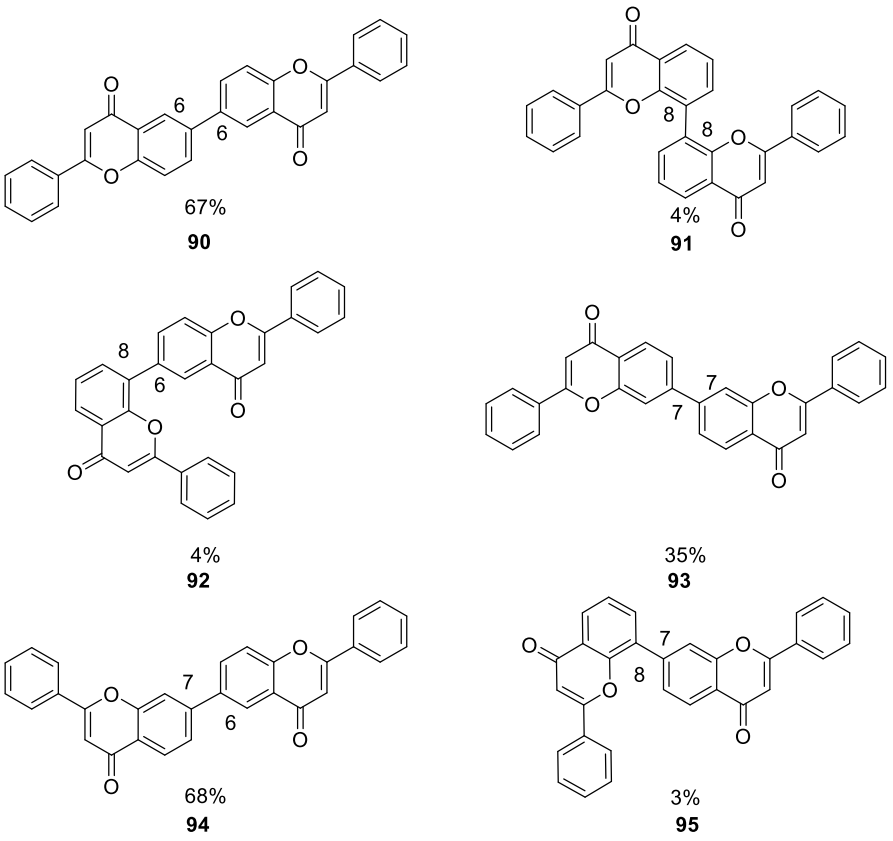

Figure 21 C-C biflavones, yields shown are for Suzuki coupling

A synthetic approach, somewhere between the two previously mentioned is also possible, where one of the pseudo dimers is synthesised, then the central link is formed after which the other flavone is built up. An example of this approach can be seen in the recent total synthesis of biapigenin A **101** (*scheme 21*). The authors initially tried to couple the two flavones monomers together using Suzuki coupling, however due to steric issues none of their attempts worked. They therefore used Sonogashira coupling to attach the aromatic alkyne **97** to iodoflavone **96** and then used cyclisation after the addition of benzophenone **99** to get their desired biflavone **101** after deprotection. They also synthesised

ridiculuflavone using the same reaction conditions in 36% from the iodoflavone in three steps.

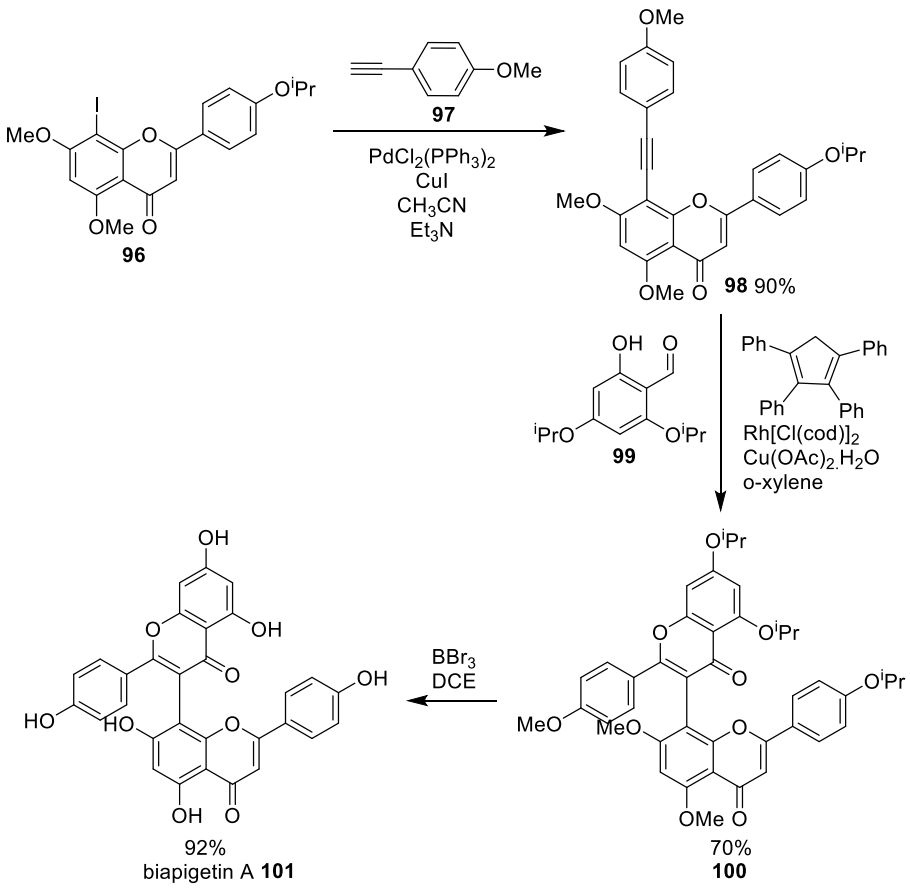

Scheme 21

A completely different take on library synthesis was taken by Sum *et al*. when they synthesised a library of unnatural bi- and triflavones **103** to screen for anticoagulants against the amyloid ß-peptide, a pathological hallmark of Alzheimer's disease (*scheme 22*). They attempted to cover a wide area of chemical space by synthesising a number of structurally diverse scaffolds. By using di- and tribenzaldehydes and a biaryldiketone for the formation of the initial chalcones **102** they managed to synthesise a number of fused bi- and triflavones. The biaryldialdehyde allowed for the synthesis of C4'-C4' biflavones.[77]

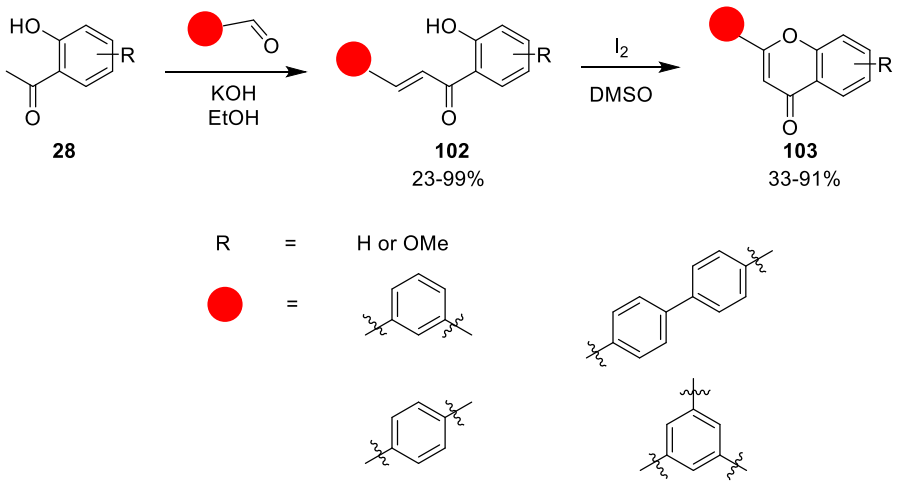

Scheme 22

2.2.2 Synthesis of C-O-linked biflavones

Just as the C-C linked biflavone could be synthesised by late stage as well as early stage bridging bond formation, so can the ether linked biflavones. A nice example of the late stage ether formation is the synthesis of a 17 membered library of substituted 6-O-7'' biflavones **106** (*scheme 23*). The library was synthesised in order to search for ether linked biflavones that would act as COX2 inhibitors, a target for novel anti-inflammatory drugs mentioned earlier. The library was synthesised by Ullman coupling 6-bromoflavone derivatives **105** to 7-hydroxyflavone derivatives **105** to form the 6-O-7'' biflavone **106** library. All the compounds synthesised were only substituted on the B and B' rings with no substitution on the A ring apart from the bromine or hydroxyl required to form the linking ether, hence lowering steric hindrance around the ether link. The unsubstituted biflavone **106** (R=R'=H) was the most active COX2 inhibitor with an IC_{50} of less than 2 μM.[78]

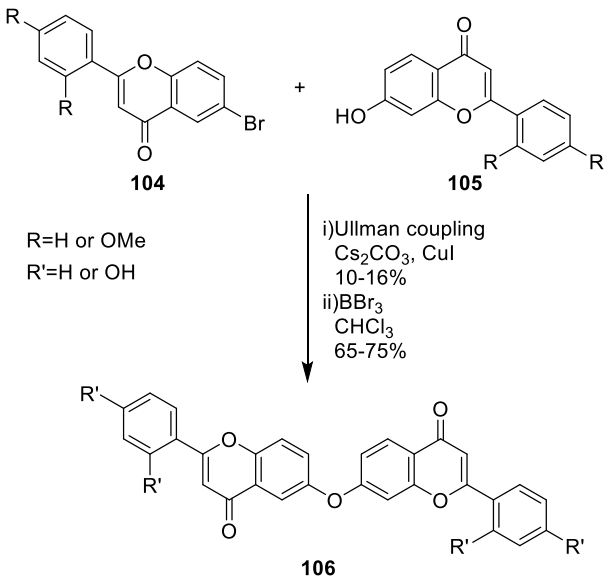

Scheme 23

The total synthesis of ochaflavone **80** published in 2013 illustrates the power of the second strategy to biflavone synthesis (*scheme 24)*.[79] Here, the central ether bond was formed first by an S_NAr reaction between phenol **107** and fluorobenzaldehyde **108** to form the biaryl ether **109**, which was subsequently used to make the dichalcone **110**. The bichalcone **110** was then cyclised using iodine in pyridine to give protected biflavone **111**. The researchers reported that the more widely utilised DMSO and iodine method only led to decomposition in their case, as did a number of other options tried. Finally the pentamethylochaflavone **111** was deprotected using boron tribromide, which yielded the natural biflavone **80** in excellent yield considering the difficulties in removing methoxy protecting groups from phenols.[79] The difficulties Ndoile *et al*. experienced in finding cyclisation conditions at quite a late stage of their synthesis really exemplifies the problems that can be encountered in a linear synthesis if reliable and widely used reactions do not work as expected. Zang *et al*. published a very similar synthesis a couple of years later using MOM protecting groups that made the protection deprotection seps much simpler. Ochaflavone was then synthesised in 6 steps with an 12.6% overall yield. Their lowest yielding step was the oxidative cyclisation to yield the protected diflavone.[80]

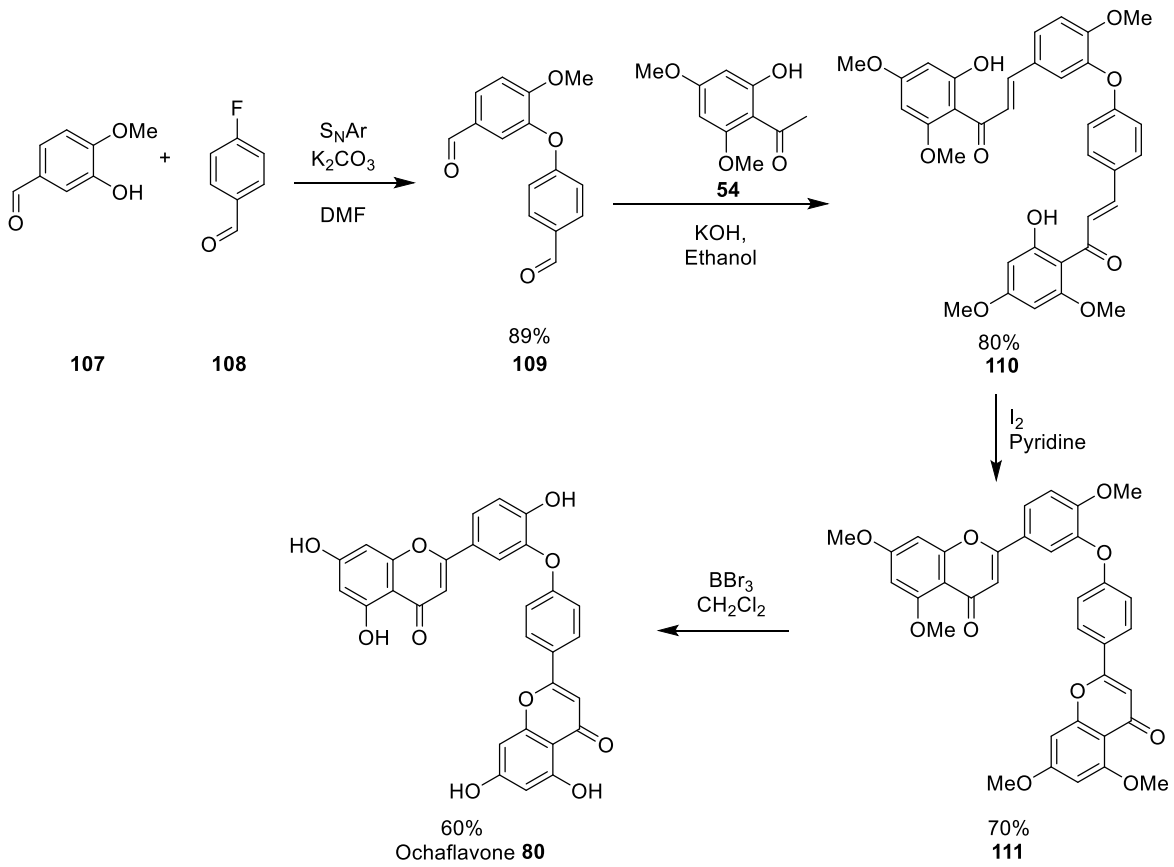

Scheme 24

2.2.3 Synthesis of hinokiflavone - previous work

The first and the total synthesis hinokiflavone **9** was made in 1967 by Nakazawa, who first published the corrected structure of hinokiflavone.[23, 24] Due to the incorrect structure having been proposed almost ten years before, the 4'-8 biflavone was synthesised first. Efforts were first turned to the Ullmann coupling of completed pseudo-monomers, however when that approach failed due to sterics different coupling conditions were sought leading eventually to S_NAr reactions.

First the methyl protected right hand side was synthesised. Since hinokiflavone was thought to have 4'-8 ether linkage the correctly substituted precursor for the incorrect flavone was made (*scheme 25*). The approach taken relied on an appropriately substituted acetophenone **114** with methoxy groups in the 4- and 6-positions and free phenolic hydroxyl groups in the 2- and 3-positions. Acetophenone **114** was therefore synthesised from acetophenone **112** in 4 steps in a 32% overall yield. After double esterification with 4-methoxybenzoyl chloride **115**, ester **116** was rearranged to the diketone **117**, which was in turn

cyclised under acidic conditions to form flavone **118**. This yielded the desired flavone RHS **119** after saponification.

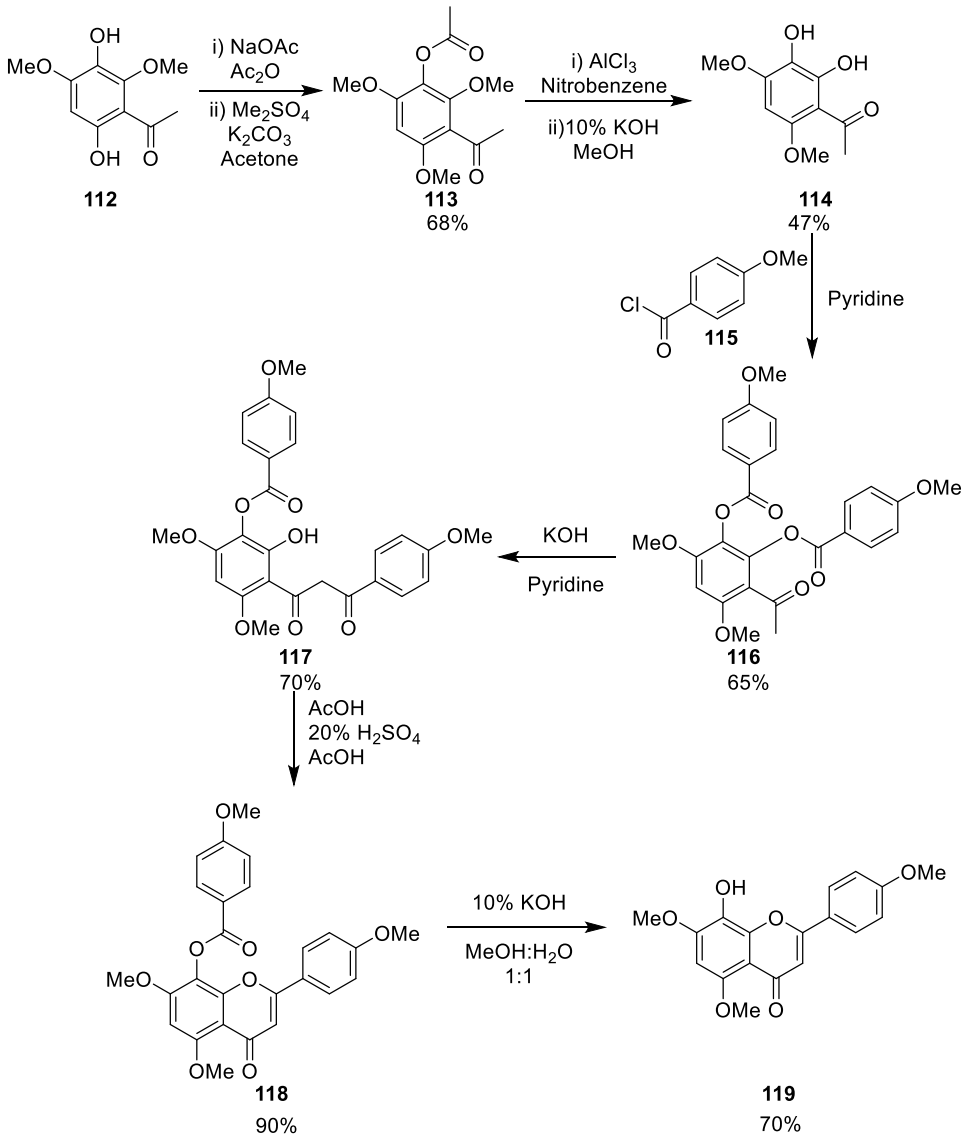

Scheme 25

Since S_NAr reactions on flavones often fail due to the aromatic rings being too electron rich, the next steps in the synthesis relied on a nitro activating group to facilitate the S_NAr reaction between flavone **119** and iodoflavone **123**. Therefore the iodo-nitro-flavone **123** was synthesised in three steps in an 17% overall yield (*scheme 26*). First the ester **121** was formed from dimethoxyacetophenone **54** and 4-iodo-3-nitrobenzoyl chloride **120**. This was then rearranged to the diketone **122** under basic conditions and then the flavone **123** formed by the cyclisation under acidic conditions.

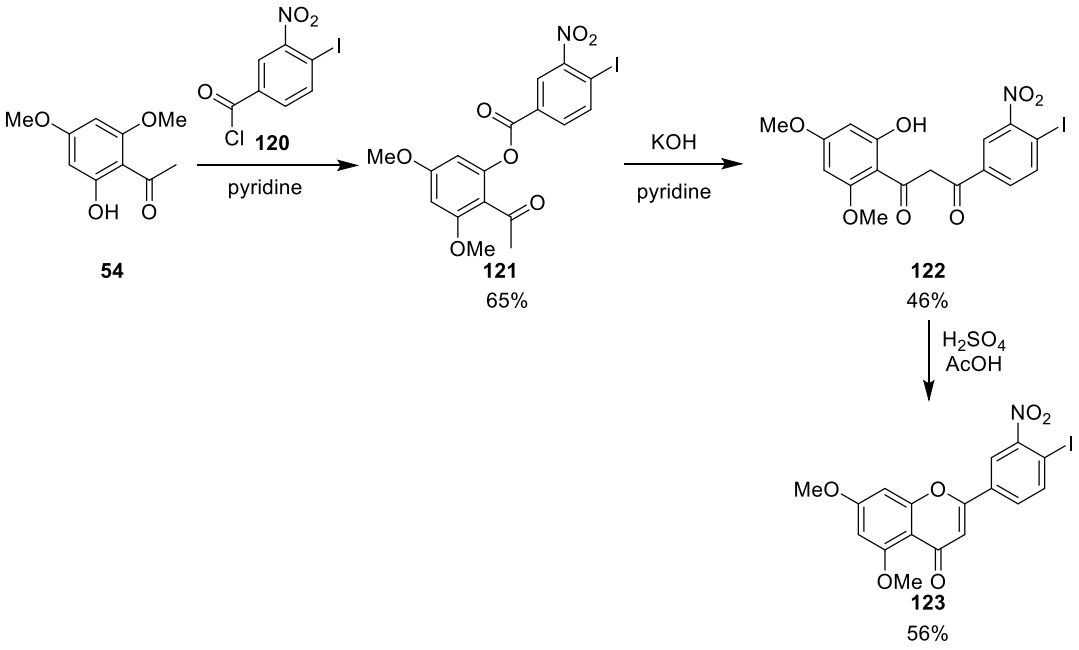

Scheme 26

With the activating nitro group the S_NAr reaction proceeded in good yield to give the biflavone **124** (*scheme 27*). The nitro arene **124** was then reduced to the amine **125** and the amino group was removed by making the diazonium ion. Attempts to deprotect the pentamethoxybiflavone **126** using HI to give the desired pentahydroxybiflavone **8** however did not proceed very well, and no yields were reported in the paper. Some of the biflavone **8** was isolated as both the pentahydroxy and the pentaacetylated structure were compared to the natural hinokiflavone **9**. Analysing the melting point and IR of natural hinokiflavone **9**, it was soon realised that the 4',8-biflavone **8** was in fact the incorrect structure. Hence the structure was revised and work began on the 4'-6 correct hinokiflavone **9** structure.

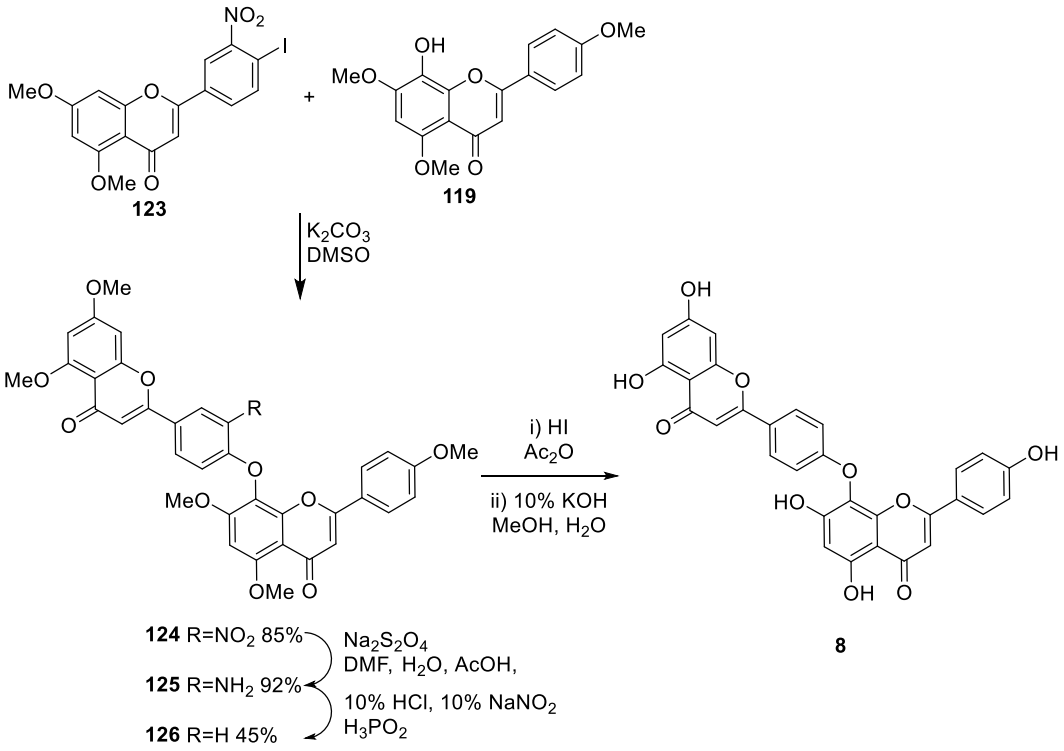

Scheme 27

To synthesise hinokiflavone the correctly substituted flavone **130** was synthesised (*scheme 28*). Double esterification of the acetophenone **112** resulted in the ester **127** that was then rearranged to the diketone **128**. The diketone underwent oxidative cyclisation to form the flavone **129** which after saponification yielded the desired RHS **130** in four steps with a 37% overall yield. The paper however did not reference the synthesis of acetophenone **112** itself, which the Hartley group later found, was low-yielding.

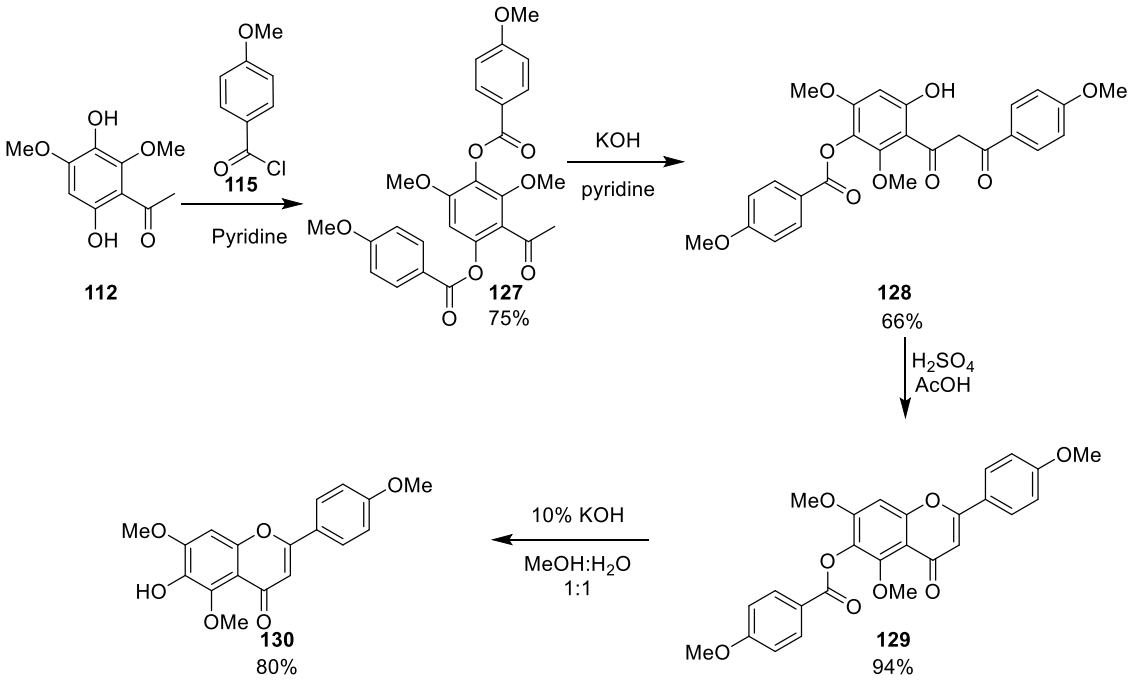

Scheme 28

The previously synthesised activated iodoflavone **123** was then coupled to the new hydroxylflavone **130** to give the nitro-biflavone **131** in a good yield (*scheme 29*). The nitro group was again removed by first forming the aminobiflavone **132**, which then was then converted into the pentamethyl hinokiflavone **133**.

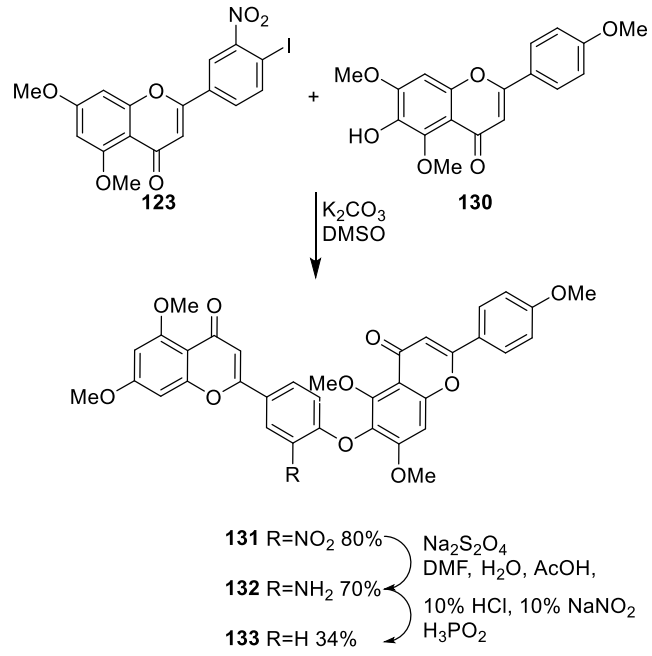

Scheme 29

Removal of the methyl groups with aluminium chloride gave what was presumably diol **134**, but no yield was recorded (*scheme 30*). While treatment with HI in acetic anhydride yielded the pentaacetylated derivative **135** in what can be presumed to have been modest yield as no yield was reported, which was then deprotected to give hinokiflavone **9**. Again no yield was recorded, so presumably very little was isolated. The identity of hinokiflavone **9** was confirmed by microanalysis, IR and melting point in comparison to natural hinokiflavone **9**. Since the work was prior to widespread use of NMR, no NMR data were included for any compounds made and there was also no MS data included. We concluded that better synthesis would certainly be possible.

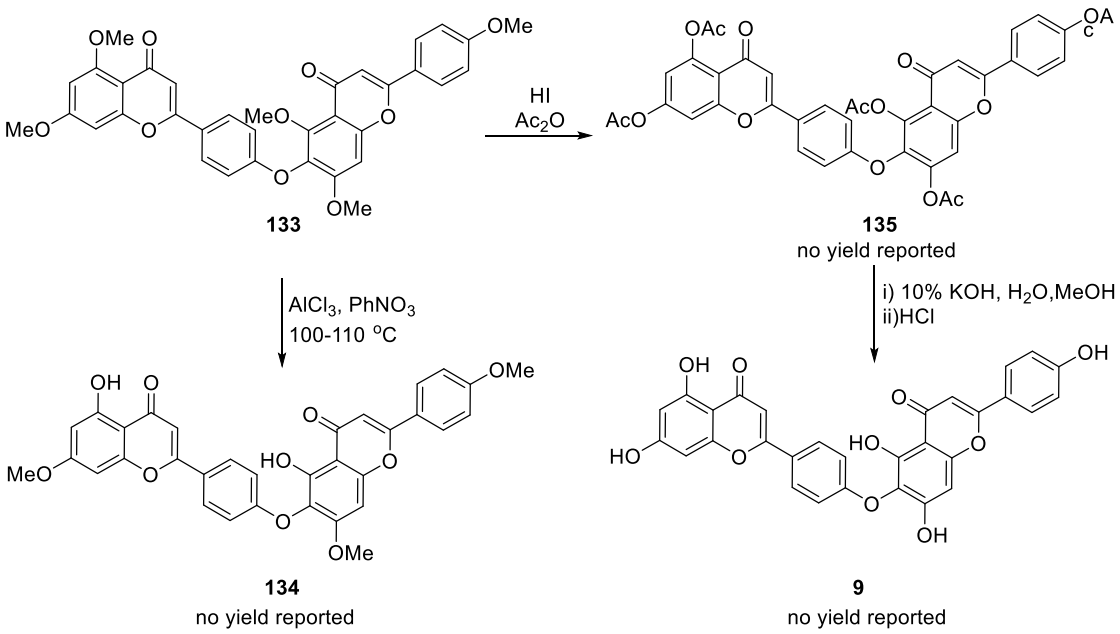

Scheme 30

To supply more hinokiflavone **9**, as global stores of hinokiflavone **9** fell short of even a gram of the compound and to establish a structure activity relationship for the observed phenotypic and splicing effects, a synthetic approach to hinokiflavone **9** that would yield quantitative amounts of compound and simplified analogues was necessary. Previous work on hinokiflavone **9** in the Hartley group had attempted the synthesis of hinokiflavone **9** by assembling the two halves forming an ether linkage after the synthesis of each of the pseudo-monomers separately.

The A, B, C flavone system **140** was synthesised from chrysin **137** in 4 steps in an 17% overall yield (*scheme 31*). The chrysin **137** was used to allow for the correct

substitution pattern on the A ring by setting up the correct pattern of benzyl protection for the starting acetophenone **138**.[81, 82] Acetophenone **138** was then reacted with *p*-fluorobenzaldehyde **109** to form the chalcone **140**, which was then cyclised with iodine to form the LHS ring system **140** of the biflavone **9**.

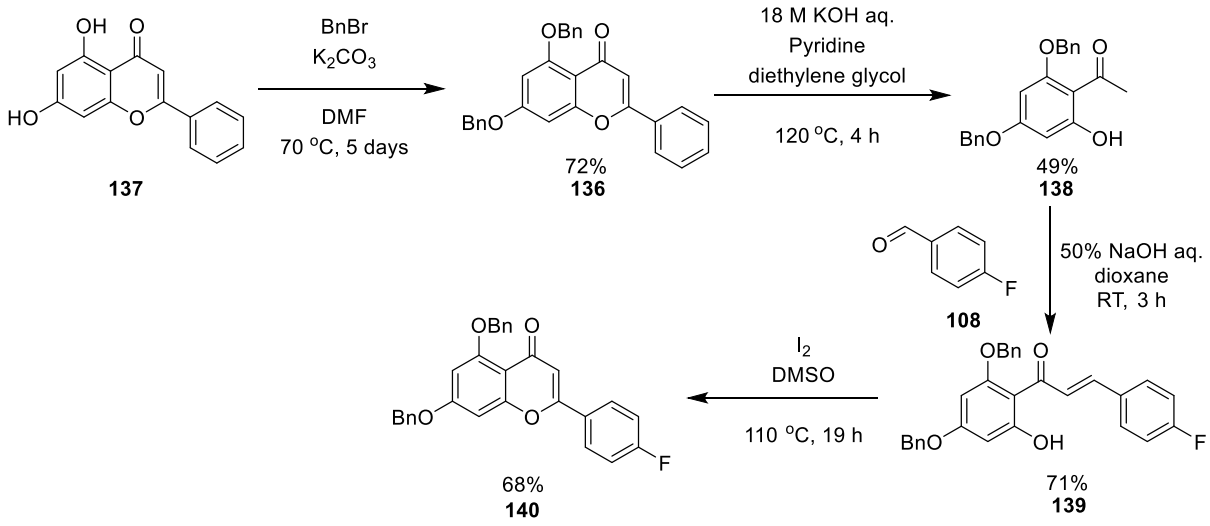

Scheme 31

To synthesise the RHS, trihydroxyacetophenone **141** was selectively methyl protected to yield the dimethoxyacetophenone **54** (*scheme 32*). This time the selectively was achieved by relying on the hydrogen bonding between the carbonyl and a neighbouring phenol which makes that position harder to deprotonate. It should be noted that even though the ketone is actually *ortho* to two phenols, only one of them can be hydrogen bonded at any one time and hence the other is deprotonated and alkylated. An extra hydroxyl group was then introduced using an Elbs oxidation,[83] *para* to the free hydroxyl group to yield the dimethoxydihydroxyacetophenone **112**. The new hydroxyl group was then THP protected to form acetophenone **142** which was used to form a chalcone **144** from benzyloxybenzaldehyde **143**. Finally the chalcone **144** was cyclised using iodine to form the protected A'C'B' ring system **145**. Overall the synthesis of the RHS fragment **145** was carried out over five steps with a 9% total yield. The yield of the RHS fragment **145** suffers considerably from the low yielding Elbs oxidation.

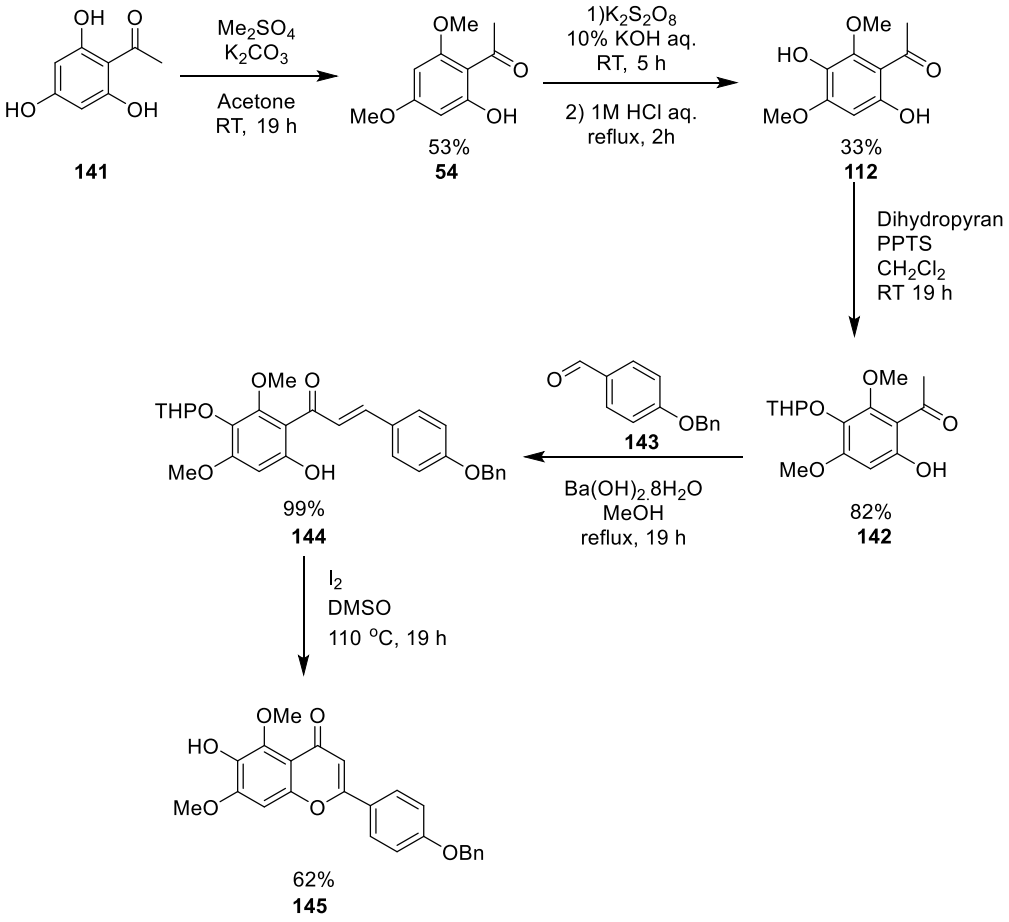

Scheme 32

Substantial effort was then put into trying to couple the two halves (compounds **140** and **145**) together to form the protected hinokiflavone **146** (*scheme 33*).[81] Among the various conditions used were aromatic substitutions and Ullman couplings. Unfortunately all the attempts were unsuccessful. This was thought to be the result of the central ring systems being too sterically hindered by the protected phenols on the A' ring, and the B ring is also quite electron rich and hence less likely to undergo nucleophilic aromatic substitution.[81] Steric hindrance on the A' ring prevented any reaction from taking place on substrates where the A' ring was fully substituted. For analogues without two methoxy groups on the A' ring the coupling did take place.[81]

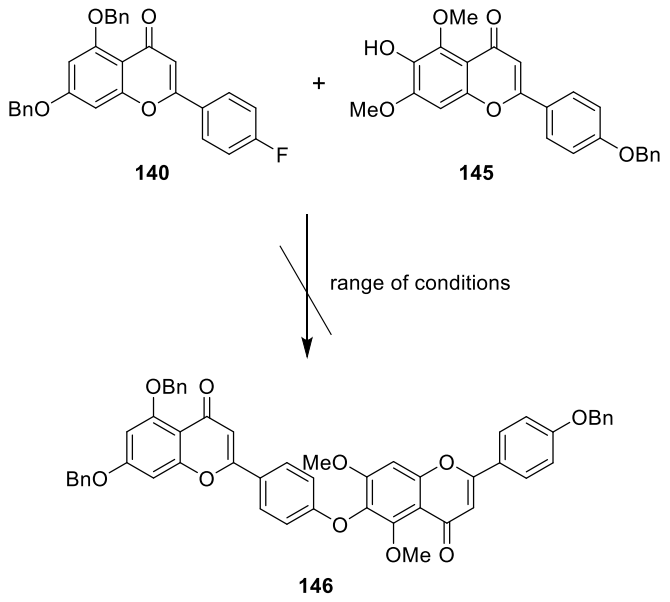

Scheme 33

Several analogues of hinokiflavone **9** were synthesised successfully using similar synthetic routes to the one described above (*figure 22*). As all of them are less substituted, especially around the central ether linkage, they underwent the S_NAr reaction more readily, though forcing reaction conditions were still required. [81, 84] Nonetheless, upon testing, none of them were found to form the same megaspeckles that hinokiflavone **9** did in living cells.

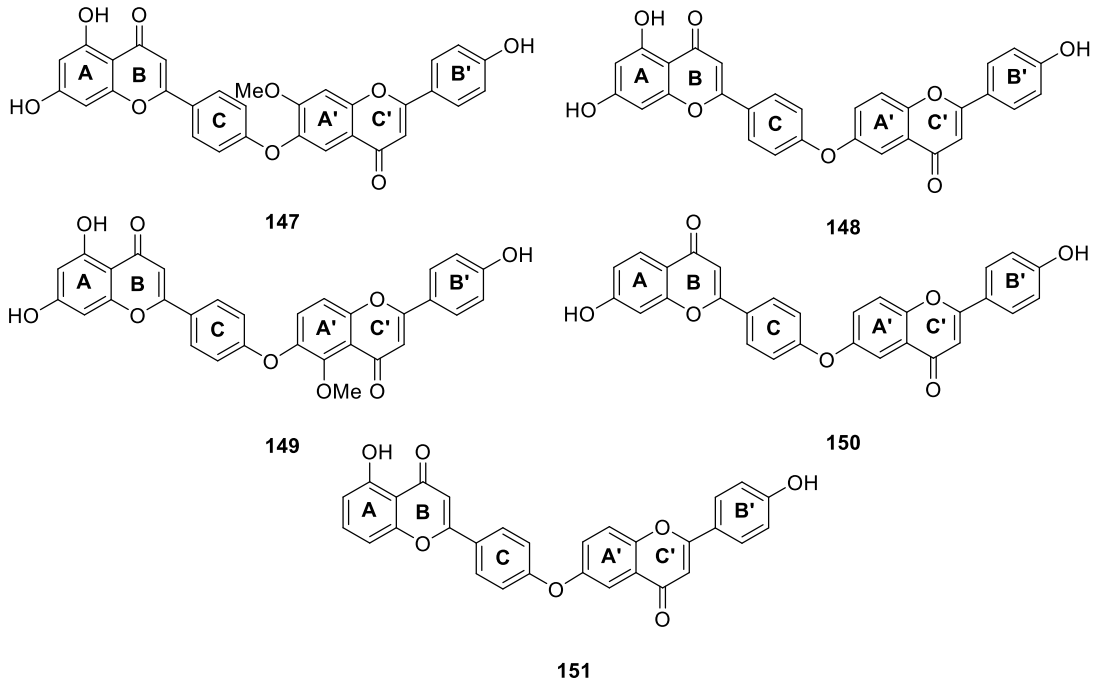

Figure 22 Hinokiflavone analogues

Although these analogues covered a wide range of substitution patterns, none of them had the two hydroxyl groups on A' ring present in hinokiflavone. The two hydroxyl groups on the A' ring force hinokiflavone **9** to have a twist in its conformation (*figure 23*). Since none of these analogues were found to be active it suggested that this twist in the shape of hinokiflavone **9** is important for its biological activity.

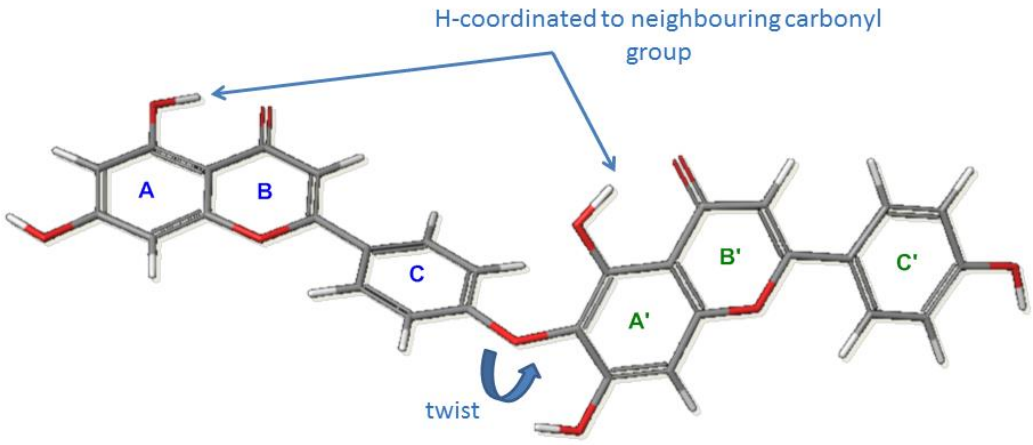

Figure 23 Computational model of hinokiflavone

Hence, a new strategy was required for making this biflavonoid. Since the problematic step seemed to be the coupling to make the biaryl ether, it was decided that it should be done relatively early in the synthesis. This way the unsuccessful coupling conditions could be disregarded early and with minimum cost to time and materials. As the flavones would be built up during the synthesis it would be possible to synthesise libraries of analogues with late stage divergent synthesis The simpler coupling partners would also not have such poor solubility as they would not be quite as flat, and they would be more reactive, since reactivity would be easier to control earlier in the synthesis. The reactivity could be controlled by choosing particular functional groups to favour the electronics of the system towards nucleophilic aromatic substitution. In addition, better solubility and smaller size would make these compounds easier to work with and potentially less sensitive to high temperatures if it would be necessary to force the reaction. As the monomers had already been synthesised they would be utilised for the total synthesis, once the key nucleophilic coupling was optimised.[81]

As well as the total synthesis of hinokiflavone **9**, it was the aim of this project to synthesise structural analogues of hinokiflavone **9** to perhaps find an analogue with better physical properties and cellular activity than hinokiflavone **9**. We also wanted to study the structure activity relationships of hinokiflavone **9** with its target and find the target protein of hinokiflavone **9**. Since a number of analogues that differed by their substitution patterns had already been synthesised by Haahr and Logan; analogues that relied on simplified structures would also be explored in this work. [81, 84]

2.2.4 Hinokiflavone and target identification

To study the spliceosome and find the target that was causing the cellular effects, small molecular probes, based on hinokiflavone **9**, were required. The main aim was to isolate and then study hinokiflavone's cellular target. Possible probes needed to fulfil two main functions: binding to the protein target and allowing for the isolation or identification of that target. These probes needed to be composed of several units: a small molecule ligand, a linker and a reporter molecule such as a fluorophore, to facilitate identification, or biotin, to facilitate isolation.[85] Hence probes composed of hinokiflavone **9** and linkers that could be attached to either fluorophores or biotin were designed (*figure 24*). They would be composed of either hinokiflavone itself or a suitable analogue linked to a tag for biorthogonal chemistry, biotin or to a fluorophore that could then be used to elucidate the exact target of hinokiflavone in the cell.

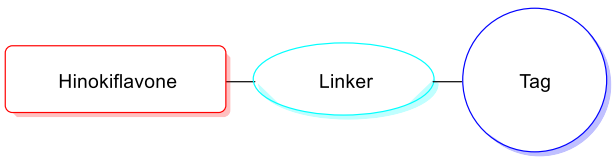

Figure 24

There now exist over 20 different biorthogonal reactions that can be chosen from when designing molecular probes.[86] As there was minimal information about hinokiflavones **9** target when this project was started, a versatile approach to probe design was needed. Hence our probes were designed to have an azide tag **152** attached by a linker to hinokiflavone **9** (*scheme 34*). The azide **152** could then be used in different ways. It could be used to attach a fluorescent marker or a biotin affinity tag either *in vitro* using copper catalysed

click chemistry[85] or *in vivo* by using copper free click chemistry with strained alkynes **155**. Azides **152** can also be reacted using Straudinger ligation[87] or if need be reduced to amines **160** to make amides **161**. Hence basing our probe design around azides would give a lot of flexibility in the eventual use of the probes. Azides can also be used as photoactivated crosslinkers.[88]

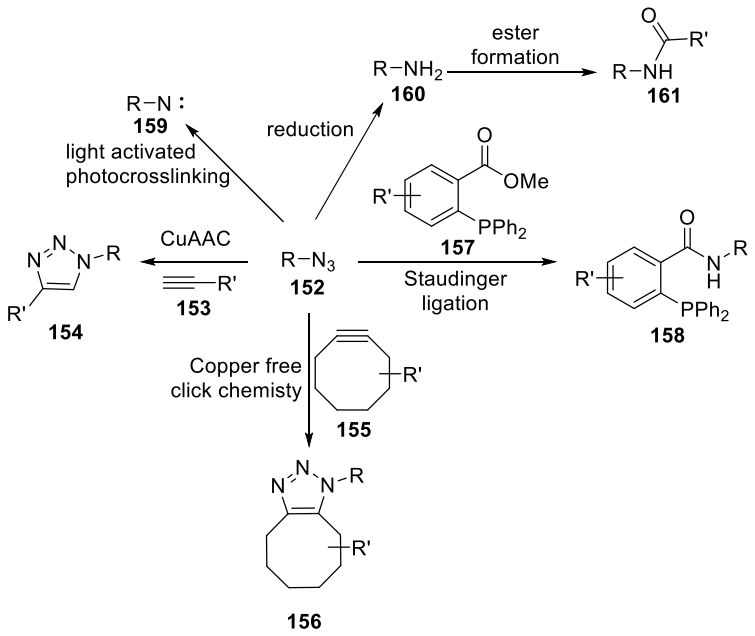

Scheme 34

3 Synthetic efforts towards Hinokiflavone

3.1 Binary ether formation and synthetic approach 1

Since the central coupling step had caused problems in the synthesis before, it was decided that by bringing it forward in the synthesis these problems could perhaps be circumvented. Hence, the new synthetic approach would first construct the central ether linkage and then focus on the building of the flavone ring systems (*Scheme 35*). Protected hinokiflavone **162** would be constructed from the compound **163**. The central ether in **163** would be made by an S_nAr reaction from benzoic acid **164** and a protected RHS system **165**.

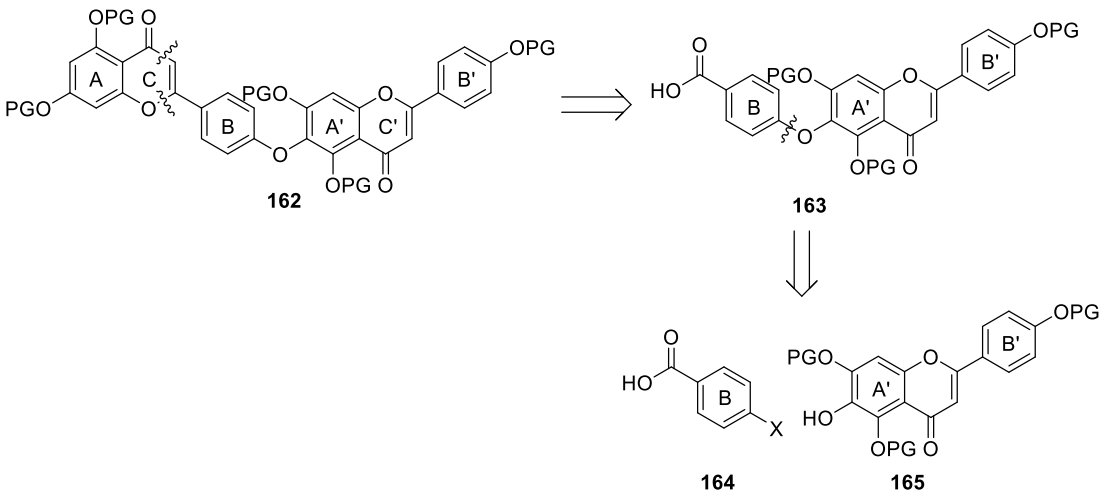

Scheme 35

To optimise conditions for the central coupling, first a model system was used. Trimethoxyphenol **167** was chosen as a mimic of the A' ring on the A'C'B' also referred to from here on as the right hand side (RHS) ring systems. It was synthesised from trimethoxybenzaldehyde **166** in good yield using acid-catalysed Dakin oxidation[8] (*scheme 36*). The substitution pattern in phenol **167** was thought to be a good model of the A'C'B' ring systems of hinokiflavone, mimicking the rather sterically hindered central phenol on the A' ring. The analogues without di-substitution around the A' ring had already been shown not to be active by previous research in the Hartley group. Hence reaction that would work under there sterically hindered conditions would be developed. *P*-Fluorobenzoic acid **168** was used as a mimic for the B ring. It also contains

appropriate functionality to subsequently build up the A and C ring systems. The acid group of the ether **169** would improve solubility and simplify workups.

Initially direct coupling between *p*-fluorobenzoic acid **168** and trimethoxyphenol **167** was attempted. The reaction failed to work in the model system (*scheme 36*). This was thought to be due to steric hindrance around the reacting phenoxide and the relatively high pKa of the electron-rich phenol **167**.

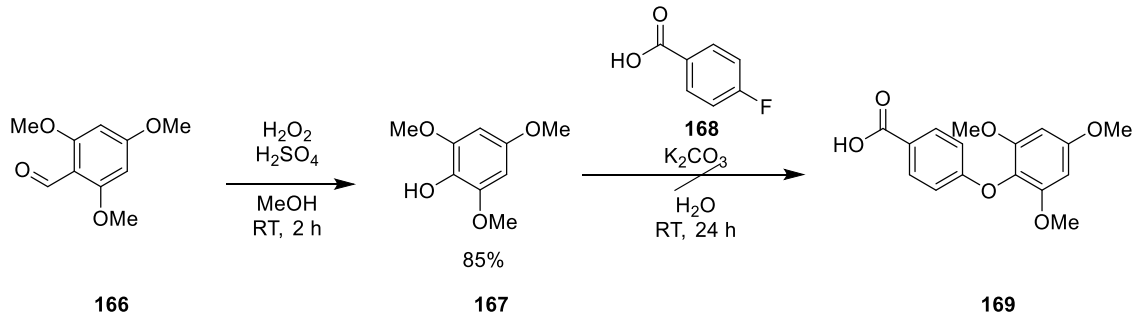

Scheme 36

The acid group on the *p*-fluorobenzoic acid **168** was protected under Fisher esterification[9] conditions in good yield. The S_NAr reaction was then reattempted with the methyl ester **167** (*scheme 37*). This still did not produce the desired product **171**.

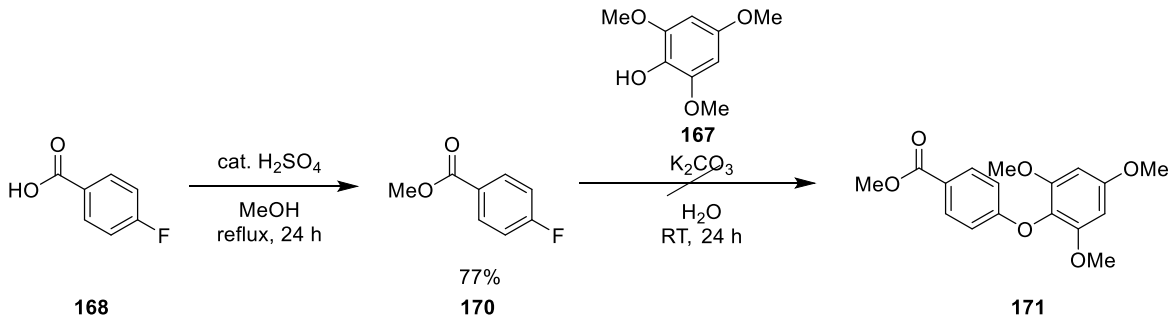

Scheme 37

Therefore, attention was turned towards reactivity of the starting materials, and an attempt was made to increase the electrophilicity of the aryl fluoride. To improve reactivity an electron-withdrawing nitro group was inctroduced on the *p*-fluorobenzoic acid (compound **172**). With the ring thus activated towards nucleophilic attack, the reaction proceeded in good yield to give the diaryl ether **173** (*scheme 38*).

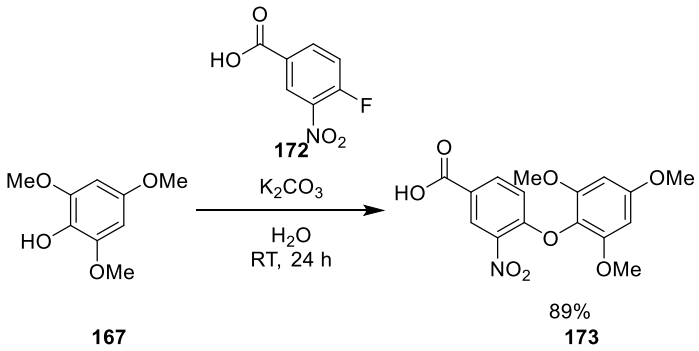

Scheme 38

With the activating group in place, the coupling between the *para*-fluorobenzoic acid **172** and phenol **174**, was attempted (*scheme 39*). The dimethyl protected flavanol **174**, a model of the RHS A'C'B' rings systems, was synthesised previously by Adam Haahr in the Hartley group; it differs from the actual hinokiflavone RHS by having no substituents on the B' ring. The reaction proceeded in good yield illustrating the power of the activating nitro group in facilitating these S_NAr reactions. It was expected that the central ether formation would proceed equally well with an additional 4-methoxy substituent on the B' ring and thus attention was turned towards building up the AC ring system.

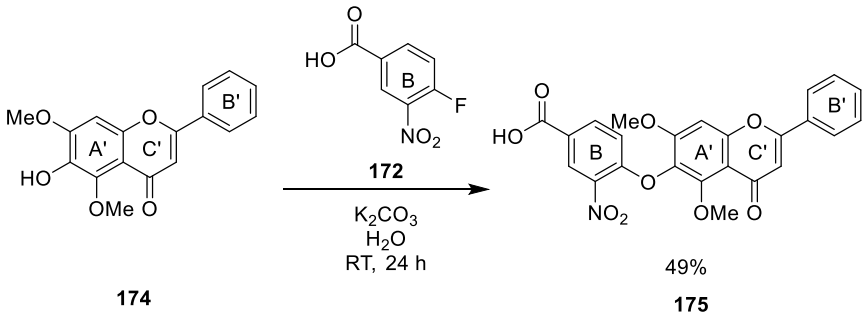

Scheme 39

To explore the different synthetic approaches that could lead to hinokiflavone attention was turned again towards the model system **173**. It was not clear to begin with whether the activating nitro group should be removed right away to give acid **169** or further along the synthesis when the A and C the ring systems of the LHS had already been formed in flavone **176**. Both routes to flavone **177** were therefore explored to find the superior one (*scheme 40*).

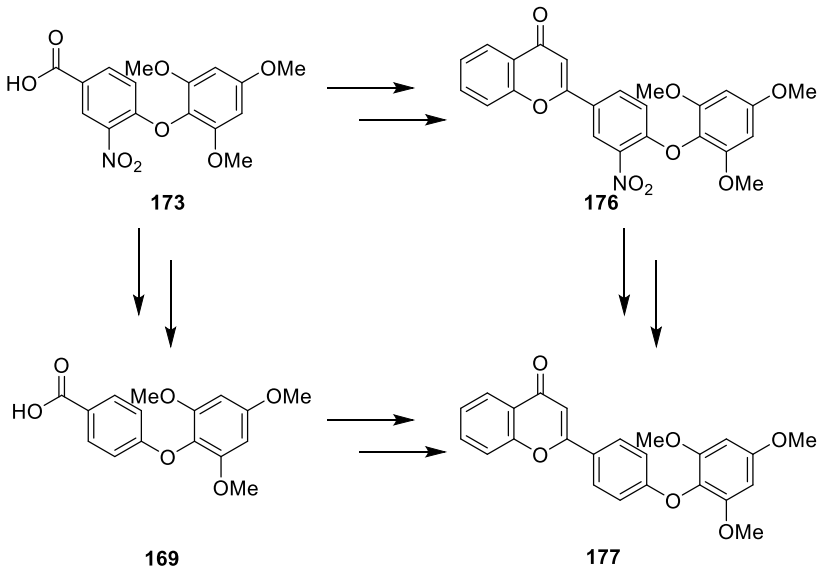

Scheme 40

Initial ACB ring constructions were attempted with the nitro group still in place, with the aim of removing it further along the synthesis. Hence the diaryl ether **173** was coupled to 2-hydroxyacetophenone **64** using DCC in acetonitrile in good yield to form the ester **178** (identified by ^{1}H NMR only) (*scheme 41*). This intermediate **178** was then cyclised to flavone **177** utilising previously used cyclisation conditions from the Hartley group.[34] The cyclisation proceeded in a poor yield, but was never optimised as the following reduction reaction, to reduce the nitro group, failed to proceed at all (*scheme 41*).

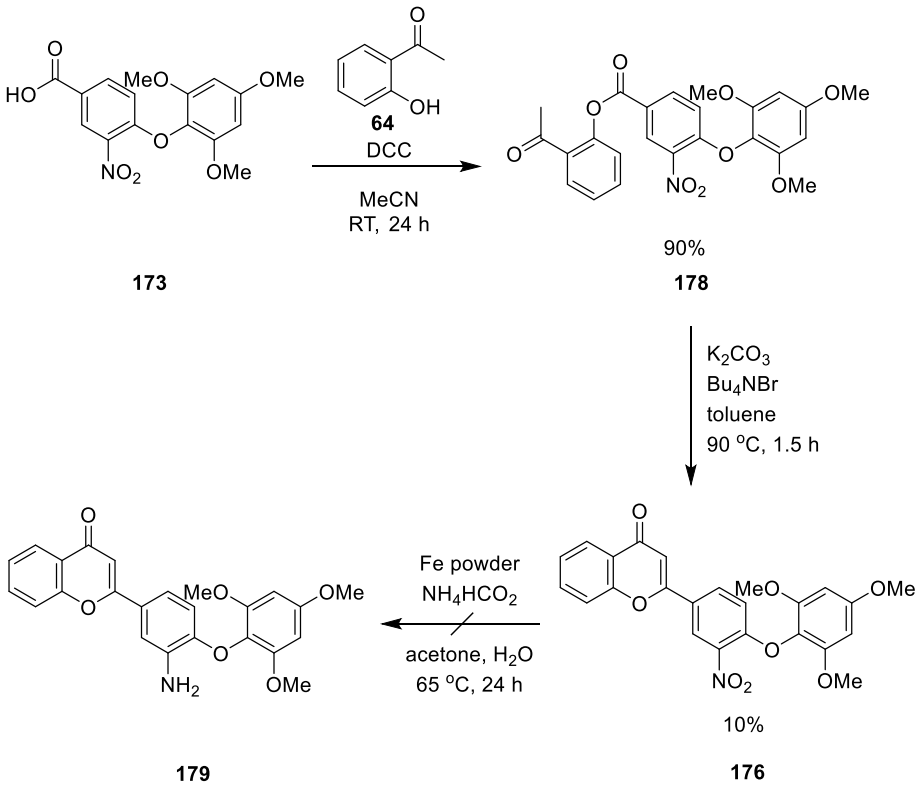

Scheme 41

The problems encountered in the experiments that followed, and indeed throughout this synthesis were due to the abysmal solubility of flavonoids in most organic and aqueous solvent systems. This makes them difficult to isolate and purify and complicates the characterisation but most importantly impacts reactivity under some conditions.

To follow the other line of enquiry then, the removal of the nitro group at the start of the synthesis was also investigated. Reduction of nitroarene **173** using hydrogen gas with palladium on carbon were first tested but failed with starting material **173** recovered unchanged.

Iron powder with ammonium formate was tested next in a mixture of water and acetone. Ammonium chloride is usually used for this type of reduction, but formate was used as the counter-ion in this case in the hope of increasing the water-solubility of the nitroarene **173** and aniline product **180** by deprotonating the acid group. The reaction proceeded particularly well on the model system **173** (*scheme 42*).

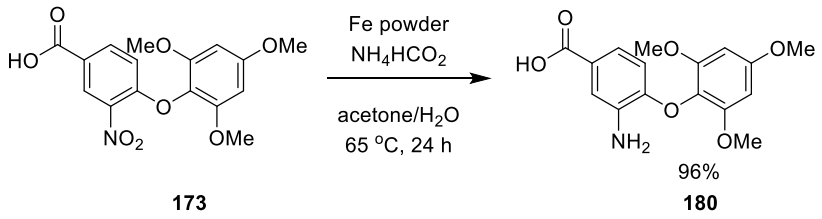

173 **180**

Scheme 42

The amino group was then removed under standard conditions, by first converting it to a diazonium ion and then reducing it with phosphinic acid. This afforded the desired diaryl ether **169** in good yield (*scheme 43*). The ether **169** was then coupled to 2-hydroxyacetophenone **64**, and this time HBTU afforded the best yield for the formation of ester **181**.

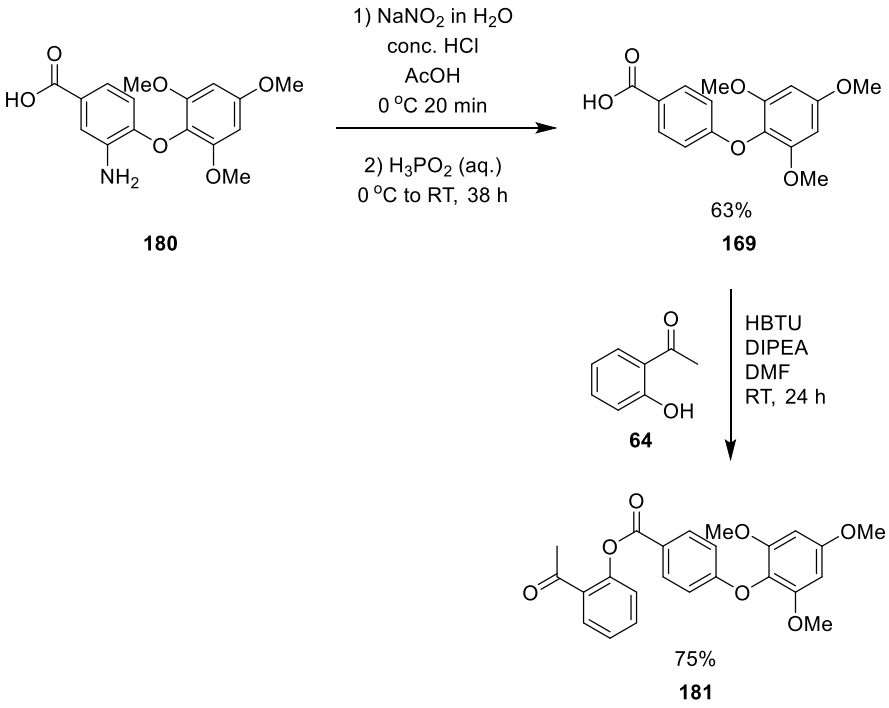

180 **169** **64** **181**

Scheme 43

At this point the attention was turned again to the more complete model of the hinokiflavone LHS to see if the optimised conditions developed for the model would work. The iron powder reductions that had been very reliable on the model system **173** failed to work on **175** and only traces of the desired amino compound **182** were isolated. It should be noted that the yield was not poor because the reaction did not proceed to the product, rather there was very little mass recovery from the reaction (*scheme 44*). The small scale of the reactions made it initially difficult to determine what was happening but eventually the

following hypothesis was reached. The solubility, already poor for most of these compounds, was further decreased by the product being a zwitterion. It was concluded that as the product formed, it must have crystallised onto the iron powder. Several attempts were made to recover the product, however these were not successful. A different reduction strategy was therefore sought.

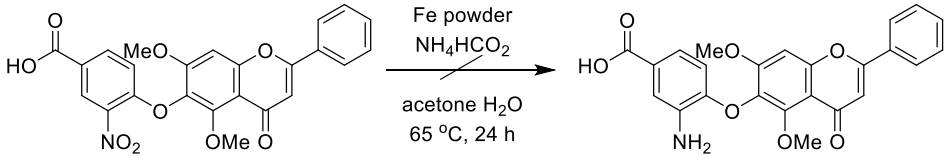

175 **182**

Scheme 44

The new reduction strategy was first tested on the model compound **173**. Reduction with sodium dithionate in a mixture of DMF, water and acetic acid produced the desired aniline **180** in an inferior yield compared to the iron reduction method that had been used before (*scheme 45*). It did have the advantage of being a homogeneous reaction and therefore less likely to result in irretrievable precipitation of product.

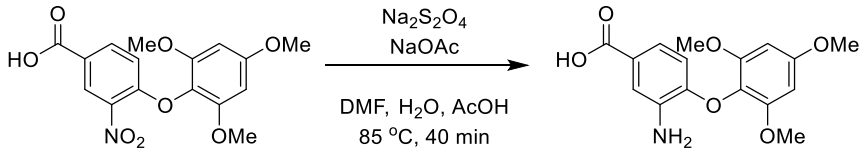

173 39% **180**

Scheme 45

At this point in the synthesis the methyl and benzyl protected RHS flavonoid **145** was used instead of the model used previously, these were also available from the work of Adam Haahr. The ether formation proceeded even better in the case of flavone **145**, perhaps due to the cross-conjugation of the para-oxygen atom and the electron withdrawing ketone marginally lowering the pKa of the phenolic hydroxyl group. The desired aryl ether **184** was isolated in excellent yield (*scheme 46*).

The nitro compound **184** was then subjected to the reduction conditions using sodium dithionite (*scheme 46*). This time the product **185** was isolated in good

yield (product tentatively identified by ^{1}H NMR only). The poor solubility of the amino compound **185** simplified the efforts to isolate it as compound **185** crystallised out of solution and was therefore easy to purify by filtration. The amino group was then removed, as before, with sodium nitrite followed by phosphinic acid to give ester **186** in excellent yield (product tentatively identified by ^{1}H NMR only).

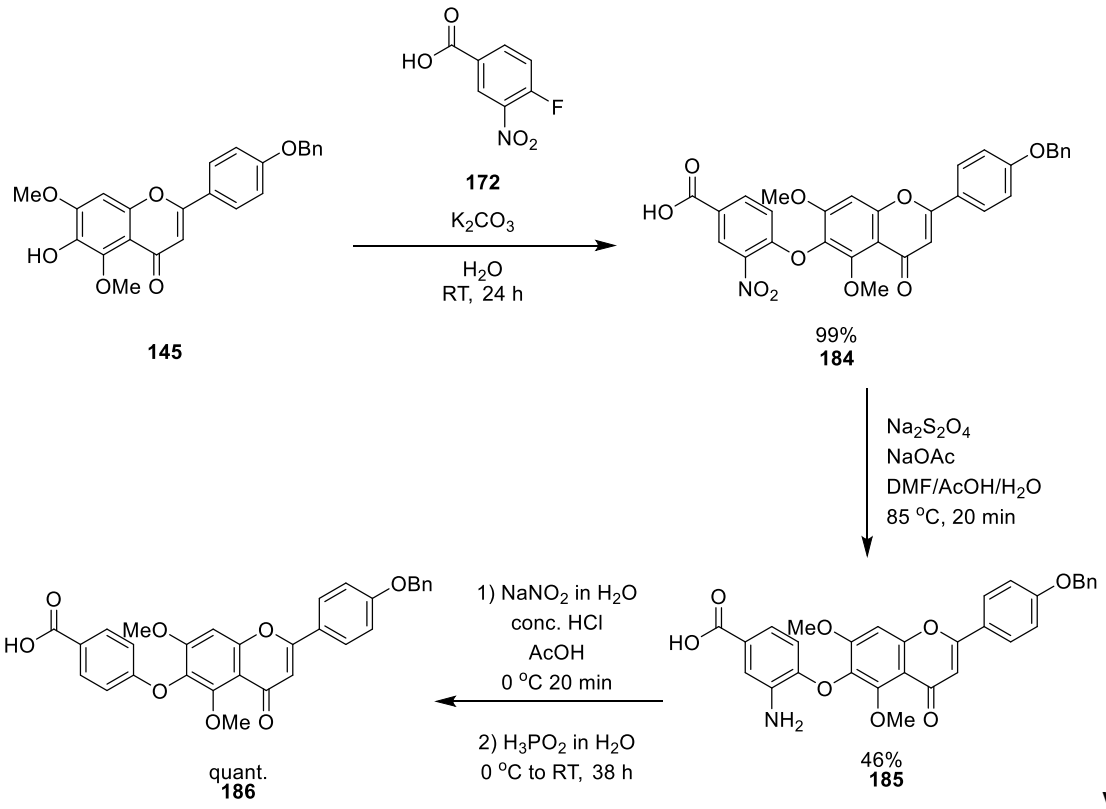

we

Scheme 46

To test the cyclisation conditions a new model system **188** was built (*scheme 47*) composed of a much simpler benzyl **187** unit with only a *p*-methoxy group and a dibenzyl protected trihydroxy acetophenone **138** (*scheme 47*). This in turn was synthesised by first benzyl protecting chrysin **137** to form chrysin derivative **136** and then hydrolysing it under basic conditions to acetophenone **138**.[34, 84] Altogether the model system was achieved in good yield.

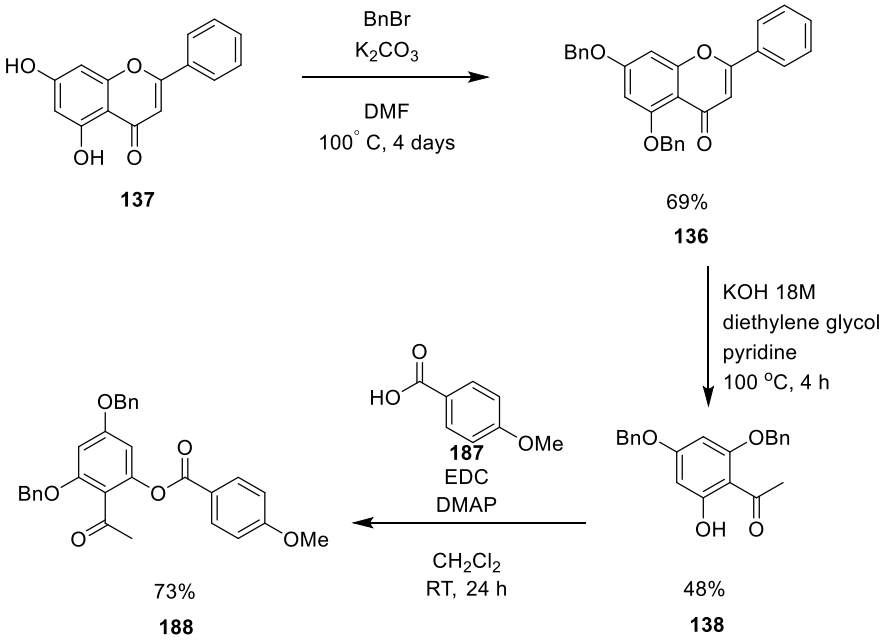

Scheme 47

An array of base catalysed Baker-Ventrakatraman reactions were then attempted (*table 1*).[34] All of these reactions resulted in very disappointing outcomes. In most cases unidentified mixtures were achieved, as with potassium carbonate, and in the case of sodium hydride, no reaction took place at all. In the cases of mixtures, these were not further analysed since they did not seem to contain the desired product **189**.

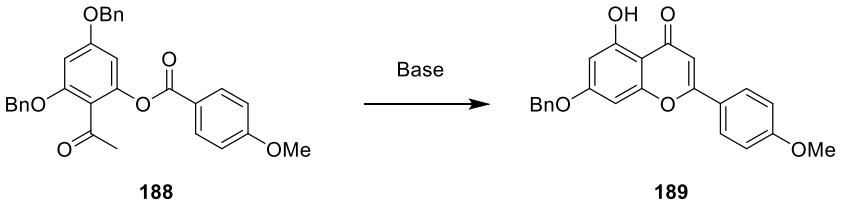

Base	Additive	Solvent	Time	Temperature	outcome
NaH	-	toluene	3.5 h	80 °C	SM
K_2CO_3	Bu_4NBr	toluene	1.5 h	90 °C	mixture
KO^tBu	-	toluene	24 h	90 °C	mixture
KOH	-	pyridine	3 h	120 °C	mixture

Table 1

A different approach was taken using phosphazene base instead of using conventional bases. Phosphazene bases are incredibly strong bases that are only weakly nucleophilic.[34] They have been used previously in the Hartley group to synthesise flavonoids. Hence the cyclisation of ester **188** was attempted with

tert-butylimino-tri(pyrrolidino)phosphorane (BTPP) base (*scheme 48*). The desired compound **189** was successfully isolated on this occasion. The mono debenzilation was expected from precedent [34]. However, an interesting point to note is that 35% of demethylated product **190** was also isolated. The demethylated product seemed to form at the same time as the desired product **189**, since stopping the reaction early did not seem to diminish the proportion of the demethylated product **190** formed. Lowering the temperature and reducing the number of equivalents of BTPP also did not affect the formation of the undesired deprotected product **190**, while both adversely affected the overall yield of the reaction.

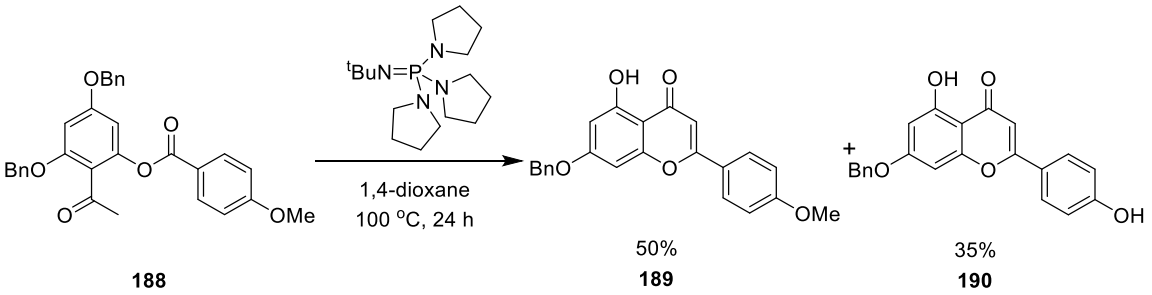

Scheme 48

With the model system conditions solved, synthesis of hinokiflavone was resumed (*scheme 49*). First, the ester was formed from acid **186** using EDC in quantitative yield then the ester **191** was cyclised with BTPP. Unfortunately the cyclisation did not proceed as expected on compound **191** and no protected hinokiflavone **192** was ever isolated. No further cyclisations were attempted with other bases due to limited material restrictions and the earlier disappointing results. Instead a different route was sought.

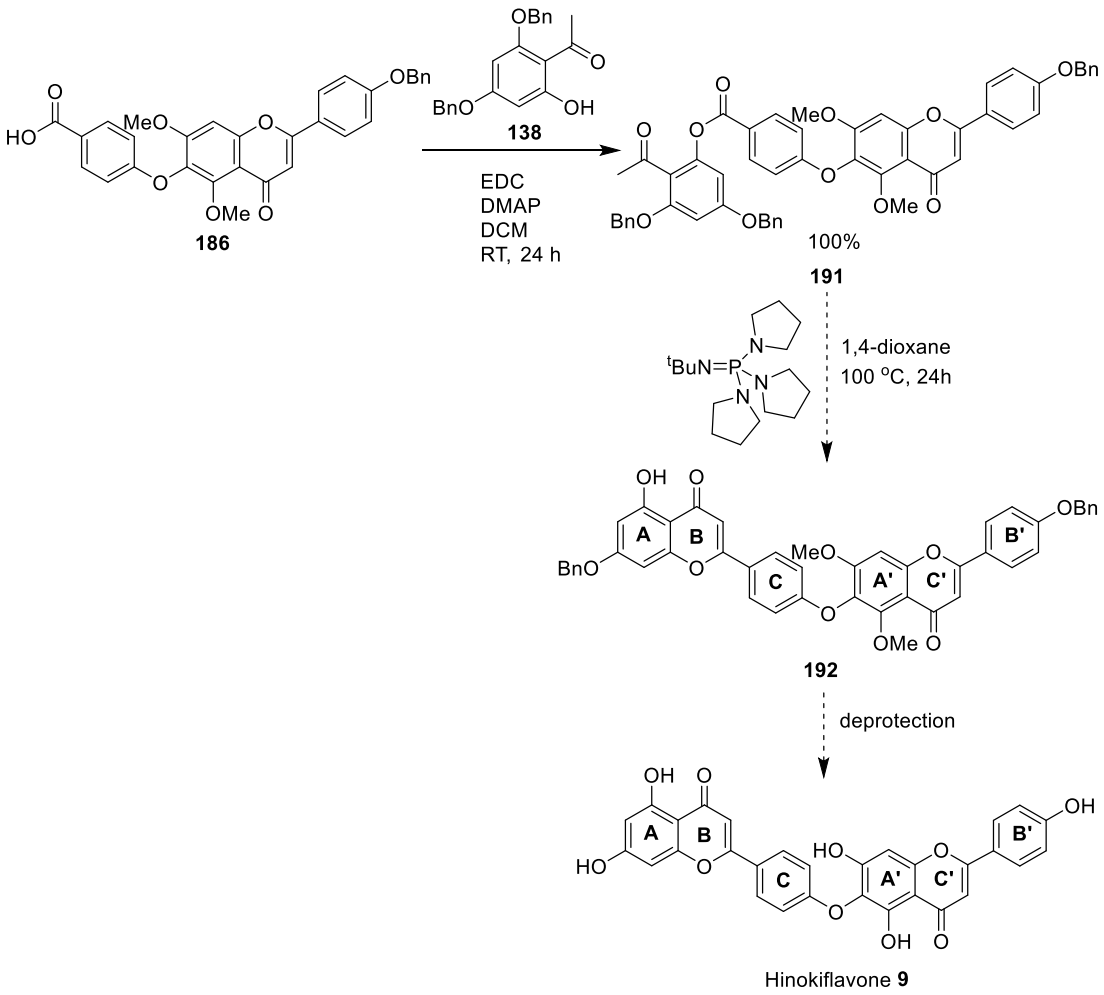

Scheme 49

3.2 Synthetic approach 2

Instead of attempting to form the LHS after the central ether formation was completed, a more convergent strategy was tested. Both the LHS **193** and the RHS **194** would be synthesised in full, with the activating group already in place. After the coupling to give a biflavonoid **195** the activation group would be removed to give protected hinokiflavone **162**, which would then be deprotected to yield hinokiflavone **9** (*scheme 50*).

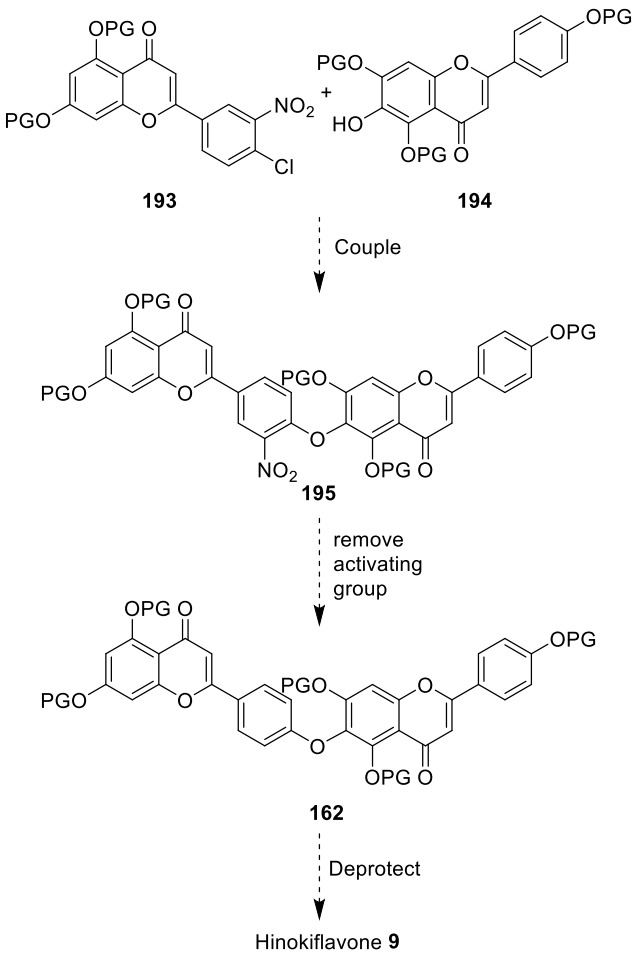

Scheme 50

This strategy was first tested by Lewis King in the Hartley group. The strategy was successful, but still suffered from the same problems as the synthetic routes before. Namely these flavones and aromatic systems had very poor solubility and the protective methyl groups were sometimes difficult to remove. Even when deprotected, the impurities with some methyl protecting groups still on, proved to be difficult to purify even on an HPLC system.

Using benzyl protecting groups made the deprotections easier but compounded the difficulties with solubility due to facilitating even more π stacking interactions. Monomethyl methyl ether (MOM) protecting groups were also used during this project, but these had opposite problems to the methyl protecting groups, not being stable enough and hence led to poorer yields. Therefore, a new protecting group was sought. The protecting group would have to be stable enough to withstand some of the harsher reaction conditions, while being labile enough to be completely removed from all five of the phenol groups in hinokiflavone. If the protecting group could also hinder some of the π-stacking

between the aromatic rings in these flavones and hence improve the solubility, all the better.

Hence the synthesis was carried out using isopropyl protecting groups that delivered all the aforementioned benefits of solubility and stability with easier deprotection conditions. The only drawback of using isopropyl protecting groups turned out to be the isopropoxy flavones exceptional solubility in organic solvents. We were unable to use some of our earlier purification methods that relied on crystallisation because the isopropyl protected compounds tended to be either oils or far too soluble to be easily precipitated.

The LHS of hinokiflavone was synthesised first, with the nitro activating group already in place (*scheme 51*). Trihydroxyacetophenone **141** was first diisopropyl protected. The hydrogen atom of the remaining *ortho*-hydroxy group is coordinated by the carbonyl group ensuring selectivity. This can be observed in the H-NMR spectra of these acetophenones as the *ortho*-hydroxyl group appears around 10 ppm while the other two hydroxyl groups appear around 3.5ppm in deuterated DMSO. The chalcone **196** was then formed by the Aldol condensation of the protected ketone **99** and the chloro-nitro-benzaldehyde **172**. The chalcone **196** was then cyclised to form the flavone **197** without further purification.

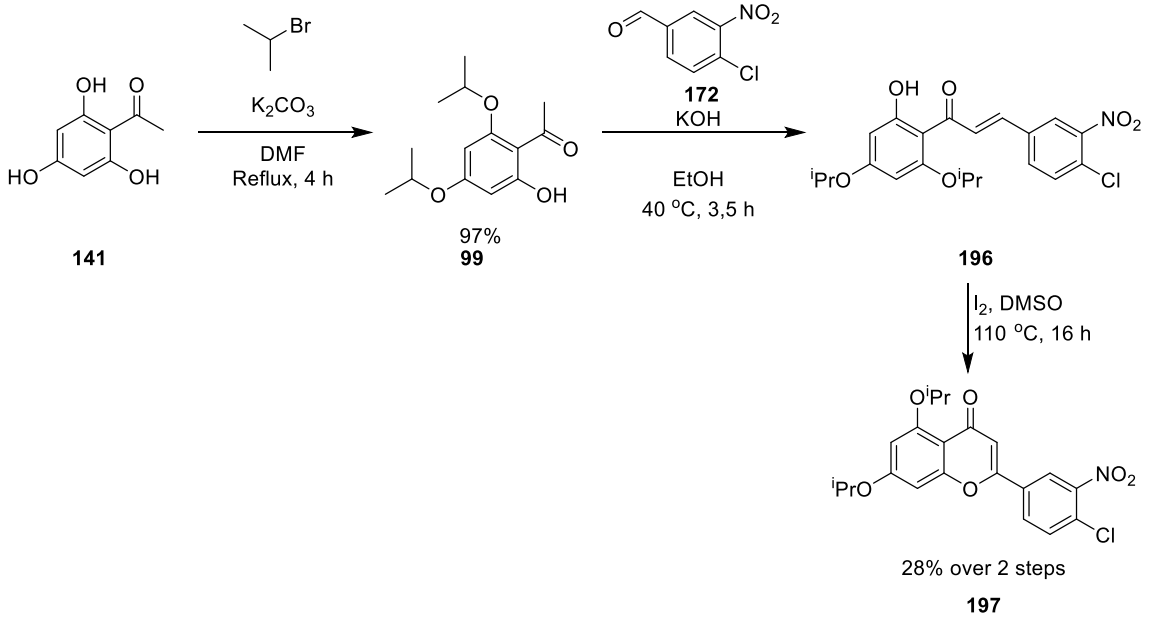

Scheme 51

The isopropyl protected LHS **197** was then coupled across to the methyl protected RHS **130** to form the ether **198**. The activating nitro group was reduced to form the amino compound **199** then removed to yield the protected hinokiflavone **200** (*scheme 52*). No purification was attempted at the amino stage, compound **199**, as the amino compounds tended to be hard to purify using column chromatography and the isopropyl compounds did not yield so easily to crystallisation.

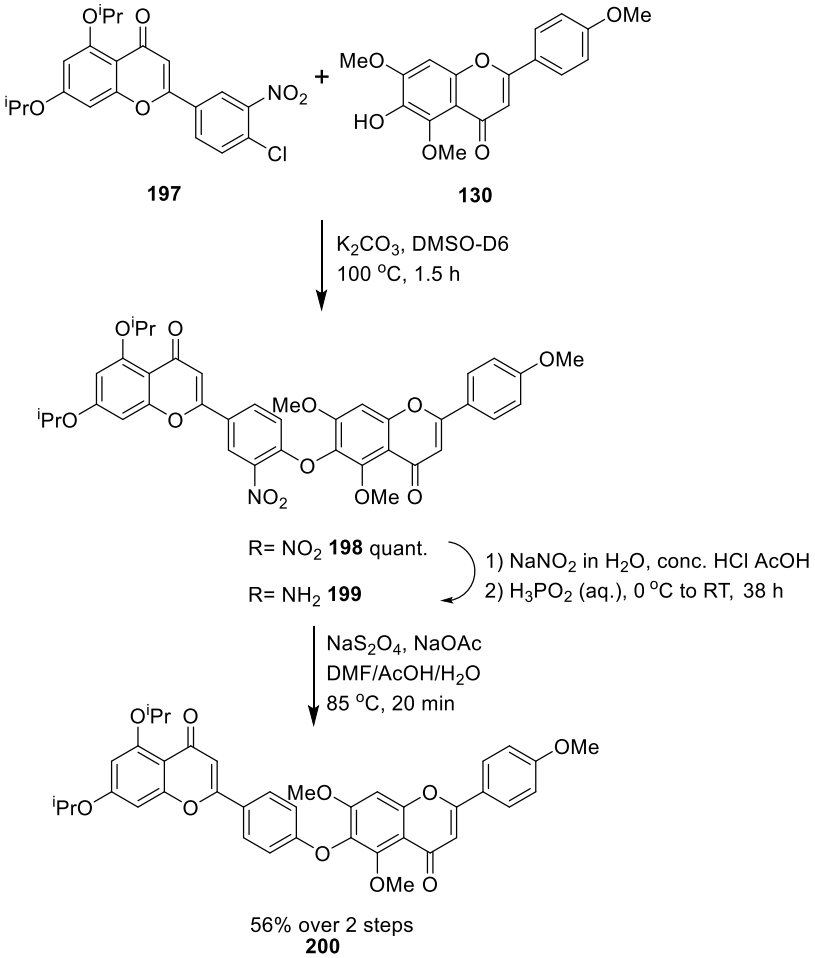

Scheme 52

Protected hinokiflavone **200** was then deprotected using boron tribromide (*scheme 53*). Here the difference between the isopropyl and the methyl protecting groups became really apparent as all the ispropyl ethers were cleaved after half an hour but the methyl groups were much harder to remove. The methoxy group at the C-7'' position proved to be impossible to remove using boron tribromide under these reaction conditions resulting in the partially protected compound **201**. This was not in itself surprising as previous synthesis of hinokiflavone **9** using methoxy protecting groups in the Hartley group resorted

to using hydroiodic acid for the deprotection step as boron tribromide was found not to be reactive enough. The reason for this is straightforward; the isopropyl groups are more easily removed than the methyl groups; the 5''-OH product is formed quickly because boron will be chelated by the 5''-OMe and the neighbouring carbonyl group and the 4'''-OMe is not sterically hindered.

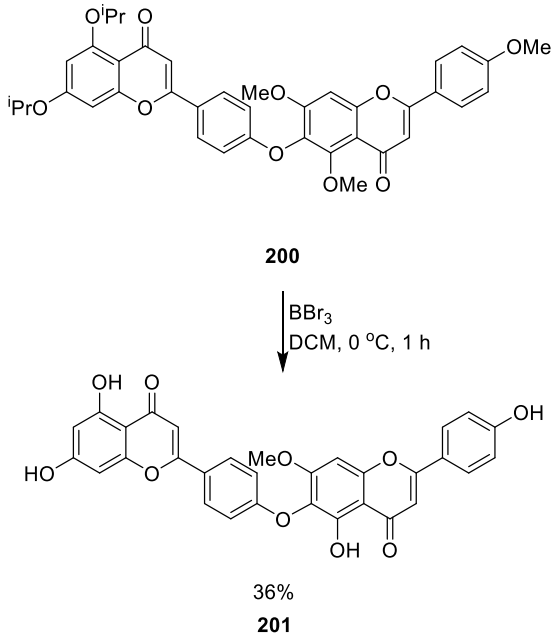

Scheme 53

Since the isopropoxy protecting groups did make a difference to the ease of synthesis and deprotection, a fully isopropoxy-protected RHS was synthesised next.

Previously prepared isopropoxy protected acetophenone **99** was converted to the desired compound **202** using the notoriously low yielding Elbs oxidation. Effort was taken to improve on the poor 21% yield but to no effect. Fortunately the synthesis of acetophenone **99** was straightforward and high yielding (*scheme 54*); hence, sufficient quantities of the *para*-diphenol **202** could be synthesised. The subsequent reactions were straightforward, monomethyl methyl ether protection of the new phenol allowed the chalchone formation to proceed in good yield, producing compound **205**. Cyclisation of chalchone **205** using the standard iodine/DMSO conditions yielded the desired flavone **206** in excellent yield. No separate deprotection steps were necessary as the MOM protecting group was labile under the cyclisation conditions.

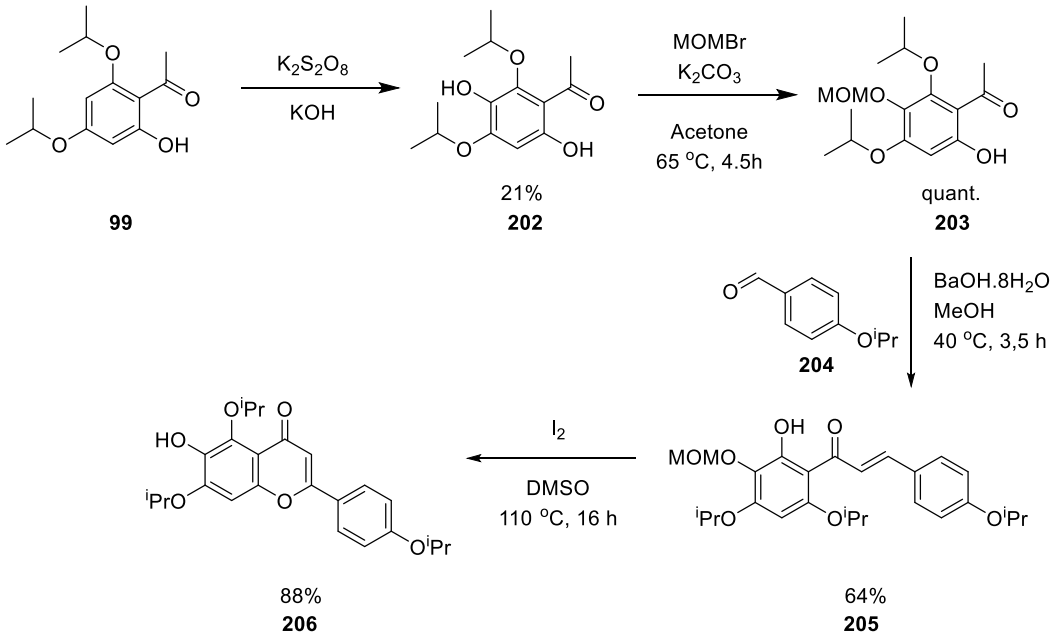

Scheme 54

The Isopropyl protected RHS **197** and LHS **206** were then coupled across (*scheme 55*) to yield compound **207**. The nitro diflavone **207** and the amino diflavone **208** were never purified as they were judged to be sufficiently pure by ^{1}H NMR conducted on the crude compounds for the subsequent reactions. Attempts to purify amine **208** by column chromatography only resulted in the loss of valuable material without any gain in purity. The overall yield of 27% over these three steps suggest individual yields of around 70% for each of the ester formation, reduction and amine removal.

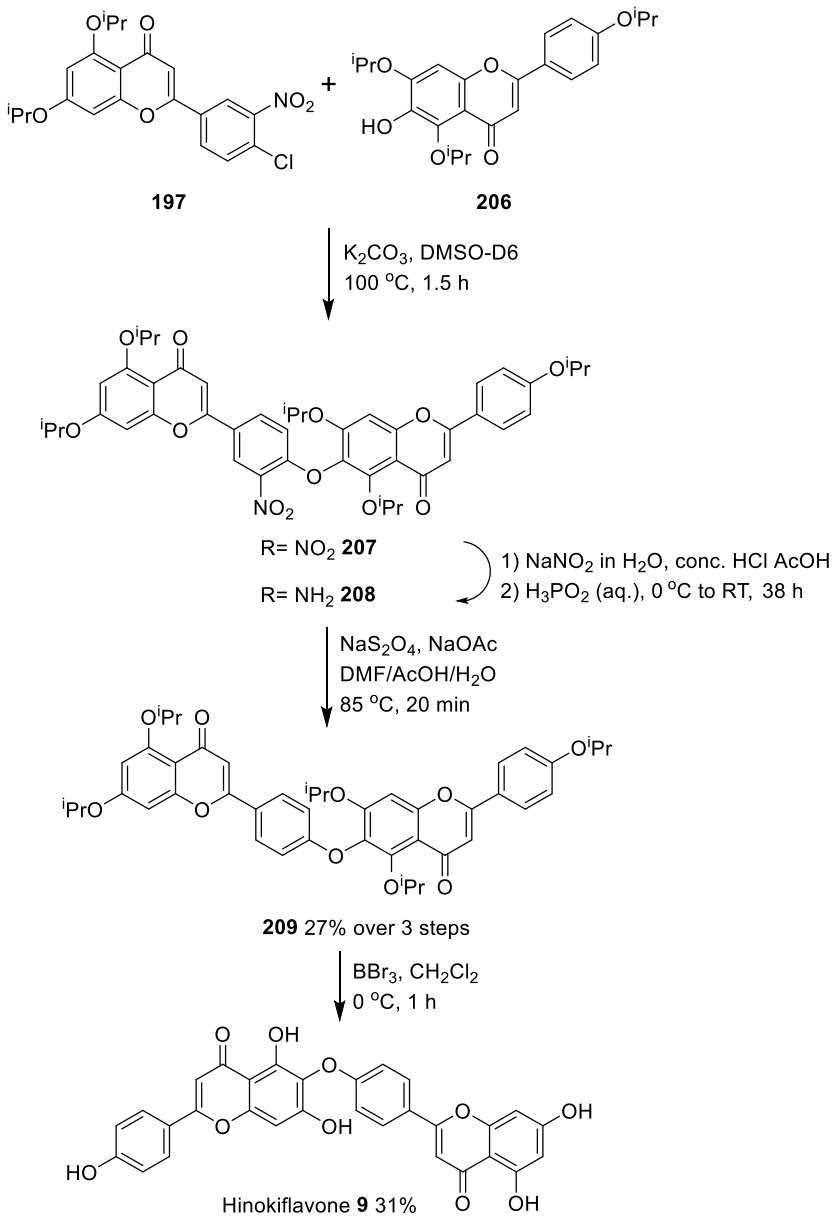

Scheme 55

After the removal of the amino group the protected hinokiflavone **209** was deprotected and recrystallised to yield pure hinokiflavone **9** (*scheme 55*). The yield for the final deprotection could be higher, the crude product was observed to be almost exclusively hinokiflavone **9**. However the recrystallisation proved to be tricky. Better yields could probably be achieved by either optimising the recrystallisation condition or by using a different purification technique, such as reverse phase column chromatography or HPLC purification.

In conclusion a robust synthetic route to hinokiflavone **9** was found, the key points in this synthesis were using a nitro activating group to facilitate the central S_NAr ether formation and using isopropoxyl protecting groups instead of

methoxyl ones. This allowed the isolation of hinokiflavone **9**, fulfilling the main aims of this thesis. The synthetic route allows for biological investigations independent of commercial availability of hinokiflavone **9**, that as mentioned before was sparse. However, to fully understand hinokiflavone's biological activity and find its binding target in the cell molecular probes based on hinokiflavone were needed. Hence tagged hinokiflavone analogues that could be used to fully elucidate its effect in cells became the next target.

4 Approaches towards tagged hinokiflavone

4.1 Direct attachment strategies

4.1.1 Attaching linkers to model system

Quercetin **210** was chosen as the model flavonol for investigating direct attachement of tags. It closely resembles the monomer unit of hinokiflavone and has the same number of phenolic hydroxy groups (*figure 25)*. Quercetin **210** itself has interesting biological activity, and there are clinical trials ongoing to demonstrate its effects on humans.[38, 89] Although results from these trials have not yet confirmed the health benefits of taking quercetin **210** as a supplement, it is available as such in some health stores. This makes it readily available and economical as a model, as well as an interesting target in its own right.

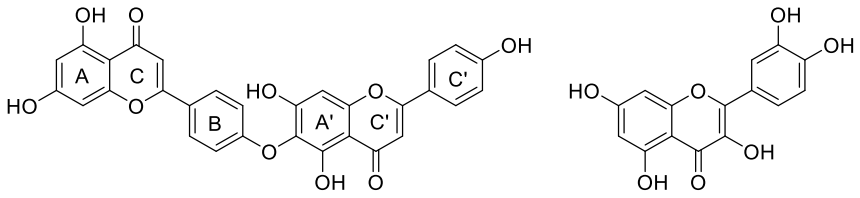

Hinokiflavone **9** Quercetin **210**

Figure 25

Since the reactivities of the phenolic hydroxyl groups in quercetin **210** differ[90] simple alkylation protocols were first investigated in the hope that this difference in reactivity would be enough to selectively synthesise one product **211** from reaction with an alkyl halide (*scheme 56*). The 4'-OH has the lowest pKa because the resulting oxyanion is in direct conjugation with the carbonyl group and is further stabilised by coordination to the hydrogen atom of the 3'OH. This means that the phenoxide produced by deprotonation at this site is the most abundant when a weak base is used, hence any reactions were predicted to occur there.[90]

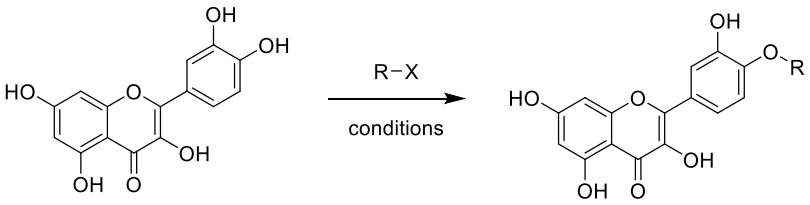

210 **211**

R = linker unit

Scheme 56

The linkers were synthesised first. These were derived from tetraethylene glycol (subsequently shortened to PEG throughout this report), designed to improve the physical properties of the flavonoids once attached. Both quercetin **210** and hinokiflavone **9** have solubility issues in general, as do most flavonoids, as they are flat aromatic molecules with many hydrogen bond donors and acceptors and hence favour π-stacking and hydrogen bonding. Attaching a PEG to them was predicted to improve their solubility in both organic solvents and water.

All of the linkers synthesised were designed to have a good leaving group for S_N2 reaction with the flavanol at one end and an azido tag at the other end to act as a handle for attaching the "chemical cargo", such as a biotin affinity tag, by biorthogonal chemistry.[91]

Following the route published by Jeong *et al.*[92] the tetraethylene glycol **212** was first mono-mesylated and then the mesylate substituted for the azido group (*scheme 57*). The yields for this reaction were moderate and un-desired di-substituted azido product **213** was also formed. Considering however, that the mono-substituted product **214** formation is entirely controlled by concentration effects, the yields are acceptable. The hydroxyl group on compound **214** was then exchanged for a chloride to form chloro-PEG **215**, using chemistry previously utilised in the Hartley group[82]. Iodinated PEG **216** was also synthesised as a more reactive analogue.

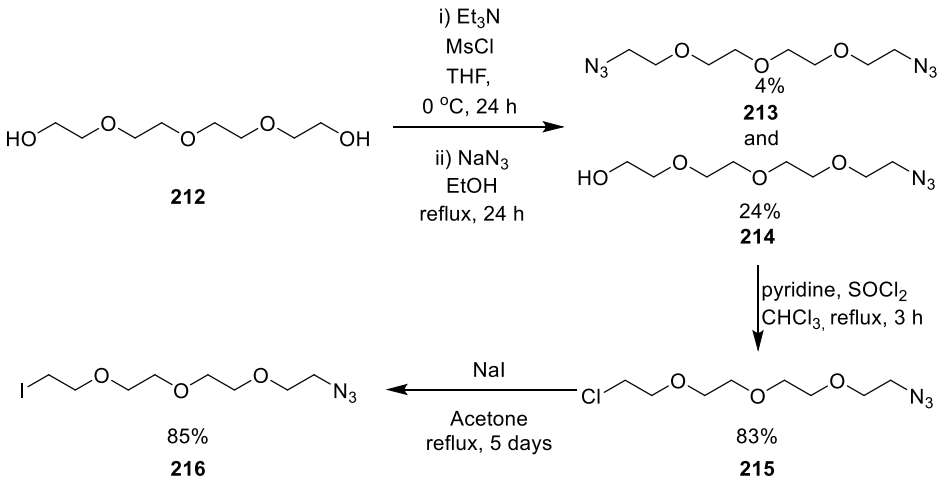

Scheme 57

The iodo compound was also prepared by a shorter, one-step synthesis directly from alcohol **216** (*scheme 58*).

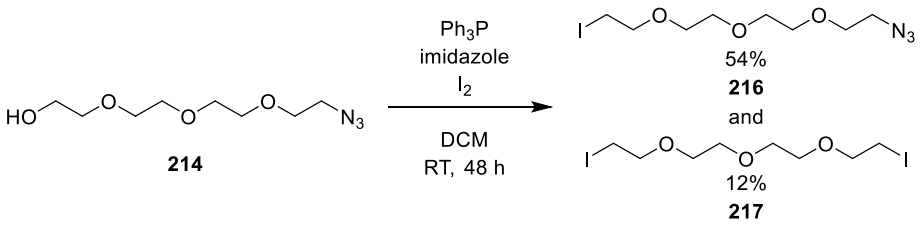

Scheme 58

Unfortunately, the chloro substituted PEG **215** did not react with quercetin **210** and only starting material could be isolated from the following reactions (*scheme 59*). The iodo compound **216** was then reacted with quercetin **210** using similar conditions (*table 2*). No single product was observed however and the reaction produced a mixture of compounds with mostly unreacted quercetin present.

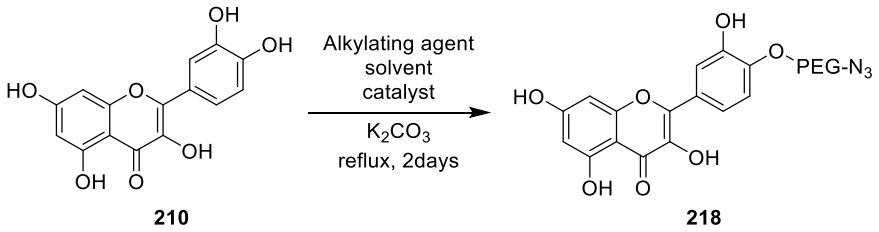

210 **218**

Scheme 59

Alkylating agent	Compound number	Solvent	Catalyst	Yield
Cl-PEG-N_3	**215**	Acetone	-	No reaction
Cl-PEG-N_3	**215**	Acetone	KI	Mixture
I-PEG-N_3	**216**	DMF	-	Mixture

Table 2

Since the simple strategy did not yield the desired results, a multistep strategy was embarked upon. Quercetin **210** was firstly be protected as the penta-acetate ester **219** and then reacted with the one of the halogenated PEG derivatives **215** or **216** (*scheme 60*). Literature precedence suggested that this could be done in one step by selective alcoholysis or hydrolysis under basic conditions.[42] In this case the 7-position was predicted to react first, as reported by Jurd because an oxyanion at this position is stabilised by conjugation to the carbonyl group and there is no 3'-OH to coordinate with for an oxyanion at the 4'-position. Hence the 7-OH is more reactive than the 4'-OH.

Quercetin **210** was protected, using methodology previously utilised in the group to yield the quercetin penta-acetate ester **219** in quantitative yield.[34] The protected quercetin **219** was then reacted with first the chloro-PEG **215** (*scheme 60*) with no apparent improvement in selectivity. The iodo-PEG **216** derivative was tested as well, again with no improvement in selectivity. Changing the base used from the literature precedented potassium carbonate to the bulky base potassium *tert*-butoxide made no difference to the selectivity of the reaction.

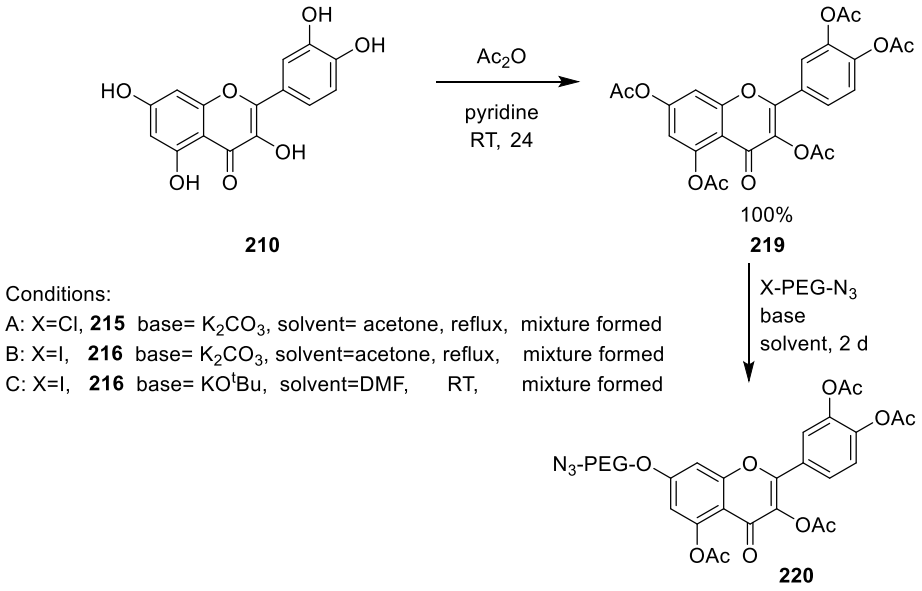

Scheme 59

Rethinking the strategy, it was realised that having several quercetin-PEG analogues where alkylation happened at different positions was perhaps not a disadvantage. Since the structure of the hinokiflavone binding protein was not yet known, it was difficult to judge which position would be best for attaching a linker to least affect binding. Having an array of molecules with linkers at different positions could be an advantage. Also, multistep syntheses, even if the reactions are selective and good yielding, are not always better than a one step, moderate yielding, synthesis. Since hinokiflavone **9** is an expensive starting material and selective reactions appeared elusive, it was decided that a better strategy would be to go for a single step alkylation and then separate the mixture afterwards, reusing any unreacted flavanol **9**. This way an array of compounds could be prepared which could be useful for biological screening later. Also, less material would be wasted than by using a multistep protection-deprotection route. However, the haloalkanes **215** and **216** suffered from slow reaction rates for the production of the aforementioned mixtures (*scheme 60 and table 2*). Since the selectivity of the reaction was already sacrificed, the speed of the reaction was judged to be non-compromisable, and hence more reactive alkylating agents were sought.

Iodoacetamides were the next target. The amide group is electron withdrawing and hence makes the adjacent carbon very susceptible to S_N2 reactions (*scheme 61*).

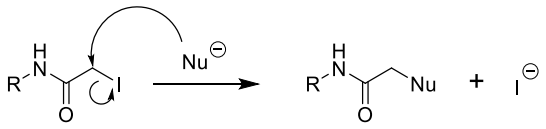

Scheme 60

To synthesise a tetraethylene glycol derived iodoacetamide, first a diazido-PEG **213** was synthesised. Mesylation and reaction with sodium azide to form the monoazido-PEG **221** had produced some of the diazido-PEG **213** as a side product, so this reaction was used (*scheme 62*).

Unexpectedly, the major product from this reaction was the mesyl-PEG derivative **221** with the desired diazido-PEG **213** produced present in only 35% yield (*scheme 62*). Reacting the mesyl-PEG **221** with more sodium azide produced the diazido-PEG **213** derivative, as expected, in 73% yield with the rest of the recovered material being starting material **212**.

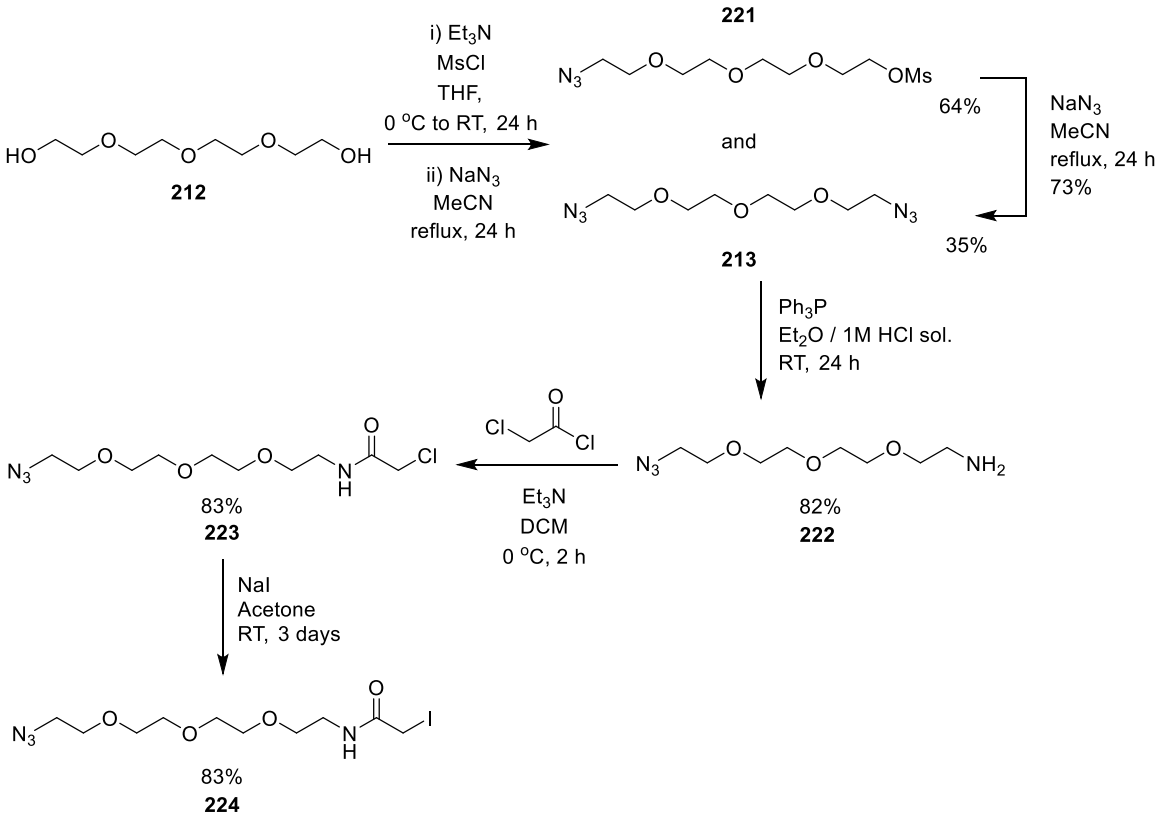

Scheme 61

Having thus made the diazido-PEG **213** derivative, it was selectively reduced to give exclusively the monoamino-PEG **222** in good yields (*scheme 62*), again utilising methodology previously employed in the Hartley group.[82]

The biphasic mixture allows for the selective Staudinger reduction of only one of the azides, as soon as one reduction has occurred the product **222** is pulled into the aqueous layer stopping the reaction. The monoamino-PEG **222** was then reacted with chloroacetyl chloride to give the chloroacetamide compound **223**. The iodoacetamide **224** was then formed by a simple Finkelstein reaction.

The unprotected quercetin **210** was then reacted with both the chloro and iodoacetamide, **223** and **224** respectively (*scheme 63*). The cloroacetamide **223** was not reactive enough and after 24 h only staring material was observed. The iodoacetamide **224** however, seemed to react much faster than any of the previously used alkylating agents.

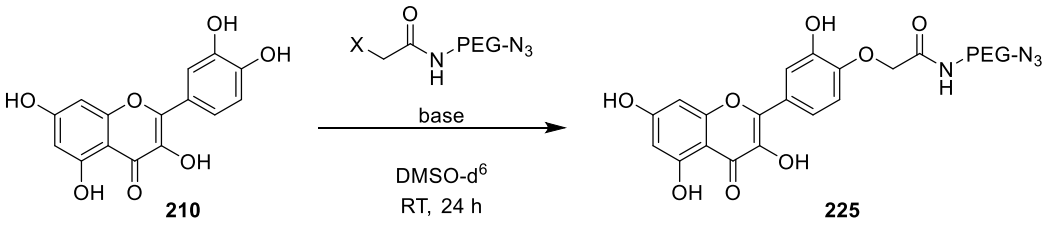

Conditions:
A: X=Cl, **223,** base= CsOH, no reaction
B: X=I, **224,** base= CsOH, mixture formed
C: X=I, **224,** base= KOH, mixture formed
D: X=I, **224,** base= Cs_2CO_3, mixture formed

Scheme 62

After caesium hydroxide several other bases were investigated. Potassium hydroxide gave similar results to caesium hydroxide, however caesium carbonate appeared to offer the fastest reaction rates, with least starting material left after 24 h based on the ^{1}H NMR spectrum of the crude material (*scheme 63*). It should be mentioned here that again all these experiments were carried out in deuterated solvents and directly in NMR tubes for the ease of monitoring with NMR. Since all the different bases tested gave similar mixtures with no selectivity apparent and differed only in the reaction rates, caesium carbonate conditions were chosen to be applied to hinokiflavone.

4.1.2 Attaching linkers to hinokiflavone

Hinokiflavone **9** was reacted with the iodoacetamide-tetraethylene glycol derivative **224** derivative under the conditions optimised using quercetin **210** (*scheme 64*). The reaction gave a promising mixture of compounds that were

separated using HPLC (C18 column, 0.1% TFA/MeCN). LC-MS suggested the presence of mono- and disubstituted hinokiflavone compounds as well as the unreacted starting hinokiflavone **9**. Separation of the mixture was attempted, unfortunately the products seemed to be unstable to even dilute concentrations of TFA (in the HPLC mobile phase) and also produced a very poor resolution on the HPLC. This was probably due to the effect of using a tetraethylene glycol linker which led to the broadening of the peaks and so making the purification and isolation of a single product problematic.

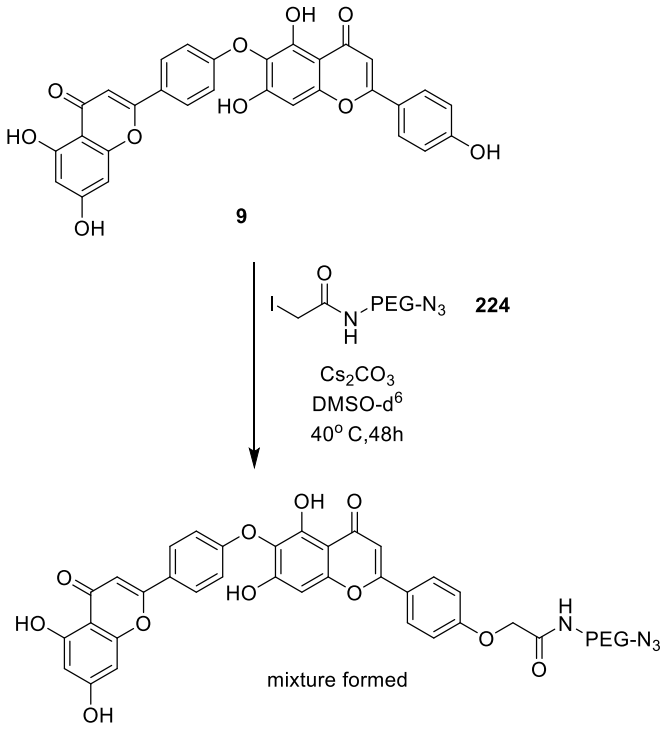

Scheme 63

In an attempt to solve the problems associated with having long polyethylene glycol chains, a smaller linker was chosen for direct functionalisation of hinokiflavone. Instead of an azido group bearing PEG, propargyl bromide was chosen because the alkyne could potentially be used for a copper (I) catalysed click reaction with an azido biotin derivative (*scheme 65*). The resulting mono-, di-, and trisubstituted hinokiflavone derivatives **226**, **227** and **228** were indeed successfully synthesised by Maria Schepinova, and separated and characterised within the group.

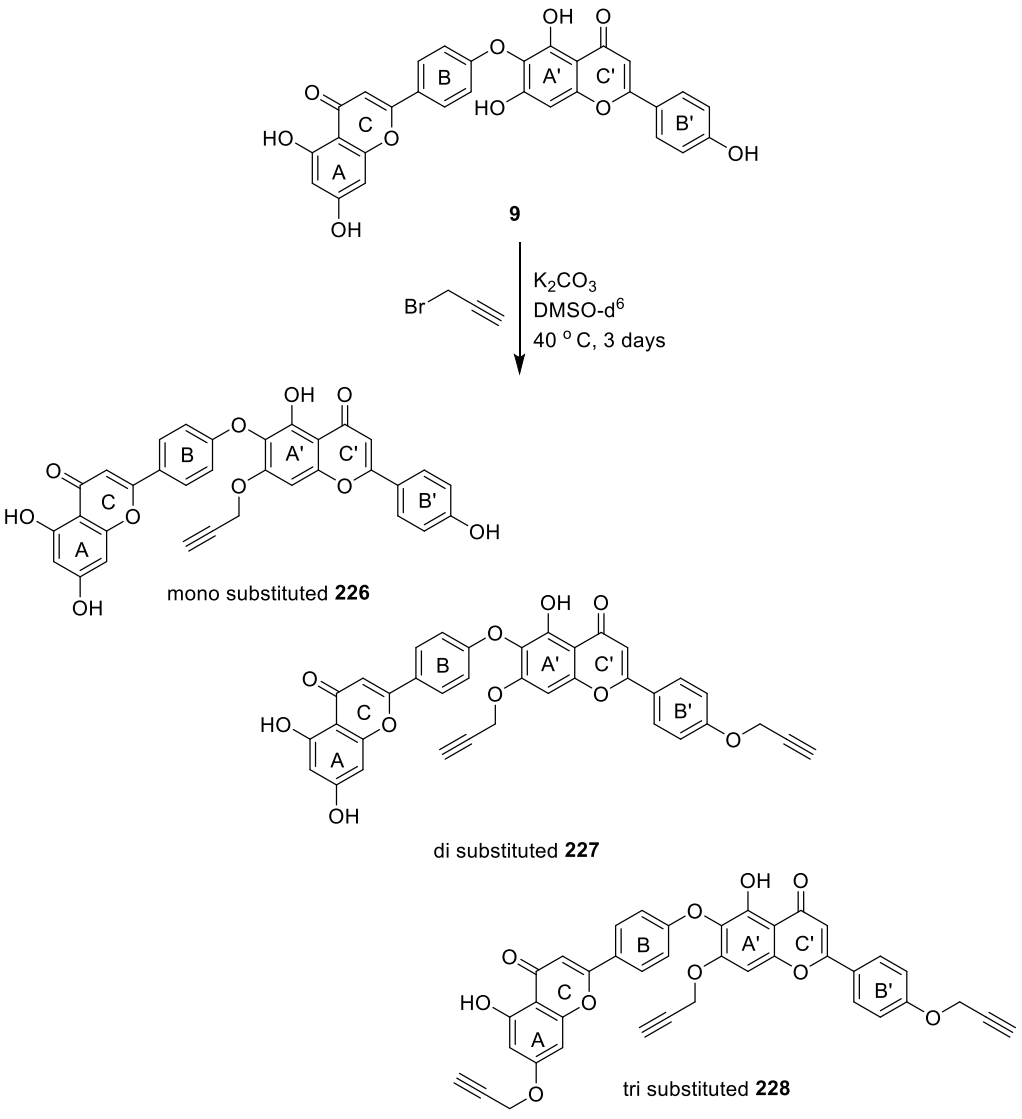

Scheme 64

After careful analysis by two dimensional H-^{1}NMR experiments it came apparent that the substitution occurred specifically first on the middle phenol (A' ring) (**226**) then on the B' ring (**227**) and finally on the A ring (**228**) (*scheme 65*). This was contrary to our prediction that the phenols A and B' ring would react first base on the reactivity observed on simple flavones such as quercetin. It was expected that the 7-OH on the A ring and the 4'''-OH on the B' ring would have the lowest pKa analogues to the 7-OH and the 4'-OH on quercetin being the most reactive. Reactivity on the 7''-OH on the A' ring was not expected as it is sterically hindered. However, this observation suggested that due to the twist around the central ether linkage the central oxygen is not conjugated to both flavone systems, only the ACB flavone. This makes it electron withdrawing by inductive effect on the A' ring lowering the pKa of the 7''-OH hydroxide. It has

already been observed that unless there is a neighbouring hydroxide the 4' position is not as reactive as the 7 position, so the 4'''-OH reacted second. The chelated phenols were untouched as predicted by the reaction conditions. This means that the 7-OH on the A ring reacted third. The following three compounds were hence obtained.

The propargyl hinokiflavone compounds **226**, **227** and **228** were sent for biological testing. Only the monosubstituted hinokiflavone **226** was found to be active in cells. This tells us that the relatively short propargyl group is tolerated on the A' ring.

4.2 Synthesising analogues with tags

To introduce tags on other positions apart from the A' ring on hinokiflavone **9**, the linkers would have to be introduced during the synthesis. This approach would allow more selectivity and control over the position of said linker. The A ring was chosen as the first target as it was not possible to install a linker on it selectively by direct alkylation of hinokiflavone.

4.2.1 Synthesis of tagged hydroxyacetophenones

One of the key intermediated in the synthesis of flavones is hydroxyacetophenone, it can be used in the synthesis of flavones *via* chalcones or any of the synthetic routes progressing through the hydroxyacetophenone itself (see section 2.1 on flavone synthesis). Hence using substituted acetophenones would allow for easy tagging of hinokiflavone on the A ring. However, it is usually not possible to directly selectively mono-alkylate trihydroxyacetophenone.

To install the linkers selectively on the A ring a strategy previously used in the Hartley group was employed, starting with chrysin **138** (*scheme 66*).[34, 81] Selective monoalkylation of the 7-OH of chrysin can be achieved easily as the 5-OH group is coordinated to the neighbouring carbonyl group and so has a higher pKa. This would allow for the synthesis of specifically modified acetophenones tagged in a specific position that could then be used to synthesise tagged hinokiflavone analogues.

Hence iodo-azido tetraethylene glycol **216** was selectively reacted with chrysin **137** in good yield. The mono-alkylated chrysin **229** was then submitted to standard base hydrolysis conditions (*scheme 66*). This however yielded no desired acetophenone **230**. It was assumed that the PEG linker decomposed under the extremely harsh hydrolysis conditions. Efforts were therefore turned towards hexane linkers. These would have less favourable solubility in aqueous systems but be more robust.

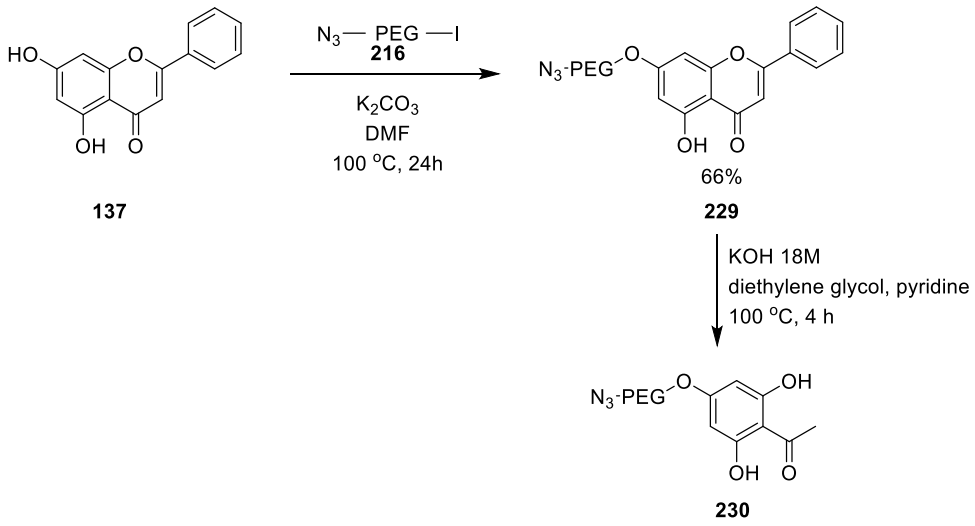

Scheme 65

At first dibromohexane **231** was used, however this did not result in the desired monoalkylated product (*scheme 67*). Instead elimination product, and perhaps predictably, chrysin dimer product **232** were isolated. Chloro-iodohexane **233** was then used as the reactivity difference might give some selectivity. At 100 °C no selectivity was observed, however, at room temperature the desired chlorohexyl product **234** was isolated in good yield. The chloride was then exchanged for an iodide (compound **235**) using the Finkelstein reaction.

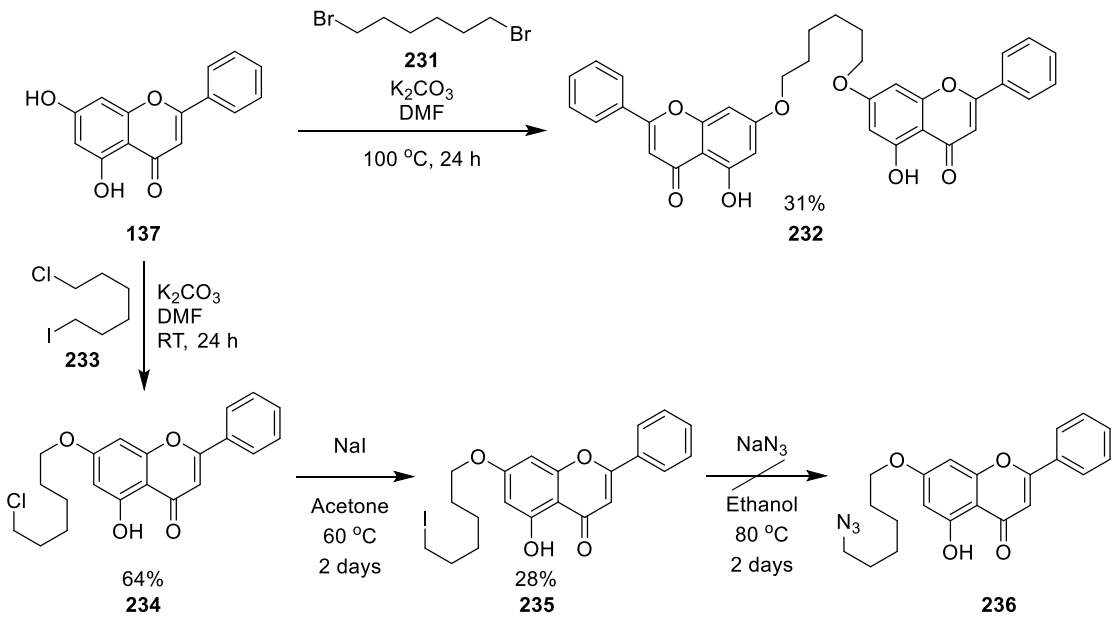

Scheme 66

The reaction to install an azido group which would have yielded compound **236** that could have been used for click reactions, did not occur as expected so a new approach was sought (*scheme 67*). Instead of starting with a hexane chain with two reactive moieties, the azido group would be installed first. Hence, starting again from chloro-iodohexane **233** the iodo functionality was first exchanged for the azido group (*scheme 68*). This reaction did not go completely cleanly. The crude mixture containing compound **237** was not purified but subjected instead to the Finkelstein reaction conditions to yield the desired azido-iodohexane **238** in 62% over two steps. The rest of the material isolated was found to be 1,6-diiodohexane.

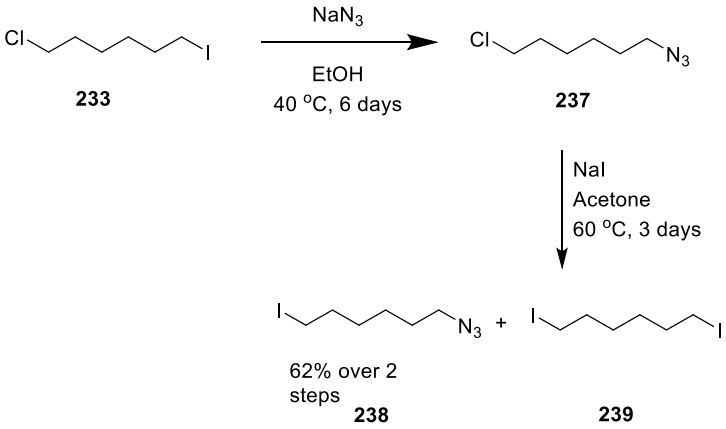

Scheme 67

The azido-iodohexane **238** was then used to monoalkylate chrysin **137** to yield the azido chrysin derivative **236** in one step (*scheme 69*). However when flavone **236** was subjected to the harsh hydrolysis conditions no product **240** could be isolated.

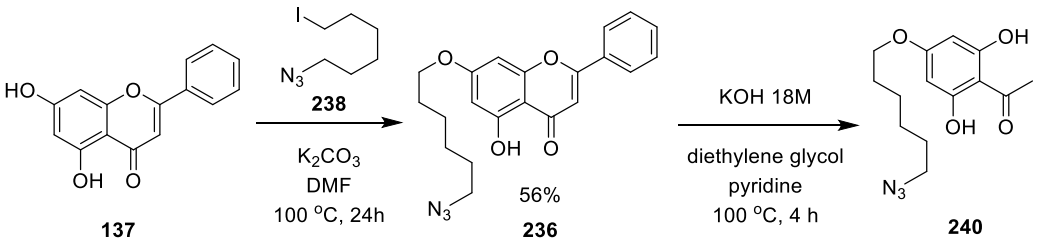

Scheme 68

Direct alkylation of trihydroxyacetophenone **141** was therefore attempted, but gave mainly the doubly alkylated product **241** instead of the monosubstituted product **240** (*scheme 70*). Though the products **240** and **241** were isolable it was thought that a better strategy would still be monoalkylation of chrysin **137**.

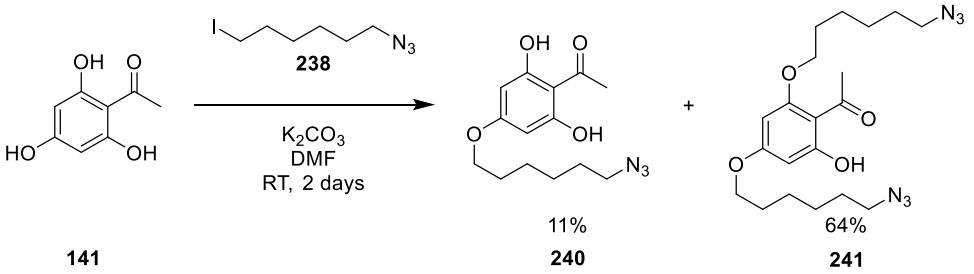

Scheme 69

A protecting group strategy was therefore sought. Previous successful attempts at this cracking reaction all had disubstituted chrysin as the starting material. The monosubstituted chrysin **236** was therefore benzyl protected. It is worth pointing out that the reaction times for the second ester formation are much longer than for the initial alkylation as the phenolic hydroxyl coordinated to the ketone is much less reactive. The cracking of this now disubstituded chrysin compound **242** proceeded well and gave the desired acetophenone **243** in an exceptionally good yield for this type of reaction (*scheme 71*).

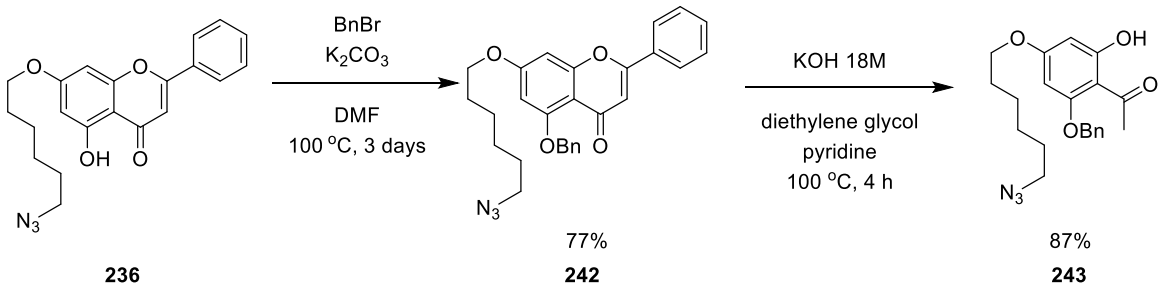

Scheme 70

To synthesise a hinokiflavone analogue with the opposite site substitution pattern on the A ring, acetophenone **246** with the opposite substitution pattern was synthesised (*scheme 72*). Chrysin **137** was first MOM protected on the non-coordinated 7-OH to form flavone **244**. This allowed for the selective alkylation of the 5-OH, to form flavone **245** in good yield. Finally, a cracking reaction furnished the desired azido-acetophenone **246** with the opposite substitution pattern to acetophenone **243**.

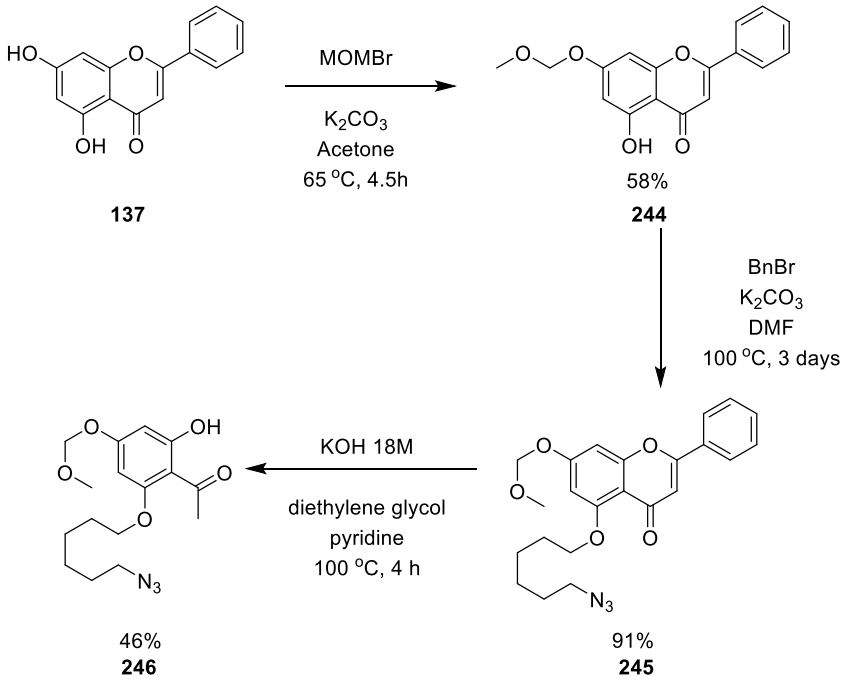

Scheme 71

Isopropyl protecting groups replaced other protecting groups around this time in our synthesis, due to their superior stability to MOM protecting groups and better solubility in organic solvents than methyl and benzyl protecting groups. Hence acetophenones with both substitution patterns using isopropyl protecting groups were also synthesised (*scheme 73*). The 4-hexylacetophenone **248** was

synthesised in two steps from the substituted chrysin **236**. The 2-hexylacetophenone **251** was synthesised in three steps from chrysin **137**.

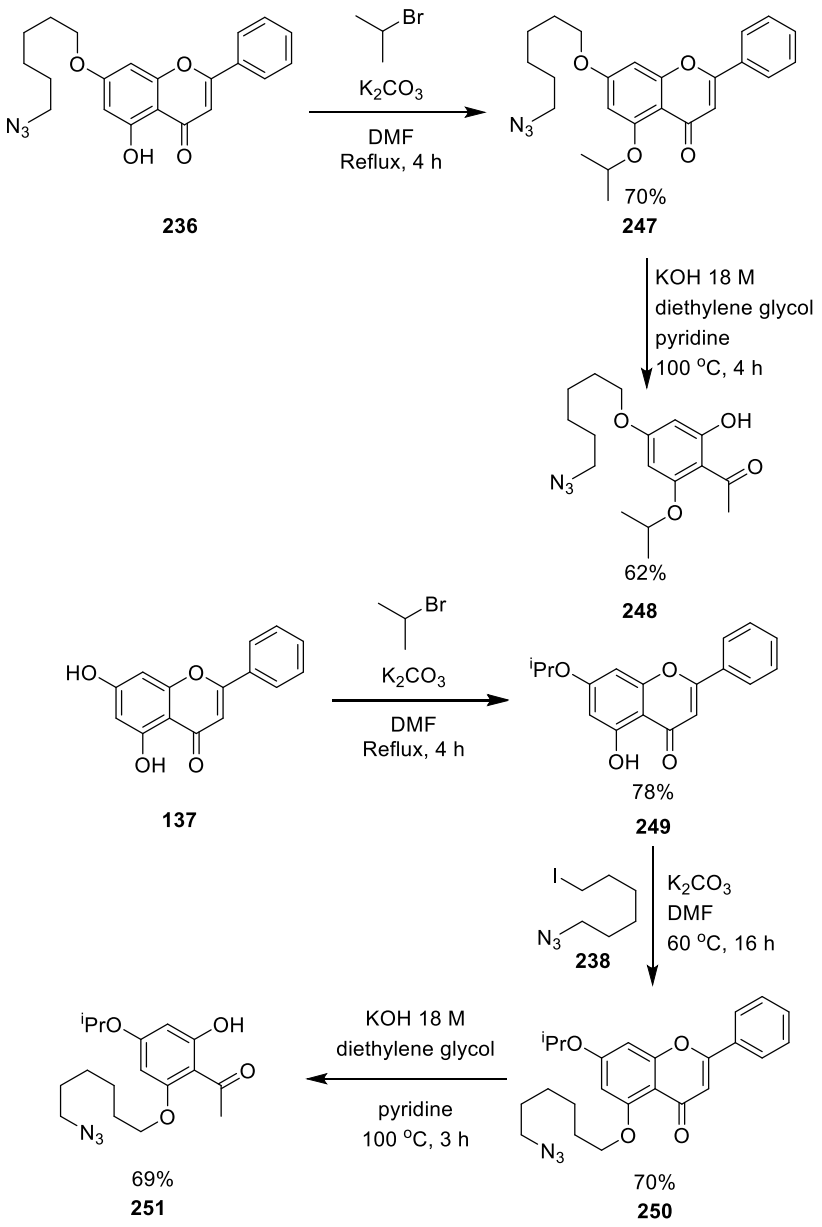

Scheme 72

4.2.2 Azido tagged hinokiflavone analogues

Both of the acetophenones **243** and **246** were then supposed to be attached to the finished BA'C'B' ring system **186** by an ester coupling using EDC (*scheme 74*). The esters **252** and **253** would then have been cyclised using the same conditions as in hinokiflavone synthesis. However, as no success was had with the hinokiflavone **9** synthesis using the same strategy, this (late stage cyclisation) strategy was abandoned for a more convergent approach.

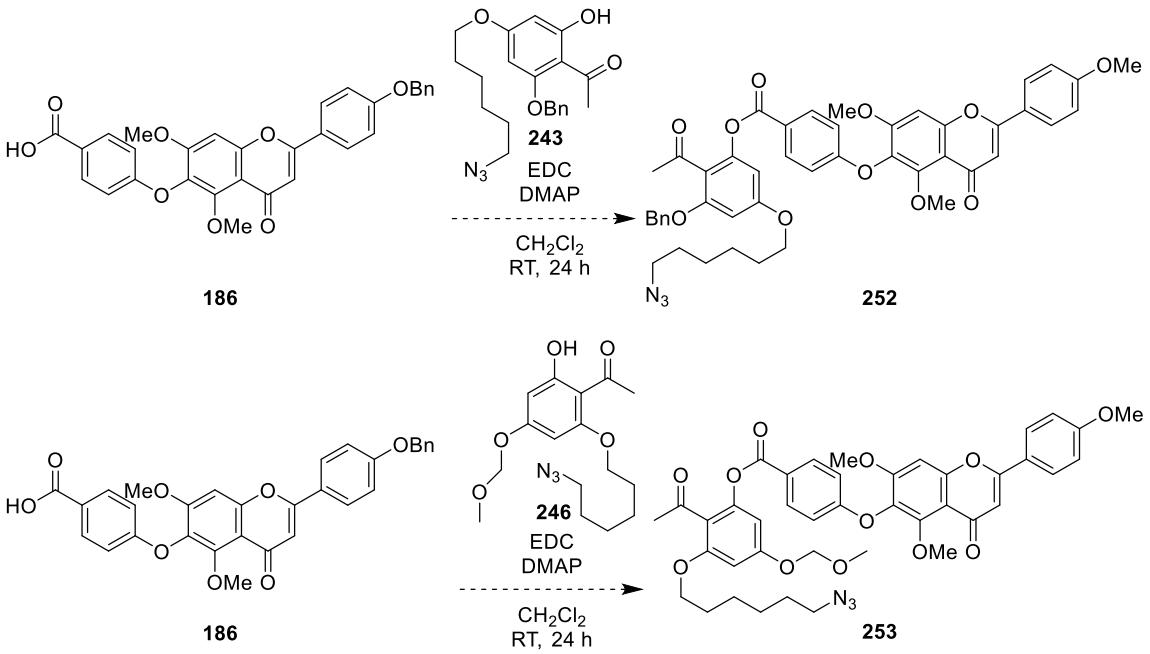

Scheme 73

Efforts were instead directed towards the synthesis of a substituted RHS that could be coupled across to a LHS to form the substituted hinokiflavone. In this early stage substitution approach linkers would have to carried through most of the synthesis, instead of being inserted later, hence hexane groups were used again as these were deemed to be much more robust than the PEG linkers.

Since reduction of the nitro activation group was impossible without damaging the azido tag, a different activating group was sought. Poly-fluoro aromatics as S_NAr activating groups were investigated in the synthesis of hinokiflavone analogues by Lewis King in the Hartley group, demonstrating that fluorides are tolerated as bioisosteres to hydrogen in hinokiflavone. The difluoro hinokiflavone **254** was found to be active in some preliminary screens like hinokiflavone (*figure 26*).

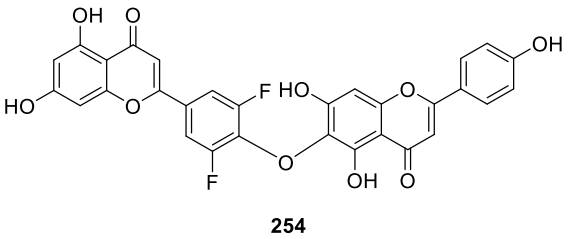

Figure 26

The use of fluorine atoms as bioisosteres for hydrogens is well accepted.[93] In fact there are drugs on the market that use this approach, most famously antimetabolites used for chemotherapy such as fluorouracil.[94] As Fluorine and hydrogen have a similar atomic radii it is usually a well-tolerated modification with respect to size in enzymes. However, fluorine has much higher electronegativity so it completely changes the electronics of the system, a useful property for antimetabolites where this can change the way these drugs are metabolised in the body. In the case of hinokiflavone synthesis, the electron withdrawing effect makes the B ring more susceptible to S_NAr reactions, removing the necessity for an activating group. Without the nitro activating group, there is no need for the steps to remove it either. This shortens the synthesis and allows for the use of reduction sensitive functional groups, such as azides.

Hence azide tagged fluorinated analogues of hinokiflavone were synthesised next (*scheme 75*). As the target for the attachment was the A ring, two different molecules were attempted; **255** where the azide tag would attached to C-5, next to the carbonyl group and **256** where the azide tag would be attached to C-7.

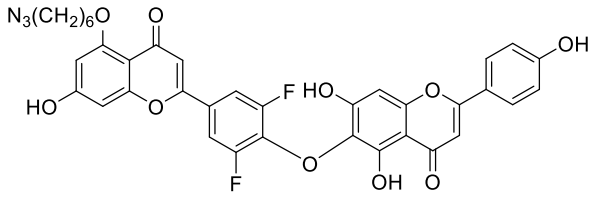

255

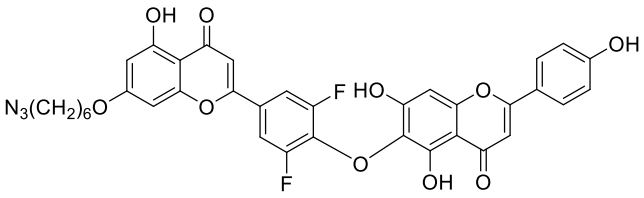

256

Scheme 74

Starting with analogue **255**, the tagged acetophenone **251** was reacted with trifluoro aldehyde **257** to form the chalcone **258** (*scheme 76*). Due to the trifluoro functionality this reaction had to be carried out under room temperature at higher temperatures side reactions reduced the overall yield of

the chalcone formation. The chalcone was then cyclised to form trifluoro flavone **259**.

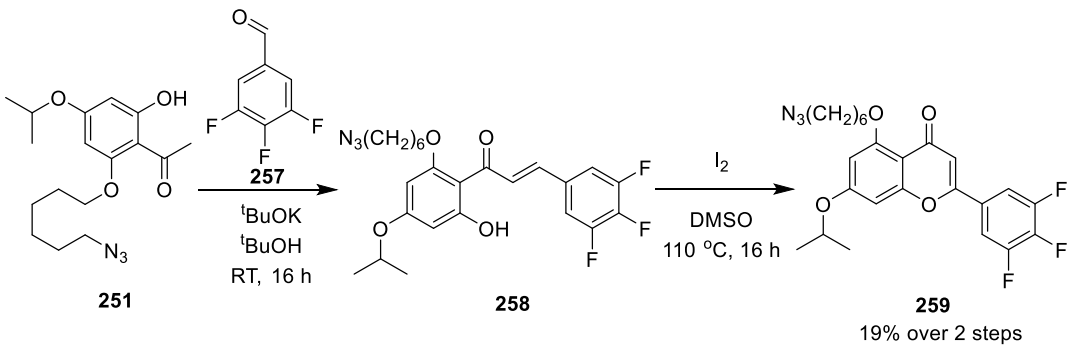

Scheme 75

The trifluoro LHS **259** was then coupled across to the isopropoxy RHS **206** using the standard coupling conditions (*scheme 77*). The deprotection was attempted with boron tribromide, however no desired product was isolated. Instead difluoro hinokiflavone analogue **254** was found, the hexyl tag probably was destabilised by its proximity to the carbonyl group. Since analogue **254** was bioactive and useful this was not the poorest result. Considering the lability of the hexyl group, if modifications on the C- position were desired, these would have to be attached by a C-C bond instead through an ether for stability.

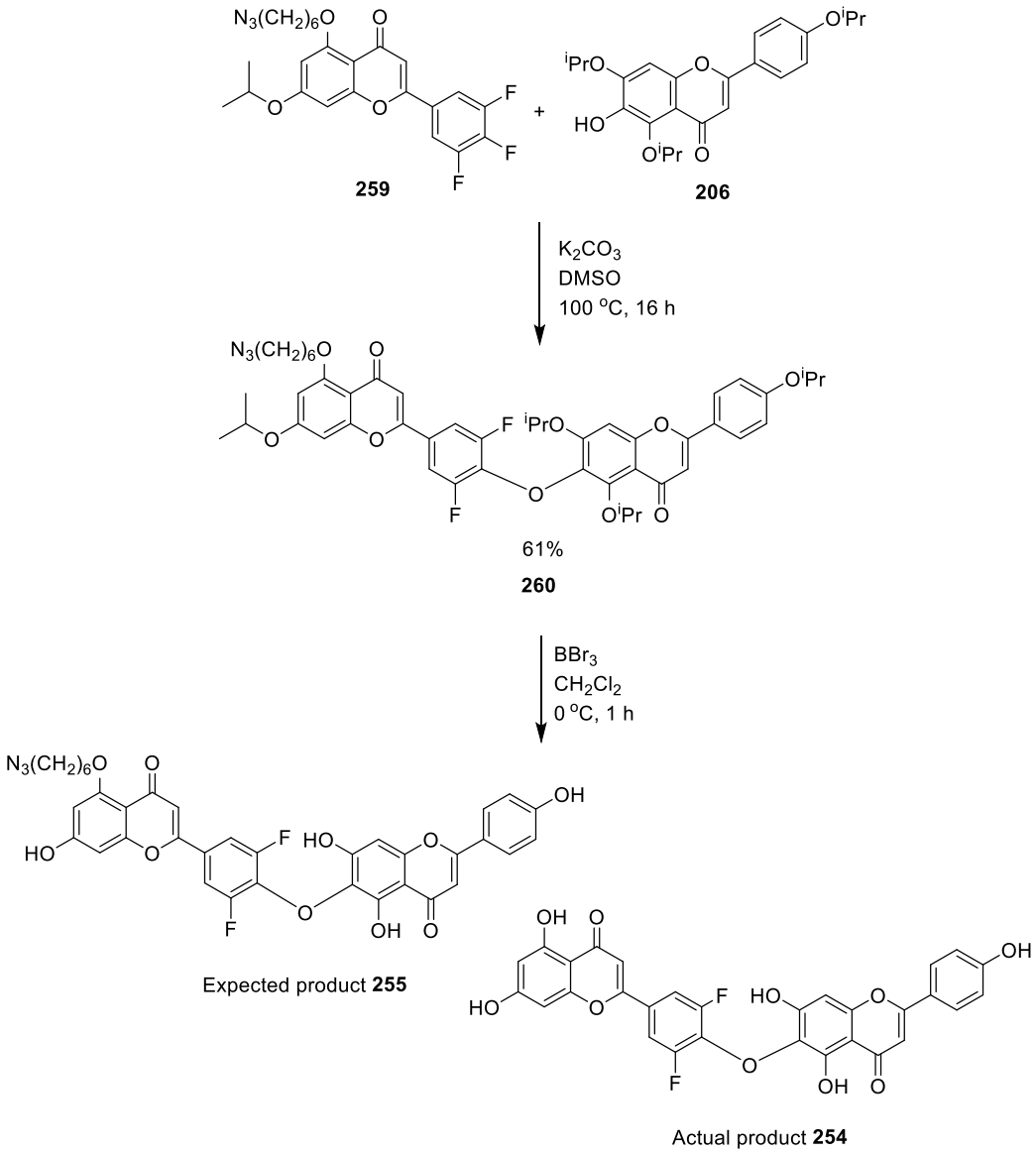

Scheme 76

The trifluoro flavonoid **256** was then made using the previously tested conditions (*scheme 78)*. Chalcone **261** was formed under milder, room temperature, condition and then cyclised to form the flavone **262** using iodine.

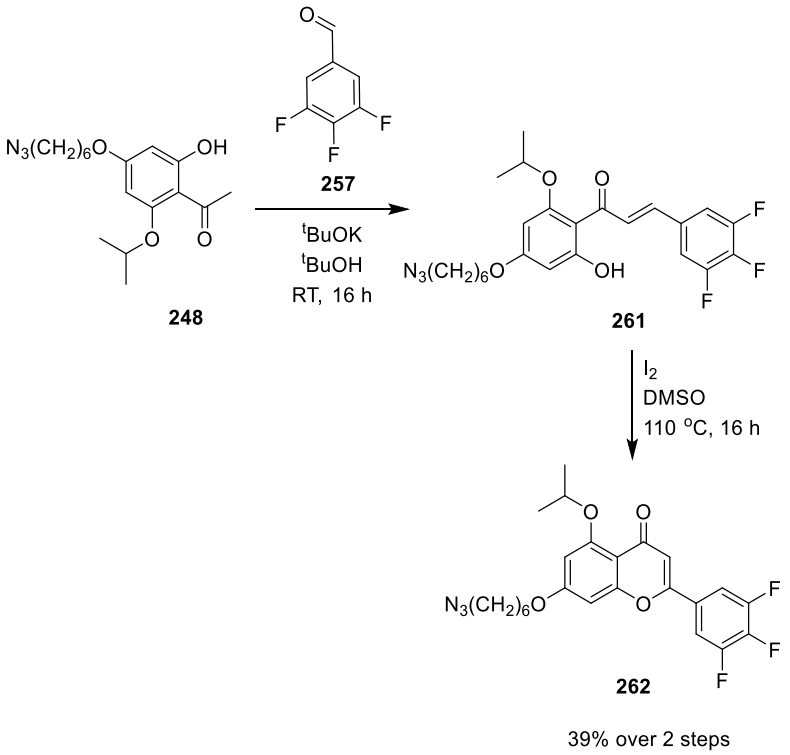

Scheme 77

The diflavone **263** was formed using previously described reaction conditions, and the deprotection step proceeded without complications from **256** that could be observed by LC-MS (*scheme 79*). However difficulties were encountered during the purification stage. Due to insufficient material and inferior resolution on the HPLC no pure sample of this material was isolated. At this point out priorities shifted to the hinokiflavone analogues and this approach was disregarded.

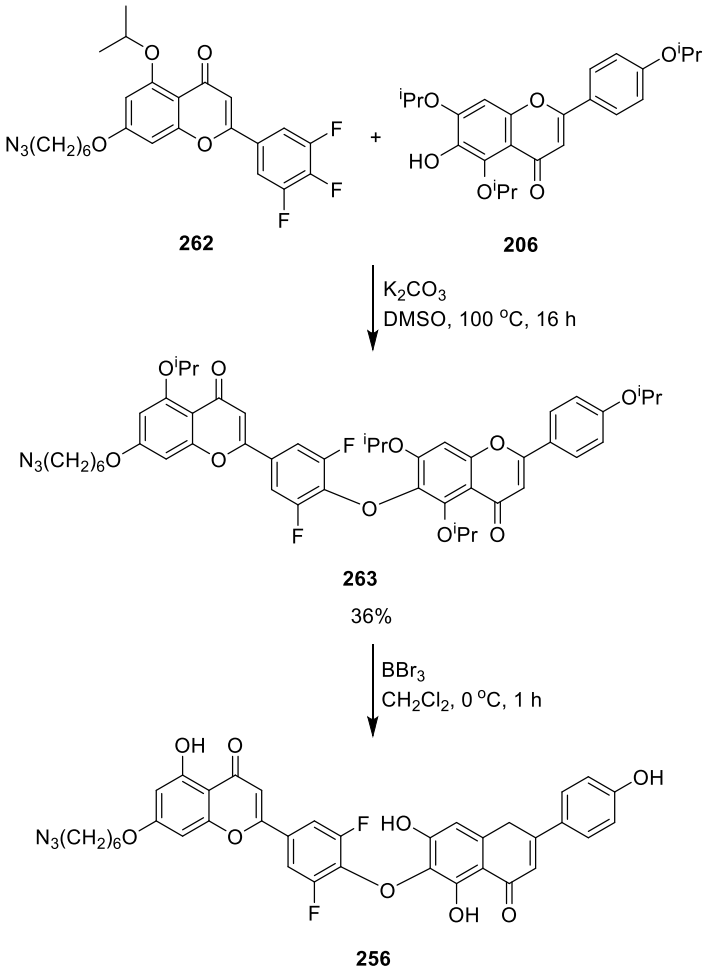

Scheme 78

Overall, a number of alkylated acetophenones were synthesised successfully. Hexane was investigated as a linker for attaching azido tags to hinokiflavone, and proved to be a much more stable and user-friendly linker than tetraethylene glycol. Hinokiflavones 5-OH position turned out to be too labile to use for tagged analogues due to its conjugation to the neighbouring carbonyl group. The 7-OH position remains a possibility for future work. Fluoro analogue **254**, an advantageous product, was synthesised and used for further biological study of the spliceosome. As the fluoro analogue **254** proved to be promising in biological studies, other bioisosteres were also investigated. If the synthesis could be simplified by structural modifications to hinokiflavone while retaining activity much larger quantities could be synthesised, useful if animal studies were carried out. Hence structural analogues of hinokiflavone **9** were investigated next.

5 SUMO

5.1 SUMO – the hinokiflavone target

While the synthesis of hinokiflavone was being carried out, the biological investigations into the activity of hinokiflavone were also progressing. Hinokiflavone's action on cells was more fully investigated, of particular interest were proteins not commonly associated with the spliceosome. This was undertaken in order to see if hinokiflavone **9** had other cellular effects

A range of other nuclear proteins were tested to see whether they changed their localisation in the nucleus under the influence of hinokiflavone. Immunofluorescence microscopy analysis, described in chapter 3 showed that SUMO, small ubiquitin like protein modifier, also co-accumulated in the megaspeckles (*figure 27*).

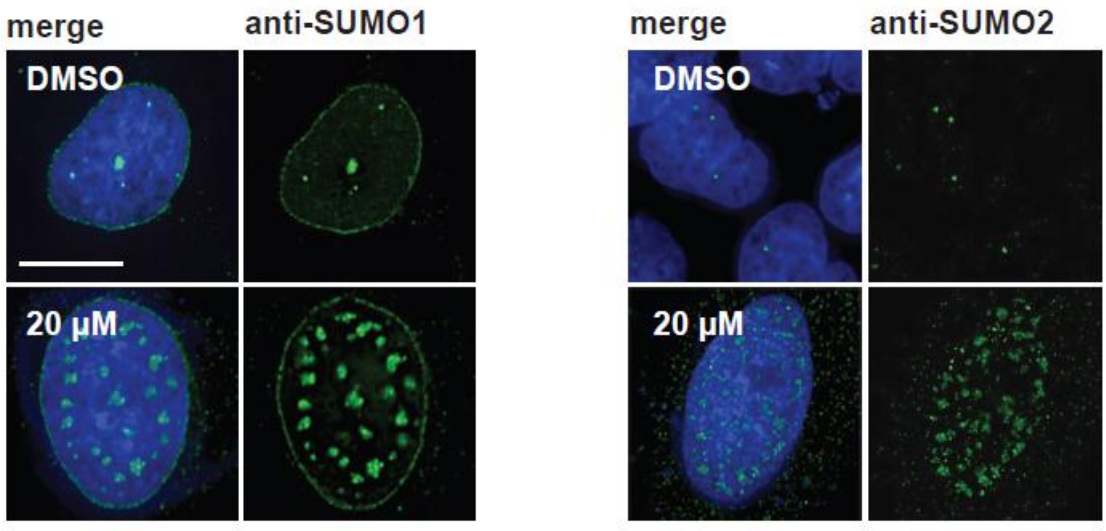

Figure 27 Immunofluorescence microscopy
HeLa cells incubated with 20µM hinokiflavone/DMSO for 24 h. The cells then fixed with 4% paraformaldehyde, permeabilised with 0.5% Triton X100 and incubated with the primary antibodies, 1 hour at RT, then incubated with the secondary dye-conjugated antibodies. Visualised with fluorescence microscope (cells stained with DAPI (blue) to show DNA and nucleus).

HeLa cells treated with hinokiflavone show accumulation of SUMO1 and SUMO2 in megaspeckles (*figure 27*) indicating that SUMO modification of proteins might be altered in these cells due to the presence of hinokiflavone **9**. That post-translational modifications are involved in the controlling of splicing has been reported before.[95] Post-translational modifications allow cells to fine-tune the

activity of proteins by covalently attaching a label to them. This way proteins can be labelled for transportation to a specific cellular compartment, their activity can be regulated up or down or the modification can tag them for degradation.[96] There is a huge range of posttranslational modifications, somewhere in the range of 300 are known to us.[97] As well as small covalent modifications like methylation and phosphorylation, cells also use small proteins as post-translational modifications. The most well knows of these is probably ubiquitin, however there exist several others such as NEDD and SUMO. As an entire protein, or multiple proteins (in the case of ubiquitin or SUMO chains) are added to the target protein this greatly increases the weight of the protein modified. Since SUMO accumulation was observed, the question arose if other protein based post-translational modifications were also affected in the same way.

To see if other post translational small protein modifiers were also increased, HEK293 cells were treated with various hinokiflavone concentrations for 24 hours then harvested, lysed and analysed by SDS-PAGE (*figure 28*). The gels were then treated with specific antibodies to detect the amount of the various proteins of interest. Looking at the size of high molecular weight spots in the DMSO control *vs* hinokiflavone treated columns tells us weather hinokiflavone is having an effect on the concentration (increased or decreased) of that post-translational modification or not. α-Tubulin was used as a loading standard, showing that the same amount of total cellular protein was loaded into each row and the increasing or decreasing size of high molecular weight spots is genuinely due to increasing concentrations of modified proteins in cells. Increasing amounts of SUMOylated proteins were seen in the experiment in response to hinokiflavone, an effect that seemed to be concentration dependent (*figure 28 a&b*). However, the other small protein modifications tested were not affected. Ubiquitin and NEDD levels were not increased by addition of hinokiflavone (*figure 28 c&d*), if anything they seemed to decrease a little (especially visible for ubiquitin).

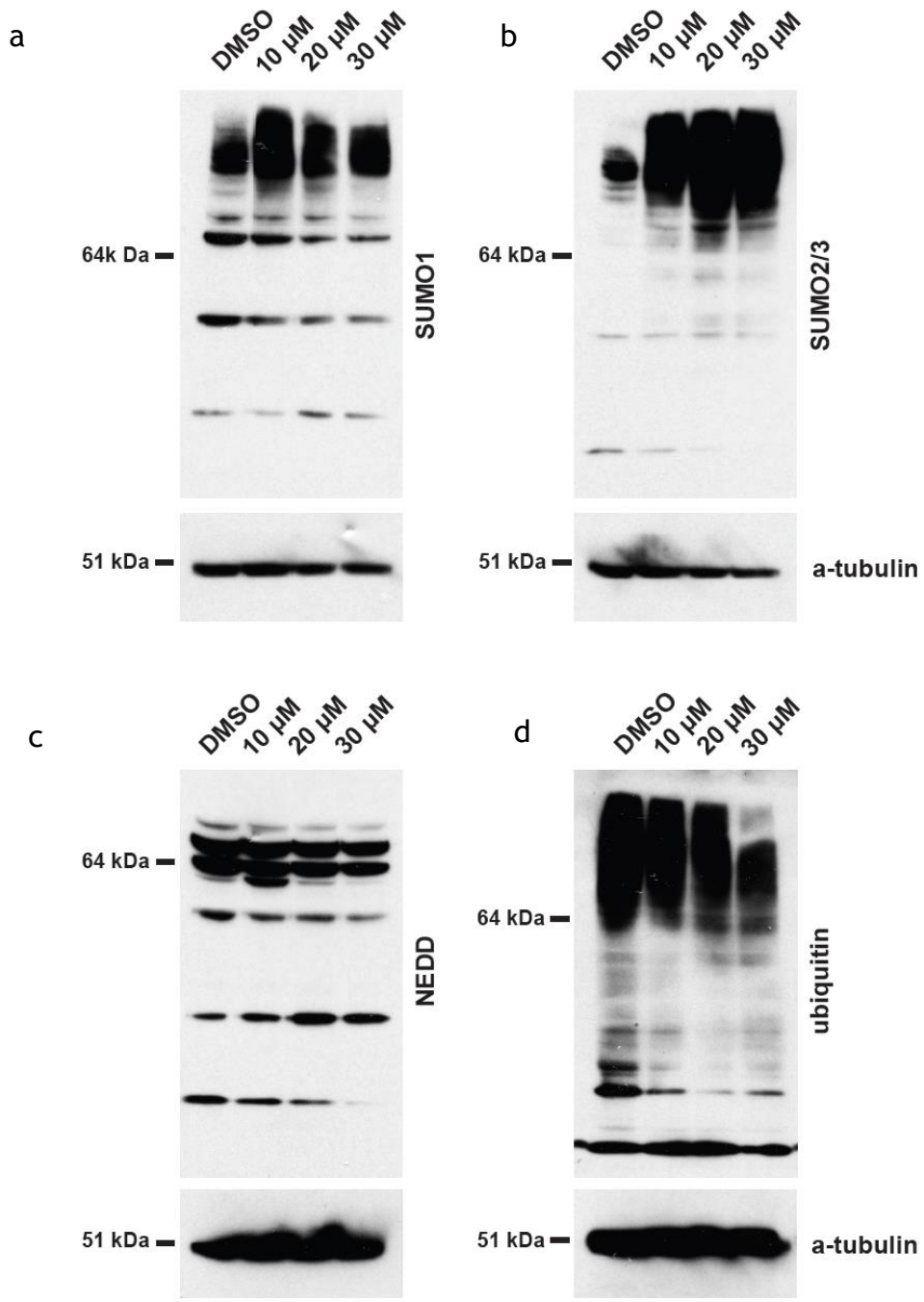

Figure 28 Western blot analysis
HeK293 cells incubated with hinokiflavone/DMSO for 24 h then harvested, washed and lysed. Cellular proteins separated on 4-12% NuPAGE Bis-Tris gel, transferred to nitrocellulose membrane labelled with antibodies and visualised using chemiluminescence; to see if concentration of post-translational modifiers was changed due to the presence of hinokiflavone. α-Tubulin was used as a loading standard.

The experiment was repeated in an *in vitro* splicing reaction (*figure 29*). The results show the same effect, increased hinokiflavone concentrations lead to increased accumulation of SUMOylated high molecular weight proteins. Here, SFRS1 is shown as the loading control.

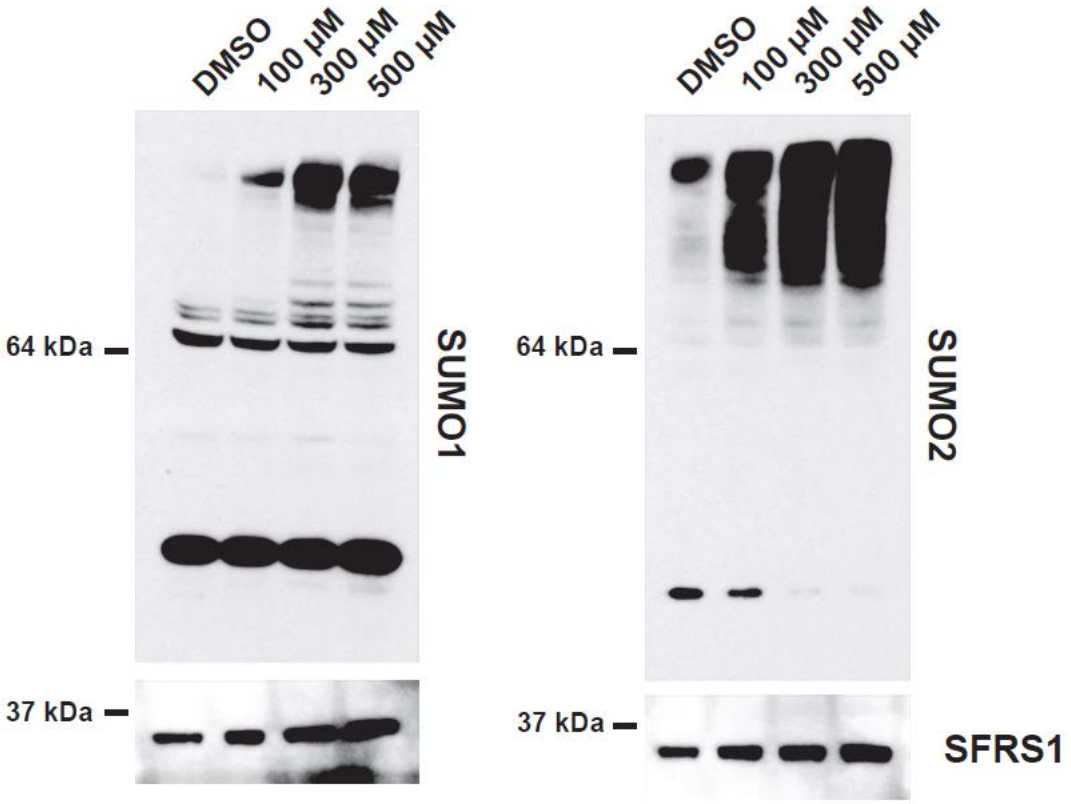

Figure 29 Western blot analysis
In vitro **splicing reactions incubated with hinokiflavone/DMSO 90 min. Proteins separated on 4-12% NuPAGE Bis-Tris gel, transferred to nitrocellulose membrane labelled with antibodies and visualised using chemiluminescence. SFRS1 used as a loading standard.**

As it was not known whether the increase in protein SUMOylation were caused by increased SUMOylation or decreased de-SUMOylation further experiments were necessary to elucidate hinokiflavone's exact effect. The de-SUMOylation hypothesis was tested first by testing hinokiflavone's effect on SENP1 (Sentrin-specific protease 1) which is one of the SUMO-removing enzymes.

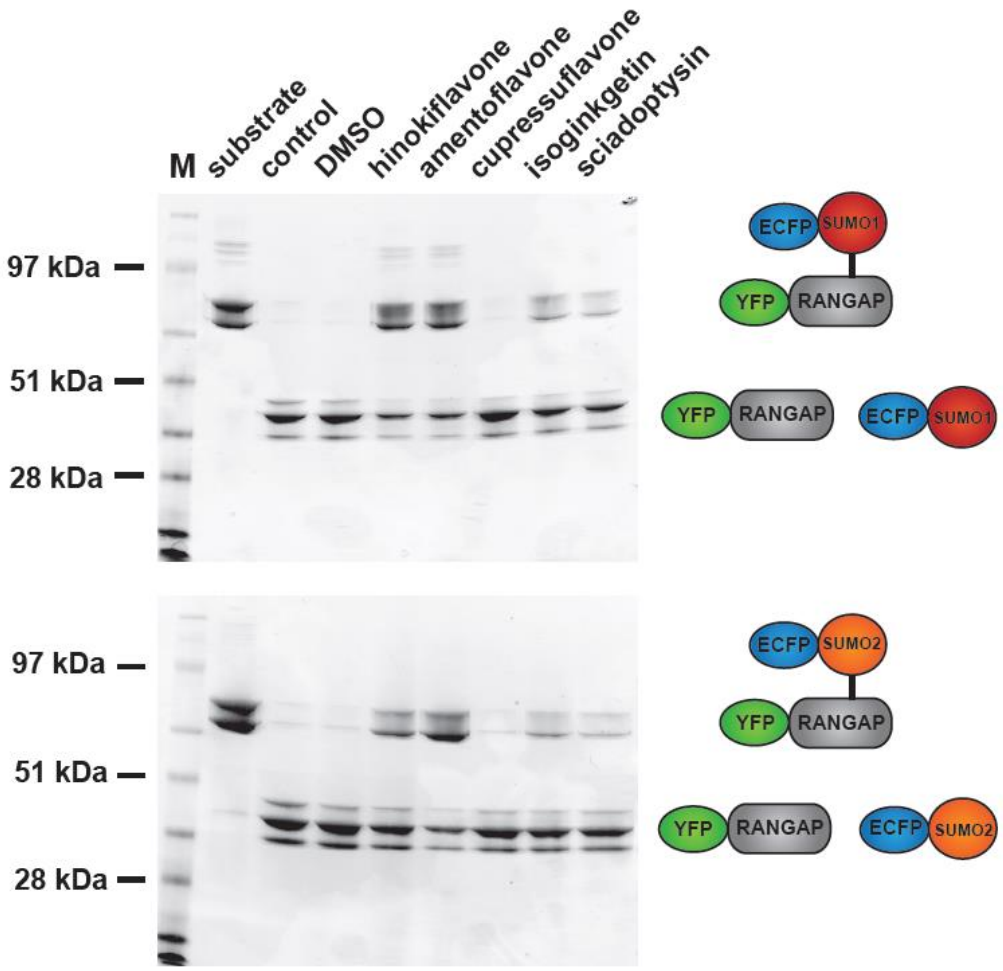

Figure 30 Gel-based SENP1 activity assay
Catalytically active SENP1 fragment (aa 415-643) expressed in *E. coli* and SUMOylated template (YFP-RANGAP-ECEP-SUMO2) were incubated with compound/DMSO in SENP buffer at 37°C for 15 min. Loading buffer added and separated on 4-12% Tris-Bis PAGE gel, visualised with Coomassie blue. Gel shows cleavage/non-cleavage of SUMOylated template depending on SENP fragment activity.

SENP activity was tested by using purified SENP1 catalytic domain together with a SUMOylated control (ECFP-SUMO2-RANGAP-YFP). The ECFP and YFP are fluorescent proteins, in this case they were not used for their fluorescent ability though as the proteins were visualised using Coomassie blue, commonly used to stain proteins. The fragments of RANGAP-YFP and ECFP-SUMO2 were then detected. In the DMSO control the SENP catalytic domain cleaves the SUMOylated control and hence only the two fragments are visible (*figure 30*). It was shown that SENP activity was inhibited by hinokiflavone and, amentoflavone and to a lesser degree by isoginkgentin and sciadoptysin, as the original SUMOylated control could still be seen . This implies that hinokiflavone is acting as a SENP1 inhibitor. The inhibition of de-SUMOylation of cellular proteins especially splicing factors caused by hinokiflavone interferes with the

spliceosome assembly and therefore pre-mRNA splicing. It also shows that controlled SUMOylation and de-SUMOylation events are required for the correct functioning of the spliceosome. This puts SUMO in the list of other post-translational modifiers already known to control and influence the spliceosome.[95]

5.2 SUMO structure and function

SUMO is one of the protein families belonging to the ubiquitin-like molecules (Ubls) group of protein modifiers. Like other Ubls, such as NEDD (involved in the control of the cell cycle), SUMO is structurally similar to ubiquitin and is also used as a post-translational modifier. Both ubiquitin and SUMO are important for mechanisms protecting DNA from damage.[98] Unlike ubiquitin, which is most often used as a marker for protein degradation, SUMO plays a role in various cellular processes. It has been implicated in transcription and protein translocation as well as formation of sub-nuclear structures.[99] An additional way SUMO differs from ubiquitin is that while ubiquitin is most often seen as a poly-ubiquitin chain, SUMO can be seen in both mono-SUMO form and poly-SUMO form depending on which isoform of SUMO is present.[99]

In mammalian cells there are 5 isoforms of SUMO that have been characterised so far. SUMO1, SUMO2 and SUMO3 are the best characterised isoforms of SUMO. SUMO4 is not characterised as well as the other three but tends to be found in immune cells only[100] and SUMO5 has not yet been characterised at all in protein form, however a gene for it has been identified so it might exist.[98, 99] All of these SUMO isoforms have a similar three dimensional shape to ubiquitin. However, they share only a moderate amount of common amino acid with the ubiquitins sequence, 18% in the case of SUMO1.[99]

SUMO1, a 101 amino acid long peptide, is unable to form poly-SUMO chains as it lacks the requisited lysine residue and therefore is usually seen as a single SUMO conjugate. SUMO2 and 3 are structurally 95% identical to each other (while being only 48% similar to SUMO1) and form poly-SUMO chains.[99] SUMO1 is seen in healthy cellular metabolism, however the amount of SUMO2 and SUMO3 found in cells increases as a response to stress.[98] Each SUMO isoform needs to be activated before use, this occurs by the liberation of a glycine near its C-

terminus by the removal of capping amino acids (these differ between the SUMO isoforms, in the case of SUMO1 the sequence is HSTV).[101] After the activation of the SUMO precursor, to form the mature SUMO protein, it is attached to its target protein by an isopeptide bond. An example of the difference between a peptide bond (forms protein backbone **266**) and an isopeptide bond (attached to the side chain **264**) is shown on the amino acid lysine **265** in *scheme 80*.

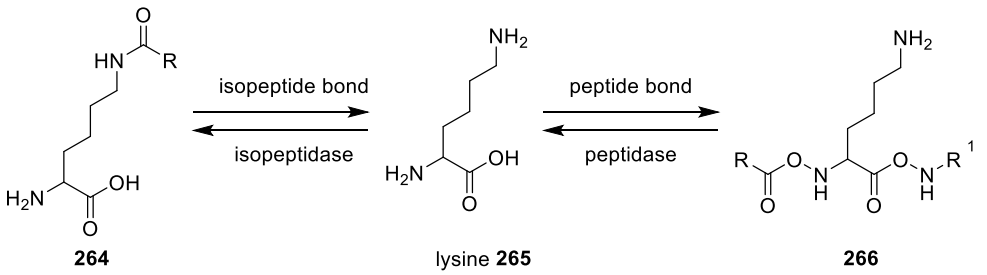

Scheme 79

SUMO conjugation to target proteins is analogues to ubiquitin conjugation (*figure 31*). The SUMO protein has to be activated first by the lysis of a capping part to form the active SUMO protein that is then attached to the target protein by a cascade of 3 different enzymes.[99] The first enzyme, SUMO-activation enzyme, forms a complex with the mature SUMO protein. In mammalian cells this activating enzyme is formed from two subunits, Aos1 and Uba2. These subunits are well-conserved between mammalian and yeast cells.[99] Uba2 contains the active site but is unable to fulfil its function without the presence of Aos1. [99]

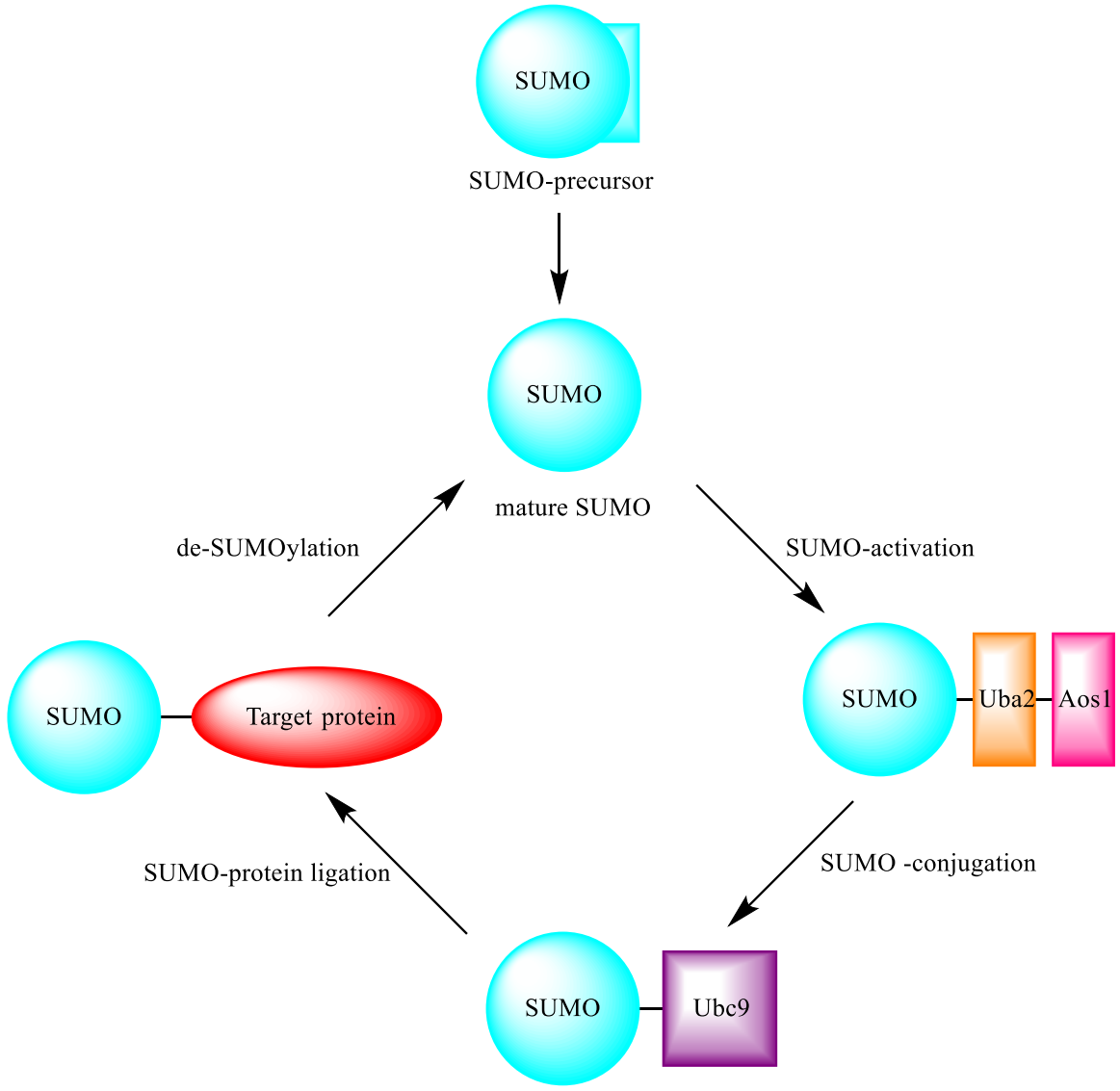

Figure 31

The second enzyme required for SUMOylation is the SUMO conjugation enzyme, Ubc9. Ubc9 is very similar to the ubiquitin conjugation enzyme, so much so that when it was first discovered it was identified as an ubiquitin conjugation enzyme, even though ubiquitin cannot actually bind to Ubc9.[99]

Unlike in the ubiquitin conjugation pathway, in the SUMO conjugation pathway the analogues SUMO protein ligases are not actually required for protein conjugation. SUMO conjugation takes place when Uba2, Aos1 and Ubc9 are present without a further conjugating enzyme, however the rate of conjugation is not very fast. Several SUMO protein ligases have been discovered. It is thought that these increase SUMOylation rates by bringing the SUMO-Ubc9 conjugate into close proximity to the protein target and hence acting as a template.[99]

The SUMO modification is removed from proteins by a SUMO-specific protease, such as SENP1, that cleaves the isopeptide bond between SUMO and its target.[99] This can be performed by the same enzymes that activate the SUMO precursor by cutting away the capping sequence and liberating the glycine residue at the C-terminus.

While antibody, peptide and nanoparticle approaches to targeting SUMO-protein interactions have been described,[102-104] targeting small molecules to interfere with protein-protein interactions has been known to be difficult. This is due to the large surface areas involved in these types of interactions, which small molecules have difficulty in interrupting. A large binding affinity is required by the small molecule to have a chance of interrupting the protein-protein interaction and this is difficult as the protein-protein surfaces tend not to have nice pockets for the small molecules to fit into. SUMO targeted small molecules are not an exception to this rule.[102]

Since SUMO controls protein-protein interactions by interacting with SUMO interaction motif (SIM), efforts have been made to disrupt this interaction with small molecules. Voet *et al*. for example screened a library of small molecules to find an inhibitor of these interactions using protein interference.[102] They found a number of inhibitors, the most potent of which of was SSI-091 **267** (*figure 32*). [102] However, as SSI-091 **267** interacts with the backbone of SUMO it does not differentiate between the different SUMO isoforms. Also, no *in vitro* or *in vivo* studies in living cells or organisms could be carried out on this compound as SSi-091 **267** is extremely toxic to cells.

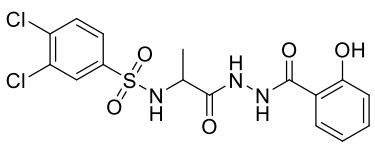

SSI-091 **267**

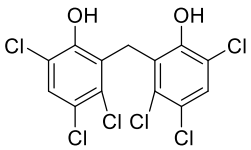

SIMI-4 **268**

Figure 32 SUMO binders

A selective SUMO1 binder has been identified by Alontaga *et al*. by utilising a specifically designed high throughput screen. The authors claim that SIMI-4 **268** (*figure 32*) interacts specifically with the active binding site on SUMO that interacts with the SIM-4 **268** by analysing the results by ^{1}H-NMR spectroscopy.

However, SIMI-4 **268** does not act as an inhibitor of this protein-protein interaction due to its weak binding and relatively small size.[105]

5.3 SENP structure and function

SENP or SUMO specific protease, is a family of cysteine peptidases that remove SUMO from SUMOylated proteins in human cells as well as activating the SUMO precursor by removing the capping amino acids from the SUMO precursor.[106] The equilibrium between SUMOylated and de-SUMOylated proteins plays an important role in healthy cell metabolism and hence SENPs are an important enzyme family as they remove and recycle SUMO in the cell. Just like Ubc9, SENP1 and SENP2 knockout is embryonically lethal, demonstrating their importance in cell metabolism.[106]

There are 6 isoforms of SENP in mammalian cells that can be roughly categorised into 3 families based on their amino acid sequence similarities. SENP1 and SENP2 belong in the first family; these enzymes can lyse both peptide bonds to form the mature SUMO proteins and isopeptide bonds to cleave SUMO1, 2 and 3 from their targets for recycling. SENP1 and 2 are found in the nucleoplasm.[106] SENP3 and SENP5 from the second family are found in the nucleolus and prefer SUMO2/3 over SUMO1. The same can be said about SENP6 and SENP7 in the third family. SUMO4 cannot be cleaved from its target protein by any of these SENPs, because its wider shape does not fit through the narrow tunnel leading to the active site of these cysteine peptidases.[106, 107]

Misalignment in the SUMO equilibrium caused by the incorrect activity of SENP enzymes has been linked to a multitude of diseases such as various cancers, heart disease and arthrosclerosis.[106] The role of SENP (particularly SENP1) has been especially well investigated with regards to prostate cancers where it was found in elevated levels in both prostate cancer and precancerous prostate tissue.[108] For example a study in prostate cancer found that HIF-1α, responsible for increasing blood flow to hypoxic cancer tissue, is stabilised by SUMO1 conjugation; however its activity was also downregulated. Hence high SENP1 levels would de-SUMOylate HIF-1α increasing its activity and hence increasing cancer viability.[109, 110] In the absence of SENP1 the HIF-1α was poly-SUMOylated and hence degraded through the ubiquitin dependent pathway.[111] In a separate

study it was shown that the lower the expression of SENP5, in over 1300 breast cancer victims analysed, the higher their chances of survival. This difference in survival rates was directly linked to the SUMOylation of TGFβRI protein that in its SUMOylated form leads to tumour invasion and hence higher mortality.[112]

The structure of SENP1 bonded to SUMO1 can be seen in *figure 33*.[113] The active site is buried in a tunnel that the SUMO tail can fit through when they are bonded. When SUMO1 is not bonded, the tunnel opens up, and the active site is merely in a narrow valley, accessible only to specific sequences of amino acids or possibly small molecule drugs.[113]

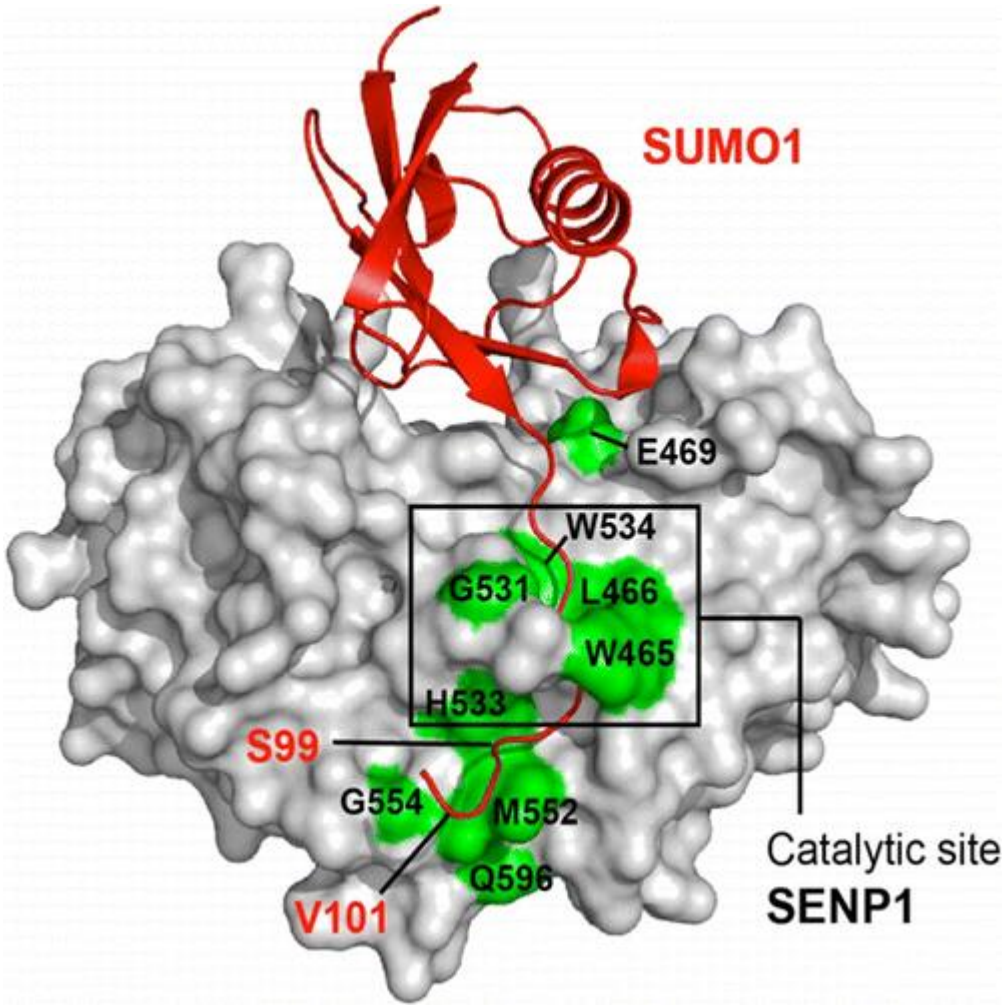

Figure 33 From Madu *et.al*[113]

Previous reports linking SUMO modification to splicing factors exist. For example when **280** (*figure 36*) was used to search for novel SUMO targets some of the most notable examples in the 900 proteins they found were splicing factors. This inspired the authors to speculate "SUMOylation of spliceosome factors may be

implicated in the pathogenesis of prostate cancer". [114] Alternative splicing of some know SUMOylation targets in cancer cells have also been reported.[115, 116] Pozzi *et al.* also liked SUMO conjugation to spliceosomal proteins to splicing control and a requirement for pre-mRNA splicing.[117] However before the paper published by Lamond *et al.* no reports of small molecule modulators of splicing that controlled specific SUMOylation and deSUMOylation events.[118]

5.4 Small molecule SENP inhibitors

Links to diseases make SENP enzymes an intriguing drug target[106] and hence a lot of effort has been spent on finding specific SENP inhibitors both for the use as molecular probes and as drugs to combat the diseases associated with SENP activity. The first SENP inhibitors were based on SUMO or parts of the SUMO protein. These peptide sequences were then modified to include a reactive moiety that would covalently bind to SENP and hence deactivate it.[119, 120] The difficulty in designing small molecules that interact with SENP is in the relatively sheltered active site. It is difficult to design molecules that fit in the narrow tunnel surrounding it while interacting strongly enough to out compete SUMO. Hence most of the molecules designed so far have been designed to covalently attach to SENP.[106] The first specific small molecule SENP1 inhibitors were based on the benzodiazepine structure that the authors expected to be a good peptide-mimetic as it has been used as such before.[121] Benzodiazepines **270** and **271** (*figure 34*) were designed to inhibit SENP1 by a covalent attachment of the electrophilic aldehyde to the active cysteine and hence potentially, to have anticancer activity. Diazepam **269**, a benzodiazepine drug used in the clinic, is shown here for structure comparison. **270** and **271** inhibited SENP1 in the μM range and were also tested against human prostate cancer cell line (PC3) where they showed activity up to IC_{50}=9.2 μM.[121]

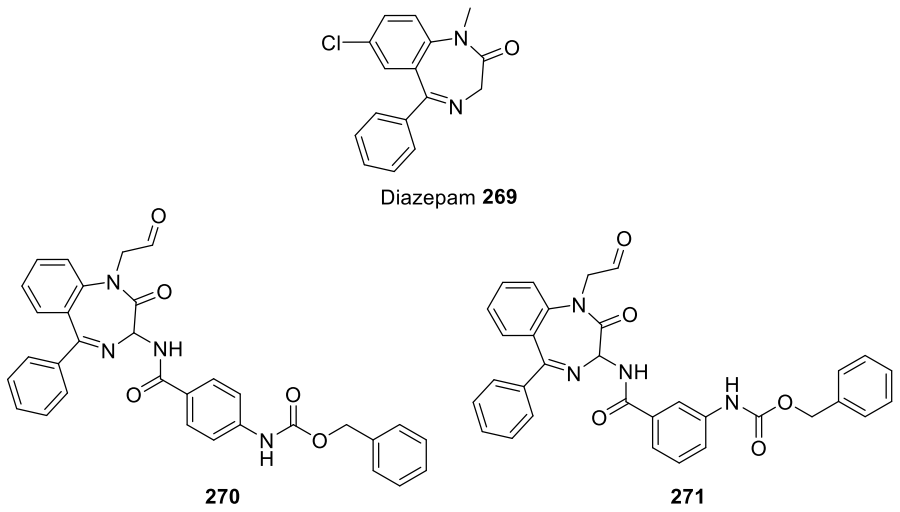

Figure 34 Diazepam and benzodiazepine based SENP1 inhibitors

Several other SENP1 inhibitors have been found since, such as GN6958 **272** (*figure 35)* that was discovered when the parent compound GN6767 **273**, a HIF-1α inhibitor, was investigated more fully. Pulldown studies using a biotinylated GN6767 **273** analogue showed that it was also binding to SENP1. Hence a better and specific SENP1 inhibitor was designed based on the parent GN6767 **273** structure. GN6958 **272** was screened against a small array of other cellular proteases (SENP2, papain, trypsin, chymotrypsin and thermolysin) representing cysteine, serine and metalloproteases respectively. GN6958 **272** did not inhibit either the serine or the metalloproteases. It did not inhibit SENP2 either, showing some selectivity. Interestingly it did show weak inhibition of papain, another cysteine protease, indicating that it might inhibit other cysteine proteases not just SENP1. However no other cysteine proteases were tested in the study. [122] Also, when looking at HIF-1α accumulation in cells, linked to SENP1 activity before, it transpired that the extent of suppression of accumulation of HIF-1α could not be explained only by SENP1 inhibition and hence it had to be assumed that GN6958 **272** has effects independent of SENP1 inhibition in cells.[122] This all indicates that it is not a very selective SENP1 inhibitor.

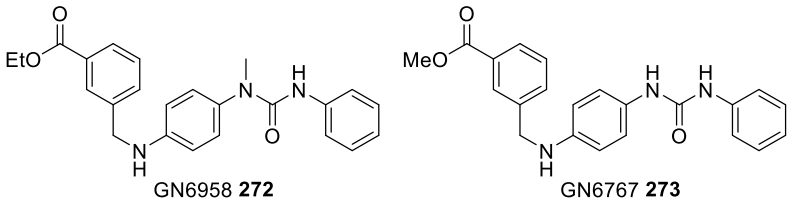

Figure 35 HIF-1α and SENP1 inhibitors

Another library of SENP inhibitors was found by Bogyo *et. al* when they searched for SENP inhibitors in a library of cysteine protease inhibitors that react with the catalytic cysteine *via* their reactive epoxide moiety.[123] The authors then synthesised a library based on the lead compound, JCP666 **274** (*figure 36*), unfortunately none of their compounds were found to be significantly more active than the lead, IC_{50}=13.8 μM for SUMO1. Their most active compound, VEA260 **275** had an IC_{50}=7.1 μM and a very similar structure to the lead. These compounds also inhibit SENP2 and SENP7 in the μM range. They did not find any compounds that inhibited SENP6 at all; SENP3 and 5 were not tested due to technical difficulties related to the screen.[123] Unfortunately when these inhibitors were tested in cells no inhibition was observed, this might have been due to the inability of these compounds to enter the cells.

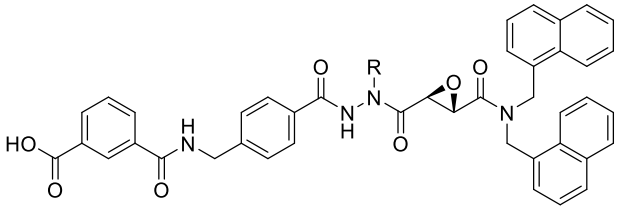

JCP666 **274** R=CH_2COOH
VEA260 **275** R=H

Figure 36 SENP inhibitors

Another family of SENP inhibitors were found when novel HIV antivirals were investigated (*figure 37*). These compounds reduced the ability of the virus to infect the cells without affecting its ability to enter cells. The viral DNA, after reverse transcription, just could not integrate into the cells genome. It turned out that the compound NSC5068 **X11** and NSC160224 **X12** were acting as SENP inhibitors.[113] A small library with the amine and sulfonic acid groups in various positions on these two skeletons was then synthesised, including the monomers of both the compounds. All the dimers tested had similar IC_{50} values of 3-6 μM for SENP1, SENP2 and SENP7 in a screen using a bioluminescent peptide substrate (pentapeptide imitating SUMO tail attached to Luciferin) assay. The monomers showed much weaker inhibitory effects in this screen. These inhibitors are active in live cells and were shown to bind to the SENP-substrate interface using NMR studies. This means that NSC5068 **276** and NSC16224 **277** do not interact with the catalytic site and the catalytic cysteine, like some of the

previously described SENP inhibitors (**270**, **271** and **275**), but instead bind to an allosteric site to inhibit enzyme activity.[113, 124]

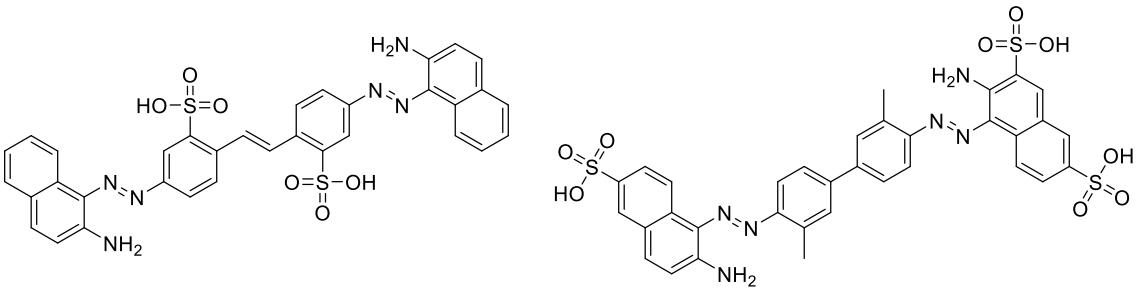

Figure 37 Allosteric SENP inhibitors

A whole range of SENP inhibitors have been found by virtual screening of compounds against the SENP enzyme. These virtual screens allow for the most promising molecular scaffolds to be weeded out and analysed before any synthesis has to take place. This has allowed for the swift discovery of several families of novel SENP inhibitors. It also allows for the purposeful differentiation between the SENP isoforms from the design phase.[106] Examples of these SENP inhibitors **278**, **279** and **280** can be seen in *figure 38*. Compounds **279** and **280** have an acyloxy methyl ketene and an α,ß-unsaturated carbonyl respectively that are both susceptible to nucleophilic attack by a cysteine.

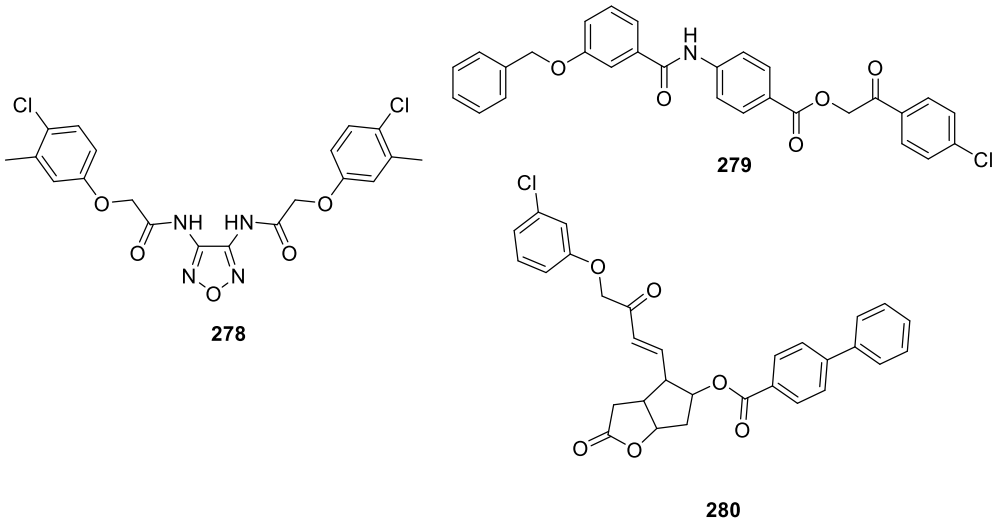

Figure 38 SENP inhibitors found by virtual screening

Compound **278** was designed by virtual screening to be a SENP2 inhibitor (*figure 38*). It is 10 times better at inhibiting SENP2 over SENP1,[125] remarkable

considering the sequence homology between SENP1 and SENP2. Compounds **279** and **280** are both SENP1 inhibitors, each with an IC_{50} of around 1 μM.[114, 126] Compound **280** was used to identify novel SUMOylation targets in human cell lines.[114] All of the SENP inhibitors described so far share some common structural motifs, high number of benzene rings and ester and amide bonds. Quite a few of them are also either dimers, pseudo-dimers or have a symmetric structure. Hinokiflavone also shares these traits, as it has a high number of aromatic rings and is a dimer.

A natural product, triptolide **281**, (*figure 39*) also seems to affect SUMOylation levels and cancer cell survival in cells. It is though that triptolide acts by downregulation of SENP expression (instead of SENP inhibition) but the effect in cells seems to be similar.[127] Triptolide does not actually bind to SENP though and the exact mechanism by which it downregulates SENP1 expression is not known yet although it is feasible that with all its epoxide and Michael addition sites triptolide **281** is also a covalent binder.

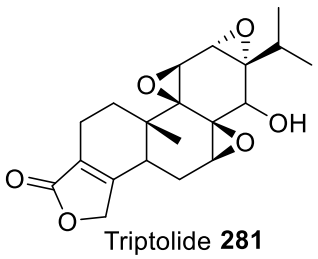

Triptolide **281**

Figure 39

There are problems associated with all of the SENP inhibitors described in this chapter, quite a few do not enter cells and are hence unsuitable for both *in cellulo* and *in vivo* work. Most are nonspecific, either by also affecting other cellular functions, inhibiting other cysteine proteases or inhibiting multiple families of SENPs. A lot of the above mentioned inhibitors work by covalently binding to the active site (for example **270**, **271** and **275**), therefore permanently deactivating the enzyme. Most of the authors even mention in their papers that further work needs to be carried out on their inhibitors before they can be widely used.[122, 125, 126]

Covalent binders do have their advantages however; they can be used to study the target enzyme by activity base profiling. The advantage of using a covalent binder to study protein activity in cells is that it is specific to activated enzymes. Enzymes that are deactivated by posttranslational modifications, for example, (and hence, not reactive) do not bind to a probe that relies on covalent attachement to the active site by enzymes own catalytic amino acids. This is in contrast to other proteomic techniques that, such as mass spectroscopy base techniques, that do not differentiate between active and inactive copies of the protein. Hence if an analogue of hinokiflavone could be designed that covalently binds to the SENP enzymes active site than this hinokiflavone based probe could be used to carry out activity based profiling of SENP1.

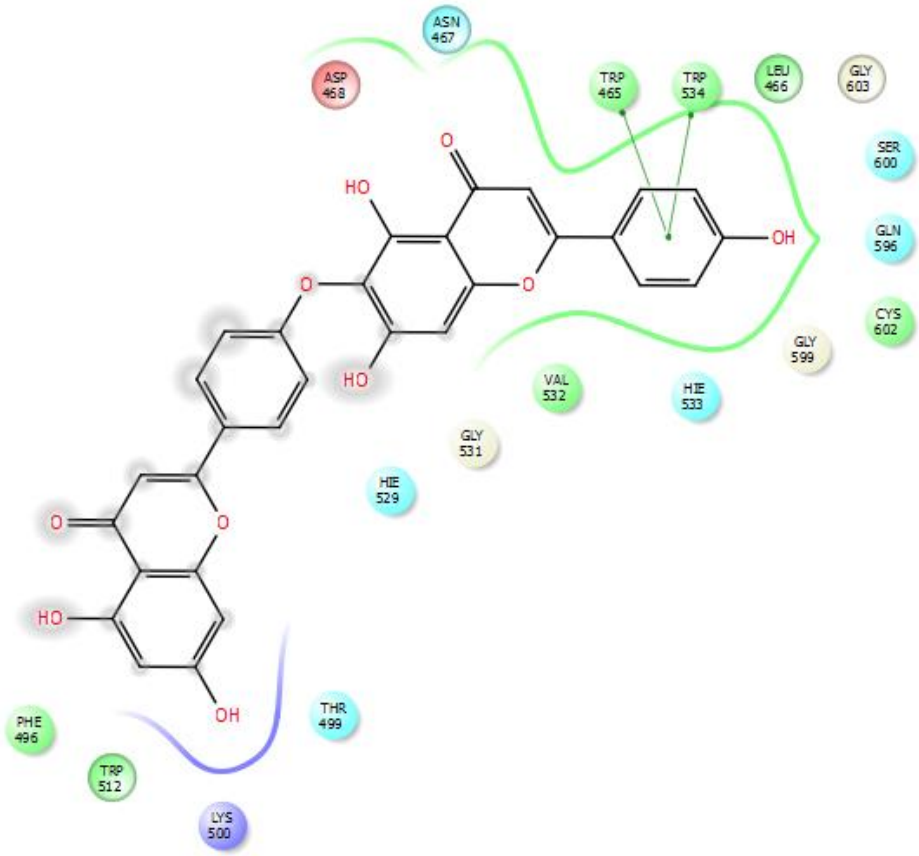

Figure 40 Model of hinokiflavone in the SENP active site

Computer modelling by David Gray in Dundee, with the SENP active site shows a possible binding site for hinokiflavone **9** (*figure 40*). This model also shows that there is a cysteine S602 right next to the proposed binding site of hinokiflavone, which would allow for potential interactions with the 4'''-OH. This allowed us to design probes that might react covalently with S602. Covalent binding of

hinokiflavone analogues to the target would allow the isolation of the protein-hinokiflavone conjugate, the exact characterisation of the binding site and other further biological experiments. Definite proof of where and how hinokiflavone interacts with the SEMP enzyme would then be helpful for designing drugs to target SEMP and hence influence splicing or designing further molecular probes. The covalently binding hinokiflavone analogue could also be used in proteomic studies of SENP.

6 Structural analogues of hinokiflavone

While efforts towards the total synthesis of hinokiflavone were being made, it became apparent that any synthesis of hinokiflavone would have to be quite lengthy and hence overall yields were expected to be small. The primary reason for the synthesis of hinokiflavone was its use in cells, and potentially in future animal studies, to further study the spliceosome. If an analogue with the same biological activity and easier synthesis was found, hinokiflavone could be replaced. The following analogues were designed to be simpler and smaller than hinokiflavone. By simplifying the flavone skeleton, molecular weight could be lowered, and the number of hydrogen bond donors and acceptors also potentially be lowered. These changes would make these analogues more drug-like, making them more likely to conform to Lipinski's rule of five.[128, 129] Hinokiflavone itself has a molecular weight of 538 amu that is high for a small molecule drug. It also has 10 hydrogen bond acceptors and 5 hydrogen bond donors. All of this puts hinokiflavone on the upper limit of what Lipinski conceived would make a good small molecule drug.[128, 129] The extensive aromatic skeleton and the numerous phenols also increase the chance of secondary metabolism; hence, hinokiflavone is not predicted to have a long half-life inside whole animals. By aiming to make more drug-like compounds, that would have the same cellular effect and the same or better physiochemical properties as hinokiflavone, but be easier and faster to synthesise and hence have the potential to become drugs targeting the spliceosome. Simplifying the structure would also allow the key interactions of hinokiflavone to be identified.

The secondary reason analogues of hinokiflavone were investigated was their use in potentially isolating and characterising hinokiflavone's **9** target protein. A covalent binder could also help to ascertain the exact binding pocket that would be then used for fragment based drug discovery.[130] The candidate target, SENP, had already been identifies by this point in time. Analogues that could help confirm this hypothesis by covalently binding to SENP but also to any other cellular targets and hence facilitating pulldown studies were needed. As SENP is a cysteine protease, analogues that could target and react with the catalytic cysteine residue were designed. Cysteine proteases are most often targeted by covalent inhibitors as the cysteine offers a convenient site for that, although

non-covalent inhibitors are also known.[131] Cysteines react with many electrophilic warheads, selective or non-selective, as long as they can reach the active site. To ensure selectivity the rest of the probe or drug should be selective to the specific cysteine protease, although this is challenging considering the multiple cysteine protease families and isoforms. To design our molecular probes an electrophilic warhead would be incorporated into a hinokiflavone analogue. A modified version of a covalent inhibitor that includes a tag could then later be used for activity based profiling.[85]

As well as designing an electrophilic warhead that then reacts with the active site, there is another method by which probes can be covalently attached to their protein targets. Photoaffinity labelling, which relies on non-covalent interactions to ensure proximity (and hence selectivity) to the target protein.[132] The probe can then be irradiated with light which activates an inbuilt photo-reactive warhead. Due to the non-covalent interaction between the probe and the target protein the light-activated warhead should be then close enough to selectively react with only the target protein. There are several light activated warheads used in photoaffinity labelling, the best ones are small (so to not affect the binding of the probe to the target) and form highly reactive species that then react with the target protein before the probe can diffuse away from the active site. The most often used groups used for this are azides, diazirines and benzophenones.[132]

To retain selectivity in our probes attention will be payed to the structural and conformational aspects because these were deemed to be important for the activity and selectivity of hinokiflavone from the SAR of inactive analogues (*chapter 2)*. A twist between the B and A' rings was thought to be the result of functionalisation of the A' ring by the two phenols on either side of the ether link, and at the onset of this work was believed to be critical to binding.

6.1 Alkene analogues of hinokiflavone

The alkene analogues were designed to be structurally similar to hinokiflavone but of lower molecular weight and with two fewer hydrogen bond acceptors and should therefore have improved solubility and pharmacokinetic properties. The alkene replaces the C' ring of hinokiflavone (*figure 41*), the analogues should

retain the molecular shape of the missing C' ring due to conjugation with the A' and B' rings. The sp^2 hybridised carbons are also flat and retain the restricted rotation positioning the B ring in the right orientation. This would hopefully provide the rigidity needed to effectively mimic hinokiflavone. Alkenes are known bioisosteres for benzene so they should also work for the 4-pyrone (ring C').[93]

Three alkenes were designed initially (*figure 41*). The simplest alkene analogue, **281** was not actually the first one attempted. Benzyl alcohol analogue **282** was chosen because benzylic alcohols are well-known phenol bioisosteres. Conveniently, benzylic chloride **282** could also be synthesised from benzylic alcohol **282** through late stage modification.[93] Benzyl chloride **283** was designed to include a leaving group instead of the phenol on the B' ring, which could perhaps anchor it to its target. This would facilitate the pull down of the target proteins by covalently modifying the active cysteine residue in SENP and potentially provide a protein bound inhibitor complex for structure determination.

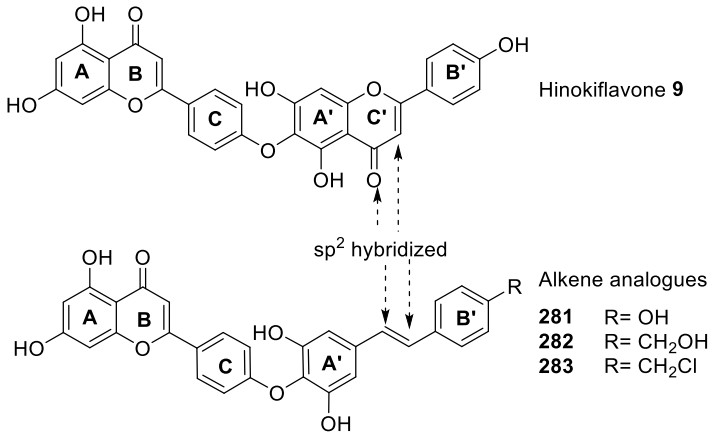

Figure 41

The Alkene analogue **282** was modelled using Spartan and the model showed that the analogue and hinokiflavone have very similar conformations (*figure 42 vs 43*). This suggests that the alkene **282** would be a good model for hinokiflavone. It is also important to note, that alkene **282** contains the two phenol groups on the A' ring which were previously shown to be important to hinokiflavone's activity. These two phenols are thought to be responsible for the twist in the conformation of hinokiflavone that was believed to be required for

activity. This twist is also observed in the alkene analogue **282** between the B ring and the A' ring.

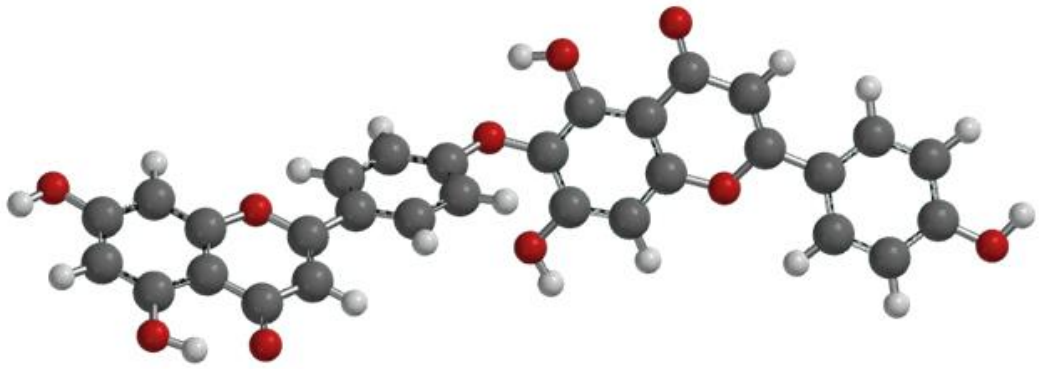

Figure 42 Computational model of hinokiflavone 9

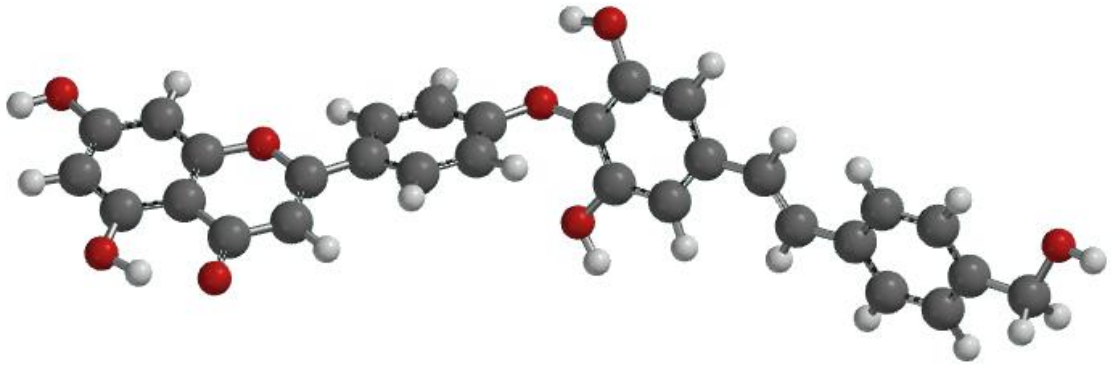

Figure 43 Computational model of analogue 282

6.1.1 Synthesis of alkene analogues:

The synthesis of alkenes was originally designed to proceed *via* the benzaldehyde intermediate **284** because this would allow for easy access to modified LHS analogues (*scheme 81*). This synthesis was designed before it became apparent, from the synthetic efforts towards hinokiflavone, that the central ether formation step was best left until later in the synthesis.

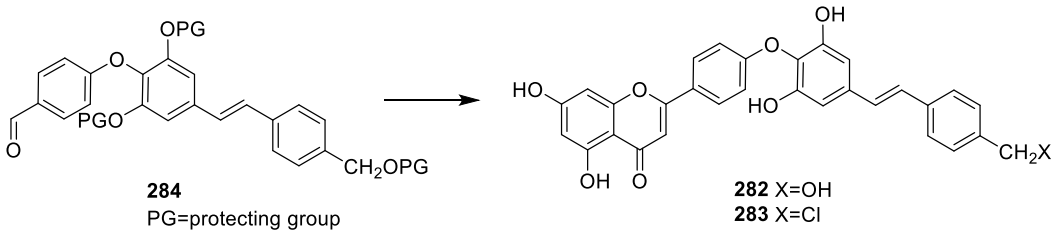

Scheme 80

Alkene **286** was synthesised from the commercially available syringaldehyde **284** and phosphonium salt **285** by a Wittig reaction (*scheme 82*). Purification of alkene **286** was initially attempted by flash column chromatography and various crystallisation procedures, but not all the phosphine oxide side product could be removed. Only very small amounts of material could be isolated completely pure. Therefore it was decided to use the crude alkene **286** in the next reaction. Hence the crude mixture was reduced using lithium aluminium hydride to give alcohol **287** in good yield over two steps after chromatography.

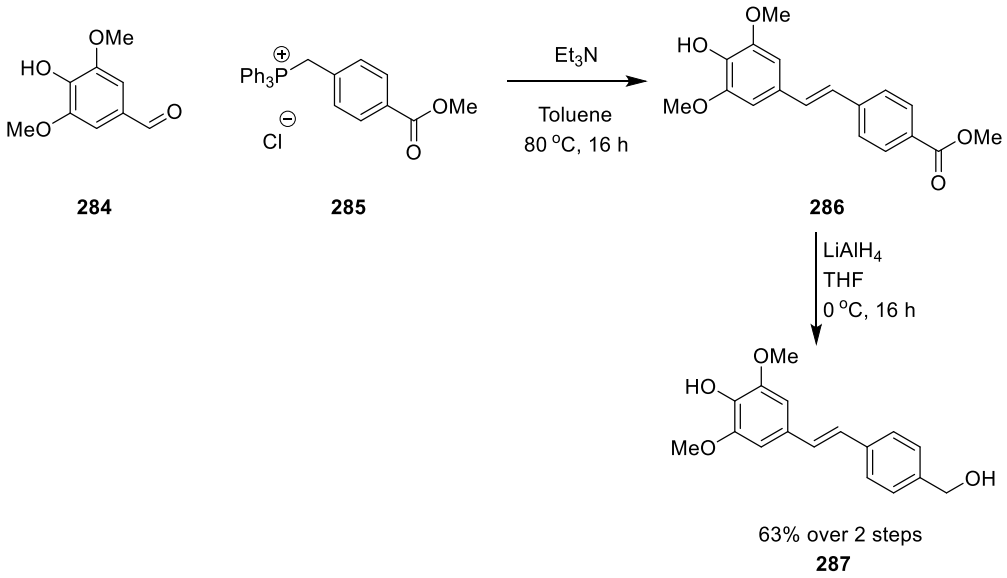

Scheme 81

The alcohol **287** was then coupled with chloro-nitro-benzaldehyde **288** using previously described conditions to yield the aldehyde **289** in good yield (*scheme 83*). With the central ether now in place, the next step was the attempted removal of the activating nitro group. However, the reduction proved problematic by all of the previously used methods, including the sodium dithionite reductions and tin chloride reductions. Palladium on carbon with hydrogen was never tried because that would most likely have reduced the alkene. It was thought that the unprotected aldehyde group was probably the cause of these problems, so a protecting group strategy was investigated.

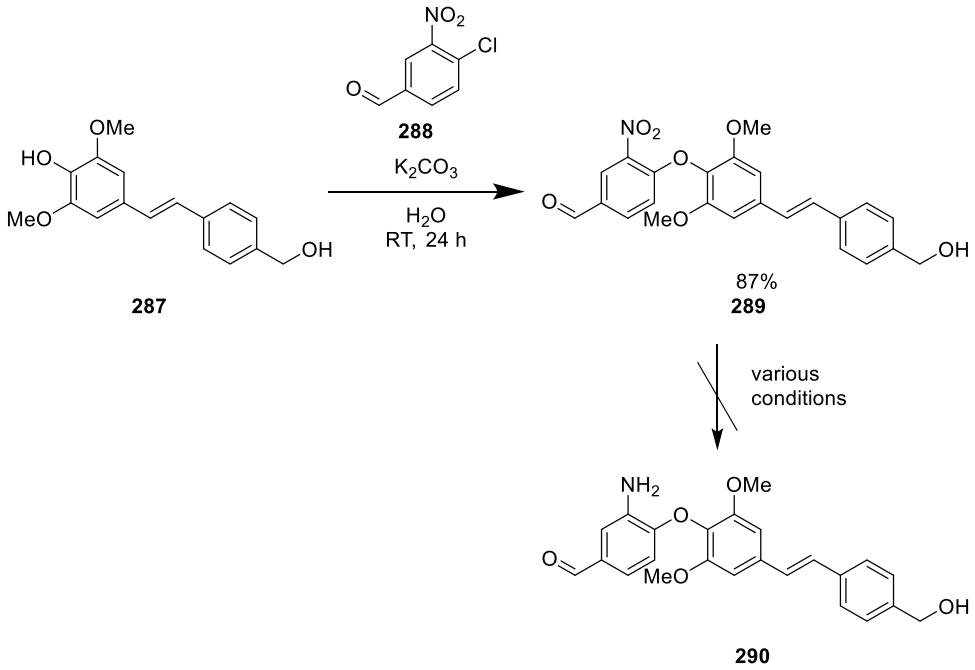

Scheme 82

The aldehyde **289** was protected as a cyclic acetal in good yield to form acetal **291** (*scheme 84*). However, reducing this compound again proved to be problematic. Even though there was some evidence of aniline **292** found by ^{1}H NMR analysis of the crude compound, no success was had with attempts to purify it. Attempts to use the crude material during the next step to make alkene **293** also resulted in decomposition of the material.

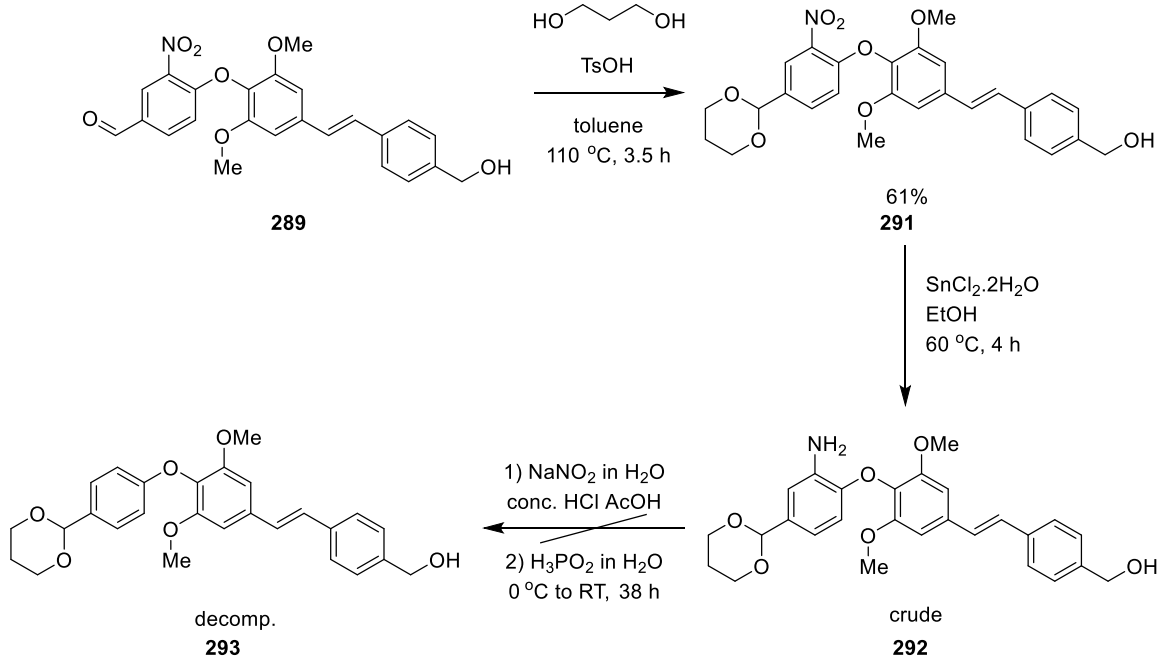

Scheme 83

At this point, since the removal of the nitro activating group had proved so difficult our approach changed and our efforts were moved toward a different route to alkene **282**. Instead of trying to synthesise the late stage common intermediate **284**, the synthesis of alkene **282** was attempted by the direct coupling of the isopropylated LHS **197** prepared earlier (see *scheme 50*) to the alkene **287** (*scheme 85*) The aromatic substitution reaction did not work as well as expected, but flavone **294** was isolated in acceptable yield. The nitro group on compound **294** was then reduced to the amine in a relatively poor yield using tin chloride (characterisation of compound **295** was based on ^{1}H NMR and ^{13}C NMR only). However all attempts to then remove the amino group from flavone **295** using the previously employed conditions resulted in total decomposition of all material. Since all attempts to synthesise compound **282** had now failed at the reduction stage, it was concluded that the system was not stable enough to survive the removal of the diazonium ion formed by nitrous acid. However, perhaps similar compounds containing alkenes could still be synthesised. It was hypothesised that intermediates in the synthesis of the phenol **281** are much more stable than those for the benzylic alcohol analogue **282** because any competing S_N1 and S_N2 reactions would be avoided.

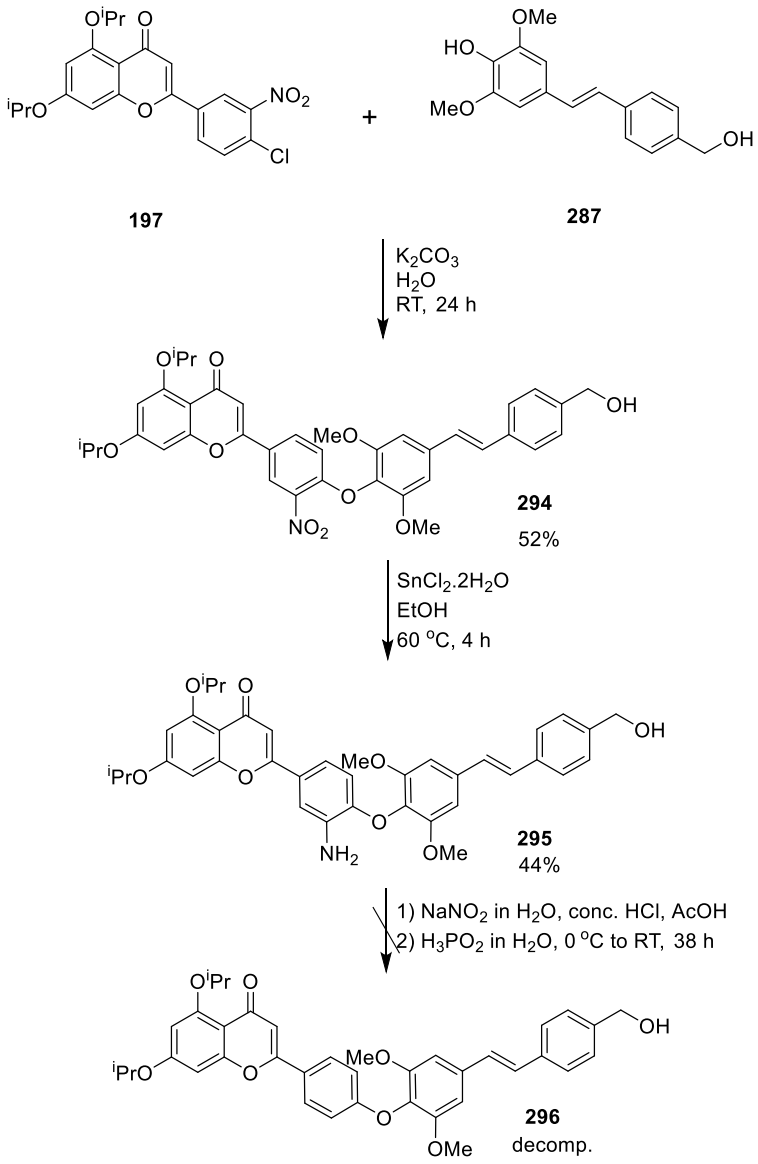

Scheme 84

Since no commercially available phosphonium salt could be found and considering the problems with the purification after the Wittig reaction, the phosphonate ester **298** was synthesised from the corresponding benzyl chloride **297** (*Scheme 86*). Since the diethylphosphate by-product of the Horner-Wadsworth-Emmons reaction[133] is easily removed by washing with water, the purification was predicted to be much simpler. The phosphonate ester **298** was then reacted with MOM-protected syringaldehyde **299** to yield the new alkene **300** in a modest yield. The MOM protecting group was then removed to yield the alkene **301** which could be used as an analogue to attach the LHS of hinokiflavone.

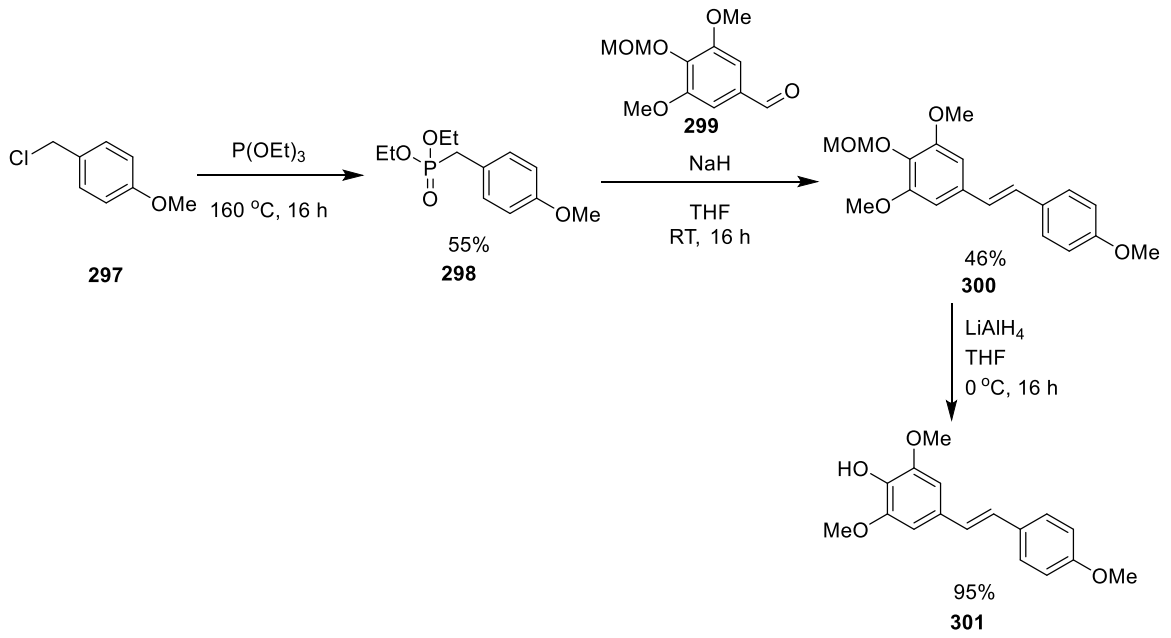

Scheme 85

The alkene analogue **301** was subsequently coupled to the isopropyl protected LHS **197** using previously employed conditions to give the ether **302** in a good yield (*Scheme 87*). The nitro activating group was again reduced using tin chloride and the crude amine **303** reacted with nitrous acid followed by phosphinic acid to yield the desired isopropoxy hinokiflavone analogue **304**. The overall yield over the two reduction steps was decidedly poor, but since these reactions only resulted in decomposition in the case of analogue **282** this was considered a success.

The alkene **304** was then deprotected using boron tribromide to yield the desired alkene analogue of hinokiflavone **281** (*scheme 87*). This deprotection did not proceed as smoothly as some previously mentioned because three of the five phenols in the analogue were methyl protected. As well as the desired deprotection product **281**, monomethyl, dimethyl and even trimethyl side products were also observed by LC/MS. These were isolated by HPLC, but due to the small scale of the reaction there was not enough material isolated for complete characterisation. The samples of the methyl side products were also not sufficiently pure for biological study.

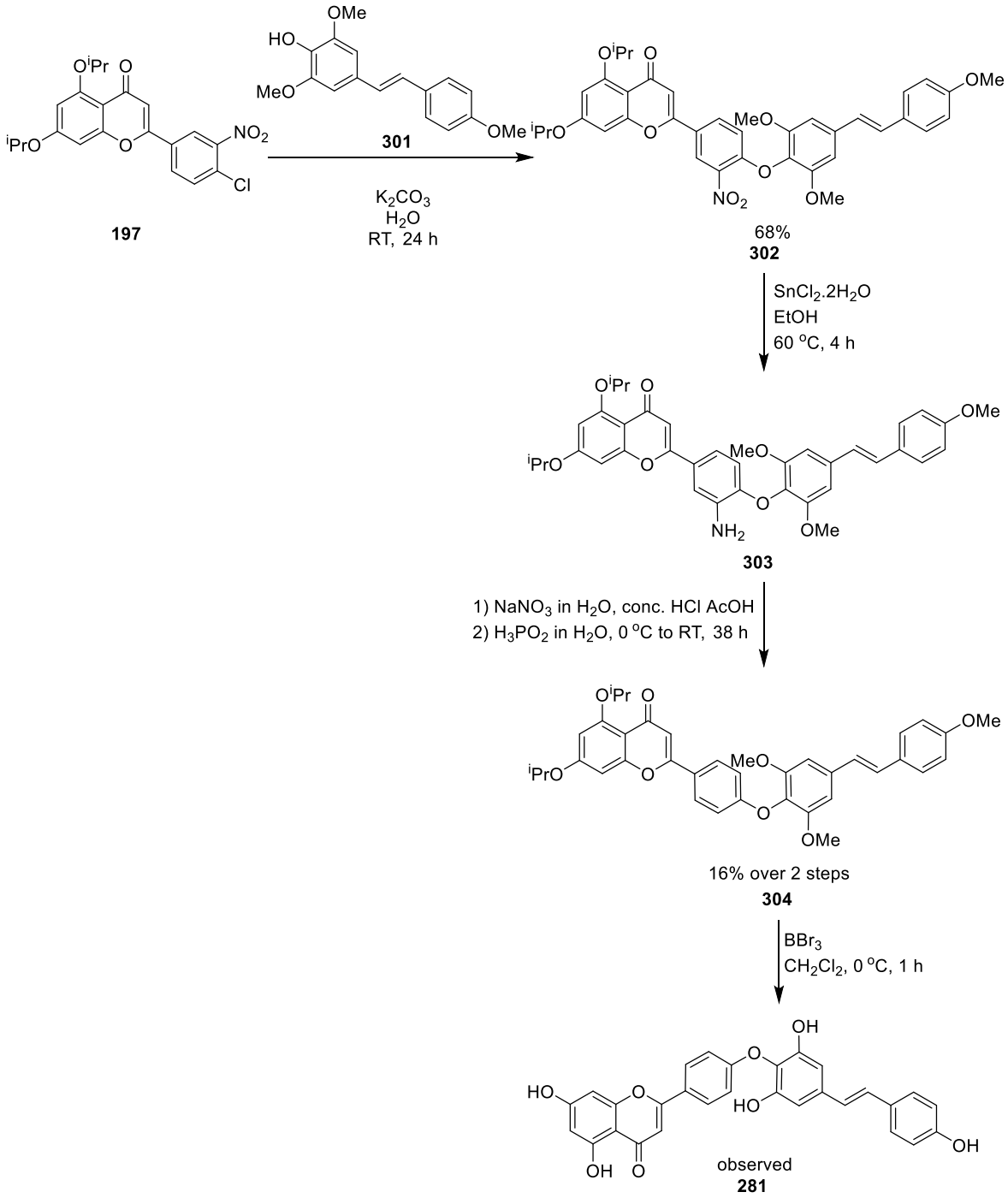

Scheme 86

Since the methyl groups caused the low yield during the deprotection, an attempt was made to synthesise an isopropyl protected RHS (*scheme 88*). First the corresponding phosphonate ester **306** was synthesised in two steps from 4-hydroxybenzyl alcohol **87**. The first step to selectively alkylate the phenol took advantage of the pKa difference between the two hydroxyl groups. The alcohol **305** was then converted by S_N2 reaction[134] into a benzylic chloride from which the phosphonate ester could be made.

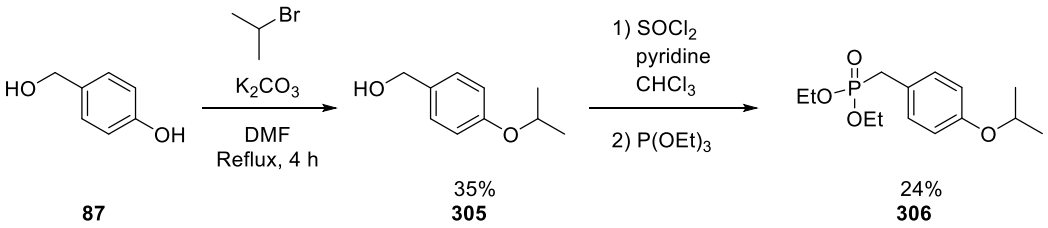

Scheme 87

The selective alkylation of the 3- and 5-hydroxy groups of 3,4,5-trihydroxybenzaldehyde is not possible.[34] Therefore it was decided that the middle hydroxyl group would be introduced last, after the formation of the alkene skeleton **309** by lithiation-borylation followed by conversion of the boronate to a phenol. Hence the 3,5-dihydroxybenzaldehyde **307** (*scheme 89*) was isopropyl protected to form the aldehyde **308** that subsequently reacted with the phosphonate ester **306** to form the alkene **309** in a modest yield. All attempts to introduce the missing hydroxyl group to the alkene **309** subsequently failed. As the HWE reaction to form the alkene proceeded in a really poor yield anyway, attempts to make this isopropyl protected RHS were abandoned.

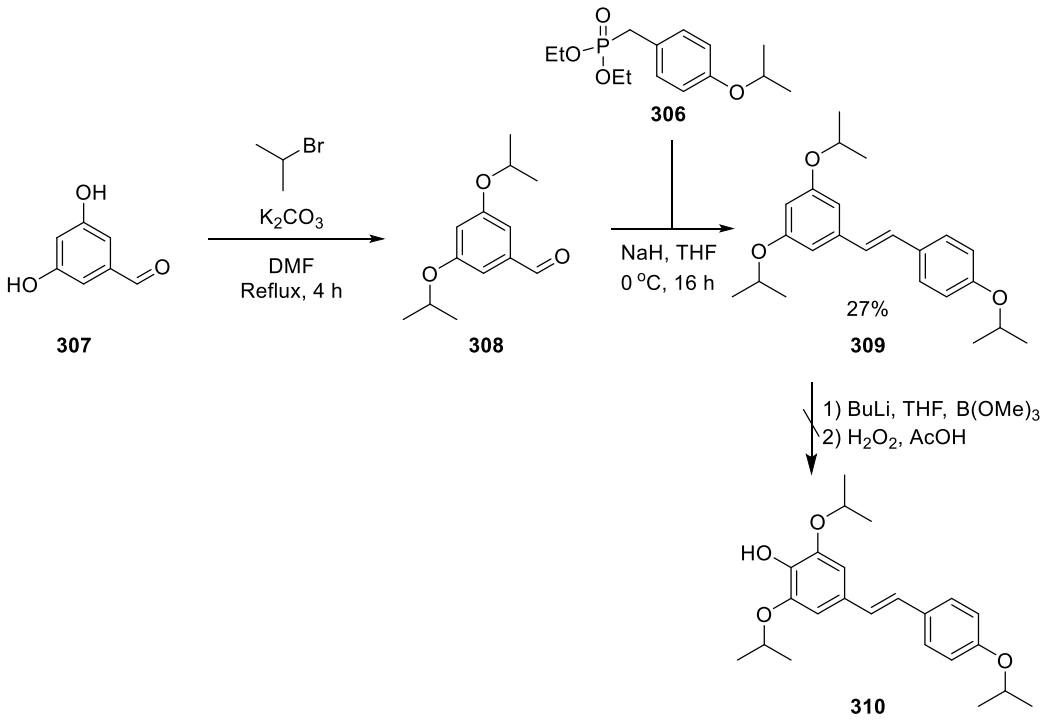

Scheme 88

During various attempts to make alkenes **281**, **282** and **283**, a consistent problem was the poor yields of the Wittig and HWE reactions. These yields were probably due to the electron rich benzylic group on the phosphonate esters that slowed down the final elimination step of the reaction. Hence a phosphonate ester with an electron withdrawing group should lead to better alkene yields. Furthermore, even though the alkene analogue **281** had a simplified skeleton and was easier to assemble then that of hinokiflavone itself, it lacked a reactive moiety allowing for covalent attachment to the target protein that was included in the alkene analogue **282**. Therefore, work began on a different set of alkene analogues that would perhaps have higher yielding reactions and a possible reactive moiety for cross-linking to the target protein.

6.2 Fluorinated analogue of hinokiflavone

Alkene analogues with nitrogen moieties were synthesised next (*figure 44*). The reasons behind this were threefold. Introducing an election withdrawing nitro group would theoretically improve the low yielding Witting reactions by stabilising the formation of the ylide. Secondly, amines are a well-known bioisostere to alcohols, both have hydrogen bond donating and accepting ability and they are of comparable size.[93] Thirdly, an aniline on the B' ring would also allow for the easy functionalisation of that position by the use of Sandmyer type reactions.[135] This would allow for the late stage introduction of azides (for the use of photoaffinity labelling) or phenols. These alkene analogues would be constructed using the fluoro LHS because the removal of the nitro activating group would also remove the nitro group on the C' ring as it was impossible to selectively reduce only one of them. The fluoro LHS would not require the removal of the activating group as the electron withdrawing fluoride atoms are hydrogen bioisosteres.

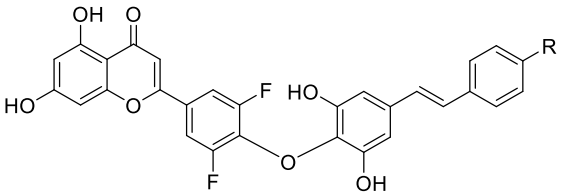

311 R=NO_2
312 R=NH_2
313 R=N_3
314 R=OH

Figure 44

The computational model of alkene analogue **140** show the same twist between the B and A' rings of this analogue than on the parent hinokiflavone molecule. The modified A' alkene B' ring system seems to have the same flat rigid conformation than the parent hinokiflavone molecule also. Lastly, the fluorine atoms on the B ring don not seem to have affected the general shape of the analogue. The analogue is smaller and lacks the two hydrogen bond acceptors on the C' ring of hinokiflavone, the importance of which is not yet clear (*figure 45*).

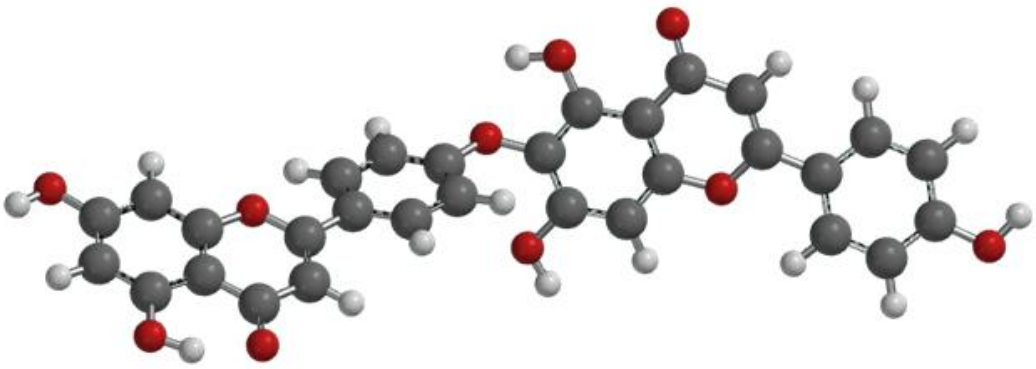

Computational model of hinokiflavone

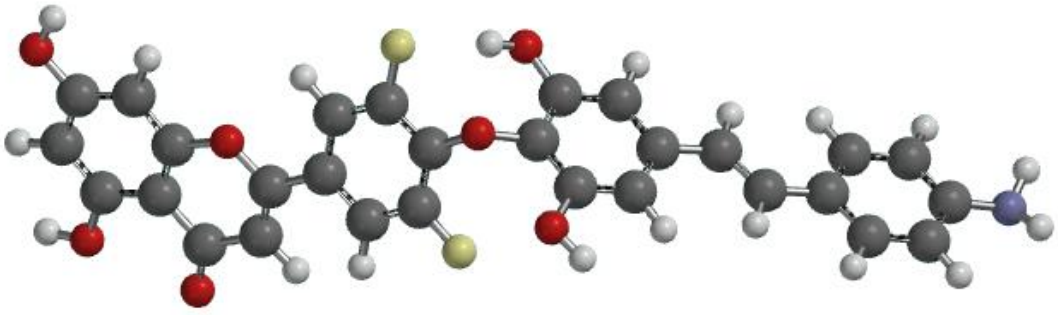

Figure 45 Molecular model of alkene analogue 140

First the phosphonate ester of the nitro compound **316** was synthesised from the corresponding benzylic bromide **315** (*scheme 90*), this was subsequently reacted with protected syringaldehyde **299** to form alkene **317** in good yield. Hence our predictions of an electron withdrawing group improving the HWE reaction yield were correct, but not as remarkable as expected. The alkene **317** was then deprotected to yield the alkene **317**, capable of the S_NAr reaction with LHS, in quantitative yield.

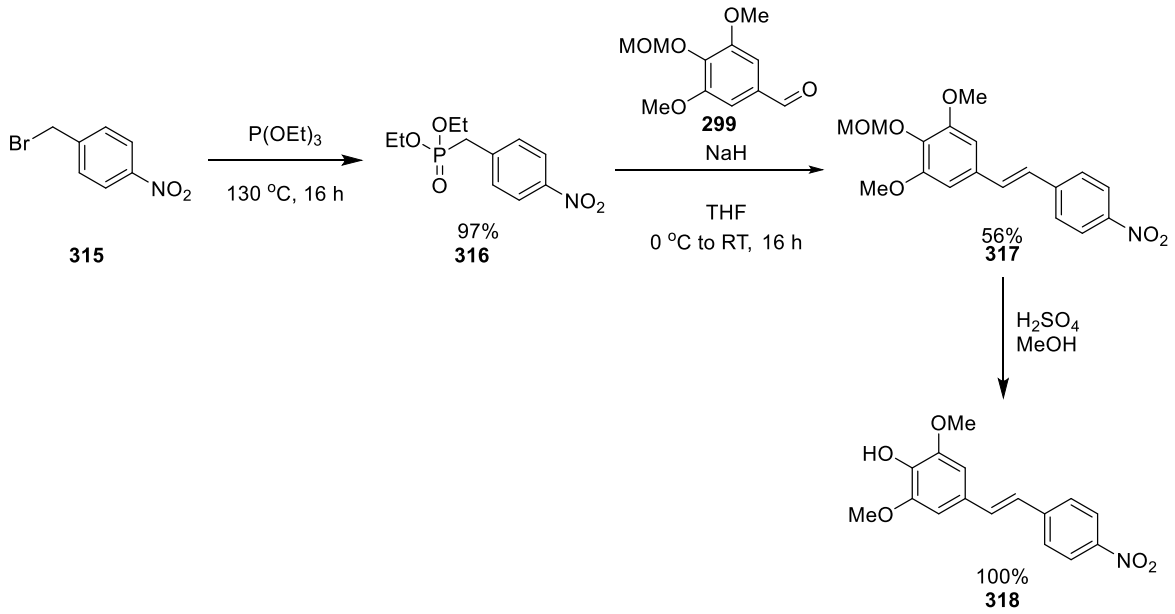

Scheme 89

Alkene **318** was then coupled with the trifluoro LHS **319** to form the protected analogue **320** of the target alkene **311** (*scheme 91*). The trifluoro LHS was used in this case because the nitro activating group of LHS **197** could not be removed without damaging the nitro group on the RHS, which was required for later reactivity. The protected analogue **320** was then subjected to the now familiar deprotection conditions using boron tribromide (*scheme 91*). Unfortunately, this resulted in complete decomposition of all material; no deprotection products (Compound **317** or mono/di-methylated side products) at all were visible using LC/MS analysis. It was thought that this was due to the nitro group, because there was evidence of the two halves in the LC-MS. It is conceivable that the electronwithdrawing nitro group caused the molecule to fragment under Lewis acidic conditions, *via* an S_NAr reaction.

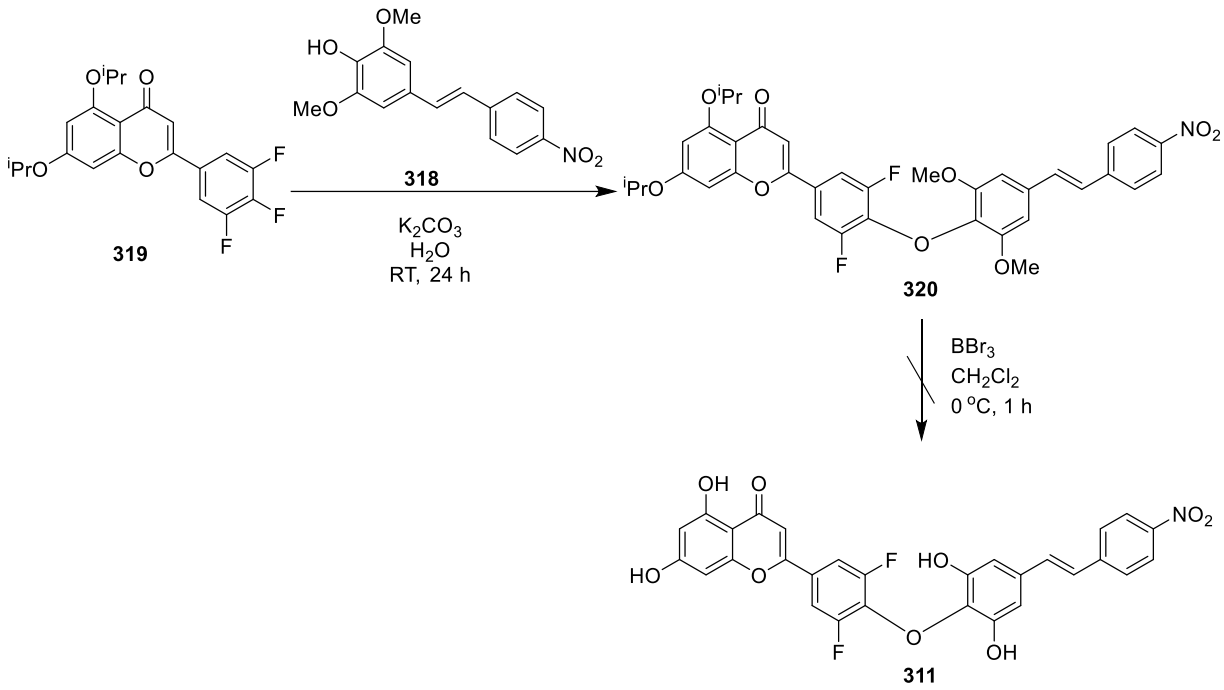

Scheme 90

Since it was thought that the nitro group was causing the decomposition during the deprotection step, efforts were made to remove it (*scheme 92*). However, the usual conditions for reduction of the nitro group using tin chloride failed in this particular case. Only starting material and an unidentified side product were visible by LC-MS analysis of the decomposition products. Hence the reduction reaction was also tried with the other reduction methods, and again, apart from starting material only decomposition products were observed. Since these reduction methods seemed to result in the fragmentation of ether **320**, the order of the steps was changed once again and various reduction conditions were attempted on alkene **318**.

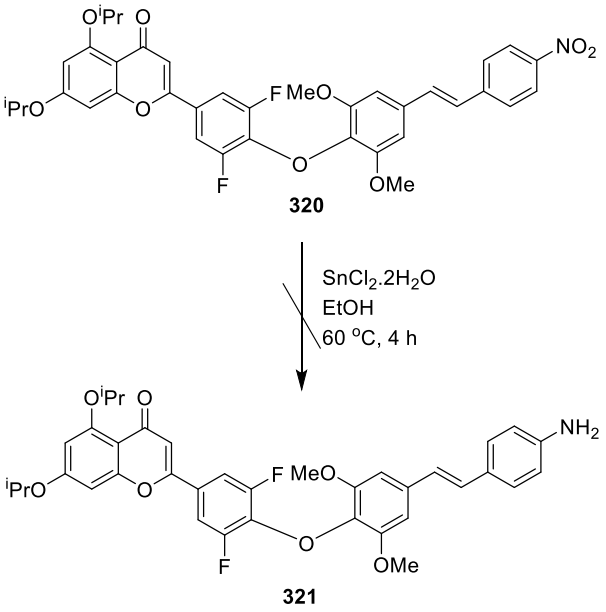

Scheme 91

However, the so far very reliable tin chloride reduction conditions failed again in the case of alkene **318**. Instead of isolating the amine **322**, just a small amount starting material was isolated (*table 3*). In an effort to reduce competing reactivities, the tin chloride reduction was also attempted on the MOM protected alkene **317**. However to no avail, the reaction produced an insoluble red precipitate that could not be characterised. Only a small amount of starting material could be reclaimed from the reaction, without the MOM protecting group.

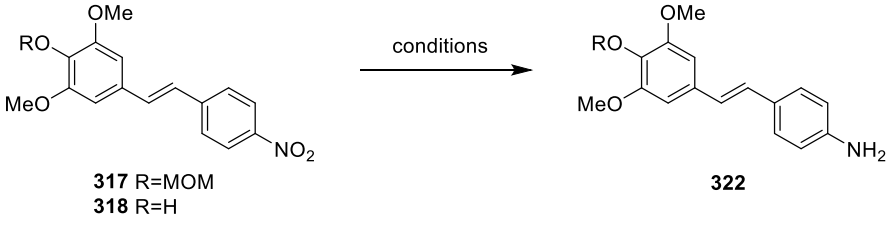

317 R=MOM
318 R=H

322

R	Conditions	Results
H	$SnCl_2.2H_2O$, EtOH, 60 °C, 4 h	Decomposition
MOM	$SnCl_2.2H_2O$, EtOH, 60 °C, 4 h	Decomposition
H	Fe powder, NH_4HCO_2, acetone/H_2O, 65 °C, 24 h	70% **322**

Table 3

On the other hand reduction using iron powder had proven reliable on small molecules (see chapter 3, *scheme 41*), but had fallen into disuse due to the

solubility issues of the various compounds encountered during this research. The iron powder used in this reduction procedure was found to induce precipitation of the amine products that were then impossible to extract from the reaction mixture. Hence these conditions were avoided. However, as all the other methods previously so reliable had failed, it was given another go. Using iron powder, ammonium formate in an acetone-water mixture alkene **322** was isolated in a good yield (*table 3*).

Since alkene **318** is a relatively small molecule with reasonable solubility, this was not a surprise; however, whether the same method would work on ether **320** was questionable. Possibly due to the presence of isopropyl protecting groups, and the smaller size of the alkene RHS compared to the original hinokiflavone skeleton, the solubility of amine **321** was good enough to be isolated in an excellent yield.

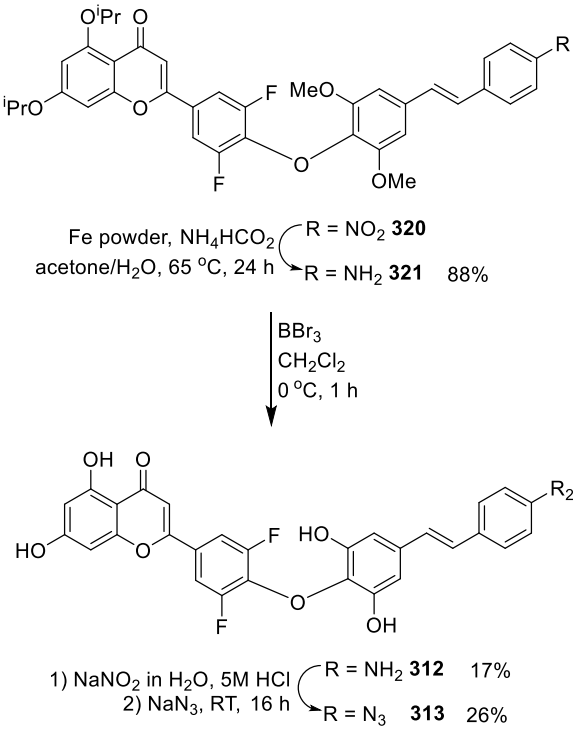

Scheme 92

The deprotection was then attempted again on the amino analogue **322**, this time proceeding without complications yielding the product **312** as essentially pure by ^{1}H NMR (*scheme 93*). Small amounts of both mono and dimethyl side products were observed by LC/MS. All efforts to further purify analogue **312** by recrystallisation from all the usual recrystallisation solvents (ethanol, methanol,

ethyl acetate, isopropanol) failed. Attempts to titurate the compound from dichloromethane-methanol also failed to give good results. Hence a portion of the compound was purified by HPLC to yield a sample for biological (17%) testing while the bulk material was used for subsequent reactions without further purification.

To produce an analogue capable of photo cross-linking to the target protein, an azido analogue was synthesised. This was done in a similar manner to the previous Sandmeyer-type reactions (*scheme 93*). The amine was converted into a diazonium salt before replacing the nitrogen leaving group with the azide nucleophile. The crude compound was again purified using HPLC to yield the azido analogue **313** in moderate yield but very small quantity. The azido compound **313** was therefore tentatively characterised based on the ^{1}H NMR, IR and LRMS data only.An effort to synthesise a phenol analogue **314** with fluoro groups was also attempted (*scheme 94*), but resulted in the total decomposition of all material present.

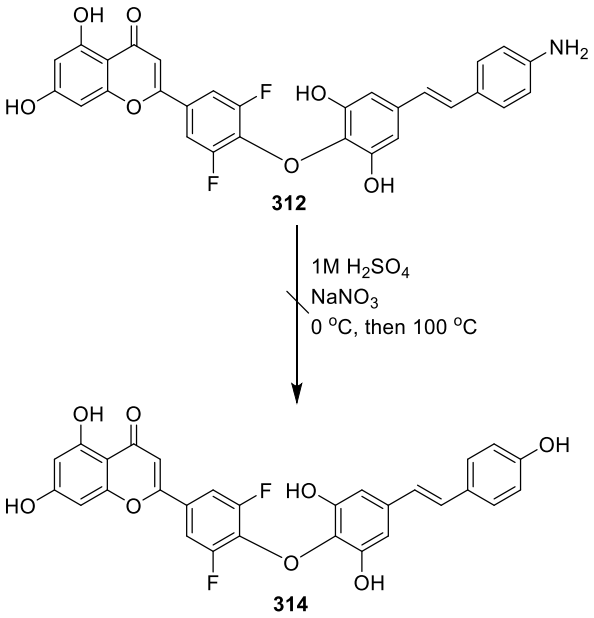

Scheme 93

6.3 Amide analogues of hinokiflavone

The second series of analogues contained an amide moiety. Amides were chosen for the ease of synthesis and the ease of introducing late stage modifications on the B' ring. The amide moiety would also provide rigidly that would hopefully

mimic the missing C' ring (*figure 46*). The synthesis was also deemed easier as the substitution pattern on the A' ring could be accessed from syringic acid. Hence the amide analogues fulfilled both the requirements to be good analogues. As amide bonds could be made after the central ether was formed an array of amide analogues were designed. The simplest of these was the direct analogue **323** with a *p*-hydroxyl group on the B' ring.

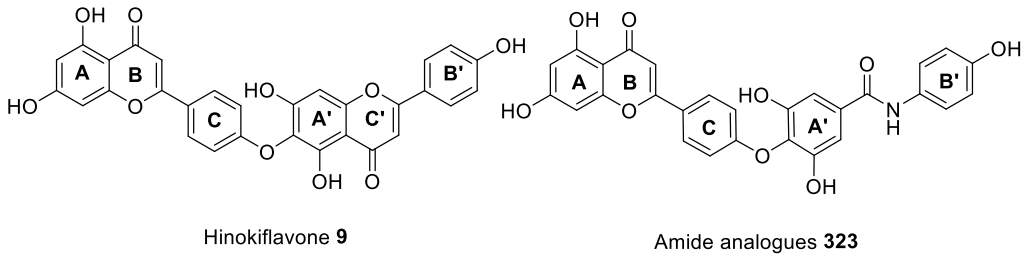

Figure 46

6.3.1 Computational modelling

The amide analogue **335** was modelled by Spartan to analyse the structural similarity to hinokiflavone. Computational modelling of analogue **335** confirmed our design (*figure 47 vs. 48*), the A'B' ring system of the amide analogue **335** closely resembles the physical shape of the A'C'B' ring system of hinokiflavone. There is a small twist visible through the amide bond but on the whole it seems to occupy the same physical space.

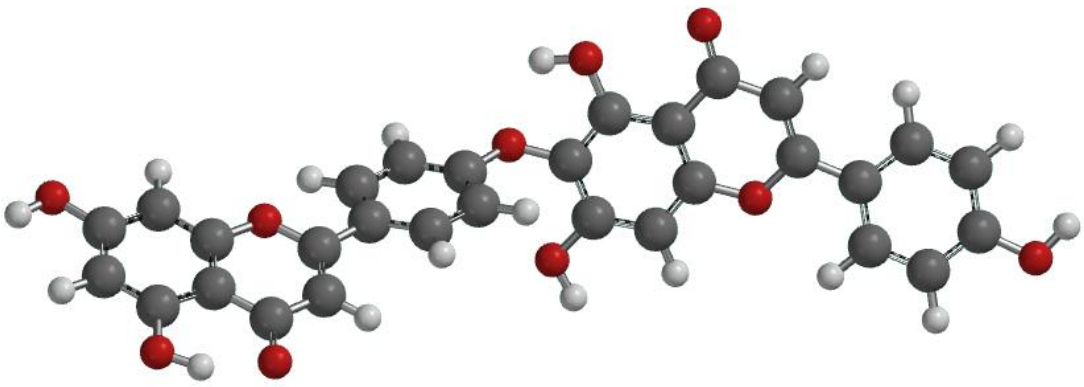

Figure 47 Molecular model of Hinokiflavone 9

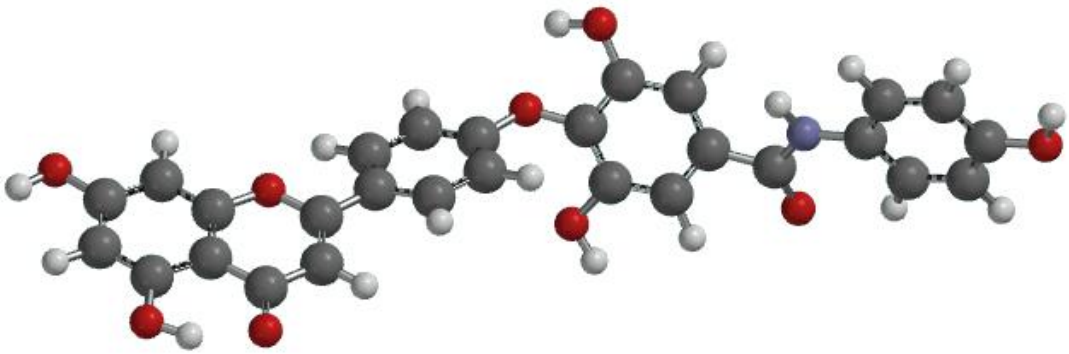

Figure 48 Computational model of amide analogue 335

6.3.2 Synthesis of amide analogue of hinokiflavone

To start the synthesis the common starting material **328** of all the amide analogues was synthesised by a nucleophilic aromatic substitution reaction between the isopropyl protected LHS **197** and the methyl ester of syringic acid **324** (*scheme 95*). This reaction proceeded in a modest yield with no difficulties. The nitro activating group was then removed from ether **325** using the previously utilised tin chloride reduction to acquire the amine **326**. The amino group was then removed by the usual method to yield the ester **327** in a good yield. The methyl ester **327** was hydrolysed to give the carboxylic acid **328**, which would be used for all the subsequent amide formations.

The first amide synthesised was from a cyclohexylamine (*scheme 95*). This was chosen as a type of validation for the design, to see if these amides could be formed. The cyclohexane ring would also interfere with the π-stacking that made these compounds so insoluble and hard to work with. Hence the analogue **333** was expected to have better solubility than hinokiflavone while still having the same rough shape.

The synthesis proceeded without much difficulty (*scheme 95*). The moderate yield for the formation of amide **329** could have been due to the small scale on which this reaction was carried out, because on smaller scales any residual moisture has a much more pronounced effect on the yield. The deprotection using boron tribromide proceeded in an unprecedentedly excellent yield to furnish the deprotected hinokiflavone analogue **333**. This was most likely due to the much better solubility of this analogue **333** compared to the other flavones

encountered during this project. The better solubility of **333** in dichloromethane would have prevented the partially deprotected product from crystallising out of solution and hence helped drive the reaction to completion.

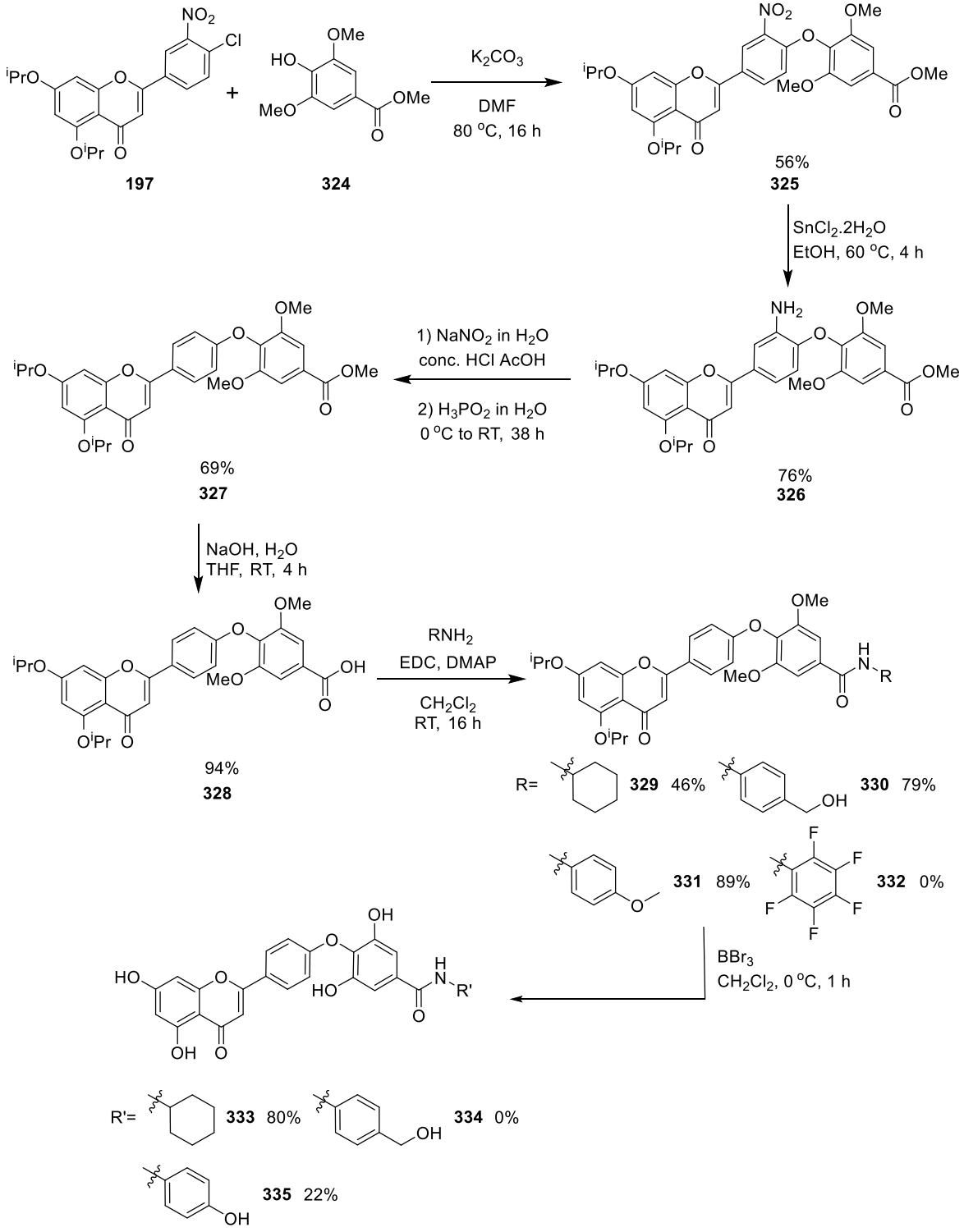

Scheme 94

As the shape of hinokiflavone was believed to be important to the role of binding, an analogue more closely resembling the shape of hinokiflavone was

designed (*scheme 95*). To synthesise analogue **335**, *para*-methoxy-aniline was reacted with the syringic acid derivative **328** to yield the protected amide **331** in excellent yield. The boron tribromide deprotection did not proceed in as high a yield as for the cyclohexane analogue **333**, but this was to be expected. Analogue **335** has the same general aromatic flat structure as hinokiflavone and the majority of previously synthesised analogues. Hence, it suffers from the same solubility and reactivity problems. It has to be remarked that a 22% yield after HPLC purification for a hinokiflavone analogue is more than adequate, especially considering the difficulties previously encountered in removing the methoxy protecting groups. Hence analogue **335** fulfils the requisites outlined for analogues in general as it has both a simpler higher yielding synthesis and much better solubility in organic solvents.

Since amide analogue **335** seemed promising two other amide analogues were attempted (*scheme 95*), both with potential reactive groups on the B' ring that could be used for covalent linkage to the target protein. Amide analogue **334** would potentially allow access to a leaving group on the B' ring. The synthesis was started from 4-aminobenzyl alcohol and the previously used syringic acid derivative **328**. The amide **330** was formed in a good yield, but the deprotection step once again proved problematic. While the product **334** was visible by LC/MS, it was not possible to isolate enough for characterisation. This was due to the small scale of the reaction and the difficulty in separating the fully deprotected desired analogue **334** from the partially methyl protected side products.

A second reactive analogue **332** was also designed, the pentafluoro moiety would make this ring very susceptible to nucleophilic aromatic substitution reactions by nucleophilic groups nearby (e.g. the cysteine in the binding pocket of SENP1). However, despite trying various different amide formation conditions, only starting acid **332** was ever isolated from these reactions along with various decomposition products of the coupling reagents.

7 Biological results

7.1 Theoretical calculations of physical properties

Altogether, four hinokiflavone analogues (figure 49) synthesised and four different fragments (figure 50) were tested in biological assays. The analogues were all based on the structure of hinokiflavone 9 with modifications that were designed to either simplify the synthesis or deliver better physiochemical properties. The difluoro analogue 254 (figure 49) has the exact structure of hinokiflavone 9 with the only difference being the replacement of two hydrogen atoms in the C ring for fluorine atoms. As fluorine atoms are bioisosteres of hydrogen no difference in bioactivity was expected, the change was introduced to simplify the synthesis. Analogue 335 has a simplified skeleton with respect to hinokiflavone. The C' ring has been mostly removed and replaced by an amide. This was done to see if the C ring was necessary for hinokiflavone function, having the carbonyl opposite the ether linkage also simplified the synthesis and allowed for different B' rings to be added with ease. Alkenes **213** and **213** were also synthesised with a simplified C' ring, this time replaced by an alkene. We wanted to see if the two hydrogen bond acceptors on the C' ring were actually required for activity. These analogues are also much smaller than hinokiflavone **9** itself.

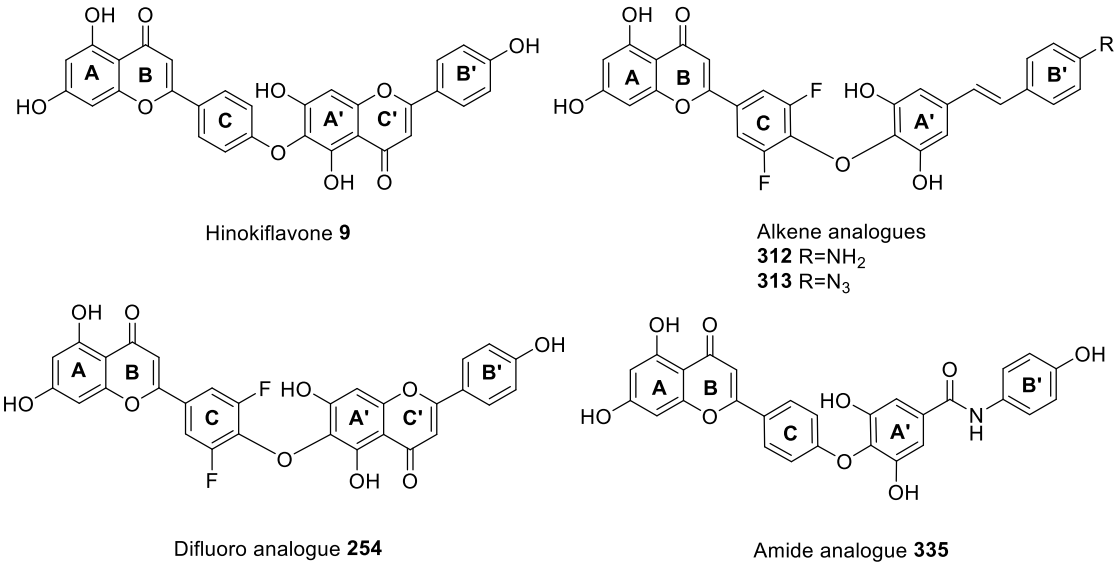

Figure 49

Some fragments (**169**, **175**, **176** and **178**) acquired during the synthetic efforts towards hinokiflavone **9** itself were also tested (*figure 50*). This was done to see if partial hinokiflavone skeleton would have the same biological effect as hinokiflavone itself.

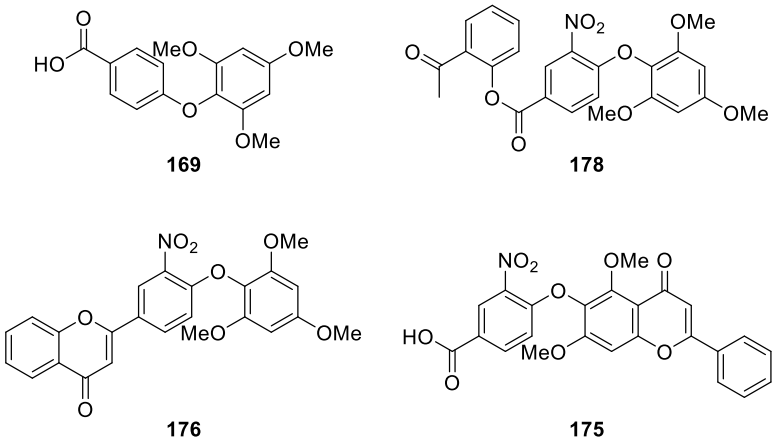

Figure 50

To evaluate our analogues some calculations were done to find their theoretical cLogP (logarithm of the theoretical partition between n-octanol and water, used to describe the relative solubility of a compound in the lipophilic and aqueous compartments of cells), cLogS (logarithm of the theoretical water solubility of the compound) and the likeliness that the molecule would make a good drug by looking at the number of hydrogen bond donors and acceptors. These values were then compared to hinokiflavone to see if the analogues could be predicted to have better properties in cells (*table 1)*. The calculations were done by Data warrior, an open soured program designed to analyse large sets of chemical compounds.

cLogP was calculated by the Actelion[136] method based on atom properties that are then combined for the molecule. This method has been reviewed by an independent review paper and verified to be considered reliable.[136] The optimal cLogP for drugs was set to be in the range of 0-5 by Lipinski.[129] Lipinski also used molecular mass as a proxy for the molecules size. Obviously smaller molecules tend to be more soluble and have an easier time passing plasma membranes and Lipinski suggested molecular weights of less than 500 amu are best. Hinokiflavone **9** has cLogP of 4.75, even though it is within the limits set by Lipinski for orally bioavailable drug, this is a rather high value. Out of all our

compounds only the fractions had cLogP approaching 3, a stricter limit set for drug design.[137] The fluoro analogue **254** has a higher cLogP than hinokiflavone **9** at 4.95 and the alkene analogues are even higher than that at cLogP=5.11 for **312** and cLogP=6.07 for **313**. The amine analogue **335** has a cLogP in the more reasonable range of 4.19, which is a great improvement over hinokiflavone.

cLogS was calculated by a similar method using atomic properties. Calculating cLogS by this method does not take into account the tendency of the molecules examined to stack into crystals making them very insoluble is all solvents. This means that the cLogS values for the biflavones are unlikely to be accurate. Most of the drugs on the market have a Log S of greater than -4. The better the water solubility the easier the drug is to administer, to both cells and animals. Hinokiflavone **9** was found to have cLogS of -6.69, appropriate for a compound with such poor solubility. The only compound synthesised that had a cLogS of greater than -4 was the small central fraction of **169** with a cLogS of -3.98, only marginally higher. The rest of the compounds all had cLogS values below that of hinokiflavone in the calculations, though they were all much more soluble in acetone and methanol. Indicating that, while the analogues did had better solubility in organic solvents than hinokiflavone **9**, the same might not apply to aqueous solutions.

Structure	Total Mol. weight	cLogP	cLogS	H-Acceptors	H-Donors
Hinokiflavone **9**	538	4.75	-6.69	10	5
169	304	2.33	-3.98	6	1
175	463	3.19	-6.55	10	1
176	449	3.64	-6.56	9	0
178	467	3.23	-6.58	10	0
254	574	4.95	-7.32	10	5
312	531	5.12	-7.70	8	5
313	557	6.07	-8.32	10	4
335	513	4.19	-6.07	10	6

Table 4

As already mentioned, hinokiflavone **9** is on the upper end of the scale of drug-likeness with regards to the number of hydrogen bond acceptors and donors. As the fluoro analogue **254** differs from hinokiflavone **9** by the presence of two fluroro substituents, it has the same number of hydrogen bond donors (5) and acceptors (10) as hinokiflavone **9** according to Lipinski.[129] The fractions containing the nitro group, compounds **175**, **176** and **178** have an extra two hydrogen bond acceptors due to that group so actually also approach 10 hydrogen bond acceptors though due to the methoxy protecting groups they did not contain many (any) hydrogen bond donors. This might have affected their biological activity as hydrogen bonding can be very important to protein ligand relationships. The two alkene analogues **312** and **313** were very similar to hinokiflavone with respect to hydrogen bond donors but had two fewer hydrogen bond acceptors on the backbone due to the double bond replacing the C' ring, the nitro alkene **313** have one fewer hydrogen bond donor as the phenolic hydroxyl on the B' ring was replaced by the azide group. The amide analogue **335** actually gained a hydrogen bond donating group with respect to hinokiflavone **9**, with 6 hydrogen bond donating groups and an amide bond it does not adhere to best practice rules with respect to oral bioavailability, but as it is much simpler to synthesise than hinokiflavone and had a simpler structure we expected it to make a very useful probe.

7.2 Fragments of hinokiflavone

Andrea Pawellek at the University of Dundee tested the four fragments from the synthesis to see if these could be used instead of hinokiflavone and to get some sense of the structure activity relationship. Three of these compounds were tested for their ability to modulate pre-mRNA splicing of the endogenous MCL1 transcription in HeLa cells (*figure 51*). None of the fragments altered pre-mRNA splicing of MCL1 at the concentrations tested. However we note that there is a loss of MCL1 RNA after treatment with **176** (most likely due to transcription inhibition). It was therefore assumed that the full hinokiflavone skeleton was required for activity.

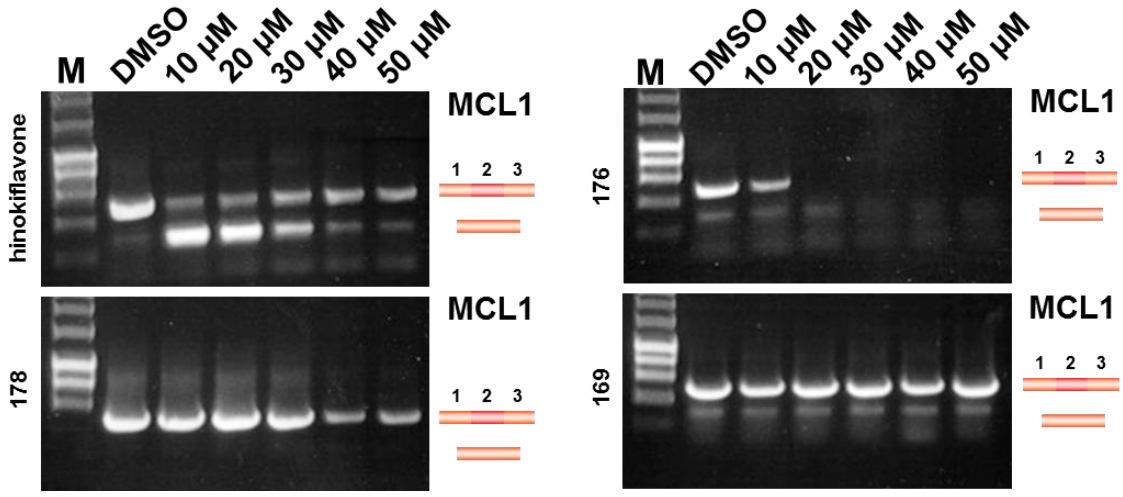

Figure 51 *Cell based* splicing assay
HeLa cells treated with compound/DMSO incubated 24 h. total RNA was extracted, reverse transcribed then amplified by semi quantitative RT-PCR using primers specific to sequences examined. Separated on 1% agarose gel with SYBR safe DNA gel stain.

Once the protein target had been identified, thermal profiling assays (*figure 52*) were done to see if the fragments would bind to SENP1 directly; thermal stability of SENP was measured either in the presence of DMSO (control) or in the presence of the compound. Proteins are denatured by heat treatment and precipitate when ultracentrifuged and hence cannot be seen in the gel of the supernatant. If a compound binds to its target protein there is a shift in the temperature needed for the denaturing of the protein. Hence the thermal test allows for a robust test to see if the compound binds to SENP1 or not.

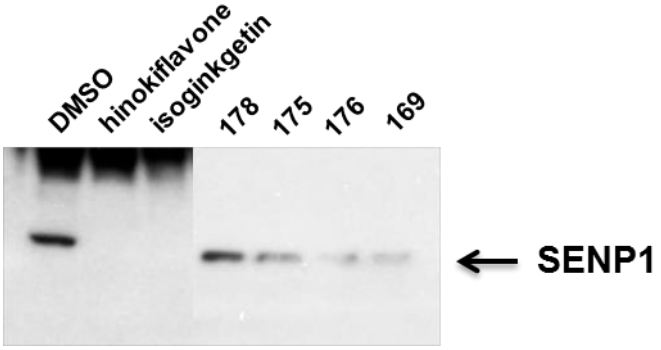

Figure 52 – Thermal SENP1 assay

HeLa nuclear extract treated with 100 µM compound and heat treated (37 ºC, 3 min), centrifuged to remove precipitate. Suspension analysed by SDS page. Gel cut and aligned.

Incubation of hinokiflavone and isoginkgetin with HeLa nuclear extract followed by heat treatment led to a complete loss of SENP1 from the supernatant when

compared to the DMSO control, indicating that hinokiflavone as well as isoginkgetin interact with SENP1. Two of the fragments (**176** and **169**) showed a partial loss of SENP1 from the supernatant, indicating a weak SENP1 binding in the thermal assay. However none of the compounds affected splicing of the endogenous MCL1 transcript in HeLa cells, therefore we can assume that the binding was not strong enough to actually inhibit SENP1 or the compound was not cell-permeable. Carboxylic acid **169** composed of only the B and A' rings shows some SENP1 binding in the thermal assay. However, which implies that it might not be cell-permeable because it is predominantly in the carboxylate form at pH 7, it shows no splicing modulation of MCL1. Compound **178** and **175** did not change the thermal stability of SENP1 hence it can be assumed that they do not bind to SENP1. Since ester **178** is much less rigid, has different electronics due to the nitro group and contains no hydrogen bond donors, this does not come as a surprise. What is more interesting is the difference between compounds **176** and **175**. One of them contains a flavone LHS (**176**) and the other the flavone RHS (**175**), both have the twist between the B ring and A' rings. LHS flavone **176** binds to and the RHS flavone **175** does not bind to SENP1 in the thermal shift assay (*figure 52*). Hence even though the LHS was not predicted to be that close to the active cysteine of SENP by computer modelling it must play an important role in binding. The results are summarised in *table 5*.

	Compound	Changes in MCL1 splicing	Thermal SENP assay
169	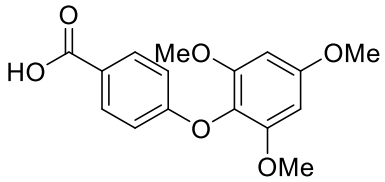	None	Weak binding
178	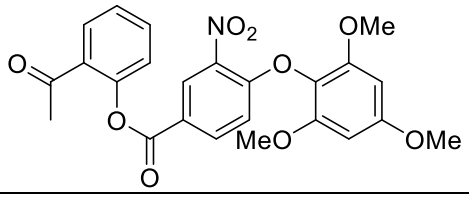	None	No binding
176	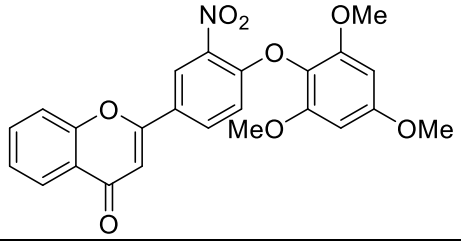	Loss of MCL1 RNA	Binding
175	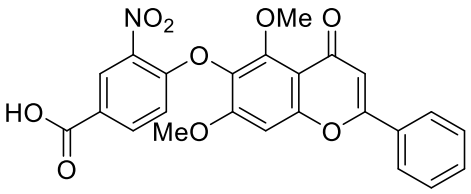	None	No binding

Table 5

7.3 Analogues of hinokiflavone

The four hinokiflavone analogues were also tested by Andrea Pawellek in HeLa cells for their ability to alter the splicing of the MCL1 pre-mRNA. The cells were treated with 10 µM, 20µM, 30µM, 40µM and 50 µM compound or DMSO for 24h (*figure 53*).

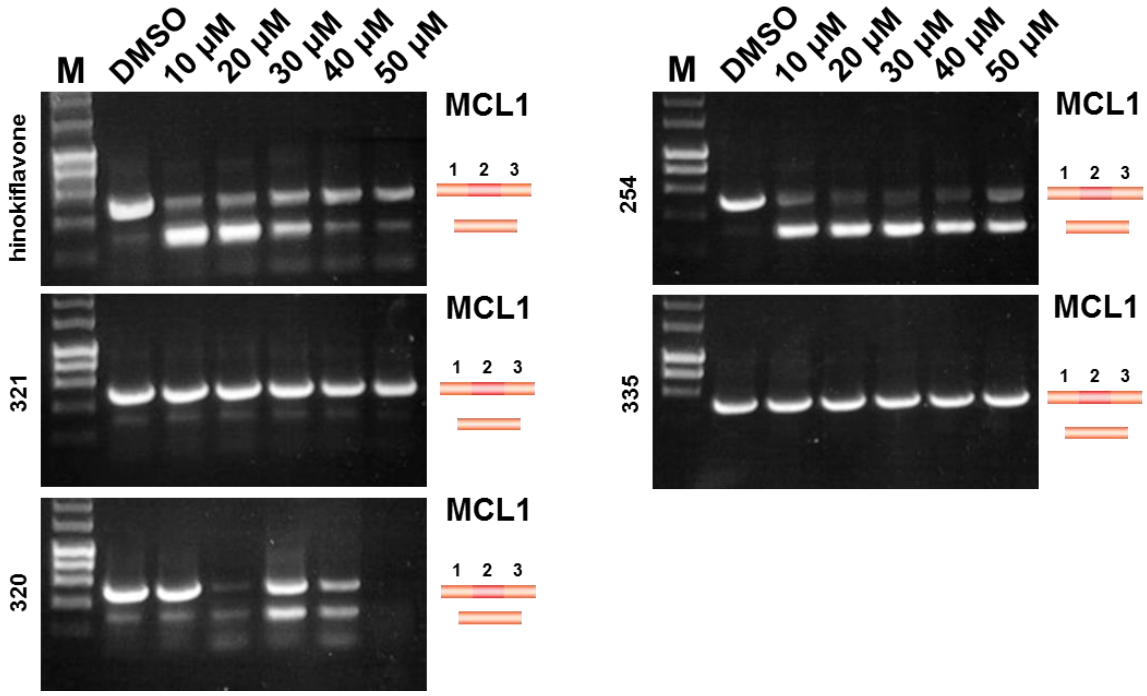

Figure 53 *Cell based* splicing assay
HeLa cells treated with compound/DMSO incubated 24 h. total RNA was extracted, reverse transcribed then amplified by semi quantitative RT-PCR using primers specific to sequences examined. Separated on 1% agarose gel with SYBR safe DNA gel stain.

Fluoro analogue **254** was the most promising compound synthesised. In cells difluoroflavone **254** showed a near complete shift of the MCL1 pre-mRNA splicing towards the production of the mRNA for the smaller isoform at all concentrations tested. Additionally, RT-PCR results in treated HEK293 cells also showed changes in the alternative splicing of MCL1 and RBM5 (*figure 54*) in a concentration dependent way.

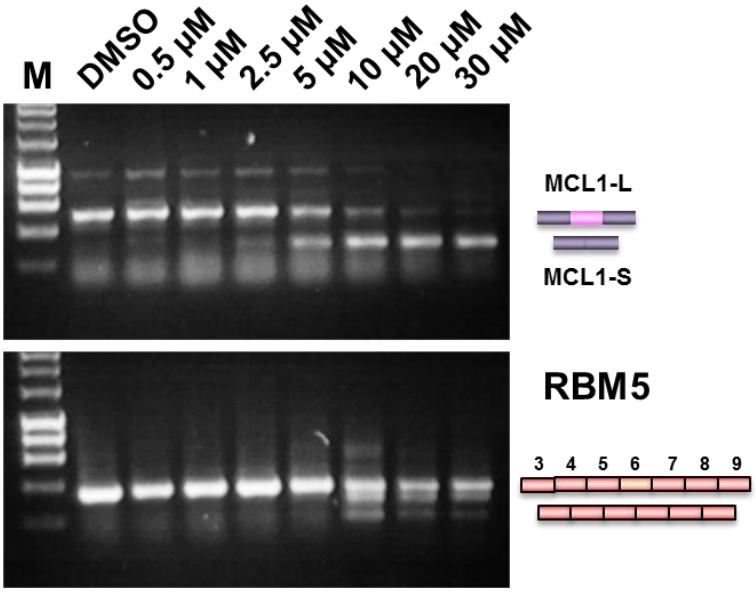

Figure 54
Pre-mRNA, 30% HeK293 cell extract and 500 µM compound 254/DMSO incubated for 30 min at 90 ºC. RNA amplified by RT-CPR then separated on 1% agarose gel with SYBR safe DNA gel stain. Intron retention in MCL1-L and RBM5 as a result of treatment with 500 µM of compound/DMSO.

The thermal assay of difluoro analogue **254** also shows complete loss of SENP1 like hinokiflavone **9** (*figure 55*). This suggests analogue **254** is modulating splicing *via* the inhibition of SENP1 in the same way as hinokiflavone **9**.

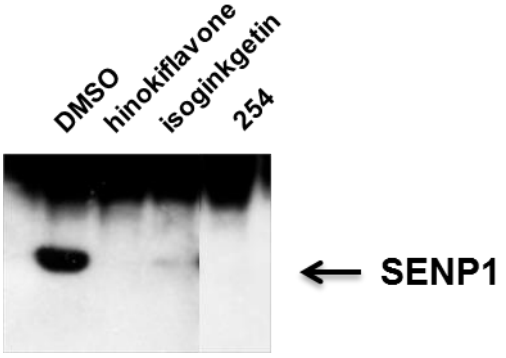

Figure 55 Thermal SENP1 assay
HeLa nuclear extract treated with 100 µM compound and heat treated (37 ºC, 3 min), centrifuged to remove precipitate. Suspension analysed by SDS page. Gel cut and aligned.

One striking feature of hinokiflavone is the relocation of early splicing factors in the nucleus. Immuno-fluorescence images of difluorohinokiflavone **254** treated cells also showed a dose-dependent concentration of PRPF40 and TMG to megaspeckles in the nucleus (*figure 56*), further confirming that difluorohinokiflavone **254** is behaving analogously to hinokiflavone in cells.

Considering the structural similarity of difluorohinokiflavone **254** and hinokiflavone **9** this is not surprising, fluorine atoms, as mentioned already, are a well-known hydrogen bioisostere. The activity of difluorohinokiflavone **254** does open up avenues to large-scale synthesis since the ether formation step does not require the addition and removal of the nitro activating group for the S_NAr reaction to proceed (see chapter 6 on analogue synthesis). This also opens up the possibility of other structural analogues of hinokiflavone that could be synthesised without the need of a nitro activating group.

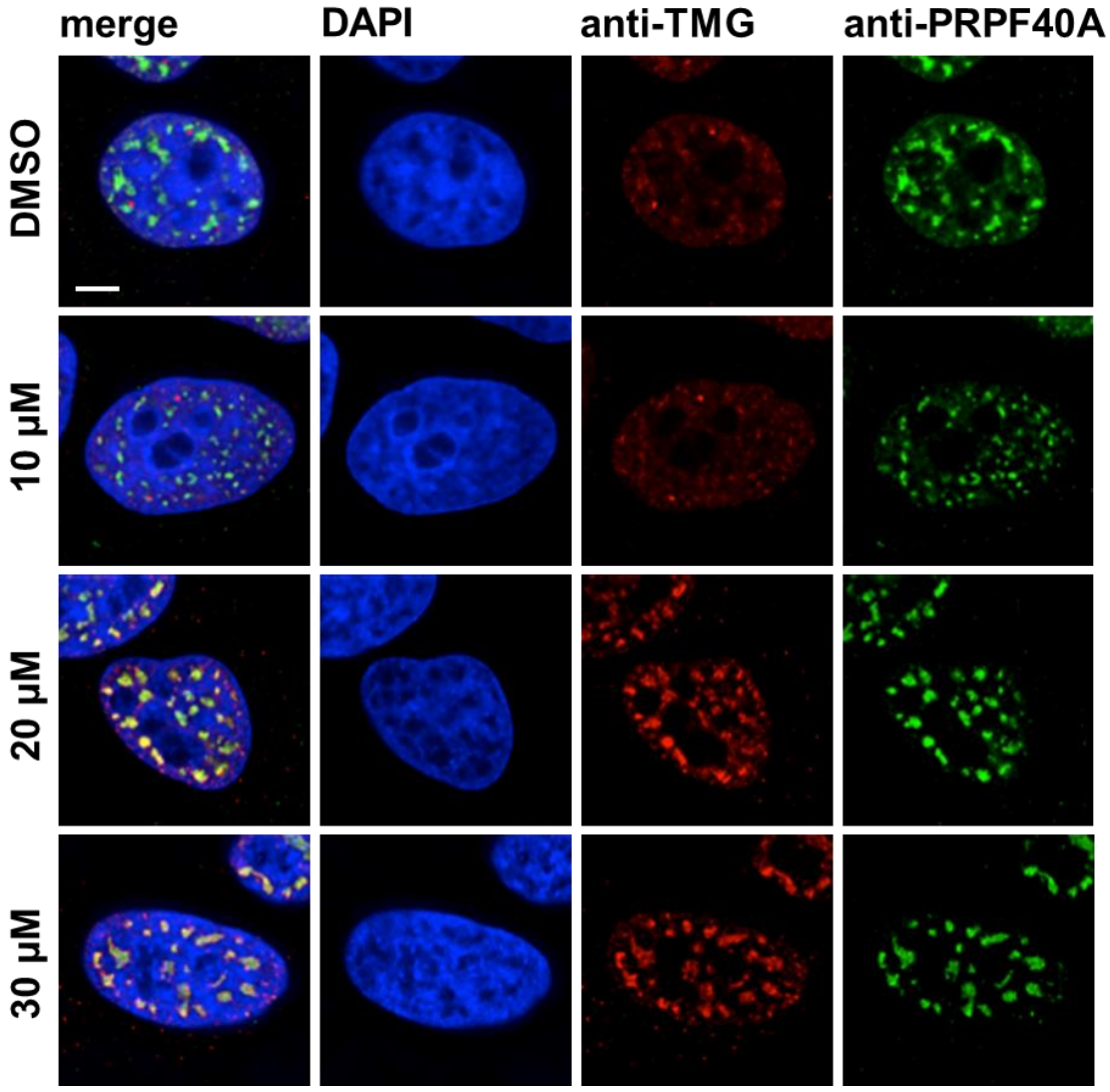

Figure 56 Immunofluorescence assay
HeLa cells incubated with fluoro compound /DMSO for 24 h. The cells were then fixed with 4% paraformaldehyde, permeabilised with 0.5% Triton X100 and incubated with the primary antibodies, 1 hour at RT, then incubated with the secondary dye-conjugated antibodies. Visualised with fluorescence microscope (cells stained with DAPI (blue) to show DNA and nucleus).

The amide analogue **335**, and the alkene analogues **320** and **321** were also tested in a gel-based SENP1 activity assay (*figure 57*). SUMOylated ubiquitin was

incubated with a SENP1 active site fragment with or without compound. The first line shows the ubiquitin-SUMO2 compound without added SENP1, the compound is not degraded. In the case of DMSO control the SUMO2 is removed from the ubiquitin by SENP1 activity. After the addition of hinokiflavone, some of the SUMO2 conjugated ubiquitin can again be seen as SENP1 activity is inhibited. The amide **335** and one of the alkenes **312** clearly inhibit SENP1**.**

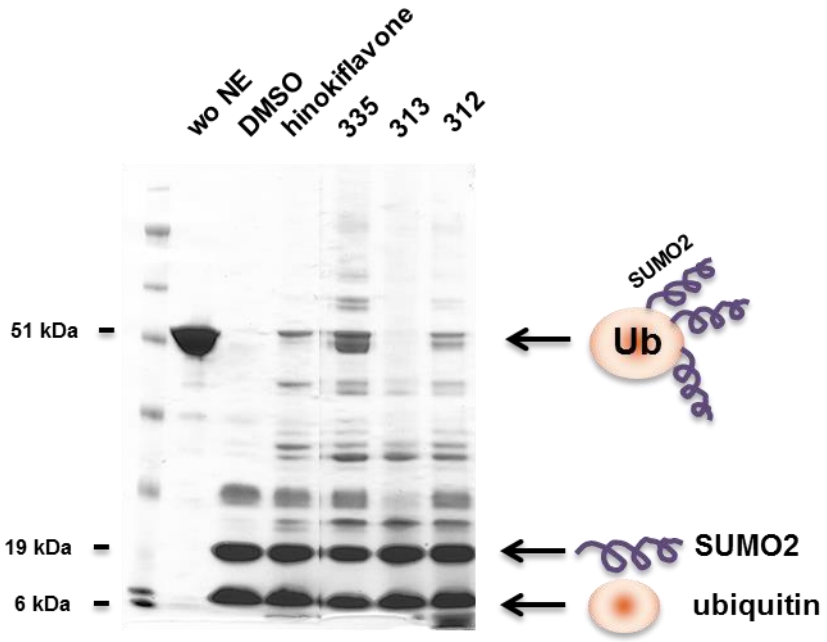

Figure 57 Gel-based SENP activity assay
Catalytically active SENP1 fragment (aa 415-643) expressed in *E. coli* and SUMOylated ubiquitin were incubated with 500 µM compound/DMSO in SENP buffer at 37 ºC for 15 min. Loading buffer added and separated on 4-12% Tris-Bis PAGE gel, visualised with Coomassie blue. Gel shows cleavage/non-cleavage of SUMOylated ubiquitin depending on SENP fragment activity. (gel cut, realigned)

The three analogues were also tested for splicing modification in an *in vitro* assay using HeLa nuclear extract. Here we see the two isoforms of E6/E7 pre-mRNA (exon-intron-exon and exon-exon) are present in an equal amount in the DMSO control. After the introduction of hinokiflavone **9** less of the smaller isoform of E6/E7 pre-mRNA (exon-exon) can be seen.

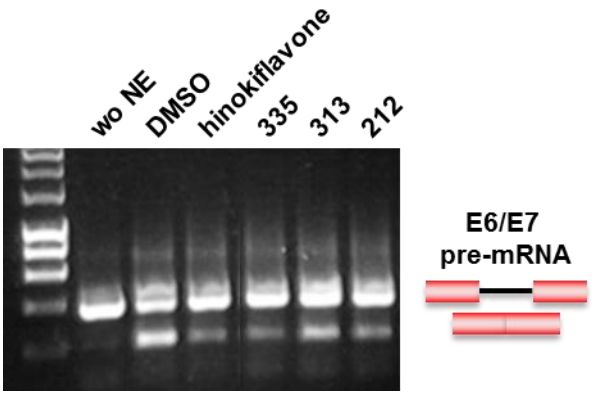

Figure 58 *In vitro* splicing assay
HeLa nuclear extract, 10 ng in vitro transcribed pre-mRNA (HPV18 E6/E7) with 500 μM compound/DMSO incubated for 30 min at 90 ºC. RNA amplified by RT-CPR then separated on 1% agarose gel with SYBR safe DNA gel stain. Looking or intron retention in Ad1 and HPV18E6/7

The amide analogue **335**, did not alter the splicing of the MCL1 transcript in HeLa cells (*figure 53*), but treatment of *in vitro* splicing assays with **335** showed similar intron retention level when compared with hinokiflavone **9** treated samples (*figure 58*). Using an *in vitro* SENP assay with SUMOylated ubiquitin as a target protein, amide **335** showed the strongest SENP inhibitory effect when compared to the other compounds (*figure 57*). Cells treated with amide **335** failed to display the same phenotype (megaspeckles) as hinokiflavone treated cells. One possibility is that the aryl amide binds SENP1 but is quickly hydrolysed in cells so the *in cellulo* assays so not show activity. Hydrolysis of aryl amides is particularly thermodynamically favoured.[138] Another plausible explanation is that the extra hydrogen bond donor in the amide is enough to prevent its uptake by cells. Further work on amides is clearly necessary, but amide **335** or another amide derivative may be useful in protein-inhibitor complexes for binding structure determination.

When the alkene analogues **313** and **312** were tested for their ability to modulate splicing of the MCL1 gene, alkene **313** had no effect and alkene **312** induced a moderate switch towards the expression of the smaller isoform (*figure53*). In the *in vitro* splicing (*figure 58*) and gel-based SENP1 (*figure 57*) assays, alkene **313** did not show activity while alkene **320** showed an effect. However alkene **313** was found to be very toxic to cells, leading to concentration dependent cell death with 100% death at 30 μM. However, the mechanism is currently unknown. Since alkene **312** altered pre-mRNA splicing of

cells, further experiments were carried out to investigate it in cells. It transpired that compound **312** also led to the formation of megaspeckles. *Figure 59* shows that alkene **312** led to the relocation of SUMO2 to the speckles in the nucleus, SUMO1 showed striking aggregates in the cytoplasm and the nucleus. In the presence of 20 μM of alkene **312** cells also showed abnormal nuclei which is assumed to be due to problems to cell division.

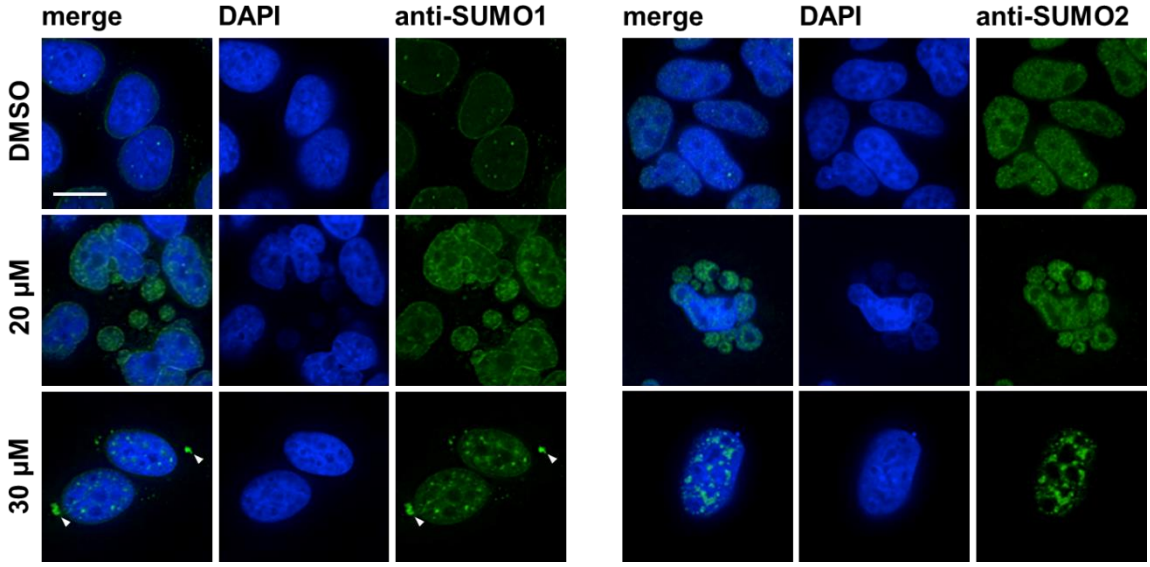

Figure 59 Immunofluorescence staining
HeLa cells incubated with compound 312/DMSO for 24 h. The cells were then fixed with 4% paraformaldehyde, permeabilised with 0.5% Triton X100 and incubated with the primary antibodies, 1 hour at RT, then incubated with the secondary dye-conjugated antibodies. Visualised with fluorescence microscope (cells stained with DAPI (blue) to show DNA and nucleus).

Direct comparison between hinokiflavone **9** and the alkene skeleton could only be possible with the parent *para*-hydroxyl alkene analogue **314** for which the synthesis unfortunately failed. Differences in bioactivity could be due to the change of the phenolic hydroxyl on the B' ring to an azido group in compound **313** and an amino group in compound **312**. Although both the alkene analogues **312** and **313** also contain fluorine groups instead of hydrogens on the B ring, this was not though to affect their activity as the fluorine analogue **254** did not have altered activity. No studies attempting to photo cross-link the alkene analogues **313** to SENP has been attempted yet, and would seem unlikely to succeed since it showed no SENP1 inhibition and did not affect splicing.

A summary of the MCL1 splicing assay and the gel-based SENP1 assay can be found in *table 6*.

	Compound	Changes in the alternative splicing of MCL1	Gel-based SENP1 assay
254	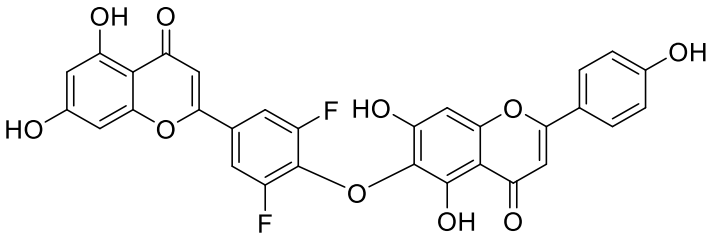	Splicing changes	Inhibited
335	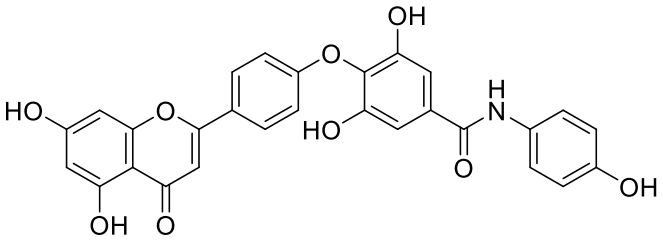	None	Inhibited
313	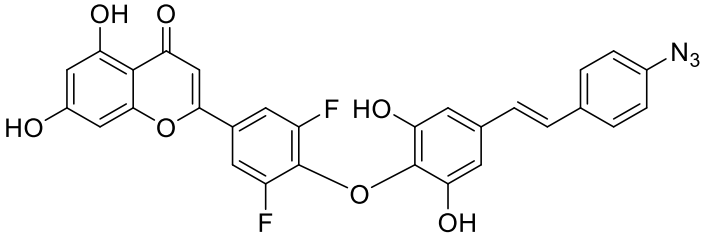	None	No effect
312	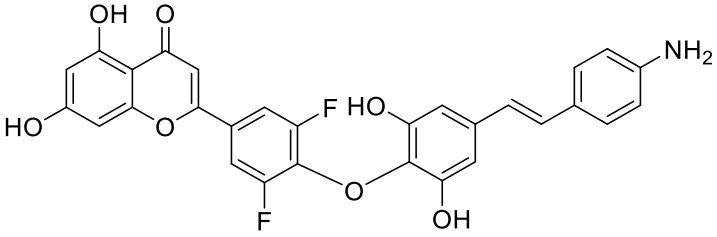	Splicing changes	Inhibited

Table 6

7.4 Conclusions

In conclusion, the twist between the B and A' rings could be important for hinokiflavone's **9** biological activity since only analogues that have this twist have been shown to be active. Fluoro analogue **254** turned out to be the most effective analogue, which is unsurprising considering the close structural similarity. This opens up an easier synthetic route for future analogue design. The amide analogue **335** seems to be a good analogue *in vitro* but has troubles *in cellulo*, possibly due to the instability of the amide group *in vivo* due to peptidases. Alkene analogue **312** also shows promise in these preliminary tests.

Although alkene **313** did not seem to exhibit the same biological effects as hinokiflavone **9**, it did seem to be highly toxic to cells. The reason behind this activity is still unclear. In summary compounds **254**, **335** and **312** synthesised during this project seem to have interesting bioactivity. The amides and alkenes in general should be further investigated since these scaffolds seem to be good mimics for hinokiflavone *in vitro* at least.

8 Conclusions

Over the last three years the following objectives have been achieved: a synthetic route was found to hinokiflavone that gave measurable quantities of this bioactive natural biflavonoid.

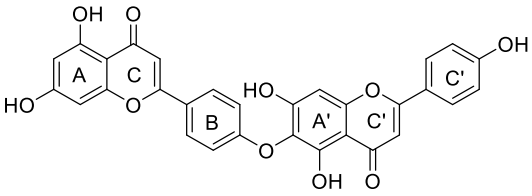

Hinokiflavone **9**

Members of three different families of bioactive analogues of hinokiflavone were also synthesised. Two of these analogues were based on alternative scaffolds to hinokiflavone itself, alkene **312** and amide **335**. The fluoro analogue **254** was based on fluorine being a bioisostere to hydrogen. All three families of analogues followed much simpler synthetic sequences than the synthesis of hinokiflavone itself.

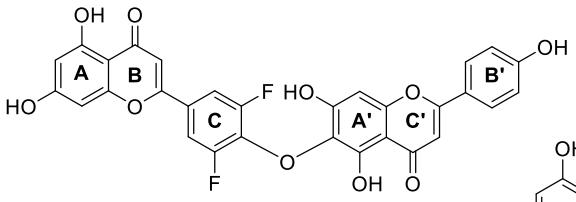

Difluoro analogue **254**

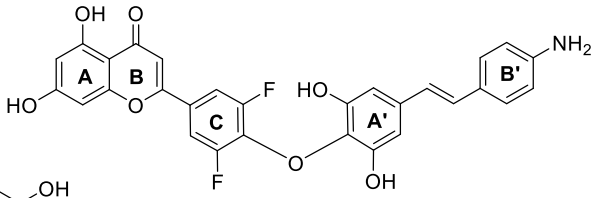

Alkene analogue **312**

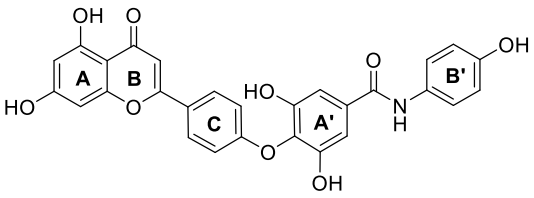

Amide analogue **335**

Various routes to making tagged hinokiflavone analogues were investigated. Both polyethylene glycol and simple hydrocarbon linkers were explored with the aim of introducing functional groups capable of biorthogonal chemistry. Synthesis of tagged hinokiflavone analogues will require further work.

Hinokiflavone and its bioactive analogues will now be used for the elucidation of how splicing is controlled in human cells lines. Advances in our understanding of splicing should in turn lead to the discovery of new ways to tackle diseases caused by defective splicing control.

9 Experimental

General

All reactions under an inert atmosphere (N_2 gas) were carried out using oven-dried or flame-dried glassware and solvents were added *via* syringe. Reagents were obtained from commercial suppliers and used without further purification. Dry solvents were collected from a Puresolv solvent purification system or obtained from commercial suppliers. Acetone was dried by stirring with 4 Å molecular sieves. ^{1}H NMR spectra were obtained using Bruker DPX400 spectrometer operating at 400 MHz and Bruker AVIII spectrometers operating at 400 and 500 MHz, ^{13}C NMR spectra at 100 and 126 MHz, ^{31}P NMR spectra at 162 MHz. All coupling constants were recorded in Hz and reported uncorrected. All NMR chemical shifts were reported to two decimal places. DEPT was used to assign the signals in ^{13}C NMR spectra as C, CH, CH_2 and CH_3. 2D techniques including COSY, HSQC, HMBC and NOESY were used to aid assignment. All spectra were assigned using the following reference solvent peaks for residual non-deuterated solvent in the^{1}H NMR spectra and for the deuterated solvent in the ^{13}C NMR spectra: $CDCl_3$ (7.26 ppm for ^{1}H NMR; 77.16 ppm for ^{13}C NMR), CD_3OD (3.31 ppm for ^{1}H NMR; 49.00 for ^{13}C NMR); DMSO-D_6(2.50 ppm for ^{1}H NMR, 39.52 ppm for ^{13}C NMR), Acetone-D_6 (2.05 ppm for ^{1}H NMR; 29.84 for ^{13}C NMR). LRMS (ESI+) and HRMS (ESI+) spectra were collected on a Bruker MicroTOF-Q, EI MS spectra were collected on a JeolJMS700 (MStation) spectrometer. IR spectra were obtained using Shimadzu FTIR-8400S. Melting points were determined on a Reichert platform melting point apparatus. Purification of products was carried out by either recrystallisation, column chromatography (using silica gel [70-230 mesh] or Biotage® Isolera™ One Flash Chromatography system using Biotage® SNAP Ultra silica gel cartridges) or by RP-HPLC. RP-HPLC buffers were 0.1% TFA in H_2O (Buffer A) and 100% MeCN (Buffer B). C18 column (Phenomenex Gemini-NX 10µ C18 250 × 21.20 mm) was used. Samples dissolved in 1 mL of 25% MeCN in 0.1% TFA (aq) were filtered manually through a 0.45 µm PTFE filter (Sartorius Stedim Biotech) and loaded onto a column *via* a 10 mL injection loop. Samples were eluted at 12 mL/min flow rate using different gradients (Spectra System P2000). A_{220} of the column eluent was detected using UV/Vis spectrophotometer

(Spectro Monitor 3200) and visualised with Chrom Quest software. After the HPLC purification, the solvents were removed under reduced pressure.

Hinokiflavone 9

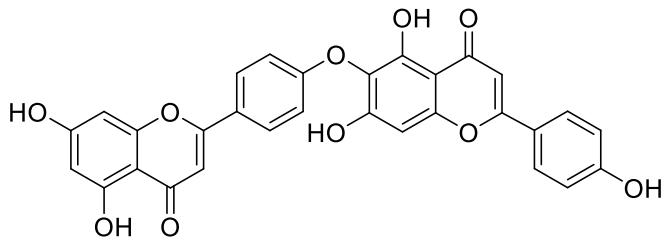

Isopropoxy hinokiflavone **209** (0.178 mg, 0.24 mmol) was taken up in dry dichloromethane (7.0 mL) and cooled to 0 ºC. Boron tribromide solution in dichloromethane (1M, 2.4 mL) was then added dropwise, and the resultant solution stirred for 30 minutes at 0 ºC. The reaction was then quenched with water and filtered. The crude compound was recrystallised form hot methanol to yield pure hinokiflavone **9** as a beige powder (36.0 mg, 28%). Decomposes at 316 ºC (Lit.[24] decomposes at 343 ºC. ν_{max} (ATR): 1649 (C=O) 1608 (C=O), 1166 (C-O) cm^{-1}. δ_H (400 MHz, DMSO-D_6): 13.22 (1H, s, OH), 12.89 (1H, s, OH), 11.31 (1H, s, OH), 10.88 (1H, s, OH), 10.41 (1H, s, OH), 8.02 (2H, d, *J* = 8.9 Hz, H-2'/6'), 7.98 (2H, d, *J* = 8.7 Hz, H-2'''/6'''), 7.04 (2H, d, *J* = 8.9 Hz, H-3'/5'), 6.95 (2H, d, *J* = 8.7 Hz, H-3'''/5'''), 6.87 (2H, s, H-3/3'''), 6.74 (1H, s, H-8''),6.50 (1H, d, *J* = 1.9 Hz, H-8), 6.21 (1H, d, *J* = 1.8 Hz, H-6). δ_C (100 MHz, DMSO-D_6): 182.59 (C), 182.27 (C), 164.73 (C), 164.66 (C), 163.61 (C), 161.92 (C), 161.80 (C), 161.09 (C), 157.83 (C), 157.57 (C), 154.22 (C), 153.57 (C), 129.11 (CH), 128.85 (CH), 125.07 (C), 124.69 (C), 121.56 (C), 116.47 (CH), 115.77 (CH), 104.64 (C), 104.42 (CH), 104.26 (C), 103.05 (CH), 99.39 (CH), 95.05 (CH), 94.51 (CH). HRMS [ESI]: 537.0815 *m/z*. $C_{30}H_{17}O_{10}$ requires $[M-H]^-$ 537.0827 *m/z*. Copy of the ^1H NMR and a magnified version of the ^1H NMR can be found in the appendix. IR data agree with leterature.[24]

5,7 -Dibenzyloxy flavone 137

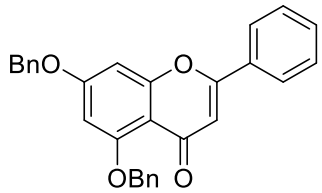

Chrisin **138** (2.02 g, 7.9 mmol), benzyl bromide (9.40 g, 79 mmol) and potassium carbonate (11.0 g, 79 mmol) were dissolved in anhydrous dimethyl formamide (40 mL) then stirred at 100 ºC for 4 days. The reaction was then quenched with 1 M aq. HCl solution (100 mL), extracted into a mixture of ethyl acetate (120 mL) and dichloromethane (12 mL). The dichloromethane was left to evaporate overnight and the product crystallised out of solution, the crystals were collected by filtration and washed with cold ethyl acetate to yield the product **137** (2.38 g, 69%). Mp: 136-140 ºC. ν_{max} (ATR): 2359 (C-H), 1643 (C=O) cm^{-1}. δ_H (400 MHz, $CDCl_3$): 7.91-7.85 (2H, m, H-Ar), 7.65-7.95 (2H, m, H-Ar), 7.54-7.48 (3H, m, H-Ar), 7.45-7.29 (8H, m, H-Ar), 6.68 (1H, s, H-C=C), 5.67 (1H, d, *J* = 2.3 Hz, H-Ar), 5.51 (1H, d, *J* = 2.3 Hz, H-Ar), 5.25 (2H, s, CH_2), 5.13 (2H, s, CH_2). δ_C (100 MHz, $CDCl_3$): 177.3 (C), 162.9 (C), 160.7 (C), 159.8 (C), 159.7 (C), 136.4 (C), 135.6 (C), 131.6 (C), 131.1 (CH), 128.9 (CH), 128.8 (CH), 128.6 (CH), 128.4 (CH), 127.6 (CH), 126.5 (CH), 125.0 (CH), 109.9 (C), 109.1 (CH), 98.4 (CH), 94.2 (CH), 70.7 (CH_2),70.5 (CH_2). Reported data agree with literature.[34]

2,4-Dibenzyloxy-6-hydroxy acetophenone 139

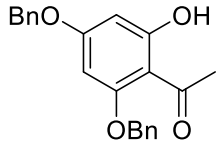

The dibenzylated chrisin **137** (1.93 g, 4.5 mmol) was taken up in a mixture of 18 M aqueous potassium carbonate solution (7.3 mL) and pyridine (7.3 mL) and diethylene glycol was added to the suspension (7.3 mL). The mixture was heated at 100 ºC for 16 h then allowed to cool to room temperature. The reaction was quenched with 1 M aqueous HCl solution (15 mL) then extracted into dichloromethane (2 × 10 mL). The combined organic layers were washed with brine (20 mL) then dried over magnesium sulfate and concentrated under

reduced pressure. The crude product was purified by column chromatograpy (Isolera: 0%-80% ethyl acetate in hexane) to yield the product acetophenone **139** as a white powder (0.743 g, 48%). Mp: 89-90 ºC. ν_{max} (ATR): 1610 (C=O), 1585 (C-C) cm^{-1}. δ_H (400 MHz, $CDCl_3$): 14.04 (1H, s, OH), 7.44-7.33 (10H, m, H-Ar), 6.17 (1H, d, *J* = 2.4 Hz, H-Ar) 6.10 (1H, d, *J* = 2.4 Hz, H-Ar), 5.06 (4H, d, *J* = 1.3 Hz, CH_2) 2.56 (3H, s, CH_3). δ_C (100 MHz, $CDCl_3$): 203.2 (C=O), 167.5 (C), 165.1 (C), 162.0 (C), 135.8 (C), 135.6 (C), 128.7 (CH), 128.7 (CH), 128.5 (CH), 128.3 (CH), 128.0 (CH), 127.6 (CH), 106.3 (C), 94.7 (CH),94.7 (CH), 71.1 (CH_2), 70.2 (CH_2), 33.3 (CH_3). The reported data agrees with literature.[34]

4-(2',4',6'-Trimethoxyphenyl) benzoic acid 169

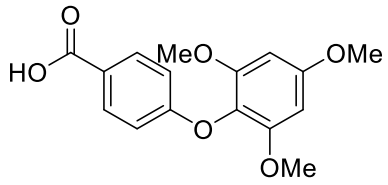

Nitro compound **173** (0.201 g, 0.58 mmol) and ammonium formate (0.159 g, 2.3 mmol) were dissolved in a mixture of acetone (2.1 mL) and water (0.75 mL), iron powder (0.161 g, 2.9 mmol) was added to the solution. The suspension was heated at 65 ºC for 24 h. The reaction was allowed to cool then filtered through celite with acetone. The filtrate was concentrated under reduced pressure and the precipitate taken up in water (10 mL). It was then extracted with dichloromethane (3 × 20 mL). The combined organic layers were washed with brine (20 mL) then dried over magnesium sulphate and concentrated under reduced pressure to yield the desired amino compound **180** as an off-white powder (0.176 g, 96%).

Carboxyphenylamine **180** (0.068 g, 0.21 mmol) was dissolved in a mixture of concentrated aqueous HCl (0.61 mL) and glacial acetic acid (1.2 mL) and cooled to 0 ºC. A solution of sodium nitrite (0.018 g, 0.27 mmol) in water (0.2 mL) was added to the mixture slowly and the resulting solution left to stir for 20 mins. Hypophosphinic acid (0.2 mL) was then added to the mixture and the reaction left to warm to room temperature overnight. It was then diluted with 1 M aqueous HCl solution (20 mL) and extracted with dichloromethane (3 × 20 mL). The combined organic layers were washed with brine (30 mL) then dried over

magnesium sulphate and concentrated under reduced pressure to yield the product **169** was a yellow powder (0.049 g, 75%). Mp: 180-182 °C. ν_{max} (ATR): 1603 (C=O), 1503 (C=C) cm^{-1}. δ_H (400 MHz, $CDCl_3$): 8.01 (2H, d, *J* = 9.0 Hz, H-2, 6), 6.91 (2H, d, *J* = 9.0 Hz, H-3, 5),6.23 (2H, s, H-3',5'), 3.85 (3H, s, CH_3), 3.77 (6H, s, 2 CH_3). δ_C (100 MHz, $CDCl_3$): 171.49 (C), 163.43 (C), 158.05 (C), 153.53 (C), 132.23 (CH), 125.47 (C), 122.44 (C), 114.67 (CH),91.78 (CH), 56.21 (CH_3), 55.62 (CH_3). HRMS [ESI]: 327.0845 *m/z*. $C_{16}H_{16}NaO_6$ requires $[M+Na]^+$ 327.0839 *m/z*.

Methyl-4-fluoro-benzoate 170

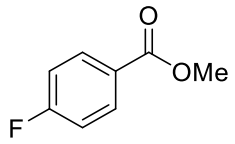

4-Fluorobenzoic acid (0.506 g, 3.6 mmol) was dissolved in methanol (20 mL), 3 drops of sulpfuric acid was added and the reaction heated at 70 °C for 24 h. It was then allowed to cool to room temperature; methanol was removed under reduced pressure and the residue taken up in ethyl acetate (15 mL). The solution was washed with sat. aq. sodium bicarbonate solution (2 × 10 mL) then dried over magnesium sulphate, filtered and concentrated under reduced pressure to yield the desired product **170** as a yellow oil (0.431 g, 77%). δ_H (400 MHz, $CDCl_3$): 8.08-8.00 (2H, m, H-Ar), 7.14-7.06 (2H, m, H-Ar), 3.91 (3H, s, CH_3). δ_C (100 MHz, $CDCl_3$): 166.8 (C=O), 165.4 (J_{C-F} = 22.0 Hz, $_{C-F}$), 132.1 (J_{C-F} = 3.7 Hz, CH), 126.4 (J_{C-F} = 9.8 Hz, C), 115.5 (J_{C-F} = 176.9 Hz, CH), 52.2 (CH_3). The reported data agrees with literature.[139]

2-Nitro-4-carboxyphenyl-2,4,6-methoxyphenoxy ether 173

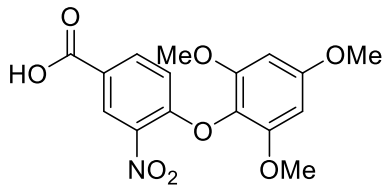

2,4,6-Trimethylphenol **167** (0.588 g, 3.2 mmol), 4-fluoro-3-nitrobenzoic acid **172** (0.611 g, 3.3 mmol) and potassium carbonate (0.596 g, 4.3 mmol) were

dissolved in water and stirred under reflux for 24 h. The reaction was then allowed to cool to RT and extracted with diethyl ether (3 × 20 mL). The aqueous layer was then acidified to pH 1 using 1M HCl solution and extracted with dichloromethane (3 × 20 mL). The combined dichloromethane layers were then washed with brine (20 mL), dried over magnesium sulphate and concentrated under reduced pressure to yield the desired product **173** as a yellow powder (0.756 g, 68%). Mp.: 210-215 ºC. ν_{max} (ATR): 2944 (COOH), 1696 (C=O), 1355 (NO_2) cm^{-1}. δ_H (400 MHz, $CDCl_3$): 8.69 (1H, d, *J* = 2. Hz, H-Ar), 8.09 (1H, dd, *J* = 8.8, 2. Hz, H-Ar), 6.82 (1H, d, *J* = 8.8 Hz, H-Ar), 6.22 (2H, s, H-Ar), 3.84 (3H, s, OMe), 3.76 (6H, s, OMe). δ_C (100 MHz, $CDCl_3$): 169.43 (C), 158.70 (C), 156.65 (C), 153.09 (C), 138.85 (C), 135.49 (CH), 128.26 (CH), 124.70 (C), 122.41 (C), 116.28 (CH), 90.77 (CH), 56.27 (CH_3), 55.65 (CH_3). HRMS: 372.0676 *m/z*. $C_{16}H_{15}NNaO_8$ requires $[M+Na]^+$ 372.0690 *m/z*.

3'-Nitro-4'-[2'',4'',6''-(trimethoxy)phenoxy]-flavone 176

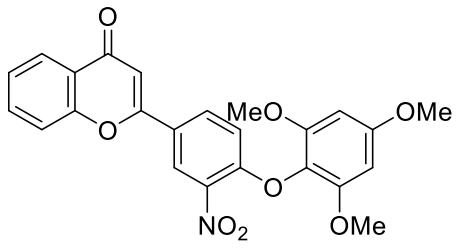

Ester **178** (0.070 g, 0.15 mmol) and phosphazene (0.18 mL, 0.18 mmol) base were taken up in anhydrous dioxane (1 mL) and heated at 100° C for 24 hours. The reaction was then allowed to cool to room temperature, diluted with ethyl acetate (10 mL) and washed with water (2 × 10 mL) then brine (2 × 10 mL). The organic layer was then dried over magnesium sulfate and concentrated under reduced pressure. The resulting powder was taken up in anhydrous dichloromethane (1 mL) and trimethylsilyl trifluoromethanesulfonate added, the mixture was allowed to stir for 45 minutes then diluted with dichloromethane (10 mL), washed with water (2 × 10 mL) then brine (2 × 10 mL), dried over magnesium sulfate and again concentrated under reduced pressure. The crude product was purified on Isolera (0-10% methanol in dichloromethane) to yield the product **176** (0.026 g, 39%). Mp: 170-174 ºC. ν_{max} (ATR): 3734 (Ph), 1647 (C=O), 1506 (NH_2), 1130 (NO_2) cm^{-1}. δ_H (400 MHz, $CDCl_3$): 8.59 (1H, d, *J* = 2.3 Hz, H-2'), 8.22 (1H, dd, *J* = 7.9, 1.5 Hz, H-Ar), 7.87 (1H, dd, *J* = 9.0, 2.4 Hz, H-6'), 7.75-

7.70 (1H, m, H-Ar), 7.59 (1H, d, *J* = 8.5Hz, H-Ar), 7.44 (1H, t, *J* = 7.5 Hz, H-Ar), 6.90 (1H, d, *J* = 8.9 Hz, H-5'), 6.76 (1H, s, H-C=C), 6.23 (2H, s, H-3'', 5''), 3.85 (3H, s, OMe), 3.78 (6H, s, OMe). δ_C (100 MHz, $CDCl_3$): 178.0, 160.9, 158.7, 156.1, 155.0, 153.2, 139.4, 134.0, 131.3, 125.8, 125.5, 125.0, 125.0, 123.9, 118.1, 117.1, 107.4, 91.9, 56.3, 55.6. HRMS: 472.0983 *m/z*. $C_{24}H_{19}NNaO_8$ requires $[M+Na]^+$ 472.1003 *m/z*.

2''-Acetylphenyl-3-nitro-4-[2',4',6'-(trimethoxy)phenoxy]benzoate 178

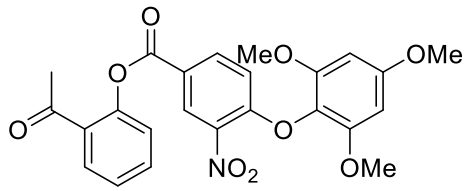

Hydroxyacetophenone **64** (141 mg, 0.40 mmol) and ester **173** (71 mg, 0.52 mmol) were dissolved in anhydrous acetonitrile (2.0 mL) under argon along with DCC (0.145 g, 0.70 mmol). The reaction mixture was stirred for 3 d at RT. The mixture was then filtered through cotton wool and the solvent removed under reduced pressure. The residue was purified by column chromatograpy (Isolera 40%-80% dichloromethane in hexane) to yield ester **178** (163 mg, 90%). δ_H (400 MHz, $CDCl_3$): 8.80 (1H, d, *J* = 2.1 Hz, H-2), 8.18 (1H, dd, *J* = 8.8, 2.2 Hz, H-6), 8.87 (1H, dd, *J* = 7.8, 1.6 Hz, Ar), 7.60(1H, ddd, *J* = 8.0, 7.5, 1.6 Hz, Ar), 7.38 (1H, td, *J* = 7.6, 1.2 Hz, Ar), 7.20 (1H, dd, *J* = 8.1, 1.0 Hz, Ar), 6.85 (1H, d, *J* = 8.8 Hz, H-5), 6.22 (2H, s, H-3',5'), 3.84 (3H, s, CH_3), 3.78 (6H, s, CH_3), 2.55 (3H, s, CH_3). Tentative characterisation based on ^{1}H NMR.

4'-Benzyloxy-5,7-dimethoxy-(2''amino-4''carboxy-phenoxy)-flavone 185

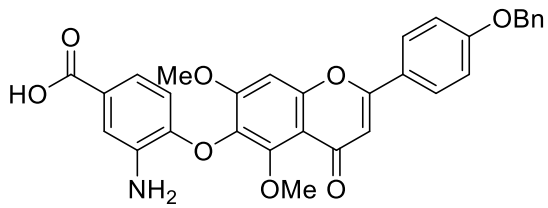

Benzyl protected chrysin derivative **146** (72 mg, 0.18 mmol) and 4-fluoro-3-nitrobenzoic acid **172** (47 mg, 0.25 mmol) were dissolved in a mixture of water (0.5 mL) and dimethyl sulfoxide (0.5 mL) along with potassium carbontate

(27 mg, 0.20 mmol). The solution was heated at 100 ºC for 24 h. It was then allowed to cool, acidified with 0.5 M aqueous HCl solution until precipitation occurred then extracted into dichloromethane (5 × 10 mL). The combined organic layers were washed with brine (10 mL) then dried over magnesium sulfate, filtered and concentrated under reduced pressure to yield **184** (99 mg, 99%).

A solution of nitro compound **184** (97 mg, 0.17 mmol) in a mixture of dimethyl formamide (3.4 mL), water (1.7 mL) and acetic acid (0.9 mL) was heated to 85 ℃. Sodium dithionate was added to the solution over 20 min, then heated for a further 40 min. Sodium acetate was then added and reaction mixture allowed to cool to RT overnight. The amine was then extracted into dichloromethane (5 × 20 mL). The combined organic layers were washed with brine (20 mL) then dried over magnesium sulfate, filtered and concentrated under reduced pressure. Water (10 mL) was added to the remaining liquid to induce percipitation. Crystals of **185** were collected by filtration, washed with water and dried under reduced pressure. (42 mg, 46%). δ_H (400 MHz, DMSO-D_6): 8.96 (2H, d, J = 9.0 Hz, H-2'',6''), 7.52-7.47 (2H, m, H-Ar), 7.45-7.39 (3H, m, H-Ar), 7.38-7.33 (2H, m, H-2,8'), 7.21 (2H, d, J = 9.0 Hz, H-H-3'',5''), 7.06 (1H, dd, J = 8.4, 2.1 Hz, H-6), 6.78 (1H, s, H-3'), 6.30 (1H, d, J = 8.4 Hz, H-5), 5.24 (2H, s, CH_2), 3.89 (3H, s, CH_3), 3.73 (3H, s, CH_3). Tentative characterisation based on ^{1}H NMR.

4'-Benzyloxy-5,7-dimethoxy-(4''carboxy-phenoxy)-flavone 186

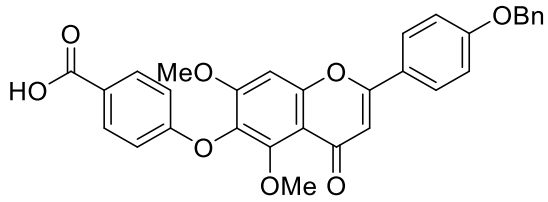

Aryl amine **185** (29 mg, 0.05 mmol) was dissolved in a mixture of conc. HCl (0.15 mL) and glaciar acetic acid (0.30 mL) and cooled to 0 ºC. A solution of sodium nitrite (8.0 mg, 0.12 mmol) in water (0.1 mL) was added to the reaction mixture slowly and the solution left to stir for 20 min. Hypophosphinic acid (0.05 mL, 0.46 mmol) was then added to the mixture and the reaction left to warm to RT overnight. It was then diluted with 1 M aqueous HCl solution (5 mL)

then extracted with dichloromethane (3 × 10 mL). The combined organic layers were washed with brine (10 mL) then dried over magnesium sulfate, filtered and concentrated under reduced pressure. Ether **186** was purified by column chromatography on the Isolera (0-10% methanol in dichloromethane) to yield the product as a grey powder (30 mg, 98%). δ_H (400 MHz, $CDCl_3$): 8.03 (2H, d, *J* = 8.8 Hz, H-2',6'), 7.85 (2H, d, *J* = 8.6 Hz, H-2'',6''), 7.48-7.33 (5H, m, H-Ar), 7.10 (2H, d, *J* = 8.6 Hz, H-3'',5''), 6.94 (2H, d, *J* = 8.8 Hz, H-3',5'), 6.89 (1H, s, H-), 6.66 (1H, s, H-Ar), 5.16 (2H, s, CH_2), 3.90 (6H, s, CH_3). Tentative characterisation based on ^{1}H NMR.

2'-Acetoxyphenyl-3',5'-(benzyloxy)phenoxy-4-methoxy-benzoate 188

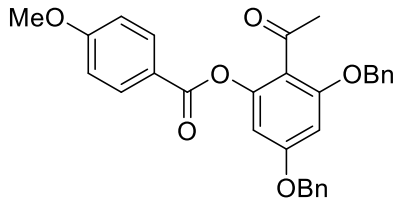

Dibenzyl protected acetophenone **139** (0.152 g, 0.43 mmol) and paramethoxy benzoic acid **187** (67.7 mg, 0.44 mmol) were dissolved in anhydrous dichloromethane (2 mL) along with EDC (0.137 g, 0.72 mmol) and DMAP (6.0 mg, 0.05 mmol). The reaction mixture was stirred overnight at room temperature. The solvent was then removed under reduced pressure. The residue was purified by column chromatography (Isolera 10%-60% ethyl acetate in hexane) to yield the ester **188** as a colourless oil (0.153 g, 73%). ν_{max} (ATR): 1605 (C=O), 1730 (C=O), 1252 (C–O), 1096 (C–O) cm^{-1}. δ_H (400 MHz, $CDCl_3$): 8.10 (2H, d, *J* = 9.1 Hz, H-2&6), 7.42-7.31 (10 H, m, H-Ph), 6.98 (2H, d, *J* = 9.0 Hz, H-3&5), 6.55 (1H, d, *J* = 2.2 Hz, H-4'/6'), 6.48 (1H, d, *J* = 2.2 Hz, H-4'/6'), 5.09 (2H, s, CH_2), 5.05 (2H, s, CH_2), 3.90 (3H, s, OMe), 2.48 (3H, s, CH_3). δ_C (100 MHz, $CDCl_3$): 199.37 (C), 164.69 (C), 164.06 (C), 161.22 (C), 158.12 (C), 149.87 (C), 136.08 (C), 135.96 (C), 132.49 (CH), 128.74 (CH), 128.34 (CH), 128.29 (CH), 127.68 (CH), 127.49 (CH), 121.53 (C), 118.17 (C), 114.20 (CH), 113.94 (CH), 101.57 (CH), 98.48 (CH), 70.97 (CH_2), 70.47 (CH_2), 55.53 (CH_3), 32.09 (CH_3). HRMS (ESI): 505.1606 *m/z*. $C_{30}H_{26}NaO_6$ requires $[M+Na]^+$ 505.1622 *m/z*.

7-Benzyloxy-5-hydroxy-flavone 189

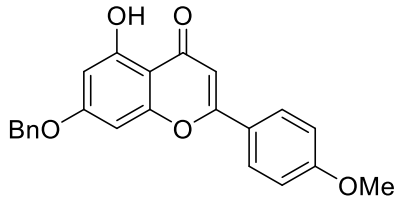

Ester **188** (0.0117 g, 0.024 mmol) and phosphazene base (0.03 mL) were taken up in anhydrous 1,4-dioxane (0.5 mL) and heated at 100 ºC for 24 h. The mixture was then diluted with ethyl acetate (10 mL) and washed with water (2 × 10 mL), then brine (10 mL); dried over magnesium sulfate and concentrated under reduced pressure. The residue was purified on Isolera (Isolera 20%-80% ethyl acetate in hexane) to yield product **189** (0.0056 g, 50%) δ_H (400 MHz, $CDCl_3$): 12.82 (1H, s, OH), 9.08 (2H, d, *J* = 9.1 Hz, H-2', 6'), 7.44-7.37 (5H, m, H-Ar), 7.02 (2H, d, *J* = 9.0 Hz, H-3', 5'), 6.58 (1H, s, H-3), 6.56 (1H, d, *J* = 2.2 Hz, H-6/8), 6.45 (1H, d, *J* = 2.2 Hz, H-6/8), 5.15 (2H, s, CH_2), 3.89 (3H, s, CH_3). δ_C (100 MHz, $CDCl_3$): 182.46 (C), 164.50 (C), 163.16 (C), 162.61 (C), 162.22 (C), 157.68 (C), 135.82 (C), 128.76 (CH), 128.60 (C), 128.37 (CH), 128.07 (CH), 127.50 (CH), 114.52 (CH), 105.74 (C), 104.41 (CH), 98.81 (CH), 93.49 (CH), 70.44 (CH_2), 29.61 (CH_3). Tentative characterisation based on the ^{1}H NMR and ^{13}C NMR only. Known compound CID 70341749 no characterisation in literature.[150]

5,7-Diisopropoxy-4'-chloro-3'-nitro-flavone 197

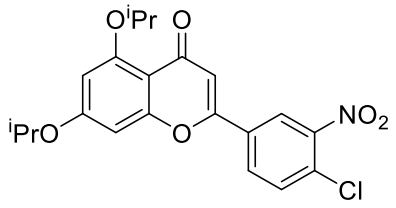

Diisopropoxy acetophenone **99** (3.08 g, 12 mmol) and 4-chloro-3-nitrobenzaldehyde **172** (2.27 g, 12 mmol) were dissolved in ethanol (60 mL) along with potassium hydroxide (0.689 g, 12 mmol). The mixture was then heated at 40 ºC for 3.5 hours, then allowed to cool to room temperature. Ethanol was removed under reduced pressure and the resulting precipitate taken up in ethyl acetate (100 mL). The solution was washed with 1 M aqueous HCl

solution (100 mL), water (100 mL), then brine (100 mL), dried over magnesium sulfate, filtered and concentrated under reduced pressure.

The resulting crude yellow crystals of the chalcone **196** were dissolved in dry DMSO (120 mL) and iodine (0.311 g, 1.2 mmol) was added. The suspension was heated at 100 ºC for 16 hours. The reaction was then cooled to room temperature and quenched with sodium bicarbonate solution (250 mL) and then extracted with dichloromethane (2 × 200 mL). The combined organic layers were then washed with sodium bicarbonate solution (300 mL) then brine (300 mL) and dried over magnesium sulfate; filtered and concentrated under reduced pressure. The crude product was purified by column chromatograpy (Isolera: 0%-10% methanol in dichloromethane) to yield the product **197** as a yellow powder (4.49 g, 45%). Mp: 182-186 ºC. ν_{max} (ATR): 2978 (Ar-H), 1651 (C=C). δ_H (400 MHz, $CDCl_3$): 8.40 (1H, d, *J* = 2.1 Hz, H2'), 7.95 (1H, dd, *J* = 8.5,2.2 Hz, H6'), 7.65 (1H, d, *J* = 8.5 Hz, H5'), 6.59 (1H, s, H3), 6.54 (1H, d, *J* = 1.9, H6/8),), 6.34 (1H, d, *J* = 2.0, H6/8), 4.67 (1H, septet, *J* = 6.0 Hz, CH), 4.60 (1H, septet, *J* = 6.1 Hz, CH), 1.46 (6H, d, *J* = 6.1 Hz, $2CH_3$), 1.42 (6H, d, *J* = 6.1 Hz, $2CH_3$). δ_C (100 MHz, $CDCl_3$): 176.31 (C=O), 162.60 (C), 159.59 (C), 159.46 (C), 156.40 (C), 148.21 (C), 132.47 (CH), 131.80 (C), 129.71 (CH), 129.22 (C), 122.67 (CH), 110.19 (CH), 109.77 (C), 100.58 (CH), 94.03 (CH), 72.26 (CH), 70.70 (CH), 21.83 (CH_3), 21.74 (CH_3). HRMS [ESI]: 440.0846 *m/z*. $C_{21}H_{20}NNaO_6{}^{35}Cl$ requires $[M+Na]^+$ 440.0871 *m/z*.

5,7-Diisopropoxy-5'',7'',4'''-trimethoxy-3'-nitrohinokiflavone 198

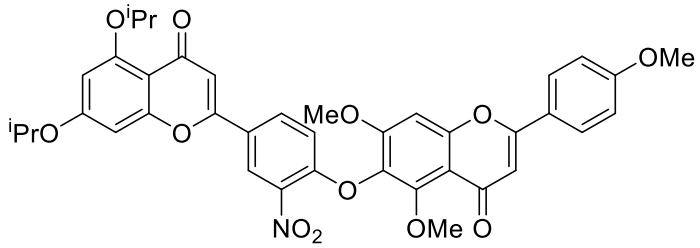

Nitroflavone **197** (20.5 mg, 0.05 mmol) and methoxyflavone **132** (16.5mg, 0.05 mmol) were taken up in DMSO-D_6 (0.3 mL) and heated in a sealed vial at 100 ºC for 1.5 h. The reaction was cooled to room temperature and diluted with 1M HCl (10 mL), extracted into a mixture of chloroform and isopropanol (4:1, 2 × 10 mL). The combined organic layers were washed with brine (20 mL) and dried

over magnesium sulphate. A small amount was purified for characterisation purposes the rest was taken on as crude. Decomposes at 256 ºC. ν_{max} (ATR): 2928 (NO_2), 1643 (C=O) 1604 (C=C) cm-1. δ_H (400 MHz, DMSO-D_6): 8.67 (1H, d, *J* = 2.3 Hz, H-2'), 8.19 (1H, dd, *J* = 9.0, 2.3 Hz, H-6'), 8.09 (2H, d, *J* = 9.0 Hz, H-2''', 6'''), 7.49 (1H, s, H-3/3''/8''), 7.15 (2H, d, *J* = 9.0 Hz, H-5''', 3'''), 7.00 (1H, d, *J* = 8.9 Hz, H-5'), 6.88 (1H, d, *J* = 2.2 Hz, H-6/8), 6.83 (1H, s, H-3/3''/8''), 6.78 (1H, s, H-3/3''/8''), 6.46 (1H, d, *J* = 2.2 Hz, H-6/8), 4.80 (1H, sept., *J* = 6.1 Hz, CH), 4.67 (1H, sept., *J* = 6.1 Hz, CH), 3.94 (3H, s, CH_3), 3.88 (3H, s, CH_3), 3.76 (3H, s, CH_3), 1.34 (6H, d, J = 6.1 Hz, ^{i}Pr), 1.30 (6H, d, J = 6.1 Hz, ^{i}Pr). Too insoluble to take ^{13}C NMR in DMSO-D_6. HRMS [ESI]: 732.1982 *m/z*. $C_{46}H_{31}NNaO_7$ requires $[M+Na]^+$ 732.1993 *m/z*.

5,7-Diisopropoxy-5'',7'',4'''-trimethoxyhinokiflavone 200

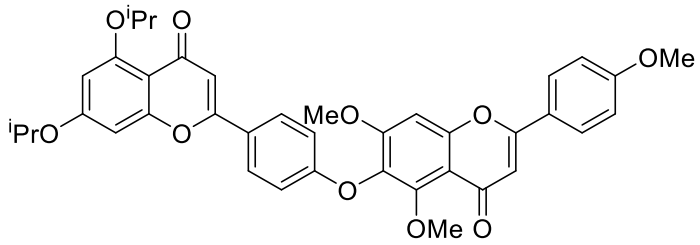

A solution of nitro compound **198** (55 mg, 0.077 mmol) in a mixture of dimethyl formamide (1.4 mL), water (0.7 mL) and acetic acid (0.45 mL) was heated to 85 ºC. Sodium dithionate (75 mg, 0.43 mmol in 0.3 mL of water) was added to the solution over 20 min, the resulting solution was heated for a further 40 min. Sodium acetate (42 mg, 0.51 mmol) was then added and reaction mixture allowed to cool to room temperature overnight. The solution was basified using dilute sodium hydroxide solution (0.5 m, 10 mL). Percipitate of **199** was collected by filtration, washed with water and dried under reduced pressure to yield the aminoflavone **199** as a beige powder. This was then dissolved in a mixture of conc. HCl (0.2 mL) and glaciar acetic acid (0.40 mL) and cooled to 0 ºC. A solution of sodium nitrite (8.0 mg, 0.12 mmol) in water (0.1 mL) was added to it slowly and the solution left to stir for 20 min. Hypophosphinic acid (0.03 mL, 0.30 mmol) was then added to the mixture and the reaction left to warm to RT overnight. It was then diluted with 1 M aqueous HCl solution (5 mL), then extracted with dichloromethane (3 × 10 mL). The combined organic layers were washed with brine (10 mL) then dried over magnesium sulfate, filtered and

concentrated under reduced pressure to yield the protected flavone **200** as a beige powder (21 mg, 56%). Decomposes at 314 °C. ν_{max} (ATR): 2977 (C-H), 1639 (C=O) 1603 (C=O) cm-1. δ_H (400 MHz, $CDCl_3$): 7.84 (2H, d, *J* = 8.9 Hz, H-2', 6'), 7.77 (2H, d, *J* = 9.0 Hz, H-2''', 6'''), 7.01 (2H, d, *J* = 9.0 Hz, H-3', 5'), 6.99 (2H, d, *J* = 9.0 Hz, H-3''', 5'''), 6.90 (1H, s, H-3/3''/8''), 6.61 (1H, s, H-3/3''/8''), 6.50 (1H, s, H-3/3''/8''), 6.49 (1H, d, *J* = 2.2 Hz, H-6/8), 6.34 (1H, d, *J* = 2.2 Hz, H-6/8), 4.63 (1H, sept., *J* = 6.1 Hz, CH), 4.57 (1H, sept., *J* = 6.1 Hz, CH),3.90 (6H, s, $2CH_3$), 3.88 (3H, s, CH_3), 1.44 (6H, d, *J* = 6.0 Hz, ^{i}Pr), 1.39 (6H, d, *J* = 6.0 Hz, ^{i}Pr). δ_C (100 MHz, $CDCl_3$): 177.38 (C), 176.86 (C), 162.29 (C), 162.07 (C), 161.42 (C), 160.56 (C), 160.20 (C), 159.89 (C), 159.42 (C), 157.07 (C), 155.85 (C), 152.91 (C), 134.01 (C), 127.72 (CH), 127.60 (CH), 125.63 (C), 123.61 (C), 115.52 (CH), 114.48 (CH), 113.08 (C), 110.04 (C), 108.01 (CH), 107.16 (CH), 100.69 (CH), 96.68 (CH), 94.50 (CH), 72.47 (CH), 70.54 (CH), 56.53 (CH_3), 55.53 (CH_3), 21.94 (CH_3), 21.88 (CH3). HRMS [ESI]: 687.2170 *m/z*. $C_{39}H_{36}NaO_{10}$ requires $[M+Na]^+$ 687.2201 *m/z*.

2,4,-Diisopropoxy-3,6-dihydroxy acetophenone 202

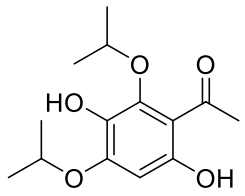

2,4,-di-isopropoxy acetophenone **99** (3.44 g, 13 mmol) was added to a cooled solution of aqueous potassium hydroxide (10%, 28 mL) at 0 °C. Potassium persulfate solution (2.81 g, 50 mmol, in 84 mL of water) was then added to the stirring solution over 2 hours. The reaction was left to stir for 16 h. The pH was then adjusted to pH 2 using 1 M hydrochloric acid solution. Sodium bisulfate (6.123 g, 59 mmol) was then added and the reaction heated at 110 °C for 2 hours, then allowed to cool. The solution was extracted using ethyl acetate (2 × 100 mL). The combined organic layers were washed with brine (100 mL), dried over magnesium sulfate, filtered and concentrated under reduced pressure. The crude product was purified by column chromatograpy (Isolera: 5%-7% ethyl acetate in hexane) to yield the product **202** as a colourless oil (0.783 g, 21%). ν_{max} (ATR): 3410 (O-H), 2981 (Ar-H), 1624 (C=O) cm^{-1}. δ_H (400 MHz, $CDCl_3$): 13.05 (1H, s, OH), 6.21 (1H, s, H5), 5.17 (1H, s, O-H), 4.89 (1H, sept.,

J = 6.2 Hz, CH), 4.64 (1H, sept., *J* = 6.1 Hz, CH), 2.68 (3H, s, CH_3), 1.40 (6H, d, *J* = 6.1 Hz, $2CH_3$), 1.32 (6H, d, *J* = 6.2 Hz, $2CH_3$). δ_C (100 MHz, $CDCl_3$): 203.93 (C=O), 158.45 (C), 151.47 (C), 144.97 (C), 131.59 (C), 109.10 (C), 96.10 (CH), 75.43 (CH), 72.01 (CH), 32.52 (CH_3), 22.59 (CH_3), 21.98 (CH_3). HRMS [ESI]: 291.1198 *m/z*. $C_{14}H_{20}NaO_5$ requires $[M+Na]^+$ 291.1203 *m/z*.

2,4,-Diisopropoxy-6-hydroxy-3-(methoxymethoxy) acetophenone 203

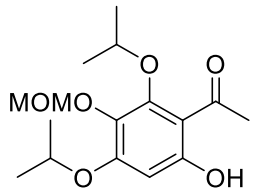

Phenol **202** (0.444 g, 4.7 mmol) and diidopropylamine (1.2 mL, 13 mmol) were dissolved in anhydrous dichloromethane (7.5 mL). The reaction mixture was cooled to 0 ºC and bromomethyl methyl ether (0.27 mL, 3.3 mmol) added. The reaction was left to warm to room temperature over 16 hours. It was then diluted with dichloromethane (20 mL) and washed with 1 M hydrochloric acid solution (3 × 50 mL) then brine (50 mL). The organic layer was dried over magnesium sulfate, filtered and concentrated under reduced pressure. The crude product was purified by column chromatograpy (Isolera: 0%-20% ethyl acetate in hexane) to yield the product **203** as a colourless oil (0.348 g, 67%). ν_{max} (ATR): 2976 (C-H), 2933 (OH), 1614 (C=O) cm^{-1}. δ_H (400 MHz, $CDCl_3$): 13.29 (1H, s, OH), 6.21 (1H, s, H5), 5.01 (2H, s, CH_2), 4.89 (1H, sept., *J* = 6.2 Hz, CH), 4.60 (1H, sept., *J* = 6.1 Hz, CH), 3.61 (3H, s, CH_3), 2.67 (3H, s, CH_3), 1.39 (6H, d, *J* = 6.1 Hz, $2CH_3$), 1.28 (6H, d, *J* = 6.2 Hz, $2CH_3$). δ_C (100 MHz, $CDCl_3$): 203.78 (C=O), 161.68 (C), 158.13 (C), 153.05 (C), 132.07 (C), 110.32 (C), 98.63 (C), 97.03 (CH), 75.84 (CH), 70.94 (CH), 57.50 (CH_3), 32.61 (CH_3), 22.33 (CH_3), 21.85 (CH_3). HRMS [ESI]: 335.1449 *m/z*. $C_{16}H_{24}NaO_6$ requires $[M+Na]^+$ 335.1465 *m/z*.

4-Isopropoxybenzaldehyde 204

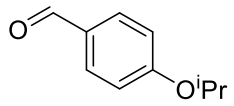

4-Hydroxybenzaldehyde (3.04 g, 25 mmol) and potassium carbonate (6.80 g, 49 mmol) were dissolved in anhydrous dimethyl formamide (120 mL). 2-Bromopropane (2.5 mL, 27 mmol) was added to the reaction flask and the reaction mixture heated at 60 ºC under argon atmosphere for 3 hours. It was then cooled to room temperature, quenched with LiCl solution (5%, 100 mL), and extracted into ethyl acetate (2 × 100 mL) The combined organic layers were then washed with LiCl solution (5%, 5 × 50 mL) and brine (100 mL), dried over magnesium sulfate, filtered and concentrated under reduced pressure. The crude product was purified by column chromatograpy (Isolera: 0%-20% ethyl acetate in hexane) to yield the product **204** as a pale yellow oil (3.05 g, 75%). ν_{max} (ATR): 2978 (C-H), 1688 (C=O), 1597 (C-C) cm^{-1}. δ_H (400 MHz, $CDCl_3$): 9.87 (1H, s, CHO), 7.81 (2H, d, *J* = 8.8 Hz, CH), 6.97 (2H, d, *J* = 8.8 Hz, CH), 4.67 (1H, septet, *J* = 6.1 Hz, CH), 1.38 (6H, d, *J* = 6.1 Hz, $2CH_3$). δ_C (100 MHz, $CDCl_3$): 190.74 (HC=O), 163.18 (C), 132.02 (CH), 129.57 (C), 115.60 (CH), 70.32 (CH), 21.87 (CH_3). Reported data agrees with literature.[140]

4,2',4'-Triisopropoxy-6'hydroxy-3'-(methoxymethoxy)-chalcone 205

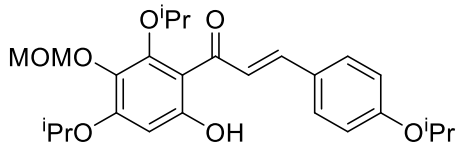

Acetophenone **203** (0.345 g, 1.1 mmol) and aldehyde **204** (0.175 g, 1.1 mmol) were dissolved in methanol (6.0 mL) along with barium hydroxide octahydrate (0.383 g, 1.2 mmol). The mixture was heated at 60 ºC for 3 hours. The solvent was then removed under reduced pressure. The residue was taken up in ethyl acetate (20 mL) and washed with 1 M hydrochloric acid solution (20 mL), water (2 × 20 mL) then brine (20 mL); dried over magnesium sulfate, filtered and concentrated under reduced pressure. The crude product was purified by column chromatograpy (Isolera: 0%-20% ethyl acetate in hexane) to yield the product **205** as an orange powder (0.324 g, 64%). ν_{max} (ATR): 2978 (O-H), 1626 (C=O) 1550.82 (C=C) cm^{-1}. δ_H (400 MHz, $CDCl_3$): 13.51 (1H, s, OH), 7.91 (1H, d, *J* = 15.6 Hz, CH), 7.77 (1H, d, *J* = 15.7 Hz, CH), 7.57 (2H, d, *J* = 8.8 Hz, H-Ar), 6.91 (2H, d, *J* = 8.7 Hz, H-Ar), 6.27 (1H, s, H-Ar), 5.09 (2H, s, CH_2), 4.68-4.51 (3H, m, 3CH), 3.66 (3H, s, CH_3), 1.41 (6H, d, *J* = 6.1 Hz, $2CH_3$), 1.37 (6H, d,

J = 6.0 Hz, 2CH_3), 1.23 (6H, d, *J* = 6.2 Hz, 2CH_3). δ_C (100 MHz, $CDCl_3$): 193.15 (C=O), 162.14 (C), 159.95 (C), 158.06 (C), 152.73 (C), 142.41 (CH), 132.99 (C), 130.30 (CH), 127.70 (C), 124.94 (CH), 115.95 (CH), 110.59 (C), 98.77 (CH_2), 97.49 (CH), 70.94 (CH), 70.02 (CH), 57.43 (CH_3), 22.36 (CH_3), 22.01 (CH_3), 21.88 (CH_3). HRMS [ESI]: 481.2178 *m/z*. $C_{26}H_{34}NaO_7$ requires $[M+Na]^+$ 481.2197 *m/z*.

5,7,4'-Triisopropoxy-6-hydroxyflavone 206

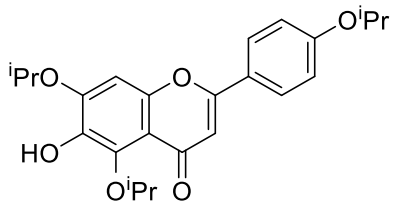

Chalcone **205** (0.324 g, 0.71 mmol) and iodine (13.7 mg, 0.054 mmol) were dissolved in dry DMSO and heated at 100 ºC for 16 hours. The reaction was then cooled to room temperature and quenched with sodium bicarbonate solution (50 mL), followed by extraction with dichloromethane (2 × 30 mL). The combined organic layers were then washed with sodium bicarbonate solution (50 mL), water (50 mL), and brine (50 mL), dried over magnesium sulfate, filtered and concentrated under reduced pressure. The crude product was purified by column chromatograpy (Isolera: 0%-10% methanol in dichloromethane) to yield the product **206** as an orange oil (0.257 g, 88%).). ν_{max} (ATR): 2978 (O-H), 1632 (C=O) 1508 (C=C) cm^{-1}. δ_H (400 MHz, $CDCl_3$): 7.80 (2H, d, *J* = 8.9 Hz, H-Ar), 6.98 (2H, d, *J* = 8.9 Hz, H-Ar), 6.80 (1H, s, H-Ar), 6.54 (1H, s, H-Ar), 5.84 (1H, s, H-Ar), 4.73 (1H, d, *J* = 6.1 Hz, CH), 4.69-4.58 (2H, m, CH), 1.48 (6H, d, *J* = 6.0 Hz, 2CH_3), 1.40 (6H, d, *J* = 5.6 Hz, 2CH_3), 1.38 (6H, d, *J* = 5.9 Hz, 2CH_3). δ_C (100 MHz, $CDCl_3$): 177.21 (C=O), 162.29 (C), 160.51 (C), 152.04 (C), 150.18 (C), 141.55 (C), 138.06 (C), 127.65 (CH), 123.60 (C), 115.85 (CH), 112.14 (C), 106.57 (CH), 97.84 (CH), 78.78 (CH), 71.95 (CH), 70.14 (CH), 22.35 (CH_3), 21.95 (CH_3), 21.91 (CH_3). HRMS [ESI]: 435.1758 *m/z*. $C_{24}H_{28}NaO_6$ requires $[M+Na]^+$ 435.1778 *m/z*.

Pentaisopropoxyhinokiflavone 209

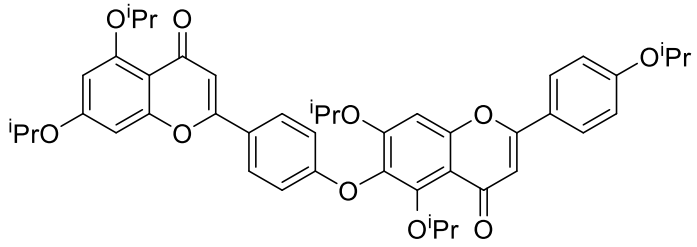

Chloroflavone **197** (0.127 g, 0.30 mmol) and hydroxylavone **206** (0.130 g, 0.32 mmol) were dissolved in anhydrous dimethyl formamide along with anhydrous potassium carbonate (54.2 mg, 0.39 mmol) and heated at 100 ℃ for 16 hours. The reaction was then cooled to room temperature and quenched with water. The product biflavone **207** was filtered and washed with water.

The precipitate **207** was taken up in ethanol along with tin (II) chloride (0.185 g, 0.82 mmol). The reaction was heated at 60 ºC for 6 hours, allowed to cool and the solvent removed under reduced pressure. The residue was taken up in dichloromethane and washed with sodium bicarbonate solution (3 × 50 mL) then brine (50 mL), dried over magnesium sulfate, filtered and concentrated under reduced pressure. The residue **208** was then dissolved in a mixture of conc. aq. HCl (0.50 mL) and glacial acetic acid (1.0 mL) and cooled to 0 ºC. A solution of sodium nitrite (13.3 mg, 0.19 mmol) in water (0.1 mL) was added to it slowly and the solution left to stir for 20 min. Hypophosphinic acid (0.14 mL) was then added to the mixture and the reaction left to warm to room temperature overnight. It was then diluted with 1 M aqueous HCl solution (20 mL) and extracted with dichloromethane (2 × 20 mL). The combined organic layers were washed with sodium bicarbonate solution (30 mL), brine (30 mL) then dried over magnesium sulphate and concentrated under reduced pressure. The crude product was purified by column chromatography (Isolera: 0%-10% methanol in dichloromethane) to yield the product **209** as a viscous brown oil (62.5 mg, 27%). ν_{max} (ATR): 2978 (O-H), 1626 (C=O) 1550.82 (C=C) cm^{-1}. δ_H (400 MHz, $CDCl_3$): 13.51 (1H, s, OH), 7.91 (1H, d, *J* = 15.6 Hz, CH), 7.77 (1H, d, *J* = 15.7 Hz, CH), 7.57 (2H, d, *J* = 8.8 Hz, H-Ar), 6.91 (2H, d, *J* = 8.7 Hz, H-Ar), 6.27 (1H, s, H-Ar), 5.09 (2H, s, CH_2), 4.68-4.51 (3H, m, 3CH), 3.66 (3H, s, CH_3), 1.41 (6H, d, *J* = 6.1 Hz, $2CH_3$), 1.37 (6H, d, *J* = 6.0 Hz, $2CH_3$), 1.23 (6H, d, *J* = 6.2 Hz, $2CH_3$). δ_C (100 MHz, $CDCl_3$): 193.15 (C=O), 162.14 (C), 159.95 (C), 158.06 (C), 152.73

(C), 142.41 (CH), 132.99 (C), 130.30 (CH), 127.70 (C), 124.94 (CH), 115.95 (CH), 110.59 (C), 98.77 (CH_2), 97.49 (CH), 70.94 (CH), 70.02 (CH), 57.43 (CH_3), 22.36 (CH_3), 22.01 (CH_3), 21.88 (CH_3). HRMS [ESI]: 771.3115 *m/z*. $C_{45}H_{48}NaO_{10}$ requires $[M+Na]^+$ 771.3140 *m/z*.

7-(6''-Chlorohexoxy)-5-hydroxyflavone 234

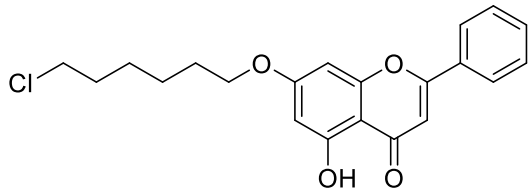

Chrysin **138** (0.103 g, 0.41 mmol), iodo-hexane compound **237** (0.62 mL, 4.1 mmol) and potassium carbonate (0.118 g, 0.86 mmol) were dissolved in anhydrous dimethyl formamide (2.0 mL) then heated to 100 ºC for 24 h. The reaction was allowed to cool to room temperature then quenched with aqueous LiCl solution (5%, 20 mL) and extracted into dichloromethane (3 × 10 mL). The combined organic layers were then washed with brine (10 mL), dried over magnesium sulfate and concentrated under reduced pressure. The crude product was purified by column chromatograpy (Isolera: 100% dichloromethane) to yield the product **234** as white crystals (0.103 g, 66%). Mp.: 110-112 ºC. ν_{max} (ATR): 2940 (C=C), 1165 (C=O), 823 cm^{-1}. δ_H (400 MHz, $CDCl_3$):12.71 (1H, s, OH), 7.92-7.86 (2H, m, H-2',6'), 7.58-7.49 (3H, m, H-3',4',5'), 6.67 (1H, s, H-3), 6.50 (1H, d, *J* = 2.2 Hz, H-6/8), 6.37 (1H, d, *J* = 2.2 Hz, H-6/8), 4.05 (2H, t, *J* = 6.4 Hz, CH_2), 3.57 (2H, t, *J* = 6.4 Hz, CH_2), 1.89-178 (4H, m, CH_2), 1.58-1.47 (4H, m, CH_2). δ_C (100 MHz, $CDCl_3$): 182.6 (C=O), 165.3 (C), 164.1 (C),162.4 (C), 158.0 (C), 131.9 (CH), 131.5 (C), 129.2 (CH), 126.5 (CH), 106.1 (CH), 105.8 (C), 98.7 (CH), 93.3 (CH),68.6 (CH_2), 45.1 (CH_2), 32.6 (CH_2), 29.0 (CH_2), 26.7 (CH_2), 25.5 (CH_2). HRMS: 395.1004 *m/z*. $C_{21}H_{21}N_3NaO_3O_4{}^{35}Cl$ requires $[M+Na]^+$ 395.1021 *m/z*.

7-(6''-Iodohexoxy)-5-hydroxyflavone 235

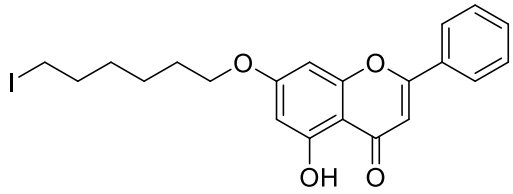

Chloro-hexane chrysin derivative **234** (0.080 g, 0.22 mmol) was dissolved in acetone (1.0 mL) along with sodium iodide (0.230 g, 1.5 mmol). The mixture was heated to 60 ºC for 2 days. The reaction was allowed to cool to room temperature then filtered through celite and concentrated under reduced pressure to yield the product **235** (0.028 g, 28%) as off white crystals. Mp.: 122-124 ºC. ν_{max} (ATR): 2928 (C–C), 1659 (C=O), 1167 (C-O). δ_H (400 MHz, Acetone-D_6): 12.85 (1H, s, OH), 8.11-8.07 (2H, m, H-2',6'), 7.66-7.57 (3H, m, H-3',4',5'), 6.83 (1H, s, H-3), 6.74 (1H, d, *J* = 2.2 Hz, H-6/8), 6.36 (1H, d, *J* = 2.2 Hz, H-6/8), 4.17 (2H, t, *J* = 6.5 Hz, H-1'), 3.11 (2H, t, *J* = 7.0 Hz, H-6'), 1.92-1.79 (4H, m, H-2',5'), 153-1.48 (4H, m, H-3',4'). δ_C (100 MHz, Acetone-D_6): 182.46, 165.10, 163.95, 162.19, 157.81, 131.80, 131.39, 129.08, 126.29, 105.88, 105.65, 98.59, 93.12, 68.42, 30.31, 30.16, 28.77, 24.97, 6.78. HRMS(ESI): 487.0360 *m/z*. $C_{21}H_{21}INaO_4$ requires $[M+Na]^+$ 487.0377 *m/z*.

7-(6''-Azidohex-1''-oxy)-5-hydroxyflavone 236

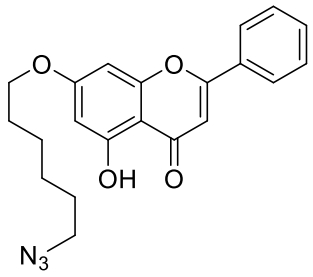

Chrysin **138** (0.511 g, 2.0 mmol), iodo-hexane compound **238** (0.463 g, 1.8 mmol) and potassium carbonate (0.518 g, 3.7 mmol) were dissolved in anhydrous dimethyl foramide (9.0 mL) then stirred at room temperature for 2 d. The reaction was then quenched with aqueous LiCl solution (5%, 20 mL), and extracted into dichloromethane (2 × 15 mL). The combined organic layers were washed with LiCl solution (5%, 5 × 20 mL) and brine (20 mL), dried over magnesium sulfate, filtered and concentrated under reduced pressure. The crude product was purified by column chromatograpy (Isolera: 10%-100% ethyl acetate in hexane) to yield the chrysin derivative **236** as a beige powder (0.374 g, 56%). MP 94-96 ºC. ν_{max} (ATR): 2928 (OH), 2095 (CH_2N_3), 1657 (C=O). δ_H (400 MHz, $CDCl_3$):12.71 (1H, s, OH), 7.92-7.86 (2H, m, H-2',6'), 7.59-7.48 (3H, m, H-3',4',5'), 6.67 (1H, s, H-Ar), 6.50 (1H, d, *J* = 2.2 Hz, H-6/8), 6.38 (1H, d, *J* = 2.2 Hz, H-6/8), 4.05 (2H, t, *J* = 6.5 Hz, CH_2), 3.30 (2H, t, *J* = 6.8 Hz, CH_2),

1.89-1.79 (2H, m, CH_2), 1.70-1.37 (6H, m, CH_2). δ_C (100 MHz, $CDCl_3$): 182.45 (C=O), 164.06 (C), 163.92 (C), 162.15 (C), 157.78 (C), 131.79 (CH), 131.79 (CH), 131.35 (C), 129.07 (CH), 126.26 (CH), 105.86 (CH), 105.63 (C), 98.56 (CH), 93.08 (CH), 68.38 (CH_2), 51.34 (CH_2), 29.68 (CH_2), 28.81 (CH_2), 26.44 (CH_2), 25.58 (CH_2). LRMS (ESI^+): 402.14 [$(M+Na)^{+\bullet}$, 100%]. HRMS(ESI+): 402.1406 *m/z*. $C_{21}H_{21}N_3NaO_4$ requires $[M+Na]^+$ 402.1424 *m/z*.

1-Azido-6-iodohexane 238

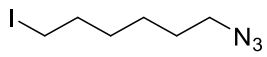

1-Chloro-6-iodo-hexane **233** (2.3 mL, 15 mmol) and sodium azide (1.03 g, 16 mmol) were dissolved in ethanol and heated at 40 ºC for 6 days. The solvent was then removed under reduced pressure and the residue taken up in dichloromethane (20 mL). The suspension was washed with water (2 × 20 mL) then brine (20 mL), dried over magnesium sulfate, filtered and concentrated under reduced pressure. The yellow oil obtained was then dissolved in acetone (75 mL) and sodium iodide (15.8 g, 110 mmol) added. The reaction mixture was heated at 60 ºC for 2 d, the solvent was then removed under reduced pressure. The residue was taken up in dichloromethane, filtered through celite and concentrated under reduced pressure. The crude oil was purified by column chromatograpy (Isolera: 100% hexane) to yield the 1-azido-6-iodohexane **238** as a yellow oil (2.35 g, 62%). δ_H (400 MHz, $CDCl_3$): 3.28 (2H, t, *J* = 6.9 Hz, CH_2N_3), 3.19 (2H, t, *J* = 6.9 Hz, CH_2I), 1.89-1.78 (2H, m, CH_2), 1.66-1.57 (2H, m, CH_2),1.49-1.35 (4H, m, $2CH_2$). δ_C (100 MHz, $CDCl_3$): 51.33 (CH_2), 33.27 (CH_2), 30.03 (CH_2), 28.70 (CH_2), 25.70 (CH_2), 6.90 (CH_2). The reported data agree with literature.[141]

2,4-Di-(6'-azidohex-1'-oxy)-6-hydroxy acetophenone 241

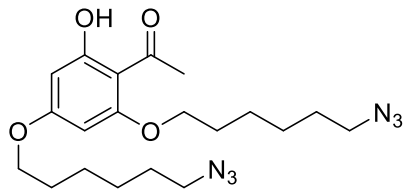

2,4,6-Acetophenone **142** (15.9 mg, 0.95 mmol), hexane derivative **237** (46.5 mg, 1.9 mmol) and potassium carbonate (52.6 mg, 3.8 mmol) were dissolved in anhydrous dimethyl formamide (5.0 mL) then stirred at 60 °C for 24 h. The reaction was allowed to cool to room temperature then quenched with 1 M aqueous HCl solution (20 mL), and extracted into dichloromethane (2 × 20 mL) The combined organic layers were then washed with LiCl solution (5%, 5 × 20 mL) and brine (20 mL), dried over magnesium sulfate, filtered and concentrated under reduced pressure. The crude product was purified by column chromatograpy (Isolera: 0%-20% ethyl acetate in hexane) to yield acetophenone **241** as a colourless oil (26.2 mg, 66%). ν_{max} (ATR): 2938 (OH), 2861 (C-H), 2091 (CH_2N_3), 1616 (C=O) cm^{-1}. δ_H (400 MHz, $CDCl_3$): 14.03 (1H, s, OH), 6.12 (1H, d, *J* = 2.3 Hz, H-3/5), 5.89 (1H, d, *J* = 2.3 Hz, H-3/5), 3.99 (2H, t, *J* = 6.4 Hz, CH_2OAr), 3.67 (2H, t, *J* = 6.4 Hz, CH_2OAr), 3.29 (2H, t, *J* = 6.8 Hz, CH_2N_3), 3.28 (2H, t, *J* = 6.8 Hz, CH_2N_3), 2.62 (3H, s, CH_3), 1.92-1.73 (4H, m, CH_2), 1.69-1.40 (12H, m, CH_2). δ_C (100 MHz, $CDCl_3$): 202.91 (C=O), 167.55 (C), 165.51 (C), 162.25 (C),105.91 (C), 93.80 (CH), 91.54 (CH), 68.62 (CH_2), 67.99 (CH_2), 51.31 (CH_2), 33.08 (CH_3), 28.91 (CH_2), 28.82 (CH_2), 28.74 (CH_2), 26.44 (CH_2), 26.43 (CH_2), 25.88 (CH_2), 25.58 (CH_2). LRMS(ESI$^+$): 441.22 [$(M+Na)^{+\bullet}$, 100%]. HRMS(ESI+): 441.2201 *m/z*. $C_{20}H_{30}N_6NaO_4$ requires $[M+Na]^+$ 441.2221 *m/z*.

4-(6'-Azidohex-1'-oxy)-2-benzyloxy-6-hydroxy-acetophenone 243

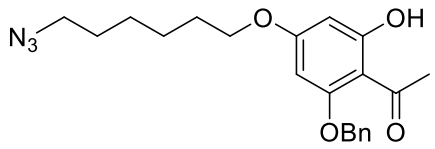

Monosubstituted chrysin **236** (0.151 g, 0.41 mmol), benzyl bromide (0.20 g, 1.7 mmol) and potassium carbonate (0.236 g, 1.7 mmol) were dissolved in anhydrous dimethyl foramide (2.0 mL) then stirred at 100 °C for 3 d. The reaction was then quenched with 1 M aqueous HCl solution (10 mL), and extracted into dichloromethane (2 × 10 mL). The combined organic layers were washed with LiCl solution (5%, 5 × 10 mL) and brine (20 mL), dried over magnesium sulfate, filtered and concentrated under reduced pressure. The crude product was purified by column chromatography (Isolera: 0%-50% ethyl acetate in hexane) to yield the benzylated chrysin derivative **242** (0.150 g, 77%). The disubstituted chrysin derivative **242** (0.0519 g, 0.11 mmol) was then taken

up in a mixture of 18 M aqueous potassium carbonate solution (0.2 mL) and pyridine (0.2 mL) and diethylene glycol was added to the suspension (0.2 mL). The mixture was heated at 100 ºC for 4 h then allowed to cool to room temperature. The reaction was quenched with 1 M aqueous HCl solution (5 mL) then extracted into dichloromethane (2 × 10 mL). The combined organic layers were washed with brine (10 mL) then dried over magnesium sulfate, filtered and concentrated under reduced pressure. The crude product was purified by column chromatography (Isolera: 0%-20% ethyl acetate in hexane) to yield the acetophenone **243** as a colourless oil (0.037 g, 87%). ν_{max} (ATR): 2938 (OH), 2862 (C-H), 2093 (CH_2N_3), 1584 (C=O). δ_H (400 MHz, $CDCl_3$): 14.05 (1H, s, OH), 7.43-7.35 (5H, m, H-2', 3', 4', 5', 6'), 6.05 (1H, d, *J* = 2.4 Hz, H-3/5), 6.01 (1H, d, *J* = 2.4 Hz, H-3/5), 5.07 (2H, s, OC*H*$_2$Ph), 3.97 (2H, t, *J* = 6.4 Hz, CH_2), 3.29 (2H, t, *J* = 6.7 Hz, CH_2N_3), 2.55 (3H, s, CH_3), 1.85-1.74 (2H, m, CH_2), 1.69-1.59 (2H, m, CH_2), 1.50-1.42 (4H, m, CH_2). δ_C (100 MHz, $CDCl_3$): 203.05 (C=O), 167.57 (C), 165.44 (C), 161.94 (C), 135.64 (C), 128.71 (CH), 128.42 (CH), 127.95 (CH), 106.08 (C), 94.21 (CH), 92.06 (CH), 71.06 (CH_2), 68.04 (CH_2), 51.32 (CH_2), 33.23 (CH_3), 28.79 (CH_2), 28.74 (CH_2), 26.42 (CH_2), 25.57 (CH_2). HRMS [ESI]: 406.1724 *m/z*. $C_{21}H_{25}N_3NaO_4$ requires $[M+Na]^+$ 406.1737 *m/z*.

5-Hydroxy-7-(methoxymethoxy)flavone 244

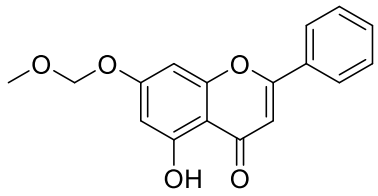

Chrysin **138** (2.51 g, 9.9 mmol), bromomethyl methyl ether (0.89 mL, 11 mmol) and potassium carbonate (4.02 g, 29 mmol) were dissolved in acetone (50 mL) then stirred at 60 ºC for 4 h. The reaction was allowed to cool to room temperature then concentrated under reduced pressure. The precipitate was taken up in dichloromethane (30 mL) then washed with 1 M aqueous HCl solution (3 × 15 mL), water (25 mL), and brine (25 mL). The solution was dried over magnesium sulfate, filtered and concentrated under reduced pressure. The crude product was purified by column chromatography (Isolera: 20%-80% ethyl acetate in hexane) to yield the protected chrysin **244** as a yellow powder (1.14 g, 58%). Mp: 108-110 ºC. δ_H (400 MHz, $CDCl_3$): 12.68 (1H, s, OH), 7.91-7.88

(2H, m, H-2',6'), 7.56-7.56 (3H, m, H-3',4',5'), 6.69 (1H, d, *J* = 2.2 Hz, H-6/8), 6.69 (1H, s, H-3), 6.50 (1H, d, *J* = 2.2 Hz, H-6/8), 5.25 (2H, s, CH_2), 3.51 (3H, s, CH_3). δ_C (100 MHz, $CDCl_3$): 182.54 (C), 164.07 (C), 163.08 (C), 162.04 (C), 157.64 (C), 131.85 (CH), 131.24 (C), 129.06 (CH), 126.29 (CH), 106.35 (C), 105.87 (CH), 100.17 (CH), 94.37 (CH), 94.23 (CH_2), 56.41 (CH_3). The reported data agree with literature.[142]

5-(6''-Azidohex-1''-oxy)-7-(methoxymethoxy)-flavone 245

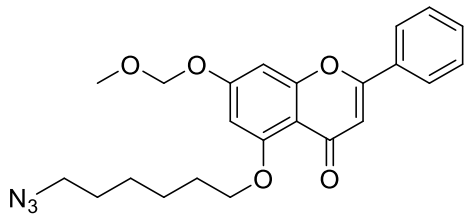

Mono protected chrysin **244** (39.8 mg, 1.3 mmol), iodochexane compound **237** (38.1 mg, 1.5 mmol) and potassium carbonate (37.5 mg, 2.7 mmol) were dissolved in anhydrous dimethyl formamide (7.0 mL) then stirred at 30 °C for 3 d. The reaction was allowed to cool to RT then quenched with LiCl solution (5%, 20 mL), extracted into dichloromethane (20 mL). The organic layer was then washed with LiCl solution (5%, 5 × 20 mL) and brine (20 mL), dried over magnesium sulfate, filtered and concentrated under reduced pressure. The crude product was purified by column chromatograpy (Isolera: 0%-60% ethyl acetate in hexane) to yield disubstituted chrysin **245** as yellow crystals (51.1 mg, 91%). MP: 90-91 °C. ν_{max} (ATR): 2095 (CH_2N_3), 1606 (C=O) 1150 (C-O) cm^{-1}. δ_H (400 MHz, $CDCl_3$): 7.90-7.85 (2H, m, H-2',6'), 7.52-7.46 (3H, m, H-3',4',5'), 6.77 (1H, d, *J* = 2.3 Hz, H-6/8), 6.64 (1H, s, H-3), 6.45 (1H, d, *J* = 2.3 Hz, H-6/8), 5.25 (2H, s, $\underline{CH_2}OMe$),4.07 (2H, t, *J* = 6.4 Hz, $CH_2\underline{CH_2}OAr$), 3.53 (3H, s, CH_3), 3.30 (2H, t, *J* = 6.9 Hz, CH_2N_3), 1.99-1.91 (2H, m, CH_2), 171-160 (4H, m, CH_2), 153-146 (2H, m, CH_2). δ_C (100 MHz, $CDCl_3$): 177.48 (C=O), 161.45 (C), 160.64 (C), 160.42 (C), 159.57 (C), 131.57 (C), 131.14 (CH), 128.90 (CH), 125.97 (CH), 110.11 (C), 109.00 (CH), 97.86 (CH), 95.50 (CH), 94.32 (CH_2), 69.15 (CH_2), 56.46 (CH_3), 51.40 (CH_2), 28.76 (CH_2), 26.44 (CH_2), 25.53 (CH_2). HRMS [ESI]: 446.1666 *m/z*. $C_{23}H_{25}N_3NaO_5$ requires $[M+Na]^+$ 446.1686 *m/z*.

2-(6'-Azidohex-1'-oxy)-6-hydroxy-4-(methoxymethoxy) acetophenone 246

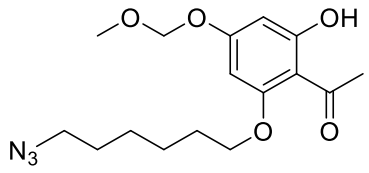

The disubstituted chrysin **245** (44.7 mg, 1.1 mmol) was taken up in a mixture of 18 M aqueous potassium carbonate solution (2.0 mL) and pyridine (2.0 mL) and diethylene glycol was added to the suspension (2.0 mL). The mixture was heated at 100 ºC for 4 h then allowed to cool to room temperature. The reaction was quenched with 1 M aqueous HCl solution (30 mL) then extracted into dichloromethane (2 × 20 mL). The combined organic layers were washed with brine (20 mL) then dried over magnesium sulfate, filtered and concentrated under reduced pressure. The crude product was purified by column chromatography (Isolera: 0%-20% ethyl acetate in hexane) then the fractions containing the product washed with saturated aqueous solution of sodium bicarbonate (3 × 20 mL) then with brine (20 mL), dried over magnesium sulfate, filtered and concentrated under reduced pressure to yield the acetophenone **246** as a yellow oil (16.5 mg, 46%). ν_{max} (ATR): 2938 (O-H), 2093 (CH_2N_3), 1582 (C=O) 1148 (C-O). δ_H (400 MHz, $CDCl_3$): 13.85 (1H, s, OH), 6.20 (1H, d, *J* = 2.3 Hz, H-3/5), 6.01 (1H, d, *J* = 2.3 Hz, H-3/5), 5.18 (2H, m CH_2OMe), 4.01 (2H, t, *J* = 6.4 Hz, CH_2CH_2OAr), 3.47 (3H, s, CH_3), 3.30 (2H, t, *J* = 6.9 Hz, CH_2N_3), 2.63 (3H, s, CH_3), 1.88 (2H, m, CH_2), 1.64 (2H, m, CH_2), 1.56-1.40 (4H, m, CH_2). δ_C (100 MHz, $CDCl_3$): 206.19 (C=O), 167.08 (C), 163.55 (C), 162.39 (C), 109.61 (C), 96.18 (CH), 93.96 (CH_2), 91.78 (CH), 68.70 (CH_2), 56.31 (CH_3), 51.31 (CH_2), 33.22 (CH_3), 28.92 (CH_2), 28.75 (CH_2), 26.46 (CH_2), 25.89 (CH_2). HRMS [ESI]: 360.1514 *m/z*. $C_{16}H_{23}N_3NaO_5$ requires $[M+Na]^+$ 360.1530 *m/z*.

7-(6''-Azidohex-1''-oxy)-5-isopropoxyflavone 247

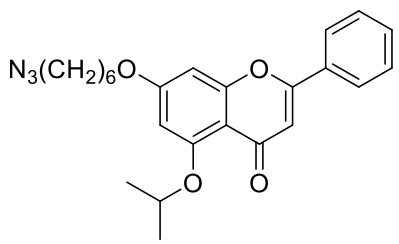

Azidohexyl chrysin **236** (0.193 g, 0.53 mmol), 2-bromopropane (0.10 mL, 1.1 mmol) and potassium carbonate (0.149 g, 1.1 mmol), were dissolved in anhydrous dimethyl formamide (2.5 mL) then heated at 165 ºC for 16 hours. The reaction mixture was cooled to room temperature then quenched with aqueous LiCl solution (5%, 20 mL), and extracted into dichloromethane (2 × 15 mL). The combined organic layers were washed with LiCl solution (5%, 5 × 20 mL) and brine (20 mL), dried over magnesium sulfate, filtered and concentrated under reduced pressure. The crude product was purified by column chromatograpy (Isolera 0-40% ethyl acetate in hexane) to yeld the product **247** as a yellow powder (0.157 g, 70%). Mp: 92-94 ºC. ν_{max} (ATR): 2091 (N_3), 1643 (C=O), 1600 (C=C) cm^{-1}. δ_H (400 MHz, $CDCl_3$): 7.91-7.83 (2H, m, H-Ar), 7.54-7.46 (3H, m, H-Ar), 6.60 (1H, s, H-3), 6.55 (1H, d, *J* = 2.3 Hz, H-6/8), 6.39 (1H, d, *J* = 2.3 Hz, H-6/8), 4.60 (1H, sept., *J* = 6.1 Hz, ^{i}Pr), 4.05 (2H, t, *J* = 6.4 Hz, CH_2), 3.31 (2H, t, *J* = 6.8 Hz, CH_2), 1.89-1.81 (2H, m, CH_2), 1.66 (2H, t, *J* = 7.1 Hz, CH_2), 1.59-1.48 (4H, m, $2CH_2$), 1.46 (6H, d, *J* = 6.0 Hz, ^{i}Pr). δ_C (100 MHz, $CDCl_3$): 177.29 (C), 163.20(C), 160.36 (C), 159.95 (C), 159.40 (C), 131.77 (C), 131.03 (CH), 128.89 (CH), 125.94 (CH), 110.42 (C), 109.11 (CH), 99.91 (CH), 93.63 (CH), 72.50 (CH), 68.26 (CH_2), 51.37 (CH_2), 28.92 (CH_2), 28.79 (CH_2), 26.49 (CH_2), 25.65 (CH_2), 21.87 (CH_3). HRMS [ESI]: 444.1869 *m/z*. $C_{24}H_{27}N_3NaO_4$ requires $[M+Na]^+$ 444.1894 *m/z*.

4-(6''-Azidohex-1''-oxy)-2-isopropoxy-5-hydroxyacetophenone 248

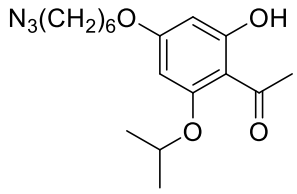

The disubstituted chrysin derivative **247** (0.428 g, 1.0 mmol) was then taken up in a mixture of 18 M aqueous potassium carbonate solution (2.0 mL) and pyridine (2.0 mL) and diethylene glycol was added to the suspension (2.0 mL). The mixture was heated at 100 ºC for 3.5 h then allowed to cool to room temperature. The reaction was quenched with 1 M aqueous HCl solution (20 mL) then extracted into dichloromethane (3 × 50 mL). The combined organic layers were washed with dilute sodium hydroxide solution (100 mL), brine (100 mL) then dried over magnesium sulfate, filtered and concentrated under reduced

pressure. The crude product was purified by column chromatograpy (Isolera: 0-15% ethyl acetate in hexane) to yield the acetophenone **248** as a yellow oil (0.213 g, 62%). ν_{max} (ATR): 2095 (N_3), 1616 (C=O), 1587 (C=C) cm^{-1}. δ_H (400 MHz, $CDCl_3$): 14.01 (1H, s, OH), 6.00 (1H, d, *J* = 2.3 Hz, H-3/5), 5.89 (1H, d, *J* = 2.3 Hz, H-3/5), 4.62 (1H, sept., *J* = 6.1 Hz, ^iPr), 3.97 (2H, t, *J* = 6.5 Hz, CH_2), 3.29 (2H, t, *J* = 6.8 Hz, CH_2), 2.62 (3H, s, CH_3), 1.83-1.75 (2H, m, CH_2), 1.68-1.60 (2H, m, CH_2), 1.52-1.43 (4H, m, CH_2), 1.41 (6H, d, *J* = 6.0 Hz, ^iPr). δ_C (100 MHz, $CDCl_3$): 203.26 (C=O), 167.61 (C), 165.50 (C), 161.17 (C), 106.62 (C), 93.51 (CH), 92.27 (CH), 70.92 (CH), 67.99 (CH_2), 51.35 (CH_2), 33.34 (CH_3), 28.87 (CH_2), 28.78 (CH_2), 26.47 (CH_2), 25.61 (CH_2), 22.03 (CH_3). HRMS [ESI]: 358.1727 *m/z*. $C_{17}H_{25}N_3NaO_4$ requires $[M+Na]^+$ 358.1737 *m/z*.

5,5'',7'',4'''-Tetraisopropoxy-3',5'-difluoro-5-(6''-azidohex-1''-oxy)-4',6''-bisflavonyl ether 255

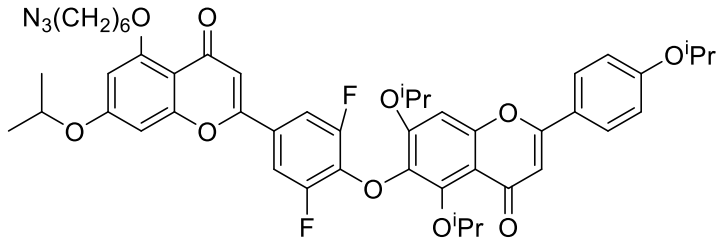

Fluoro flavone **259** (36.2 mg, 0.076 mmol) and isopropyl protected flavone **206** (31.4 mg, 0.076 mmol) were both dissolved in anhydrous dimethylsulfoxide (0.4 mL) along with anhydrous potassium carbonate (12.3 mg, 0.089 mmol) and heated at 100 ºC for 16 hours in a sealed vial. The reaction was cooled to room temperature, quenched with 1 M hydrochloric acid (15 mL), extracted into a mixture of chloroform and isopropanol (4:1, 2 × 10 mL), the combined organic layers were then washed with brine (15 mL), dried over magnesium sulfate and concentrated under reduced pressure. The crude biflavone **255** was purified using column chromatography (Isolera 20-80% ethyl acetate in hexane) to yield the desired product as a yellow oil (40.3 mg, 61%). δ_H (400 MHz, $CDCl_3$): 7.80 (2H, d, *J* = 9.0 Hz, H3', 5'), 7.38 (2H, d, *J* = 8.9 Hz, H3''', 5'''), 6.97 (2H, d, *J* = 8.9 Hz, H-2''', 6'''), 6.80 (1H, s, H-8), 6.54 (1H, s, H-3/3''), 6.50 (1H, d, *J* = 2.1 Hz, H-6/8), 6.49 (1H, s, H-3/3'''), 6.32 (1H, d, *J* = 2.1 Hz, H-6/8), 4.74-4.57 (4H, m, ^iPr), 4.04 (2H, t, *J* = 6.5 Hz, CH_2), 3.28 (2H, t, *J* = 6.9 Hz, CH_2), 1.98-1.89 (2H, m, CH_2), 1.70-1.56 (4H, m, CH_2), 1.49-1.44 (2H, m, CH_2), 1.40

(6H, d, *J* = 6.1 Hz, ^{i}Pr), 1.38 (6H, d, *J* = 6.1 Hz, ^{i}Pr), 1.34 (6H, d, *J* = 6.1 Hz, ^{i}Pr), 1.33 (6H, d, *J* = 6.1 Hz, ^{i}Pr). δ_C (100 MHz, $CDCl_3$): 177.06 (C), 176.94 (C), 162.53 (C), 161.20 (C), 160.63 (C), 160.45 (C), 159.68 (C), 157.93 (C), 155.50 (C), 154.38 (C), 154.13 (*J* = 250.4, 6.1 Hz, C), 148.88 (C), 138.23 (C), 127.69 (CH), 125.72 (C), 123.33 (C), 115.87 (CH), 112.74 (C), 109.86 (*J* = 17.4 Hz, CH), 109.09 (CH), 109.08 (C), 106.88 (CH), 98.37 (CH), 97.32 (CH), 93.83 (CH), 78.48 (CH), 71.88 (CH), 70.71 (CH), 70.16 (CH), 69.10 (CH_2), 51.41 (CH_2), 28.76 (CH_2), 26.43 (CH_2), 25.53 (CH_2), 21.94 (CH_3), 21.92 (CH_3), 21.66 (CH_3). HRMS [ESI]: 890.3397 *m/z*. $C_{48}H_{51}F_2N_3NaO_{10}$ requires $[M+Na]^+$ 890.3435 *m/z*.

5,5'',7'',4'''-Tetraisopropoxy-3',5'-difluoro-7-(6''-azidohex-1''-oxy)-4',6''-bisflavonyl ether 256

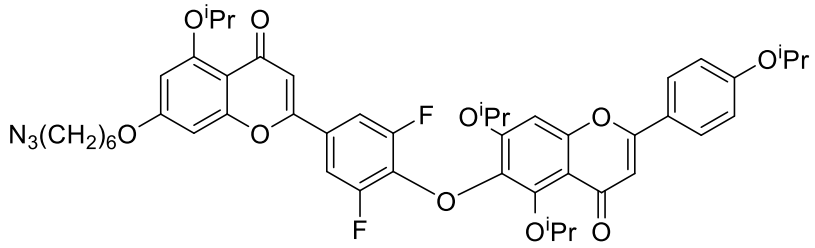

Fluoro flavone **262** (37.5 mg, 0.079 mmol) and isopropyl protected flavone **206** (32.5 mg, 0.079 mmol) were both dissolved in anhydrous dimethylsulfoxide (0.35 mL) along with anhydrous potassium carbonate (12.0 mg, 0.87 mmol) and heated at 100 ºC for 16 hours in a sealed vial. The reaction was cooled to room temperature, quenched with 1 M hydrochloric acid (10mL), extracted into a mixture of chloroform and isopropanol (4:1, 2 × 10 mL). The combined organics were then washed with brine (15 mL), dried over magnesium sulfate and concentrated under reduced pressure. The crude biflavone **256** was purified using column chromatography (Isolera 0-100% ethyl acetate in hexane) to yield the desired product as a pale yellow oil (24.4 mg, 36%). ν_{max} (ATR): 2361 (N_3), 1670 (C=O), 1605 (C=C) cm^{-1}. δ_H (400 MHz, $CDCl_3$): 7.80 (2H, d, *J* = 8.9 Hz, H-3''', 5'''), 7.38 (2H, d, *J* = 8.9 Hz, H-2', 6'), 6.98 (2H, d, *J* = 8.9 Hz, H-2''', 6'''), 6.80 (1H, s, H-3/3''/8''), 6.54 (1H, s, H-3/3''/8''), 6.52 (1H,d, *J* = 2.2 Hz, H-6/8), 6.47 (1H, s, H-3/3''/8''), 6.38 (1H,d, *J* = 2.2 Hz, H-6/8), 4.70-4.58 (4H, m, 4CH), 4.05 (2H, t, *J* = 6.4 Hz, CH_2), 3.30 (2H, t, *J* = 6.8 Hz, CH_2), 1.90-1.79 (2H, m, CH_2), 1.69-1.60 (2H, m, CH_2), 1.57-1.46 (4H, m, $2CH_2$), 1.45 (6H, d, *J* = 6.0 Hz, ^{i}Pr), 1.38 (6H, d, *J* = 6.1 Hz, ^{i}Pr), 1.34 (6H, d, *J* = 6.1 Hz, ^{i}Pr), 1.33

(6H, d, J = 6.2 Hz, ^{i}Pr). δ_C (100 MHz, $CDCl_3$): 177.05 (C), 176.85 (C), 163.38 (C), 161.18 (C), 160.63 (C), 159.71 (C), 159.41 (C), 157.83 (C), 155.49 (C), 154.38 (C), 154.13 (J_{C-F} = 250.0, 4.7 Hz, C), 148.89 (C), 138.23 (C), 127.69 (CH), 125.74 (C), 123.35 (C), 115.88 (CH), 112.76 (C), 110.22 (C), 109.87 (J_{C-F} = 18.9, 7.2 Hz, CH), 109.12 (CH), 106.90 (CH), 99.93 (CH), 97.33 (CH), 93.47 (CH), 78.47 (CH), 72.46 (CH), 71.88 (CH), 70.17 (CH), 68.33 (CH_2), 51.36 (CH_2), 28.89 (CH_2), 28.79 (CH_2), 26.48 (CH_2), 25.63 (CH_2), 21.94 ($2CH_3$), 21.84 (CH_3), 21.65 (CH_3). HRMS [ESI]: 890.3394 m/z. $C_{48}H_{51}F_2N_3NaO_{10}$ requires $[M+Na]^+$ 890.3435 m/z.

5-(6''-Azidohex-1''-oxy)-3',4',5'-fluoro-7-isopropoxyflavone 259

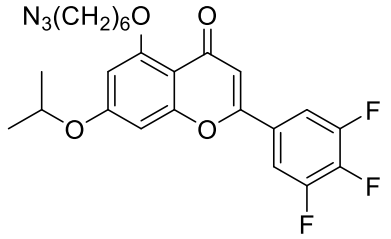

Acetophenone **251** (0.154 g, 0.50 mmol) and 3,4,5-trifluorobenzaldehyde (0.05 mL, 0.43 mmol) were dissolved in tertiary butanol (2.5 mL) along with potassium tertbutoxide (0.132 g, 0.95 mmol). The mixture was stirred at room temperature for 16 hours. The mixture was then quenched with 1 M hydrochloric acid solution (50 mL), extracted into dichloromethane (3 × 20 mL) the combined organic layers washed with 1 M hydrochloric acid solution (50 mL) then brine (50 mL); dried over magnesium sulfate, filtered and concentrated under reduced pressure to yield the crude chalcone **258**. The chalcone **258** was then taken up in anhydrous dimethylsulfoxide (2.5 mL), iodine 19.7 mg, 0.078 mmol) was added and the mixture heated at 110 ºC for 16 hours. The mixture was allowed to cool and then poured into cold water (200 mL) extracted with dichloromethane (2 × 20 mL). The combined dichloromethane layers were washed with concentrated sodium hydrogen carbonate solution (2 × 100 mL) then brine, dried over magnesium sulfate and concentrated under reduced pressure. The crude flavone was then purified by column chromatography (Isolera 23% ethyl acetate in hexane) to yield the product **259** as a brown gum (41.9 mg, 19%). ν_{max} (ATR): 2922 (N_3), 1643 (C=O) cm^{-1}. δ_H (400 MHz, $CDCl_3$): 7.50 (2H, dd, J = 8.2, 6.5 Hz, H-2',6'), 6.51 (1H, s, H-3), 6.50 (1H, d, J = 2.2 Hz H-6/8), 6.34 (1H, d, J = 2.1 Hz, H-6/8), 4.66 (1H, sept., J = 6.1 Hz, CH), 4.05 (2H,

t, J = 6.4 Hz, CH_2), 3.29 (2H, t, J = 7.0 Hz, CH_2), 1.98-1.88 (2H, m, CH_2), 1.69-1.57 (4H, m, $2CH_2$), 1.51-1.45 (2H, m, CH_2), 1.42 (1H, d, J = 6.0 Hz, CH_3). δ_C (100 MHz, $CDCl_3$): 176.68 (C), 162.74 (C), 160.62 (C), 159.62 (C), 157.03 (C), 151.52 (C, J_{C-F} = 241.2 Hz), 141.33 (C, J_{C-F} = 257.1 Hz), 127.90 (C, J_{C-F} = 4.7 Hz), 110.42 (CH, J_{C-F} = 16.8, 6.7 Hz), 109.80 (CH), 108.98 (C), 98.43 (CH), 93.76 (CH), 70.80 (CH), 69.13 (CH_2), 51.41 (CH_2), 28.76 (CH_2), 28.75 (CH_2), 26.42 (CH_2), 25.52 (CH_2), 22.08 (CH_3), 21.90 (CH_3). HRMS [ESI]: 498.1594 m/z. $C_{24}H_{24}F_3N_3NaO_4$ requires $[M+Na]^+$ 498.1611 m/z.

5-Isopropoxy-7-(6''-Azidohex-1''-oxy)-3'.4',5'-trifluoroflavone 262

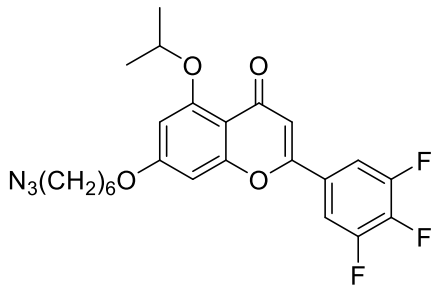

Acetophenone **248** (0.187 g, 5.6 mmol) and 3,4,5-trifluorobenzaldehyde (0.06 mL, 0.53 mmol) were dissolved in tertiary butanol (3.0 mL) along with potassium tertbutoxide (0.132 g, 1.2 mmol). The mixture was stirred at room temperature for 16 hours. The mixture was then quenched with 1 M hydrochloric acid solution (50 mL), extracted into dichloromethane (3 × 20 mL) the combined organic layers washed with 1 M hydrochloric acid solution (50 mL) then brine (50 mL); dried over magnesium sulfate, filtered and concentrated under reduced pressure. The crude product was purified by column chromatograpy (Isolera: 10-20% ethyl acetate in hexane) to yield the chalchone intermediate **261** (0.098 g, 37%). The chalcone **261** (98.3 mg, 0.21 mmol) was then taken up in anhydrous dimethylsulfoxide (2 mL), iodine (96.1 mg, 0.01 mmol) added and the mixture heated at 110 °C for 16 hours. It was allowed to cool to room temperature and then poured into cold water (200 mL). The product **262** was collected by filtration as a pale yellow oil (37.8 mg, 39%). ν_{max} (ATR): 2095 (N_3), 1647 (C=O), 1602 (C=C) cm^{-1}. δ_H (400 MHz, $CDCl_3$): 7.53-7.44 (2H, m, H-2',6'), 6.50 (1H, d, J = 2.3 Hz, H-6/8), 6.49 (1H, s, H-3), 6.38 (1H, d, J = 2.2 Hz, H-6/8), 4.59 (1H, sept., J = 6.1 Hz, ^iPr), 4.04 (2H, t, J = 6.4 Hz, CH_2), 3.30 (2H, t, J = 6.8 Hz, CH_2), 1.87-1.80 (2H, m, CH_2), 1.69-1.60 (2H, m, CH_2), 1.56-1.48 (4H, m, CH_2), 1.45

(6H, d, J = 6.0 Hz, ^{i}Pr). δ_C (100 MHz, $CDCl_3$): 176.61 (C), 163.59 (C), 159.64 (C), 159.47 (C), 156.93 (C, J_{C-F} = 1.8 Hz), 151.33 (C, J_{C-F} = 251.7, 10.2, 3.7 Hz), 141.25 (C, J_{C-F} = 257.5, 15.2 Hz),127.90 (C, J_{C-F} = 4.6 Hz), 110.39 (CH, J_{C-F} = 17.6, 5.8 Hz), 110.05 (C), 109.82 (CH), 99.78 (CH), 93.31 (CH), 72.40 (CH), 68.38 (CH_2), 51.35 (CH_2), 28.88 (CH_2), 28.78 (CH_2), 26.48 (CH_2), 25.62 (CH_2), 21.81 (CH_3). HRMS [ESI+]: 498.1600 m/z. $C_{24}H_{24}F_3N_3NaO_4$ requires $[M+Na]^+$ 498.1611 m/z.

3'5'-Dimethoxy-4-carboxyl-4'-hydroxy-stilbene 286

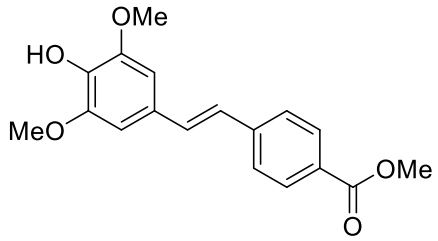

Phosphonium chloride **285** (1.55 g, 3.5 mmol) and syringaldehyde **284** (0.634 g, 3.5 mmol) were dissolved in a mixture of anhydrous THF (10 mL) and dichloromethane (10 mL). Anhydrous potassium carbonate (0.065 g, 7.7 mmol) was added and the mixture stirred at 40 ºC for 7 days. It was then quenched with 1M hydrochloric acid (100 mL), extracted with dichloromethane (2 × 50 mL), the combined organic layers washed with brine (100 mL) and dried over magnesium sulfate then concentrated under reduced pressure to give a pale yellow needles. A small portion was purified for characterisation purposes, the rest was taken on as crude. Mp: 114-120 ºC. ν_{max} (ATR): 1709 (C=O), 1605 (C=C) cm^{-1}. δ_H (400 MHz, $CDCl_3$): 7.95 (2H, d, J = 8.0 Hz, H-3,5), 7.47 (2H, d, J = 8.0 Hz, d, H-2,6), 7.07 (1H, d, J = 16.0 Hz, H-C=C), 6.91 (1H, d, J = 16.0 Hz, H-C=C), 6.71 (2H, s, H-2',6'), 5.56 (1H, s, OH), 3.89 (6H, s, CH_3), 3.85 (3H, s, CH_3). δ_C (100 MHz, $CDCl_3$): 166.91 (C), 147.27 (C), 141.98 (C), 135.40 (C), 131.40 (CH), 130.05 (CH), 128.62 (C), 128.39 (C), 126.05 (CH), 125.69 (CH), 103.70 (CH), 56.35 (CH_3), 52.06 (CH_3).

3'5'-Dimethoxy-4'-hydroxy-4-hydroxymethyl stilbene 287

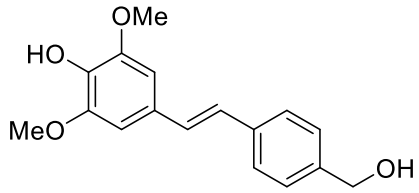

The crude stilbene derivative **286** was dissolved in anhydrous THF (10 mL) then added dropwise to a stirring solution of lithium aluminium hydride (0.410 g, 11 mmol) in anhydrous THF (17 mL) at 0 ºC. The solution was allowed to warm to room temperature overnight. It was then poured into a beaker containing 1M hydrochloric acid solution (100 mL), dichloromethane was added (100 mL) and the suspension was left to stir for 1 hour. The resulting layers were then separated and the organic layer washed with 1M hydrochloric acid (2 × 100 mL) then brine (100 mL). The solution was dried over magnesium sulfate then concentrated under reduced pressure. The crude product was purified by column chromatography (Isolera 70-100% ethyl acetate in hexane) to yield the product as a colourless oil (0.623 g, 63%).ν_{max} (ATR): 2928 (C=O), 1558 (C=C) cm^{-1}. δ_H (400 MHz, $CDCl_3$): 7.49 (2H, d, *J* = 7.6 Hz, H-3,5), 7.35 (2H, d, *J* = 7.8 Hz, H-2,6), 7.03 (1H, d, *J* = 16.4 Hz, HC=C), 6.96 (1H, *J* = 16.4 Hz, HC=C), 6.76 (2H, s, H-2',6'), 5.58 (1H, s, OH), 4.70 (2H, s, CH_2), 3.95 (6H, s, $2CH_3$). δ_C (100 MHz, $CDCl_3$): 147.24 (C), 139.96 (C), 136 (C), 134.90 (C), 128.93 (CH), 127.43 (CH), 16.46 (CH), 126.40 (CH), 103.40 (CH), 65.19 (CH_2), 56.34 (CH_3). HRMS(EI): 309.1083 *m/z*. $C_{17}H_{18}NaO_4$ requires $[M+Na]^+$ 309.1097 *m/z*.

4-Hydroxymethyl-3',5'-dimethoxy-4'(2''-nitro-4''carboxyl benzoxy)-stilbene 289

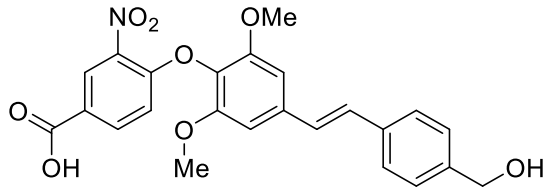

Stilbene **297** (0.200 gm 0.70 mmol), para fluoro benzoic acid **172** (0.128 g, 0.71 mmol) and potassium carbonate (0.218 g, 1.6 mmol) were taken up in water (3.5 mL) and heated to 100 ºC for 24 hours. The reaction was then allowed to

cool to room temperature and extracted into ethyl acetate (20 mL), then dried over magnesium sulfate and concentrated under reduced pressure. The crude material was purified by column chromatography (Isolera 30-100% ethyl acetate in hexane) to yield the pure stilbene ether **289** as a yellow foam (0.101 g, 31%). ν_{max} (ATR): 2936 (C=O), 1539 (NO_2), 1696 (C=C), 1128 (C=C) cm^{-1}. δ_H (400 MHz, Acetone-D_6): 8.57 (1H, d, *J* = 2.0 Hz, H-3''), 8.17 (1H, dd, *J* = 8.8, 2.0 Hz, H-5''), 7.59 (2H, d, *J* = 8.4 Hz, H-3,5), 7.40 (2H, d, *J* = 8.0 Hz, H-2,6), 7.38 (1H, *J* = 16.4 Hz, H-C=C), 7.29 (1H, *J* = 16.4 Hz, H-C=C), 7.13 (2H, s, H-2,6), 6.97 (1H, d, *J* = 8.8 Hz, H-6''), 4.67 (2H, s, CH_2), 3.89 (6H, s, 2 CH_3). δ_C (100 MHz, Acetone-D_6): 164.67 (C), 154.94 (C), 142.39 (C), 136.83 (C), 135.88 (C), 134.99 (CH), 129.45 (CH), 127.65 (CH), 126.92 (CH), 126.78 (CH), 126.41 (CH), 116.31 (CH), 103.71 (CH), 63.52 (CH_2), 55.77 (CH_2). HRMS(EI): 474.1138 *m/z*. $C_{24}H_{21}NNaO_8$ requires $[M+Na]^+$ 474.1159 *m/z*.

5,7-Diisopropoxy-3'-amino-4'-(3,5-dimethoxy-4'-hydroxymethyl-stilbene)-flavone 295

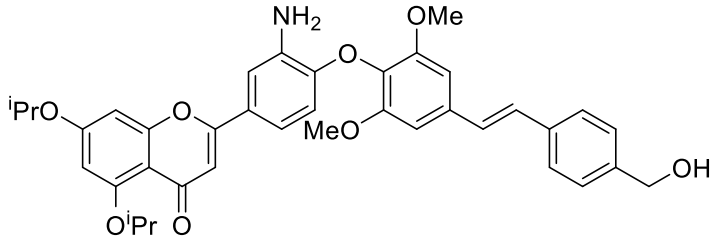

Chloro-nitro-flavone **197** (58 mg, 0.14 mmol) and stilbene derivative **287** (39 mg, 0.14 mmol) were dissolved in anhydrous dimethylformamide (0.7 mL) along with anhydrous potassium carbonate (30 mg, 0.22 mmol). The suspension was heated at 40 ºC for 16 hours then cooled to room temperature. The reaction was then quenched with 1M hydrochloric acid (10 mL), and the precipitate filtered and dried. The filtrate was then taken up in ethanol (1.0 mL) and tin chloride (66 mg, 0.29 mmol) added. The reaction was heated at 60 ºC for 3 hours then stirred at room temperature overnight. The reaction was quenched with saturated sodium bicarbonate solution (10 mL) and extracted into a mixture of chloroform and isopropanol (4:1, 2 × 10 mL), the combined organic layers were washed with brine (20 mL), then dried over magnesium sulfate and concentrated under reduced pressure. The crude product was purified by column chromatography (Isolera 0-10% MeOH in dichloromethane) to yield the product

295 as a dark red oil (16.9 mg, 23%). δ_H (400 MHz, $CDCl_3$): 7.52 (2H, d, *J* = 8.2 Hz, H-3'''',5''''), 7.38 (2H, d, *J* = 8.2 Hz, H-2'''',6''''), 7.28 (1H, d, *J* = 2.2 Hz, H-2'), 7.09 (1H, dd, *J* = 8.2, 2.3 Hz, H-6'), 7.08 (2H, s, HC=CH), 6.82 (2H, s, H-3''', 5'''), 6.52 (1H, d, *J* = 8.5 Hz, H-5), 6.59 (1H, d, *J* = 2.2 Hz, H-6/8), 6.56 (1H, s, H-3), 6.33 (1H, d, *J* = 2.2 Hz, H-6/8), 4.72 (2H, s, CH_2), 4.63 (1H, sept., *J* = 6.1 Hz, CH), 4.57 (1H, sept., *J* = 6.1 Hz, CH), 3.85 (6H, s, 2 CH_3), 1.44 (6H, d, *J* = 6.1 Hz, ^{i}Pr), 1.39 (6H, d, *J* = 6.1 Hz, ^{i}Pr). δ_C (100 MHz, $CDCl_3$): 177.53 (C), 161.96 (C), 160.83 (C), 159.91 (C), 159.38 (C), 153.29 (C), 148.65 (C), 140.66 (C), 136.60 (C), 136.36 (C), 135.17 (C), 131.81 (C), 128.73 (CH), 128.34 (CH), 127.44 (CH), 126.71 (CH),125.62 (C), 116.59 (CH),113.32 (CH), 112.86 (CH), 110.08 (C), 107.86 (CH), 103.62 (CH), 94.49 (CH), 72.45 (CH), 70.50 (CH), 65.05 (CH_2), 56.27 (CH_3), 21.95 (CH_3), 21.89 (CH_3). Tentative assignment based on ^{13}C and ^{1}H NMR only.

Diethyl-4-methoxybenzylphosphonate 298

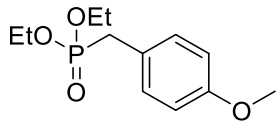

4-Methoxybenzyl chloride **297** (2.0 mL, 15 mmol) and triethylphosphite (2.8 mL, 16 mmol) were heated neat at 160 ºC for 16 hours. The mixture was then poured into water (100 mL) and extracted with ethyl acetate (2 × 40 mL). The combined ethyl acetate fractions were washed with brine (100 mL) then dried over magnesium sulfate and concentrated under reduced pressure. The product was purified by column chromatography (Isolera 0-80% ethyl acetate in hexane) to yield the product **298** as a colourless oil (2.11 g, 55%). ν_{max} (ATR): 2981 (P=O), 1512 (C-C) cm^{-1}. δ_H (400 MHz, $CDCl_3$): 7.21 (2H, dd, *J* = 8.8, 2.6 Hz, H-Ar), 6.84 (2H, dd, *J* = 8.7, 0.6 Hz, H-Ar), 4.07-3.92 (4H, m, 2O$\underline{CH_2}CH_3$), 3.79 (3H, s, CH_3), 3.08 (2H, d, *J* = 21.1 Hz, CH_2), 1.24 (6H, t, *J* = 7.1 Hz, 2O$CH_2\underline{CH_3}$). δ_C (100 MHz, $CDCl_3$): 158.38 (J_{C-P} = 3.5 Hz), 130.53 (J_{C-P} = 6.6 Hz) 123.19 (J_{C-P} = 9.1 Hz), 113.79 (J_{C-P} = 2.9 Hz), 61.85 (J_{C-P} = 6.8 Hz), 55.00, 32.52 (J_{C-P} = 139.0Hz), 16.17 (J_{C-P} = 5.9 Hz). Reported data agree with literature.[143]

3,5-Dimethoxy-4-(methoxymethoxy)benzaldehyde 299

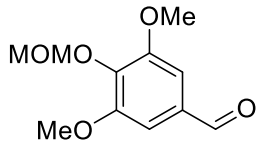

Syringaldehyde (2.07 g, 11 mmol) and potassium carbonate (4.74 g, 34 mmol) were dissolved in acetone (56 mL) and bromomethyl methyl ether (1.0 mL, 12 mmol) was then added dropwise and the reaction heated at 60 ºC for 20 hours. After cooling to room temperature the acetone was removed under reduced pressure and the residue taken up in dichloromethane (50 mL), washed with 1 M hydrochloric acid solution (3 × 20 ml) then water (20 mL) then brine (20 mL), dryed over magnesium sulfate and concentrated under reduced pressure. The crude product was purified by column chromatography (Isolera 0-50% ethyl acetate in hexane) to give the product **299** as white needles (1.400 g, 55%). Mp: 44-46 ºC. ν_{max} (ATR): 2939 (C-H), 1682 (C=O) cm^{-1}. δ_H (400 MHz, $CDCl_3$): 9.85 (1H, s, CHO), 7.12 (2H, s, H-2,6), 5.21 (2H, s, CH2), 3.91 (6H, s, $2CH_3$), 3.58 (3H, s, CH_3). δC (100 MHz, $CDCl_3$): 191.09 (CH), 15382 (C), 140.12 (C), 132.17 (C), 106.61 (CH), 98.17 (CH_2), 57.30 (CH_3), 56.23 (CH_3). Reported data agree with literature.[144]

3,5-Dimethoxy-4-hydroxy-4'methoxystilbene 301

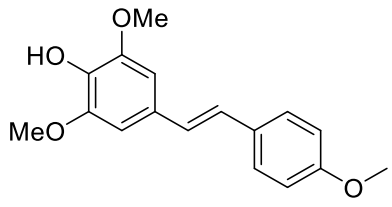

Phosphonate ester **298** (1.796 g, 7.0 mmol) was added dropwise to a stirring solution of sodium hydride (0.301 g, 7.5 mmol) in anhydrous THF (20 mL) at 0 ºC. The reaction was allowed to warm to room temperature over 30 minutes then syringaldehyde **299** (1.095 g, 4.8 mmol) was added as a solution in anhydrous THF (4 mL). The reaction was stirred for 16 hours then diluted with ethyl acetate (100 mL) and washed with water (3 × 50 mL) and brine (50 mL), dried over magnesium sulfate and concentrated under reduced pressure. The crude stilbene product was purified by column chromatography (Isolera 0-60% ethyl

acetate in hexane) to yield the product **300** (0.692 g, 43%). The protected stilbene **300** (0.241 g, 0.73 mmol) was dissolved in methanol (5 mL), a drop of concentrated sulphuric acid was added and the mixture heated at 50 ºC for 3 hours. The methanol was then removed under reduced pressure, the residue taken up in dichloromethane (20 mL) and washed with concentrated sodium hydrogen carbonate solution (20 mL) then brine (20 mL), dried over magnesium sulfate and concentrated under reduced pressure to yield the product **301** as a white solid (0.199 g, 95%). δ_H (400 MHz, $CDCl_3$): 7.43 (2H, d, *J* = 8.8 Hz, H-2',6'), 6.93 (1H, d, *J* = 16.1 Hz, H-C=C), 6.89 (2H, d, *J* = 9.0 Hz, H-3',5'), 6.88 (1H, d, *J* = 16.3 Hz, H-C=C), 6.73 (2H, s, H-2,6), 5.53 (1H, s, OH), 3.94 (6H, s, $2CH_3$), 3.83 (3H, s, CH_3). δ_C (100 MHz, $CDCl_3$): 159.10 (C), 147.20 (C), 134.47 (C), 130.23 (C), 129.47 (C), 127.47 (CH), 126.76 (CH), 126.41 (CH), 114.15 (CH), 103.06 (CH), 56.30 (CH_3), 55.34 (CH_3). The reported data agree with literature.[145]

5,7-Diisopropoxy-3'-nitro-4'-(3*,5*-dimethoxy-4-methoxy-stilbene)-flavone 302**

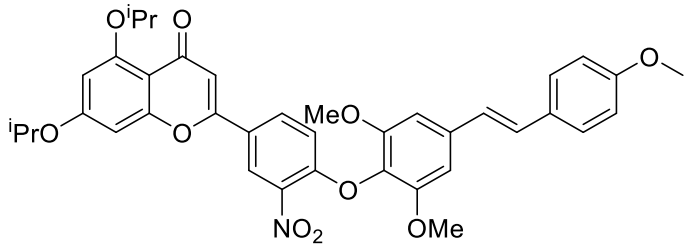

Chloro-nitro-flavone **197** (0.555 g, 1.3 mmol) and stilbene derivative **301** (0.378 g, 1.3 mmol) were dissolved in anhydrous dimethylformamide (8 mL) along with anhydrous potassium carbonate (0.225 g, 1.6 mmol). The suspension was heated at 100 ºC for 16 hours then cooled to room temperature. The reaction was then quenched with 1M hydrochloric acid (50 mL), extracted into dichloromethane (2 × 50 mL), the combined organic fractions were washed with brine then dried over magnesium sulfate and concentrated under reduced pressure. The crude product was purified by column chromatography (Isolera 20-45% ethyl acetate in hexane) to yield the product **302** as a brown foam (0.598 g, 68%). Melting point 96-100 ºC. ν_{max} (ATR): 1645 (C=O), 1604 (C=C), 1117 (C=C) cm^{-1}. δ_H (400 MHz, $CDCl_3$): 8.54 (1H, d, *J* = 2.3 Hz, H-2'), 7.80 (1H, dd, *J* = 9.0, 2.3 Hz, H-5'), 7.47 (2H, d, *J* = 9.0 Hz, H-2**,6**), 7.05 (1H, d, *J* = 15.7 Hz, H-C=C), 6.94 (1H, d, *J* = 15.7 Hz, H-C=C), 6.88 (1H, d, *J* = 15.7 Hz, H-4'),6.79 (2H,

s, H-2*,6*), 6.65 (2H, d, *J* = 8.7 Hz, H-3**,5**), 6.55 (1H, d, *J* = 2.2 Hz, H-6/8), 6.53 (1H, s, H-3), 6.36 (1H, d, *J* = 2.2 Hz, H-6/8), 4.67 (1H, sept., *J* = 6.0 Hz, ^{i}Pr), 4.59 (1H, sept., *J* = 6.1 Hz, ^{i}Pr), 3.84 (3H, s, CH_3), 3.84 (6H, s, $2CH_3$), 1.45 (6H, d, *J* = 6.1 Hz, ^{i}Pr), 1.42 (6H, d, *J* = 6.1 Hz, ^{i}Pr). δ_C (100 MHz, $CDCl_3$): 176.89 (C), 162.43 (C), 159.79 (C), 159.49 (C), 157.78 (C), 154.19 (C), 152.75 (C), 139.22 (C), 136.63 (C), 131.12 (CH), 130.04 (C), 129.56 (C), 129.21 (CH), 127.87 (CH), 125.90 (CH), 125.30 (C), 123.50 (CH), 117.15 (CH), 114.24 (CH), 109.86 (C), 108.95 (CH), 103.26 (CH), 100.65 (CH), 94.15 (CH), 72.34 (CH), 70.69 (CH), 56.32 (CH_3), 55.37 (CH_3), 21.96 (CH_3), 21.87 (CH_3). HRMS [ESI]: 690.2276 *m/z*. $C_{38}H_{37}NNaO_{10}$ requires $[M+Na]^+$ 690.2310 *m/z*.

5,7-Diisopropoxy-3'-amino-4'-(3*,5*-dimethoxy-4-methoxy-stilbene)-flavone 304**

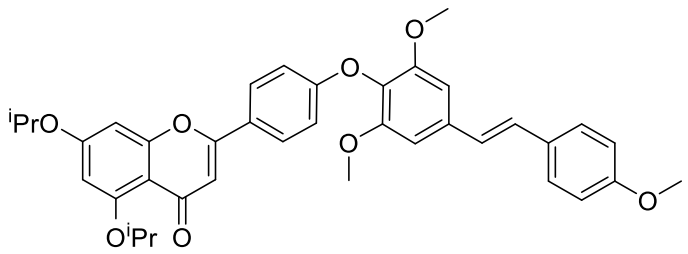

Nitro compound **302** (0.099 g, 0.15 mmol) and tin (II) chloride (0.168 g, 0.75 mmol) were taken up in ethanol (1 mL) and heated at 60 ºC for 4 hours. The solution was then cooled to room temperature and concentrated sodium hydrogen carbonate solution (10 mL) added. The resulting suspension was extracted into a mixture of isopropanol and chloroform (4:1, 3 × 10 mL), the combined organic fractions were washed with brine (20 mL) and dried over magnesium sulfate then concentrated under reduced pressure. The amino product **303** was separated from the nitro starting material **302** by column chromatography (Isolera 0-10% methanol in dichloromethane) then taken on to the next step. The amino compound **303** was then dissolved in a mixture of conc. aq. HCl (0.50 mL) and glacial acetic acid (1.0 mL) and cooled to 0 ºC. A solution of sodium nitrite (10.1 mg, 0.15 mmol) in water (0.1 mL) was added to it slowly and the solution left to stir for 20 min. Hypophosphinic acid (0.09 mL) was then added to the mixture and the reaction left to warm to room temperature overnight. It was then diluted with 1 M aqueous HCl solution (20 mL) and extracted with dichloromethane (2 × 20 mL). The combined organic

layers were washed with sodium bicarbonate solution (30 mL), brine (30 mL) then dried over magnesium sulphate and concentrated under reduced pressure. The crude product was purified by column chromatograpy (Isolera: 30-100% ethyl acetate in hexane) to yield the product **304** as a yellow oil (14.2 mg, 16%). ν_{max} (ATR): 1603 (C=C), 1503 (NO_2), 1128 (C=C) cm^{-1}. δ_H (400 MHz, $CDCl_3$): 7.77 (2H, d, *J* = 9.0 Hz, H-2',6'), 7.48 (2H, d, *J* = 8.7 Hz, H-2**,6**), 7.06 (1H, d, *J* = 16.2 Hz, H-C=C), 6.98 (2H, d, *J* = 8.9 Hz, H3',5'), 6.96 (1H, d, *J* = 16.2 Hz, H-C=C), 6.92 (2H, d, *J* = 8.8 Hz, H-3**,5**), 6.81 (2H, s, H-2*,6*), 6.50 (1H, d, *J* = 2.3 Hz, H-6/8), 6.50 (1H, s, H-3), 6.35 (1H, d, *J* = 2.3 Hz, H-6/8), 4.63 (1H, sept., *J* = 6.1 Hz, ^{i}Pr), 4.57 (1H, sept., *J* = 6.1 Hz, ^{i}Pr), 3.85 (3H, s, CH_3), 3.84 (6H, s, 2 CH_3), 1.45 (6H, d, *J* = 6.1 Hz, ^{i}Pr), 140 (6H, d, *J* = 6.1 Hz, ^{i}Pr). δ_C (100 MHz, $CDCl_3$): 177.36 (C), 162.01 (C), 160.97 (C), 160.41 (C), 159.90 (C), 159.55 (C), 159.43 (C), 153.25 (C), 135.77 (C), 129.76 (C), 128.81 (CH), 127.80 (CH), 127.57 (C), 127.49 (CH), 126.20 (CH), 125.06 (C), 115.29 (CH), 114.24 (CH), 107.83 (CH), 103.36 (CH), 100.76 (CH), 94.56 (CH), 72.51 (CH), 70.52 (CH), 56.26 (CH_3), 55.35 (CH_3), 21.94 (CH_3), 21.89 (CH_3). HRMS [ESI]: 645.2427 *m/z*. $C_{38}H_{38}NaO_8$ requires $[M+Na]^+$ 645.2459 *m/z*.

2-Hydroxy-4,6-diisopropoxy acetophenone 308

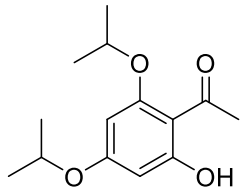

2',4',6'-Trihydroxyacetophenone monohydrate (7.42 g, 40 mmol) was taken up in anhydrous dimethyl formamide (150 mL), potassium carbonate (16.5 g, 12 mmol) and 2-bromopropane (7.5 ml, 80 mmol) were added and the mixture heated under reflux for 4 hours. It was then allowed to cool, quenched with 1 M aqueous HCl solution (200 mL) and extracted with ethyl acetate (2 × 200 mL). The combined organic layers were washed with LiCl solution (5%, 5 × 200 mL) and brine (200 mL) then dried over magnesium sulphate and concentrated under reduced pressure. The crude material was purified by flash column chromatography (Isolera: 0%-10% ethyl acetate in hexane) to yield the product **308** as a colourless oil (7.04 g, 70%). ν_{max} (ATR): 2978 (C-H), 1614 (C=O), 1578 (C=C) cm^{-1}. δ_H (400 MHz, $CDCl_3$): 14.00 (1H, s, OH), 6.00 (1H, d, *J* = 2.3 Hz, H-

Ar), 5.86 (1H, d, *J* = 2.3 Hz, H-Ar), 4.61 (1H, sept., *J* = 6.1 Hz, CH), 4.57 (1H, sept., *J* = 6.0 Hz, CH), 2.62 (3H, s, CH_3), 1.40 (6H, d, *J* = 6.0 Hz, $2CH_3$), 1.35 (6H, d, *J* = 6.1 Hz, $2CH_3$). δ_C (100 MHz, $CDCl_3$): 203.11 (C=O), 167.57 (C), 164.51 (C), 161.27 (C), 106.41 (C), 94.16 (CH), 93.05 (CH), 70.78 (CH), 70.25 (CH), 33.27 (CH_3), 22.05 (CH_3), 21.93 (CH_3). Reported data agree with literature.[146]

3',5'-Fluoro-4'-{2'',6''-dihydroxy-4''-[2'''-(4''''-aminophenyl)ethenyl]phenoxy} -flavone 312

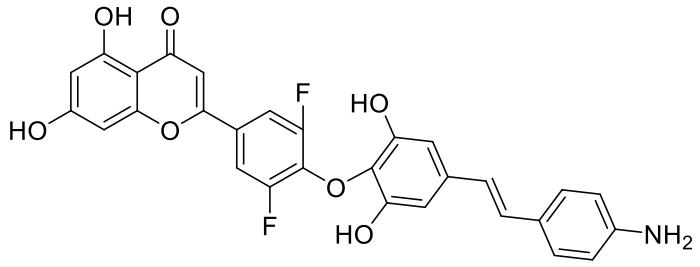

Isopropoxy compound **322** (0.139 mg, 0.22 mmol) was taken up in dry dichloromethane (2 mL) and cooled to 0 ºC. Boron tribromide solution in dichloromethane (1M, 2.2 mL) was then added dropwise, stirred for 1 hour at 0 ºC. The reaction was then quenched with water and filtered. The resulting green powder was practically pure and used as is for subsequent reactions. A small portion (10.1 mg) was further purified on the HPLC (30-50% acetonitrile in 0.01% TFA/water) to yield the pure compound as a beige powder (1.7 mg, 17%). δH (400 MHz, DMSO-D_6): 12.76 (1H, s, OH), 10.93 (1H, s, OH), 9.52 (2H, s, OH), 7.92 (2H, d, *J* = 9.4 Hz, H-2',6'), 7.25 (2H, d, *J* = 8.5 Hz, H-2''', 6'''), 7.06 (1H, s, H-3), 6.78 (1H, d, *J* = 16.4 Hz, H-C=C), 6.70 (1H, d, *J* = 16.2 Hz, H-C=C), 6.59 (1H, d, *J* = 2.0 Hz, H-6/8), 6.55 (2H, d, *J* = 8.4 Hz, H-3''', 5'''), 6.49 (2H, s, H-3'', 5''), 6.22 (1H, d, *J* = 2.0 Hz, H-6/8), 5.28 (2H, broad s, NH_2). δ_C (100 MHz, DMSO-D_6):182.24 (C), 164.95 (C), 161.86 (C), 161.58 (C), 157.90 (C), 153.47 (C), 154.68 (C, J_{C-F} = 249.1, 5.7 Hz), 138.71 (C), 137.99 (C), 133.71 (C), 133.28 (C), 130.2 (CH, J_{C-F} = 3.8 Hz), 127.58 (CH), 125.86 (CH), 123.02 (CH), 109.98 (CH, J_{C-F} = 8.44 Hz), 105.75 (CH), 104.95 (CH), 98.99 (CH), 93.83 (CH). HRMS [ESI+]: 532.1181 *m/z*. $C_{29}H_{20}F_2NO_7$ requires $[M+H]^+$ 532.1202 *m/z*.

3',5'-Fluoro-4'-{2'',6''-dihydroxy-4''-[2'''-(4''''-azidophenyl)ethenyl]phenoxy} -flavone 313

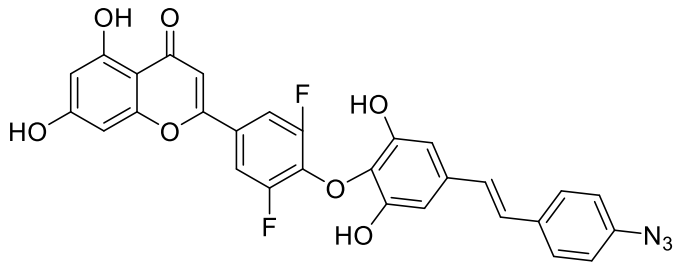

The amino starting compound **312** (17.7 mg, 0.03 mmol) was dissolved in dimethylsulfoxide (5 mL) and 5M hydrochloric acid (1 mL) sodium nitrite (6.8 mg, 0.10 mmol) was added. The reaction was stirred at room temperature for 30 minutes then sodium azide (19.4 mg, 0.30 mmol) was added and the reaction stirred for 16 hours. The reaction was quenched with water (100 mL) and the crude product extracted into a mixture of chloroform and isopropanol (4:1, 3 × 20 mL), the combined organics were then washed with brine (3 × 50 mL), dryed over magnesium sulfate and concentrated under reduced pressure. Product was purified by HPLC (55-75% acetonitrile in 0.1% THF/water) to yield the product **312** as a pale yellow powder (4.9 mg, 26%). ν_{max} (ATR): 2118 (N3), 1655 (C=O), 1038 (C=C) cm-1. δ_H (400 MHz, DMSO-D_6): 12.75 (1H, s, OH), 10.94 (1H, s, OH), 9.64 (2H, s, OH), 7.93 (2H, d, *J* = 8.8 Hz, H-2', 6'), 7.64 (2H, d, *J* = 7.5 Hz, H-3''', 5'''), 7.12 (1H, s, H-3), 7.05 (1H, d, *J* = 15.8 Hz, H-C=C), 6.96 (1H, d, *J* = 16.2 Hz, H-C=C), 6.59 (3H, s, H-6/8, 3'', 5''), 6.23 (1H, s, H-6/8). LRMS (ESI+): 558.20 *m/z*. $C_{29}H_{17}F_2N_3O_7$ requires $[M+H]^+$ 558.11 *m/z*. Compound tentatively characterised based on ^{1}H NMR, ^{13}C NMR and IR only.

Diethyl-4-nitrobenzylphosphonate 316

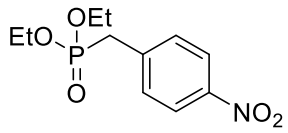

4-Nitrobenzyl bromide **315** and triethyl phosphite were stirred neat at 130 ºC for 16 hours. After cooling to room temperature the reaction was diluted with water (200 ml) then extracted into ethyl acetate (2 × 200 mL). The combined organic layers were washed with water (300 mL) then brine (300 mL) and dried over

magnesium sulfate, filtered and concentrated under reduced pressure. The crude material was purified by column chromatograpy (Isolera: 20%-70% ethyl acetate in hexane) to yield the product **316** as an yellow oil (2.454 g, 97%). ν_{max} (ATR): 2982 (P=O), 1518 (NO_2), 1344 (NO_2) cm^{-1}. δ_H (400 MHz, $CDCl_3$): 8.15 (2H, d, *J* = 8.6 Hz, H-3,5), 7.45 (2H, dd, *J* = 8.7, 2.3 Hz, H-2,6), 4.03 (4H, app.q. *J* = 7.4 Hz, $2CH_2$), 3.22 (2H, d, *J* = 2.4 Hz, CH_2), 1.24 (6H, t, *J* = 7.1 Hz, CH_3). Reported data agrees with literature.[147]

2,6-Dimethoxy-4-[2'-(4''-nitrophenyl)ethenyl]phenol 318

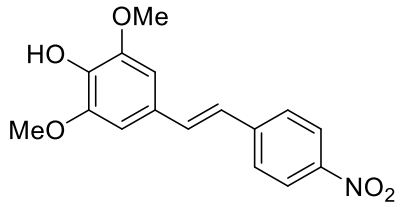

Sodium hydride (60% in mineral oil, 0.124 g, 2.9 mmol) and phosphonate **316** (0.666 g, 2.4 mmol) were taken up in anhydrous THF (10 mL) and cooled to 0 ºC. The protected syringaldehyde **299** (0.555 g, 2.4 mmol) was added dropwise and the reaction warmed to room temperature over 16 hours. The reaction was then quenched with 1 M hydrochloric acid solution (50 mL) and extracted into ethyl acetate (200 mL). The ethyl acetate layer was then washed with brine (100 mL), dried over magnesium sulfate and concentrated under reduced pressure. The residue was then taken up in methanol (12 mL) along with 8 drops of concentrated sulfuric acid. The reaction was heated at 50 ºC for 3 hours then the methanol was removed under reduced pressure, the residue taken up in dichloromethane (50 mL) and washed with concentrated sodium hydrogen carbonate solution (2 × 50 mL) then brine (50 mL) dried over magnesium sulfate and concentrated under reduced pressure to yield the pure compound **318** as a pale yellow oil (0.665 g, 90%). ν_{max} (ATR): 1587 (C=C), 1508 (N=O), 1329 (NO), 1107 (C-O-C) cm^{-1}. δ_H (400 MHz, $CDCl_3$): 8.21 (2H, d, *J* = 8.5 Hz, H-3'',5''), 7.61 (2H, d, *J* = 8.5 Hz, H-2'',6''), 7.19 (1H, d, *J* = 16.2 Hz, H-C=C), 7.00 (1H, d, *J* = 16.2 Hz, H-C=C), 6.80 (2H, s, H-3,5), 5.66 (1H, s, OH), 3.96 (6H, s, 2 CH_3). δ_C (100 MHz, $CDCl_3$): 147.32 (C), 146.52 (C), 144.05 (C), 135.94 (C), 133.52 (CH), 127.82 (C), 126.53 (CH), 124.36 (CH), 124.20 (CH), 103.97 (CH), 56.38 (CH_3).

HRMS [EI]: 301.0938 *m/z*. $C_{16}H_{15}NO_5$ requires 301.0950 *m/z*. Data agrees with patent.[148]

5,7-Diisopropoxy-3',4',5'-fluoro-flavone 319

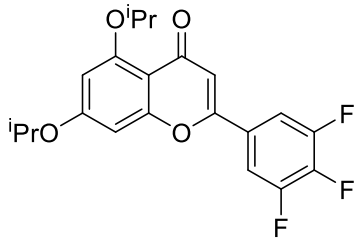

Diisopropoxy acetophenone **99** (0.520 g, 2.0 mmol) and 3,4,5-fluorobenzaldehyde (0.23 ml, 2.0 mmol) were dissolved in isopropanol (10 mL) along with potassium isopropoxide (0.458 g, 12 mmol). The mixture was then stirred at room temperature overnight. The reaction was quenched with 1 M aqueous HCl solution (50 mL), extracted into dichloromethane (2 × 20 mL). The organic fractions were washed with water (50 mL), then brine (50 mL), dried over magnesium sulfate, filtered and concentrated under reduced pressure. The resulting crude yellow crystals were dissolved in dry DMSO (10 mL) and iodine (7.0 mg, 0.027 mmol) added. Suspension heated at 100 ºC for 16 hours. The reaction was then cooled to room temperature and quenched with sodium bicarbonate solution (50 mL), extracted into dichloromethane (2 × 20 mL). The combined organic layers were then washed with sodium bicarbonate solution (30 mL) then brine (30 mL) and dried over magnesium sulfate; filtered and concentrated under reduced pressure. The crude product was purified by column chromatograpy (Isolera: 0%-10% methanol in dichloromethane) to yield the product **319** as a brown oil (0.467 g, 58%). ν_{max} (ATR): 1629 (C=O) 1528 (C=C) cm-1. δ_H (400 MHz, $CDCl_3$): 7.50 (2H, t, *J* = 7.1 Hz, H-2',6'), 6.50 (1H, d, *J* = 2.2 Hz, H-6/8), 6.49 (1H, s, H-3), 6.37 (1H, d, *J* = 2.2 Hz, H-6/8), 4.65 (1H, sept., *J* = 6.0 Hz, CH), 4.59 (1H, sept., *J* = 6.0 Hz, ^{i}Pr), 1.46 (6H, d, *J* = 6.1 Hz, ^{i}Pr), 1.41 (6H, d, *J* = 6.1 Hz, ^{i}Pr). HRMS [ESI]: 415.1115 *m/z*. $C_{21}H_{19}F_3NaO_4$ requires $(M+Na)^+$ 415.1128 *m/z*.

5,7-Diisopropoxy-3',5'-fluoro-4'-{2'',6''-dimethoxy-4''-[2'''-(4''''-nitrophenyl)ethenyl]phenoxy} -flavone 320

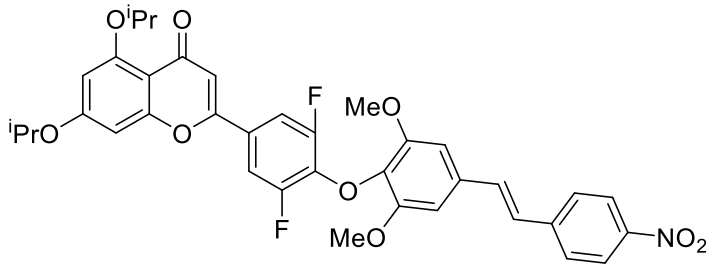

Fluoro flavone **319** (0.107 g, 0.27 mmol) and nitro stilbene **318** (0.129 g, 0.43 mmol) were both dissolved in anhydrous dimethylsulfoxide (2.0 mL) along with anhydrous potassium carbonate (0.111 g, 0.80 mmol) and heated at 110 ºC for 16 hours in a sealed vial. The reaction was cooled to room temperature, quenched with 1 M hydrochloric acid (10 mL), and extracted into dichloromethane (2 × 20 mL). The combined organics were then washed with water (20 mL) then brine (20 mL), dried over magnesium sulfate and concentrated under reduced pressure. The crude product was purified using column chromatography (Isolera 0-40% ethyl acetate in hexane) to yield the desired product **320** as a pale yellow oil (0.130 mg, 71%). δ_H (400 MHz, $CDCl_3$): 8.23 (2H, d, *J* = 8.2 Hz, H-2',6'), 7.64 (2H, d, *J* = 8.7 Hz, H-3'''',5''''), 7.40 (2H, d, *J* = 8.6 Hz, H-2'''',6''''), 7.21 (1H, d, *J* = 16.2 Hz, H-C=C), 7.08 (1H, d, *J* = 16.0 Hz, H-C=C), 6.81 (2H, s, H-3'',5''), 6.50 (1H, broad s., H-6/8), 6.48 (1H, s, H-3), 6.36 (1H, broad s., H-6/8), 4.64 (1H, sept., *J* = 6.0 Hz, CH), 4.58 (1H, sept., *J* = 5.8 Hz, ^{i}Pr), 3.87 (6H, s, CH_3), 1.45 (6H, d, *J* = 5.8 Hz, ^{i}Pr), 1.41 (6H, d, *J* = 5.8 Hz, ^{i}Pr). δ_C (100 MHz, $CDCl_3$): 176.87 (C), 162.44 (C), 159.71 (C), 159.49 (C), 157.77 (C), 154.37 (C, J_{C-F} = 249.9, 5.3 Hz), 152.00 (C), 146.77 (C), 143.58 (C), 137.25 (C, J_{C-F} = 13.1 Hz), 135.51 (C), 133.17 (C), 132.90 (CH), 126.85 (CH), 126.38 (CH), 126.02 (C, J_{C-F} = 8.9 Hz), 124.15 (CH), 109.84 (C), 109.77 (CH, J_{C-F} = 19.3 Hz), 109.04 (CH), 104.11 (CH), 100.60 (CH), 94.21 (CH), 72.38 (CH), 70.69 (CH), 56.43 (CH_3), 21.91 (CH_3), 21.84 (CH_3). Compound tentativelt characterised based on the ^{1}H NMR and ^{13}C NMR only.

5,7-Diisopropoxy-3',5'-fluoro-4'-{2'',6''-dimethoxy-4''-[2'''-(4''''-aminophenyl)ethenyl]phenoxy} -flavone 322

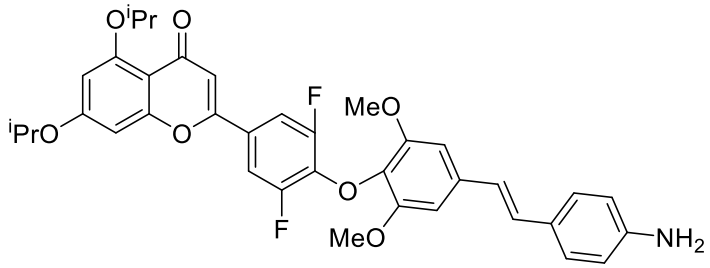

Nitro compound **320** (0.201 g, 0.58 mmol) and ammonium formate (0.159 g, 2.3 mmol) were dissolved in a mixture of acetone (2.1 mL) and water (0.75 mL), iron powder (0.161 g, 2.9 mmol) was added to the solution. The suspension was heated at 65 ºC for 24 h. The reaction was allowed to cool then filtered through celite with acetone. The filtrate was concentrated under reduced pressure and the precipitate taken up in water (10 mL). It was then extracted with dichloromethane (3 × 20 mL). The combined organic layers were washed with brine (20 mL) then dried over magnesium sulphate and concentrated under reduced pressure to yield the desired product **322** as a brown gum (0.176 g. 96%). ν_{max} (ATR): 2374 (NH_3), 1736 (C=O) cm-1. δ_H (400 MHz, $CDCl_3$):7.39 (2H, d, *J* = 9.1 Hz, H-2',6'), 7.33 (2H, d, *J* = 8.5 Hz, H-2''',6'''), 6.96 (1H, d, *J* = 16.1 Hz, H-C=C), 6.85 (1H, d, *J* = 16.1 Hz, H-C=C), 6.72 (2H, s, H-3'',5''), 6.68 (2H, d, *J* = 8.5 Hz, H-3''',5'''), 6.50 (1H, d, *J* = 2.2 Hz, H-6/8), 6.48 (1H,s, H-3), 6.36 (1H, d, *J* = 2.2 Hz, H-6/8), 4.65 (1H, sept., *J* = 6.1 Hz, CH), 4.58 (1H, sept., *J* = 6.1 Hz, CH), 3.85 (6H, s, 2 CH_3), 1.45 (1H, d, *J* = 6.0 Hz, ^{i}Pr), 1.41 (1H, d, *J* = 6.0 Hz, ^{i}Pr). δ_C (100 MHz, $CDCl_3$): 176.90 (C), 162.40 (C), 157.74 (C), 159.48 (C), 157.90 (C), 154.44 (C, J_{C-F} = 250.1, 5.5 Hz), 151.85 (C), 146.56 (C), 137.58 (C, J_{C-F} = 12.9 Hz), 135.12 (C), 134.15 (C), 129.00 (CH), 127.77 (CH), 127.44 (C), 125.73 (CH, J_{C-F} = 8.9),124.49 (CH), 115.18 (CH), 109.90 (C), 109.75 (C, J_{C-F} = 17.4, 7.9 Hz), 108.98 (CH), 103.12 (CH), 100.67 (CH), 94.27 (CH), 72.40 (CH), 70.69 (CH), 56.35 (CH_3), 21.93 (CH_3), 21.87 (CH_3). HRMS [ESI+]: 644.2432 *m/z*. $C_{37}H_{36}F_2NO_7$ requires $[M+H]^+$ 644.2454 *m/z*.

Methyl 3,5-dimethoxy-4-hydroxy-benzoate 324

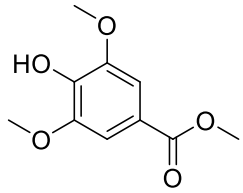

Syringic acid (2.00 g,10 mmol) was dissolved in methanol (50 mL) along with 2 drops of concentrated sulphuric acid then heated at 65 ºC for 16 hours. The methanol was then removed under reduced pressure and the resulting precipitate taken up in dichloromethane (50 mL) washed with concentrated sodium bicarbonate solution (50 mL) then brine (50 mL), dried over magnesium sulfate, filtered and concentrated under reduced pressure to yield the desired product **324** as a white powder (1.91 g, 89%). Mp: 82-84 ºC. ν_{max} (ATR): 3312 (OH), 1695 (C=C) cm^{-1}. δH (400 MHz, $CDCl_3$): 7.33 (2H, s, H-2,6), 5.88 (1H, s, OH), 3.95 (6H, s, CH_3), 3.90 (3H, s, CH_3). δ_C (100 MHz, $CDCl_3$): 166.83 (C=O), 146.58 (C), 139.13 (C), 121.07 (C), 106.58 (CH), 56.39 (CH_3), 52.08 (CH_3). Reported data agree with literature.[149]

Methyl-3,5-dimethoxy-4-[5',7'-diisopropoxy-3''-nitro-flavonoxy]-benzoate 325

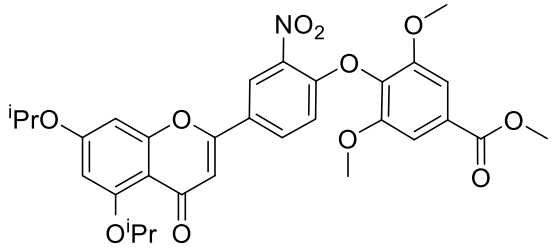

Nitro flavone **197** (1.00 g, 2.4 mmol) and methyl ester of syringic acid **324** (0.512 g, 2.4 mmol) were dissolved in dry dimethyl formamide (12 mL), anhydrous potassium carbonate (0.389 g, 2.6 mmol) was added and the suspension stirred at 80 ºC for 16 hours. After cooling to room temperature the reaction was quenched with 1 M hydrochloric acid solution (50 mL) then filtered and the filtrate washed with more 1 M hydrochloric acid solution. The filtrate was taken up in acetone, dried over magnesium sulfate and concentrated under reduced pressure. The crude product was then purified by column

chromatography (Isolera: 40-70% ethyl acetate in hexane) to yield the product **325** as a brown foam (0.780 g, 55%). Melting Point 210-212 ºC. ν_{max} (ATR): 1721 (C=O), 1602 (C=C) 1531 (NO_2) cm^{-1}. δ_H (400 MHz, $CDCl_3$): 8.54 (1H, d, *J* = 2.3 Hz, H-2''), 7.80 (1H, dd, *J* = 8.9, 2.3 Hz, H-6''), 7.39 (2H, s, H-3,5), 6.80 (1H, d, *J* = 8.9 Hz, H-5''), 6.55 (1H, d, *J* = 2.2 Hz, H-6'), 6.52 (1H, s, H-3'), 6.36 (1H, d, *J* = 2.2 Hz, H-8'), 4.67 (1H, sept., *J* = 6.1 Hz, CH), 4.59 (1H, sept., *J* = 6.1 Hz, CH), 3.96 (3H, s, CH_3), 3.85 (6H, s, CH_3), 1.46 (6H, d, *J* = 6.1 Hz, CH_3), 1.42 (6H, d, *J* = 6.1 Hz, CH_3). δ_C (100 MHz, $CDCl_3$): 176.74 (C=O), 166.14 (C), 162.41 (C), 159.71 (C), 159.44 (C), 157.52 (C), 152.26 (C), 152.49 (C), 139.32 (C), 134.42 (C), 131.04 (CH), 128.45 (C), 125.77 (C), 123.47 (CH), 116.98 (CH), 109.79 (C), 109.03 (CH), 106.65 (CH), 100.59 (CH), 94.10 (CH), 72.29 (CH), 70.65 (CH), 56.42 (CH_3), 52.51 (CH_3), 21.89 (CH_3), 21.80 (CH_3). HRMS [ESI]: 616.1763 *m/z*. $C_{31}H_{31}NNaO_{11}$ requires $[M+Na]^+$ 616.1789 *m/z*.

Methyl-3,5-dimethoxy-4-[5',7'-diisopropoxy-flavon-4''-oxy]-benzoate 327

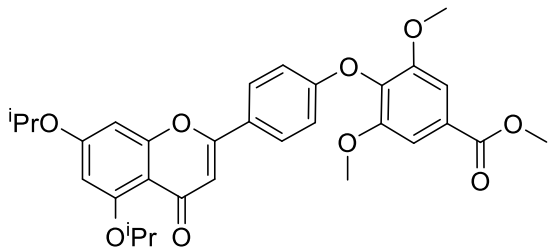

Nitro staring material **325** (1.66 g, 2.8 mmol) and tin chloride (3.196 g, 2.8 mmol) were taken up in ethanol (15 mL) and heated at 60 ºC for 4 hours. The reaction was cooled to room temperature, the ethanol removed under reduced pressure and the residue taken up in dichloromethane (30 mL). The organic fraction was then washed with sodium hydrogen carbonate solution (3 × 30mL) then brine (30 mL), dried over magnesium sulfate, filtered and concentrated under reduced pressure to yield the reduced amino product **326**.

The crude amine **326** was then taken up in a mixture of concentrated hydrochloric acid (7.8 mL) and acetic acid (15 mL) and cooled to 0 ºC. Sodium nitrite (2.46 g, 36 mmol) was added as a solution in water (0.2 mL) and the reaction warmed up to room temperature overnight. The reaction mixture was then diluted with 1M hydrochloric acid (100 mL) and extracted into dichloromethane (2 × 100 mL). The combined organic fractions were washed

with concentrated aqueous sodium hydrogen carbonate solution (2 × 150 mL) then brine (100 mL), dried over magnesium sulfate and concentrated under reduced pressure. The crude product was then purified by column chromatography (Isolera 20-60% ethyl acetate in hexane) to yield the flavone derivative **327** as a yellow oil (0.532 g, 35%). ν_{max} (ATR): 1721 (C=O), 1601 (C=C) 1225 (C-O) cm^{-1}. δ_H (400 MHz, $CDCl_3$): 7.77 (2H, d, *J* = 9.0 Hz, H-2''6''/3''5''), 7.40 (2H, s, H-3,5), 6.94 (2H, d, *J* = 9.0 Hz, H-2''6''/3''5''), 6.50 (1H, d, *J* = 2.1 Hz, H-6'/8), 6.49 (1H, 1H, s, H-3'), 6.34 (1H, d, *J* = 2.2 Hz, H-6'/8'), 4.63 (1H, sept., *J* = 6.1 Hz, CH), 4.58 (1H, sept., *J* = 6.1 Hz, CH), 1.45 (6H, d, *J* = 6.1 Hz, CH_3), 1.40 (6H, d, *J* = 6.1 Hz, CH_3). δ_C (100 MHz, $CDCl_3$): 177.26 (C), 166.34 (C), 161.97 (C), 160.18 (C), 160.13 (C), 159.80 (C), 159.34 (C), 152.92 (C), 135.22 (C), 127.60 (C), 127.45 (CH), 125.36 (C), 115.22 (CH), 109.97 (C), 107.87 (CH), 106.64 (CH), 100.58 (CH), 94.39 (CH), 72.37 (CH), 70.44 (CH), 56.30 (CH_3), 52.34 (CH_3), 21.85 (CH_3), 21.81 (CH_3). HRMS [ESI]: 645.2427 *m/z*. $C_{38}H_{38}NaO_8$ requires $[M+Na]^+$ 645.2459 *m/z*.

N-cyclohexyl-3,5-dimethoxy-4-[5',7'-diisopropoxy-flavon-4''-oxy]-benzamide 329

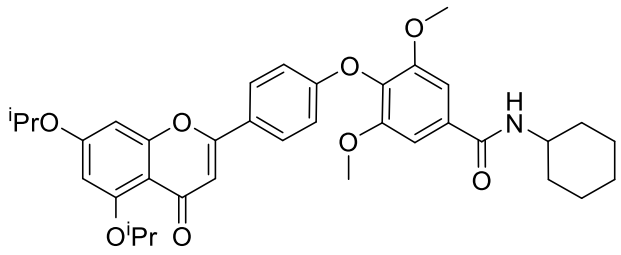

Flavone conjugated syringic acid derivative **328** (0.038 g, 0.07 mmol) and cyclohexylamine (10 µL, 0.09 mmol) were dissolved in anhydrous dichloromethane (1.0 mL) along with EDC (0.013 g, 0.11 mmol) and DMAP (1.4 mg, 0.01 mmol). The reaction mixture was stirred overnight at room temperature. The reaction mixture was purified by column chromatography (Isolera 40-60% ethyl acetate in hexane) to yield the ester **329** as a beige gum (0.021 g, 46%). ν_{max} (ATR): 1639 (C=O), 1602 (C=C) cm^{-1}. δ_H (400 MHz, $CDCl_3$): 7.76 (2H, d, *J* = 9.0 Hz, H-2'',6''/3'',5''), 7.06 (2H, s, H-2,6), 6.93 (2H, d, *J* = 9.0 Hz, H-2'',6''/3'',5''), 6.50 (1H, d, *J* = 2.2 Hz, H-6'/8'), 6.49 (1H, s, H-3'), 6.34 (1H, d, *J* = 2.2 Hz, H-6'/8'), 5.97 (1H, broad d, *J* = 8.0 Hz, NH), 4.63 (1H, sept., *J* = 6.1 Hz, ^{i}Pr), 4.57 (1H, sept., *J* = 6.0 Hz, ^{i}Pr), 2.12-2.04 (2H, m,

CH_2), 1.86-1.73 (3H, CH, CH_2), 3.84 (6H, s, 2 CH_3), 1.45 (6H, d, *J* = 6.0 Hz, ^{i}Pr), 1.40 (6H, d, *J* = 6.1 Hz, ^{i}Pr), 1.34-1.22 (6H, m, 3CH_2). δ_C (100 MHz, $CDCl_3$): 177.36 (C), 166.21 (C), 162.06 (C), 160.38 (C), 160.25 (C), 159.89 (C), 159.42 (C), 153.18 (C), 133.90 (C), 133.22 (C), 127.52 (CH), 125.36 (C), 115.24 (CH), 110.03 (C), 107.92 (CH), 104.30 (CH), 100.63 (CH), 94.45 (CH), 72.43 (CH),70.53 (CH), 56.58 (CH), 56.50 (CH_3), 33.26 (CH_2), 25.57 (CH_2), 24.98 (CH_2), 21.93 (CH_3), 21.88 (CH_3).). HRMS [ESI]: 638.2704 *m/z*. $C_{36}H_{41}NNaO_8$ requires $[M+Na]^+$ 638.2724 *m/z*.

N-4'''-hydroxybenzyl-3,5-dimethoxy-4-[5',7'-diisopropoxy-flavon-4''-oxy]-benzamide 330

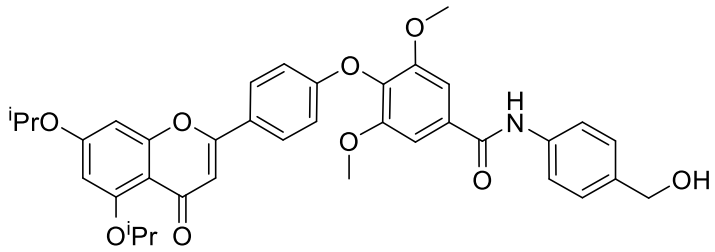

Flavone conjugated syringic acid derivative **328** (0.026 g, 0.05 mmol) and 4-aminobenzyl alcohol (0.008 g, 0.06 mmol) were dissolved in anhydrous dichloromethane (1.0 mL) along with EDC (0.014 g, 0.07 mmol) and DMAP (1.1 mg, 0.01 mmol). Reaction mixture was stirred overnight at room temperature. The reaction mixture was purified by column chromatography (Isolera 20-100% ethyl acetate in hexane) to yield the ester **330** as yellow oil (0.025 g, 79%). ν_{max} (ATR): 2976 (N-H), 1638 (C=O), 1599 (C=O) cm^{-1}. δ_H (400 MHz, $CDCl_3$): 8.86 (1H, s, NH), 7.71 (2H, d, *J* = 8.8 Hz, H-3''',5'''), 7.70 (2H, d, *J* = 8.3 Hz, H-2'',6''/3'',5''), 7.33 (2H, d, *J* = 8.5 Hz, H-2'',6''/3'',5''), 7.29 (2H, s, H-2,6), 6.90 (2H, d, *J* = 8.9 Hz, H-2''',6'''), 6.50 (1H, d, *J* = 2.1 Hz, H-6'/8'), 6.42 (1H s, H-3'), 6.32 (1H, d, *J* = 2.2 Hz, H-6'/8'), 4.66 (2H, s, CH_2), 4.63 (1H, sept., *J* = 6.1 Hz, H-^{i}Pr), 4.56 (1H, sept., *J* = 6.1 Hz, H-^{i}Pr), 3.79 (6H, s, 2 CH_3), 1.39 (12H, d, *J* = 6.1 Hz, 2^{i}Pr). δ_C (100 MHz, $CDCl_3$): 177.56 (C), 165.52 (C), 162.24 (C), 160.45 (C), 160.41 (C), 159.95 (C), 159.37 (C), 153.18 (C), 137.57 (C), 137.24 (C), 134.13 (C), 132.97 (C), 127.75 (CH), 127.55 (CH), 125.20 (C), 120.69 (CH), 115.29 (CH), 109.74 (C), 107.69 (CH), 104.49 (CH),100.24 (CH), 94.27 (CH), 72.20 (CH), 70.60 (CH), 64.88 (CH_2), 56.45 (CH_3), 21.93 (CH_3), 21.82 (CH_3). HRMS [ESI]: 662.2324 *m/z*. $C_{37}H_{37}NNaO_9$ requires $[M+Na]^{+\bullet}$ 662.2361 *m/z*.

N-4'''-methoxyphenyl-3,5-dimethoxy-4-[5',7'-diisopropoxy-flavon-4''-oxy]-benzamide 331

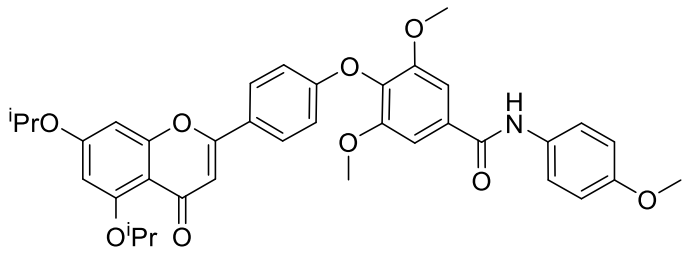

Flavone conjugated syringic acid derivative **328** (0.022 g, 0.04 mmol) and p-anisidine (0.008 g, 0.06 mmol) were dissolved in anhydrous dichloromethane (0.2 mL) along with EDC (0.013 g, 0.07 mmol) and DMAP (1.1 mg, 0.01 mmol). Reaction mixture was stirred overnight at room temperature. The reaction mixture was purified by column chromatography (Isolera 40-60% ethyl acetate in hexane) to yield the ester **331** as a pale yellow oil (0.024 g, 89%). ν_{max} (ATR): 2978 (N-H), 1637 (C=O), 1600 (C=C) cm^{-1}. δ_H (400 MHz, $CDCl_3$): 8.19 (1H, s, NH), 7.75 (2H, s, *J* = 9.0 Hz, H-2',6'/3',5'), 7.60 (2H, s, *J* = 8.9 Hz, H-2',6'/3',5'), 7.23 (2H, s, H-2,6), 6.94 (2H, s, *J* = 8.7 Hz, H-2'',6''/3'',5''), 6.92 (2H, s, *J* = 8.7 Hz, H-2'',6''/3'',5''), 6.50 (1H, d, *J* = 2.2 Hz, H-6'/8'), 6.47 (1H, s, H-3'), 6.34 (1H, d, *J* = 2.2 Hz, H-6'/8'), 4.63 (1H, sept., *J* = 6.1 Hz, ^{i}Pr), 4.57 (1H, sept., *J* = 6.1 Hz, ^{i}Pr), 3.83 (6H, s, 2 CH_3), 3.82 (3H, s, CH_3), 1.42 (1H, d, *J* = 6.0 Hz, ^{i}Pr), 1.40 (1H, d, *J* = 6.0 Hz, ^{i}Pr). δ_C (100 MHz, $CDCl_3$): 177.44 (C), 165.26 (C), 162.14 (C), 160.38 (C), 160.32 (C), 159.93 (C), 159.40 (C), 156.68 (C), 153.25 (C), 134.08 (C), 133.15 (C), 131.05 (C), 127.55 (CH), 125.31 (C), 122.26 (CH), 115.28 (CH), 114.22 (CH), 109.88 (C), 107.84 (CH), 104.54 (CH), 100.39 (CH), 94.31 (CH), 72.29 (CH), 70.56 (CH), 65.49 (CH_3), 55.52 (CH_3), 21.94 (CH_3), 21.85 (CH_3). HRMS [ESI]: 662.2315 *m/z*. $C_{37}H_{37}NNaO_9$ requires $[M+Na]^+$ 662.2361 *m/z*.

N-cyclohexyl-3,5-dihydroxy-4-[5',7'-dihydroxy-flavon-4''-oxy]- benzamide 333

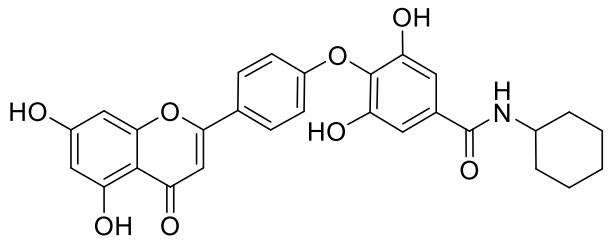

Isopropoxy protected amide **329** (9.0 mg, 0.01 mmol) was taken up in dry dichloromethane (0.3 mL) and cooled to 0 ºC. Boron tribromide solution in dichloromethane (1M, 0.1 mL) was then added dropwise, stirred for 1 hour at 0℃. The reaction was then quenched with water (10 mL) and extracted into a mixture of chloroform and isopropanol (4:1, 4 × 10 mL). The combined organic fractions were washed with water (50 mL) then dried over magnesium sulfate and concentrated under reduced pressure. The crude compound was then purified using the HP/LC system (35%-60% acetonitrile in water/0.1% TFA) to yield the pure product **333** as a beige gum (7.2 mg, 80%). ν_{max} (ATR): 2934 (O-H), 1601 (C=C) 1169 (C-O) cm^{-1}. δ_H (400 MHz, Acetone-D_6): 8.02 (1H, s, NH), 8.01 (2H, d, *J* = 8.4 Hz, H-2'',6''/3'',5''), 7.15 (2H, s, H-2,6), 7.04 (2H, d, *J* = 8.4 Hz, H-2'',6''/3'',5''), 6.69 (1H, s, H-3'/6'/8'), 6.57 (1H, s, H-3'/6'/8'), 6.29 (1H, s, H-3'/6'/8'), 3.93-3.83 (1H, m, CH), 2.02-1.92 (2H, m, CH_2), 1.82-1.75 (1H, m, H-CH_2), 1.72-1.64 (1H, m, H-CH_2), 1.49-1.16 (6H, m, CH_2). HRMS [ESI]: 526.1453 *m/z*. $C_{28}H_{25}NNaO_8$ requires $[M+Na]^+$ 526.1472 *m/z*.

N-4'''-hydroxyphenyl-3,5-dihydroxy-4-[5',7'-dihydroxy-flavon-4''-oxy]-benzamide 335

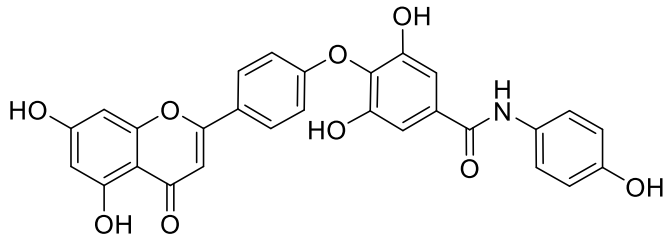

Isopropoxy protected amide **331** (0.024 mg, 0.04 mmol) was taken up in dry dichloromethane (0.5 mL) and cooled to 0 ºC. Boron tribromide solution in

dichloromethane (1M, 0.55 mL) was then added dropwise, and the resultant solution stirred for 1 hour at 0 ºC. The reaction was then quenched with water (10 mL) and extracted into ethyl acetate (2 × 10 mL). The combined organic fractions were then dried over magnesium sulfate and concentrated under reduced pressure. The crude compound was then purified using the HP/LC system (35%-60% acetonitrile in water/0.1% TFA) to yield the pure product **335** as a beige powder (4.1 mg, 22%). Decomposes at 207 ºC. ν_{max} (ATR): 3414 (O-H), 1659 (N-H), 1659 (N-H) cm^{-1}. δ_H (400 MHz, DMSO-D_6): 12.90 (1H, s, OH), 10.86 (1H, s, OH/NH), 9.95 (1H, s, OH/NH), 9.84 (2H, s, 2OH), 9.22 (1H, s, OH/NH), 8.02 (2H, d, *J* = 8.5 Hz, H-2',6'/3',5'), 7.52 (2H, d, *J* = 8.4 Hz, H-2',6'/3',5'), 6.99 (2H, s, H-2,6), 6.96 (2H, d, *J* = 8.5 Hz, H-2'',6''/3'',5''), 6.86 (1H, s, H-3'/6'/8'), 6.73 (2H, d, *J* = 8.5 Hz, H-2',6'/3',5'), 6.50 (1H, s, H-3'/6'/8'), 6.21 (1H, s, H-3'/6'/8').). δ_C (100 MHz, DMSO-D_6): 182.25 (C), 165.39 (C), 164.73 (C), 163.74 (C), 161.94 (C), 161.30 (C), 157.84 (C), 154.06 (C), 151.07 (C), 133.69 (C), 131.82 (C), 131.32 (C), 128.67 (CH), 124.33 (C), 122.49 (CH), 115.94 (CH), 115.42 (CH), 107.65 (CH), 104.67 (C), 94.51 (CH). HRMS [ESI]: 512.0974 *m/z*. $C_{28}H_{18}NO_9$ requires $[M+Na]^+$ 512.0987 *m/z*.

Bibliography

1. Berg, J. M., *Chem. Eng. News*, **2001**, *79*, 130-130.
2. Lamond, A. I., *BioEssays*, **1993**, *15*, 595-603.
3. Jurica, M. S.,Moore, M. J., *Mol. Cell*, **2003**, *12*, 5-14.
4. Nilsen, T. W., *BioEssays*, **2003**, *25*, 1147-1149.
5. Ritchie, D. B., Schellenberg, M. J.,MacMillan, A. M., *Biochim. Biophys. Acta - Gene Regulatory Mechanisms*, **2009**, *1789*, 624-633.
6. Khan, D. H., Jahan, S.,Davie, J. R., *Adv. Biol. Regul.*, **2012**, *52*, 377-388.
7. Beisel, K. W., Rocha-Sanchez, S. M., Ziegenbein, S. J., Morris, K. A., Kai, C., Kawai, J., Carninci, P., Hayashizaki, Y.,Davis, R. L., *Gene*, **2007**, *386*, 11-23.
8. Sammeth, M., Foissac, S.,Guigó, R., *PLoS Comput. Biol.*, **2008**, *4*, e1000147.
9. Ramanouskaya, T. V.,Grinev, V. V., *Mol. Genet. Genomics*, **2017**, DOI: 10.1007/s00438-017-1350-0.
10. Ward, A. J.,Cooper, T. A., *The Journal of Pathology*, **2010**, *220*, 152-163.
11. Valcárcel, J.,Ortín, J., *Nat. Microbiol.*, **2016**, *1*, 16100.
12. Pentland, I.,Parish, J., *Viruses*, **2015**, *7*, 2791.
13. Debing, Y., Jochmans, D.,Neyts, J., *Curr. Opin. Virol.*, **2013**, *3*, 217-224.
14. Zhou, Z.,Fu, X.-D., *Chromosoma*, **2013**, *122*, 191-207.
15. Koo, T.,J. Wood, M., *Hum. Gene Ther.*, **2013**, *24*.
16. Mendell, J. R., Sahenk, Z.,Rodino-Klapac, L. R., *Expert Opin. Orphan Drugs*, **2017**, *5*, 683-690.
17. Zhang, X., Yan, C., Hang, J., Finci, L. I., Lei, J.,Shi, Y., *Cell*, **2017**, *169*, 918-929.e914.
18. Leon, B., Kashyap, M., Chan, W., Krug, K., Castro, J., LaClair, J.,Burkart, M. D., *Angew. Chem., Int. Ed.*, **2017**, DOI: 10.1002/anie.201701065, n/a-n/a.
19. Debdab, M., Carreaux, F., Renault, S., Soundararajan, M., Fedorov, O., Filippakopoulos, P., Lozach, O., Babault, L., Tahtouh, T., Baratte, B., Ogawa, Y., Hagiwara, M., Eisenreich, A., Rauch, U., Knapp, S., Meijer, L.,Bazureau, J.-P., *J. Med. Chem.*, **2011**, *54*, 4172-4186.
20. O'Brien, K., Matlin, A. J., Lowell, A. M.,Moore, M. J., *J. Biol. Chem.*, **2008**, *283*, 33147-33154.
21. Miura, H., Kihara, T.,Kawano, N., *Tetrahedron Lett.*, **1968**, *9*, 2339-2342.
22. Fukui, Y.,Kawano, N., *J. Am. Chem. Soc.*, **1959**, *81*, 6331-6331.
23. Nakazawa, K., *Tetrahedron Lett.*, **1967**, *8*, 5223-5225.
24. Nakazawa, K., *Chem. Pharm. Bull.*, **1968**, *16*, 2503-2511.
25. R. Markham, K., Sheppard, C.,Geiger, H., *Phytochem.*, **1987**, *26*, 3335-3337.
26. Dongfeng, L., Dongmei, W., *China Pat.*, CN102827128 A, **2012**.
27. Mingqiu, S.; Anwei, D.; Li, Z.; Beihua, B.; Yudan, C.; Sheng, Y., *China Pat.*, CN 103130761, **2013**.
28. Jinfang, Z.; Dongmei, W., *China Pat.*, CN 103450136, **2013**.
29. Qianqian, K., *China Pat.*, CN104473948 A, **2015**.
30. Author, *Korea Pat.*, KR2015023209 A, **2015**.
31. Kalva, S., Azhagiya Singam, E. R., Rajapandian, V., Saleena, L. M.,Subramanian, V., *J. Mol. Graphics Modell.*, **2014**, *49*, 25-37.
32. Razzaghi-Asl, N., Sepehri, S., Ebadi, A., Miri, R.,Shahabipour, S., *Struct. Chem.*, **2015**, *26*, 607-621.
33. Tomás-Barberán, F. A., *Phytochem. Anal.*, **2001**, *12*, 214-214.

34. Caldwell, S., *University of Glasgow*, **2002**, *PhD thesis*.
35. Kawabata, K., Mukai, R.,Ishisaka, A., *Food Funct.*, **2015**, *6*, 1399-1417.
36. Verma, A. K.,Pratap, R., *Tetrahedron*, **2012**, *68*, 8523-8538.
37. Ferry, D. R., Smith, A., Malkhandi, J., Fyfe, D. W., deTakats, P. G., Anderson, D., Baker, J.,Kerr, D. J., *Clin. Cancer Res.*, **1996**, *2*, 659-668.
38. Burak, C., Wolffram, S., Zur, B., Langguth, P., Fimmers, R., Alteheld, B., Stehle, P.,Egert, S., *Br. J. Nutr.*, **2017**, *117*, 698-711.
39. Alqurashi, R., A Galante, L., R Rowland, I., Spencer, J.,Commane, D., *Am. J. Clin. Nutr.*, **2016**, *104*, 1-9.
40. Armelin, E. A., Donate, P. M.,Galembeck, S. E., *Tetrahedron*, **2000**, *56*, 5105-5111.
41. Mijangos, M. V., Gonzalez-Marrero, J., Miranda, L. D., Vincent-Ruz, P., Lujan-Montelongo, A., Olivera-Diaz, D., Bautista, E., Ortega, A., de la Luz Campos-Gonzalez, M.,Gamez-Montano, R., *Org. Biomol. Chem.*, **2012**, *10*, 2946-2949.
42. Jurd, L., *J. Am. Chem. Soc.*, **1958**, *80*, 5531-5536.
43. Jurd, L., *J. Org. Chem.*, **1962**, *27*, 1294-1297.
44. Jia, W. Z., Cheng, F., Zhang, Y. J., Ge, J. Y., Yao, S. Q.,Zhu, Q., *Chem. Biol. Drug Des.*, **2017**, *89*, 141-151.
45. Shah, S. P. a. U., *Asian J. Pharm. Clin. Res.*, **2017**, *10*, 403-406.
46. Lahyani, A.,Trabelsi, M., *Ultrason. Sonochem.*, **2016**, *31*, 626-630.
47. Nawghare, B. R., Sakate, S. S.,Lokhande, P. D., *J. Heterocycl. Chem.*, **2014**, *51*, 291-302.
48. Tan, C.-X., Schrader, K. K., Khan, I. A.,Rimando, A. M., *Chem. Biodiversity*, **2015**, *12*, 259-272.
49. Luxen, A. J., Christiaens, L. E. E.,Renson, M. J., *J. Organomet. Chem.*, **1985**, *287*, 81-85.
50. Chuang, D.-W., El-Shazly, M., Balaji D, B., Chung, Y.-M., Chang, F.-R.,Wu, Y.-C., *Eur. J. Org. Chem.*, **2012**, *2012*, 4533-4540.
51. Yang, D., Wang, Z., Wang, X., Sun, H., Xie, Z., Fan, J., Zhang, G., Zhang, W.,Gao, Z., *J. Mol. Catal. A: Chem.*, **2017**, *426*, 24-29.
52. Liu, J., Liu, M., Yue, Y., Zhang, N., Zhang, Y.,Zhuo, K., *Tetrahedron Lett.*, **2013**, *54*, 1802-1807.
53. Xue, L., Shi, L., Han, Y., Xia, C., Huynh, H. V.,Li, F., *Dalton Trans.*, **2011**, *40*, 7632-7638.
54. Jain, P. K., Makrandi, J. K.,Grover, S. K., *Synthesis*, **1982**, *1982*, 221-222.
55. Baker, W., *Journal of the Chemical Society (Resumed)*, **1933**, DOI: 10.1039/JR9330001381, 1381-1389.
56. Khanapur, M., Pinna, N. K.,Badiger, J., *Med. Chem. Res.*, **2015**, *24*, 2656-2669.
57. Daskiewicz, J.-B., Depeint, F., Viornery, L., Bayet, C., Comte-Sarrazin, G., Comte, G., Gee, J. M., Johnson, I. T., Ndjoko, K., Hostettmann, K.,Barron, D., *J. Med. Chem.*, **2005**, *48*, 2790-2804.
58. Gaspar, A., Matos, M. J., Garrido, J., Uriarte, E.,Borges, F., *Chem. Rev.*, **2014**, *114*, 4960-4992.
59. Feuerstein, W.,v. Kostanecki, S., *Ber. Dtsch. Chem. Ges.*, **1898**, *31*, 1757-1762.
60. Klier, L., Bresser, T., Nigst, T. A., Karaghiosoff, K.,Knochel, P., *J. Am. Chem. Soc.*, **2012**, *134*, 13584-13587.
61. Messaoudi, S., Brion, J.-D.,Alami, M., *Org. Lett.*, **2012**, *14*, 1496-1499.
62. Khoobi, M., Alipour, M., Zarei, S., Jafarpour, F.,Shafiee, A., *Chem. Commun.*, **2012**, *48*, 2985-2987.

63. Kraus, G. A.,Gupta, V., *Org. Lett.*, **2010**, *12*, 5278-5280.
64. Kim, D., Ham, K.,Hong, S., *Org. Biomol. Chem.*, **2012**, *10*, 7305-7312.
65. Shin, Y., Yoo, C., Moon, Y., Lee, Y.,Hong, S., *Chem. - An Asian Journal*, **2015**, *10*, 878-881.
66. Golshani, M., Khoobi, M., Jalalimanesh, N., Jafarpour, F.,Ariafard, A., *Chem. Commun.*, **2017**, DOI: 10.1039/C7CC02107K.
67. Gholshani, M., Khoobi, M., Jalalimanesh, N., Jafarpour, F.,Ariafard, A., *Chem. Commun.*, **2017**, DOI: 10.1039/C7CC02107K.
68. Kim, H. P., Park, H., Son, K. H., Chang, H. W.,Kang, S. S., *Arch. Pharmacal Res.*, **2008**, *31*, 265.
69. Rahman, M., Riaz, M.,Desai, U. R., *Chem. Biodiversity*, **2007**, *4*, 2495-2527.
70. Nakano, H., Hoshino, Y., Matsuyama, H.,Kohari, Y., *Heterocycles*, **2010**, *81*, 1871 - 1879.
71. Murti, V. V. S., Raman, P. V.,Seshadri, T. R., *Tetrahedron*, **1967**, *23*, 397-404.
72. Sambiagio, C., Marsden, S. P., Blacker, A. J.,McGowan, P. C., *Chem. Soc. Rev.*, **2014**, *43*, 3525-3550.
73. Ahmad, S.,Razaq, S., *Tetrahedron*, **1976**, *32*, 503-506.
74. Lim, H., Kim, S. B., Park, H., Chang, H. W.,Kim, H. P., *Arch. Pharmacal Res.*, **2009**, *32*, 1525.
75. Moon, T. C., Quan, Z., Kim, J., Kim, H. P., Kudo, I., Murakami, M., Park, H.,Chang, H. W., *Bioorg. Med. Chem.*, **2007**, *15*, 7138-7143.
76. Park, H., Kim, Y. H., Chang, H. W.,Kim, H. P., *J. Pharm. Pharmacol.*, **2006**, *58*, 1661-1667.
77. Sum, T. H., Sum, T. J., Collins, S., Galloway, W. R. J. D., Twigg, D. G., Hollfelder, F.,Spring, D. R., *Org. Biomol. Chem.*, **2017**, *15*, 4554-4570.
78. Che, H., Park, B. K., Lim, H., Kim, H. P., Chang, H. W., Jeong, J.-H.,Park, H., *Bioorg. Med. Chem. Lett.*, **2009**, *19*, 74-76.
79. M Ndoile, M.,Van Heerden, F., *Beilstein J. Org. Chem.*, **2013**, *9*, 1346-1351.
80. Zhang, Y. L., Sensen; Shi, Aihong; Yang, Yunshang; Tan, Wei *有机化学 (Organic Chemistry)*, **2015**, *35*, 2114-2118.
81. Logan, R., *University of Glasgow*, **2011**, *MSci Thesis*.
82. Cairns, A., *University of Glasgow*, **2013**, *PhD thesis*.
83. Sethna, S. M., *Chem. Rev.*, **1951**, *49*, 91-101.
84. Haahr, A., *University of Glasgow*, **2011**, *PhD thesis*.
85. Martell, J.,Weerapana, E., *Molecules*, **2014**, *19*, 1378-1393.
86. Patterson, D. M., Nazarova, L. A.,Prescher, J. A., *ACS Chem. Biol.*, **2014**, *9*, 592-605.
87. Gololobov, Y. G., Zhmurova, I. N.,Kasukhin, L. F., *Tetrahedron*, **1981**, *37*, 437-472.
88. Pham, N. D., Parker, R. B.,Kohler, J. J., *Curr. Opin. Chem. Biol.*, **2013**, *17*, 90-101.
89. https://clinicaltrials.gov/ct2/results?cond=&term=quercetin&cntry1=&state1=&recrs=, Clinical trials UK, (accessed 24/09/2017, 2017).
90. Trouillas, P., Marsal, P., Siri, D., Lazzaroni, R.,Duroux, J.-L., *Food Chem.*, **2006**, *97*, 679-688.
91. Carell, T.,Vrabel, M., *Top. Curr. Chem.*, **2016**, *374*, 9.
92. Jeong, S. W.,O'Brien, D. F., *J. Org. Chem.*, **2001**, *66*, 4799-4802.
93. Patani, G. A.,LaVoie, E. J., *Chem. Rev.*, **1996**, *96*, 3147-3176.
94. Kaye, S. B., *Br. J. Cancer*, **1998**, *78*, 1-7.

95. Heyd, F.,Lynch, K. W., *Trends Biochem. Sci.*, **2011**, *36*, 397-404.
96. García-Rodríguez, N., Wong, R. P.,Ulrich, H. D., *Front. Genet.*, **2016**, *7*.
97. Witze, E. S., Old, W. M., Resing, K. A.,Ahn, N. G., *Nat. Meth.*, **2007**, *4*, 798-806.
98. Cappadocia, L.,Lima, C. D., *Chem. Rev.*, **2017**, DOI: 10.1021/acs.chemrev.6b00737.
99. Kim, K. I. L., Baek, S. H.,Chung, C. H., *J. Cell. Physiol.*, **2002**, *191*, 257-268.
100. Huang, C.-J., Wu, D., Khan, F. A.,Huo, L.-J., *DNA and Cell Biol.*, **2015**, *34*, 652-660.
101. Bayer, P., Arndt, A., Metzger, S., Mahajan, R., Melchior, F., Jaenicke, R.,Becker, J., *J. Mol. Biol.*, **1998**, *280*, 275-286.
102. Voet, A. R. D., Ito, A., Hirohama, M., Matsuoka, S., Tochio, N., Kigawa, T., Yoshida, M.,Zhang, K. Y. J., *MedChemComm*, **2014**, *5*, 783-786.
103. Song, J., Durrin, L. K., Wilkinson, T. A., Krontiris, T. G.,Chen, Y., *Proc. Natl. Acad. Sci. U. S. A.*, **2004**, *101*, 14373-14378.
104. Li, Y.-J., Perkins, A. L., Su, Y., Ma, Y., Colson, L., Horne, D. A.,Chen, Y., *Proc. Natl. Acad. Sci.*, **2012**, *109*, 4092-4097.
105. Alontaga, A. Y., Li, Y., Chen, C.-H., Ma, C.-T., Malany, S., Key, D. E., Sergienko, E., Sun, Q., Whipple, D. A., Matharu, D. S., Li, B., Vega, R., Li, Y.-J., Schoenen, F. J., Blagg, B. S. J., Chung, T. D. Y.,Chen, Y., *ACS Comb. Sci.*, **2015**, *17*, 239-246.
106. Kumar, A.,Zhang, K. Y. J., *Comput. Struct. Biotechnol. J.*, **2015**, *13*, 204-211.
107. Liu, Y., Kieslich, C. A., Morikis, D.,Liao, J., *Protein Eng., Des. Sel*, **2014**, *27*, 117-126.
108. Wang, Q., Xia, N., Li, T., Xu, Y., Zou, Y., Zuo, Y., Fan, Q., Bawa-Khalfe, T., Yeh, E. T. H.,Cheng, J., *Oncogene*, **2013**, *32*, 2493-2498.
109. Berta, M. A., Mazure, N., Hattab, M., Pouysségur, J.,Brahimi-Horn, M. C., *Biochem. Biophys. Res. Commun.*, **2007**, *360*, 646-652.
110. Bae, S.-H., Jeong, J.-W., Park, J. A., Kim, S.-H., Bae, M.-K., Choi, S.-J.,Kim, K.-W., *Biochem. Biophys. Res. Commun.*, **2004**, *324*, 394-400.
111. Cheng, J., Kang, X., Zhang, S.,Yeh, E. T. H., *Cell*, **2007**, *131*, 584-595.
112. Cashman, R., Cohen, H., Ben-Hamo, R., Zilberberg, A.,Efroni, S., *Oncotarget*, **2014**, *5*, 1071-1082.
113. Madu, I. G., Li, S., Li, B., Li, H., Chang, T., Li, Y.-J., Vega, R., Rossi, J., Yee, J.-K., Zaia, J.,Chen, Y., *Sci Rep.*, **2015**, *5*, 17808.
114. Wen, D., Xu, Z., Xia, L., Liu, X., Tu, Y., Lei, H., Wang, W., Wang, T., Song, L., Ma, C., Xu, H., Zhu, W., Chen, G.,Wu, Y., *J. Proteome Res.*, **2014**, *13*, 3571-3582.
115. Cheng, J., Perkins, N. D.,Yeh, E. T. H., *J. Biol. Chem.*, **2005**, *280*, 14492-14498.
116. Bawa-Khalfe, T., Lu, L.-S., Zuo, Y., Huang, C., Dere, R., Lin, F.-M.,Yeh, E. T. H., *Proc. Natl. Acad. Sci.*, **2012**, *109*, 17466-17471.
117. Pozzi, B., Bragado, L., Will, C. L., Mammi, P., Risso, G., Urlaub, H., Lührmann, R.,Srebrow, A., *Nucleic Acids Res.*, **2017**, *45*, 6729-6745.
118. Pawellek, A., Ryder, U., Tammsalu, T., King, L. J., Kreinin, H., Ly, T., Hay, R. T., Hartley, R.,Lamond, A. I., *bioRxiv*, **2017**, DOI: 10.1101/123026.
119. Dobrotă, C., Fasci, D., Hădade, N. D., Roiban, G.-D., Pop, C., Meier, V. M., Dumitru, I., Matache, M., Salvesen, G. S.,Funeriu, D. P., *ChemBioChem*, **2012**, *13*, 80-84.

120. Borodovsky, A., Ovaa, H., Meester, W. J. N., Venanzi, E. S., Bogyo, M. S., Hekking, B. G., Ploegh, H. L., Kessler, B. M.,Overkleeft, H. S., *ChemBioChem*, **2005**, *6*, 287-291.
121. Qiao, Z., Wang, W., Wang, L., Wen, D., Zhao, Y., Wang, Q., Meng, Q., Chen, G., Wu, Y.,Zhou, H., *Bioorg. Med. Chem. Lett.*, **2011**, *21*, 6389-6392.
122. Uno, M., Koma, Y., Ban, H. S.,Nakamura, H., *Bioorg. Med. Chem. Lett.*, **2012**, *22*, 5169-5173.
123. Albrow, V. E., Ponder, E. L., Fasci, D., Békés, M., Deu, E., Salvesen, G. S.,Bogyo, M., *Chem. & Biol.*, **2011**, *18*, 722-732.
124. Madu, I. G., Namanja, A. T., Su, Y., Wong, S., Li, Y.-J.,Chen, Y., *ACS Chem. Biol.*, **2013**, *8*, 1435-1441.
125. Kumar, A., Ito, A., Takemoto, M., Yoshida, M.,Zhang, K. Y. J., *J. Chem. Inf. Model.*, **2014**, *54*, 870-880.
126. Chen, Y., Wen, D., Huang, Z., Huang, M., Luo, Y., Liu, B., Lu, H., Wu, Y., Peng, Y.,Zhang, J., *Bioorg. Med. Chem. Lett.*, **2012**, *22*, 6867-6870.
127. Huang, W., He, T., Chai, C., Yang, Y., Zheng, Y., Zhou, P., Qiao, X., Zhang, B., Liu, Z., Wang, J., Shi, C., Lei, L., Gao, K., Li, H., Zhong, S., Yao, L., Huang, M.-E.,Lei, M., *PLOS ONE*, **2012**, *7*, e37693.
128. Lipinski, C. A., Lombardo, F., Dominy, B. W.,Feeney, P. J., *Adv. Drug Delivery Rev.*, **2001**, *46*, 3-26.
129. Lipinski, C. A., *Drug Discovery Today: Technol.*, **2004**, *1*, 337-341.
130. Erlanson, D. A., Fesik, S. W., Hubbard, R. E., Jahnke, W.,Jhoti, H., *Nat. Rev. Drug. Discov.*, **2016**, *15*, 605-619.
131. Siklos, M., BenAissa, M.,Thatcher, G. R. J., *Acta Pharm. Sin. B*, **2015**, *5*, 506-519.
132. Smith, E.,Collins, I., *Future Med. Chem.*, **2015**, *7*, 159-183.
133. Boutagy, J.,Thomas, R., *Chem. Rev.*, **1974**, *74*, 87-99.
134. Bhattacharya, A. K.,Thyagarajan, G., *Chem. Rev.*, **1981**, *81*, 415-430.
135. Wang, Z., in *Comprehensive Organic Name Reactions and Reagents*, John Wiley & Sons, Inc., 2010, DOI: 10.1002/9780470638859.conrr558.
136. Mannhold, R., Poda, G. I., Ostermann, C.,Tetko, I. V., *J. Pharm. Sci.*, **2009**, *98*, 861-893.
137. Congreve, M., Carr, R., Murray, C.,Jhoti, H., *Drug Discovery Today*, **2003**, *8*, 876-877.
138. Hie, L., Fine Nathel, N. F., Shah, T. K., Baker, E. L., Hong, X., Yang, Y.-F., Liu, P., Houk, K. N.,Garg, N. K., *Nature*, **2015**, *524*, 79-83.
139. B. A. Tschaen, J. R. Schmink, G. A. Molander, *Org. Lett.*, **2013**, 15, 500-503. (data in supplementary information)
140. Solladié, G.; Pasturel-Jacopé, Y.; Maignan, J. *Tetrahedron* **2003**, 59, 3315.
141. Helmy, S., Leibfarth, F. A., Oh, S., Poelma, J. E., Hawker, C. J.,Read de Alaniz, J., *J. Am. Chem. Soc.*, **2014**, *136*, 8169-8172.
142. Daskiewicz, J.-B., Bayet, C.,Barron, D., *Tetrahedron*, **2002**, *58*, 3589-3595.
143. Hong, M. C., Kim, Y. K., Choi, J. Y., Yang, S. Q., Rhee, H., Ryu, Y. H., Choi, T. H., Cheon, G. J., An, G. I., Kim, H. Y., Kim, Y., Kim, D. Y., Lee, Y-S., Chang, Y-T., Lee, K. C.,, *Bioorg. Med. Chem.*, **2010**, *18*, 7724-7730.
144. Banwell, M. G., Chand, S.,Savage, G. P., *Tetrahedron: Asymmetry*, **2005**, *16*, 1645-1654.

145. Androutsopoulos, V. P., Ruparelia, K. C., Papakyriakou, A., Filippakis, H., Tsatsakis, A. M.,Spandidos, D. A., *Eur. J. Org. Chem.*, **2011**, *46*, 2586-2595.
146. Ichino, K., Tanaka, H., Ito, K., Tanaka, T.,Mizuno, M., *J. Nat. Prod.*, **1988**, *51*, 906-914.
147. Nahoum, G. A., Breen D., Clarke, J., Donoghue, G., Drummond, A. J., Ellis, E. M., Gemmell, C. G., Helesbeux, J-J., hunter, I. S., Khalaf, A. I., Mackay, S. P., Parkinson, J. A., Suckling, C. J., Waigh, R. D., *J. Med. Chem.*, **2007**, *50*, 6116–6125
148. China Patent CN106431855, **2017**, China Pharmaceutical University, Feng, F., Qu, W., Guan, L., Liu, W., Lin, Q., Chen, L., Hao, Y., Zue,
149. Chouhan, M., Kumar, K., Sharma, R., Grover, V.,Nair, V. A., *Tetrahedron Lett.*, **2013**, *54*, 4540-4543. (data found in supplementary information)
150. National Center for Biotechnology Information. PubChem Compound Database; CID=70341750, https://pubchem.ncbi.nlm.nih.gov/compound/70341750 (accessed Dec. 13, 2017).

10 Appendix: ^{1}H NMR of hinokiflavone

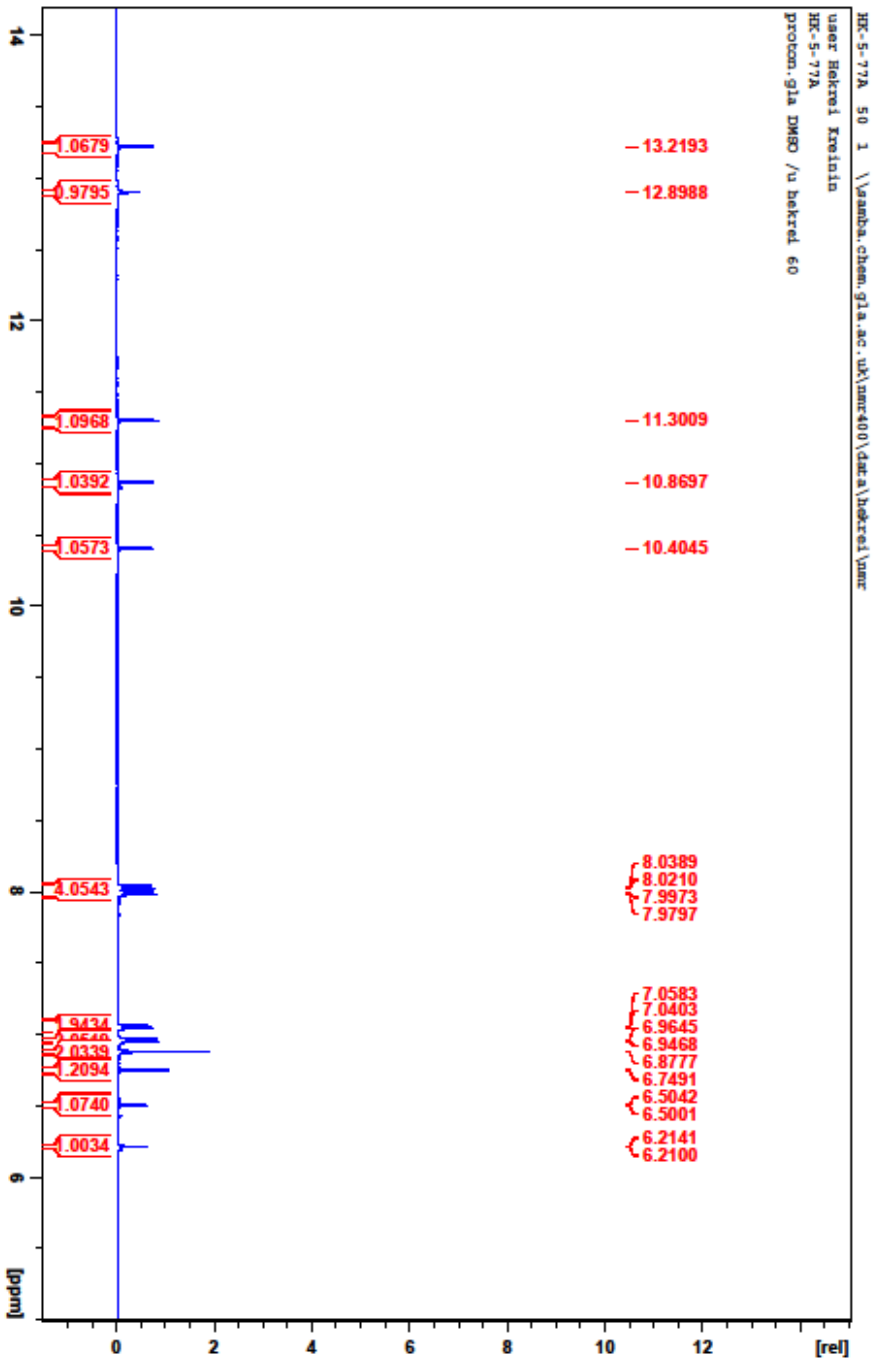

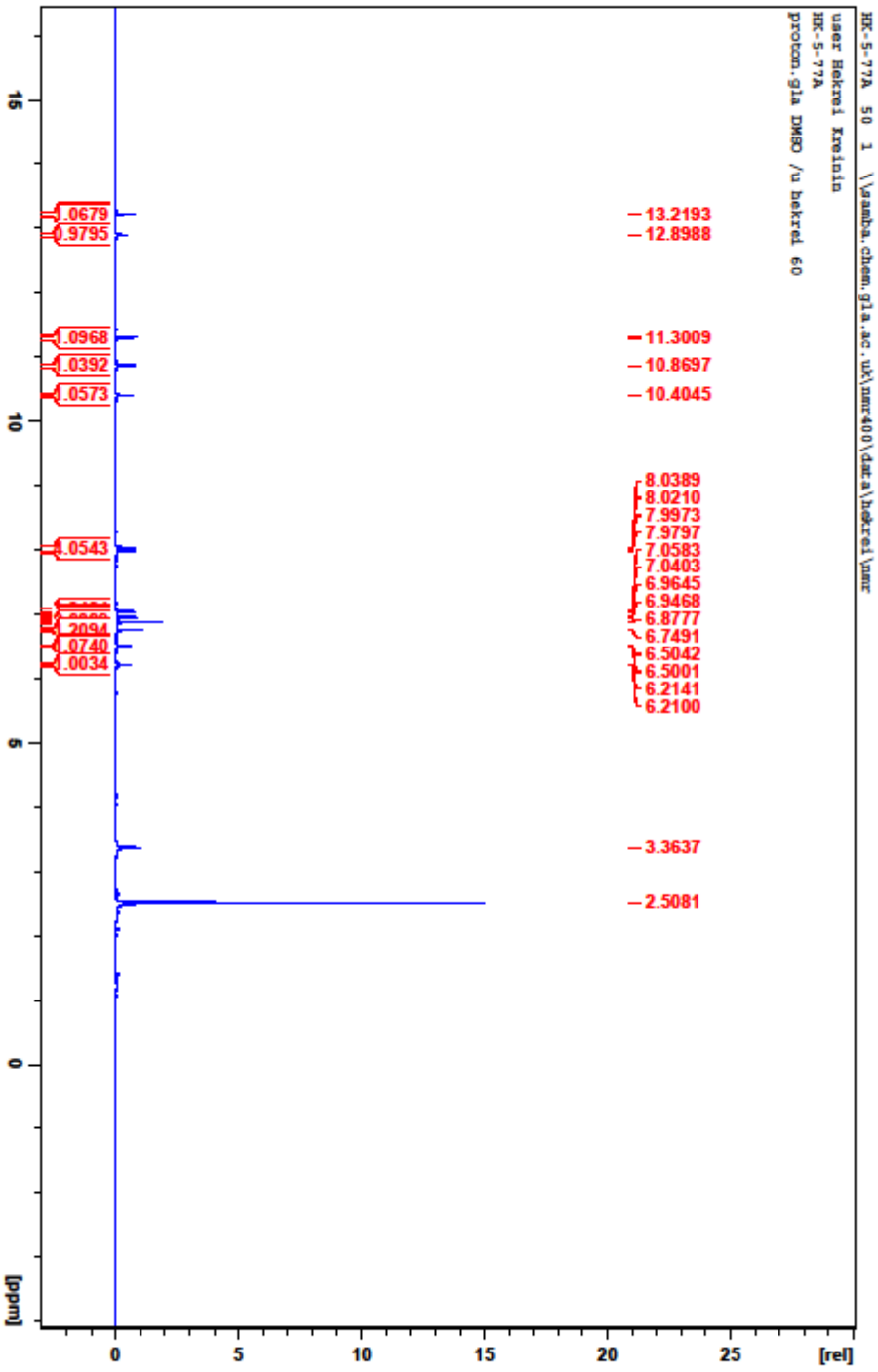
HK-5-77A 50 1 \\samba.chem.gla.ac.uk\nmr400\data\hekrei\nmr
user Hekrei Krvinin
HK-5-77A
proton.gla DMSO /u hekrei 60
1.0679
0.9795
1.0968
1.0392
1.0573
1.0543
1.2094
1.0740
1.0034
13.2193
12.8988
11.3009
10.8697
10.4045
8.0389
8.0210
7.9973
7.9797
7.0583
7.0403
6.9645
6.9468
6.8777
6.7491
6.5042
6.5001
6.2141
6.2100
3.3637
2.5081
[ppm]
[rel]